Declaration

I hereby declare that this thesis is of my own work and effort and has not been submitted in support of an application for another degree or qualification at this or any other university.

Malcolm Allan Kinninmonth

Signature: …….

Date: ……...

Abstract

Healthcare associated infections (HCAI) are a significant problem facing modern healthcare settings; therefore it is important to develop strategies aimed at reducing the number of patients contracting HCAIs. This study investigates the use of essential oils (EO) as antimicrobial additives for polymer materials, including surface coatings (paints), silicone elastomer and a thermoplastic. Conferring antimicrobial properties to surfaces made from such materials, would help to reduce the number of bacteria, reduce the risk of cross infection and therefore limit the number of HCAIs.

The antimicrobial efficacies of five EOs (manuka (MO), oregano (OO), rosewood (RO), lavender (LO) and geranium (GO)) were examined individually against three microorganisms associated with HCAI (MRSA, *Acinetobacter baumannii*, and *Pseudomonas aeruginosa*). Oregano oil provided the highest level of antimicrobial activity, inhibiting the growth of all three bacteria at 2.5 % (v/v). In an attempt to reduce the concentration of oil required for inhibition of growth, blends of the EO have been explored. A blend of oregano oil and rosewood oil exhibited the strongest synergistic antimicrobial effect at a ratio of 3:1, and was selected as the antimicrobial to be added to the polymer materials.

EOs are volatile, direct addition to polymers may allow the EO to bloom to the surface and rapidly evaporate from the polymer, resulting in loss of antimicrobial activity. Furthermore thermoplastics are processed at high temperatures which can result in degradation of the EO. Encapsulation strategies for the EO were therefore investigated in order to promote both sustained release of the EO and protection against degradation / volatilisation during blending in to thermoplastic materials. Considering the latter in particular, inorganic adsorbents were selected and the adsorption characteristics of the EOs onto a range of natural and synthetic montmorillonite type layered silicates were investigated. Using gas chromatography and flow micro-calorimetry their suitability as controlled release reservoirs was investigated. Rockwood Additives Laponite® RD provided the highest levels of adsorption, achieving approximately 170 $mg.g^{-1}$ for oregano oil and 140 $mg.g^{-1}$ for rosewood oil. Organic modification (via cation exchange) of the layered silicates with alkyl ammonium surfactants did not give the anticipated increase in the level of EO adsorption from solution. However the strength of adsorption was in some cases increased. Laponite® RD with

50 % 2HT2M organic modification (modified via cation exchange using dihydrogenated tallow dimethyl ammonium chloride) was selected as the adsorption substrate for the EO based antimicrobial.

Samples of linear low density polyethylene (LLDPE), silicone elastomer (SE) and a solvent based paint were formulated containing the oregano oil:rosewood oil blend pre-adsorbed onto Laponite® RD with 50 % 2HT2M organic modification. These materials were tested for antimicrobial efficacy against MRSA and *A. baumannii*, and the results were compared to control polymers where the EO blend had been added directly. *P. aeruginosa* was found to be unsuitable as a test organism for the polymer samples. All of the polymer samples containing the EO blend exhibited antimicrobial activity, with SE containing the pre-adsorbed EO blend performing the best achieving a 3 log reduction in MRSA cells. The SE and paint materials containing the pre-adsorbed EO blend outperformed the directly added EO controls; however the reverse was true for LLDPE. The release rates of the EO molecules from the polymers were investigated using headspace gas chromatography, and it was found that pre-adsorption of the EO onto the organically modified Laponite® RD more than doubled the time the EO molecules were retained in comparison to the directly added controls.

It has been shown that EO can be used to obtain antimicrobials with broad spectrum antimicrobial activity, and that said activity can be successfully conferred onto polymer materials. Adsorption of the EO onto layered silicates before addition to polymers improved the retention of the EO molecules, thereby increasing the antimicrobial lifetime. Further work will be undertaken to optimise the EO polymer formulations, to combine the best possible antimicrobial activity with EO molecule retention that will make the materials a viable commercial product. The mechanical properties of the polymers; such as hardness, strength and toughness, will be optimised to ensure commercial viability.

Acknowledgements

I would like to thank my Director of Studies Dr. Christopher Liauw for giving me the opportunity to undertake this project. His support and guidance through this project has been invaluable. I would also like to thank my supervisors Professor Joanna Verran, Professor Valerie Edwards-Jones and Dr. Rebecca Taylor for their help and the expert knowledge they have brought to the research. Without such a strong and knowledgeable team of supervisors I would not have succeeded in completing this research.

The whole of the technical staff in the Manchester Metropolitan Microbiology and Chemistry departments deserve thanks for their help and guidance throughout my period of learning the techniques required to complete the work. I would also like to thank Peter Skingle for being generous with his time as I synthesised the silicone elastomers, and Bill Ellison and Lee Harman for their help with the running and interpreting of gas chromatography samples.

At Rockwood Additives Ltd. I would like to thank Dr. David Shaw, Tex Timperly, Adam Brookbanks, and Debbie McCarthy for their input on the project and their guidance in helping me to fully utilise the silicate materials used. In addition I would like to thank Rockwood Additives Ltd. for the funding supplied for the research and the use of their equipment for synthesis and analysis of the silicate materials. I would also like to thank Dr. Maurice Webb for his input and ideas.

I would like to thank the Chemistry Innovation Knowledge Transfer Network for their help in securing funding from the Engineering and Physical Sciences Research Council.

Finally, I would like to thank my parents for their emotional and financial support provided throughout the course of my academic career. Special thanks goes to my fiancé Samantha Jayne Lawrence for putting up with me throughout the stressful writing up period.

Overview of Thesis

This study explored the concept of producing antimicrobial polymers via the addition of an essential oil based antimicrobial. As part of this work the use of layered silicates as an adsorption substrate for EO was also investigated. The purpose of this was to produce a range of polymer materials that would have long lasting antimicrobial activity. These polymers could be used in the manufacture and coating of surfaces for healthcare facilities, producing antimicrobial surfaces which would help to reduce the number of patients catching healthcare associated infections (HCAI).

Thesis structure

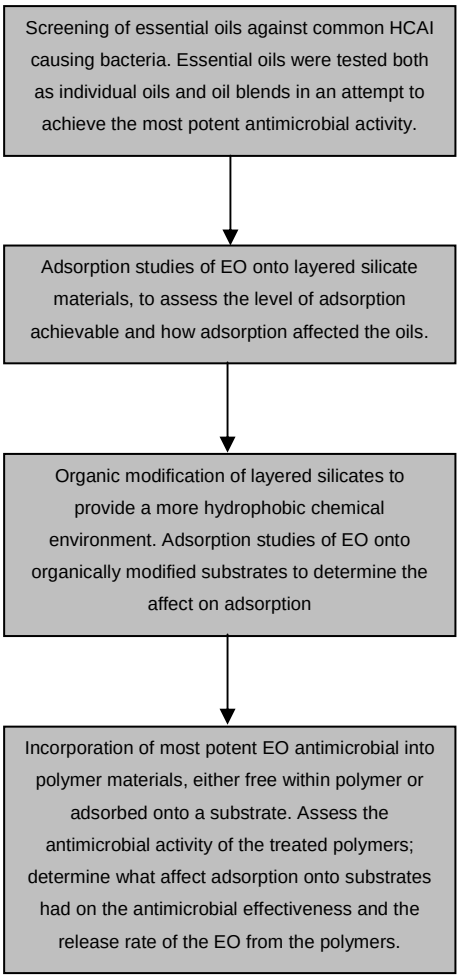

Table of Contents

Declaration i

Abstract ii

Acknowledgements iv

Overview of Thesis v

Table of Contents vi

List of Abbreviations xiii

List of Tables xix

List of Figures xxv

CHAPTER 1 1

Introduction 1

1.1 Healthcare associated infections 1

1.2 Microbiology and the structure of bacterial cells 2

1.3 Chemical makeup of essential oils and their historical uses 4

1.3.1 Controlled release of essential oils to prolong their effects 8

1.4 Physical and chemical structure of smectite minerals 9

1.5 Thesis methodology 12

CHAPTER 2 15

Antimicrobial screening of essential oils and biocides 15

Abstract 15

2.1 Introduction 15

2.1.1 Antimicrobial activity of essential oils 15

2.1.1.1 Essential oils used in this study 17

2.1.2 Bacteria used in this study 18

2.1.2.1 Methicillin resistant *Staphylococcus aureus* 18

2.1.2.2 *Pseudomonas aeruginosa* 19

2.1.2.3 *Acinetobacter baumannii* 19

2.1.3 Gas chromatography-mass spectrometry 20

2.2 Objectives 22
2.3 Materials 23
2.3.1 Culture media 23
2.3.2 Microorganisms 23
2.3.3 Essential oils and biocides 23
2.3.4 Solvents 24
2.4 Experimental 25
2.4.1 Sub culturing microorganisms 25
2.4.2 Preparation of overnight broth 25
2.4.3 Estimation of bacterial numbers 25
2.4.4 Minimum inhibitory concentration and minimum bactericidal concentration of essential oils 25
2.4.5 Oil blend MIC and MBC screening 27
2.4.6 Individual synthetic biocide MIC and MBC screening 29
2.4.7 Biocide and essential oil blend MIC and MBC screening 31
2.4.8 Gas chromatography mass spectrometry analysis of essential oils 35
2.5 Results and discussions 37
2.5.1 MIC and MBC screening of individual essential oils 37
2.5.2 MIC and MBC screening of oil blends 40
2.5.3 MIC and MBC screening of individual synthetic biocides 45
2.5.4 MIC and MBC screening of biocide and essential oil blend combinations 47
2.5.6 Gas chromatography - mass spectroscopy analysis of the chemical makeup of essential oils 57
2.6 Conclusions 66
CHAPTER 3 67
Adsorption of essential oils onto layered silicate substrates 67
Abstract 67

3.1 Introduction 67
3.1.1 Montmorillonite structure 68
3.1.2 Adsorption of organic material onto montmorillonite 68
3.1.3 Desorption of material from montmorillonite 69
3.1.4 Adsorption substrate materials 70
3.1.4.1 Naturally derived substrates from montmorillonites 70
3.1.4.2 Synthetic layered silicates; Laponites® 72
3.1.5 Analytical techniques 73
3.1.5.1 Fourier transform infrared spectroscopy 73
3.1.5.2 Diffuse reflectance infrared Fourier transform spectroscopy 73
3.1.5.3 Wide angle X-ray scattering 74
3.1.5.4 Flow micro-calorimetry 75
3.2 Objectives 78
3.3 Materials 79
3.3.1 Layered silicate substrates 79
3.3.2 Essential oils 79
3.3.3 Solvents 80
3.4 Experimental 81
3.4.1 Characterisation of substrates 81
3.4.1.1 Fourier transform infra red spectroscopy of layered silicate substrates and essential oils. 81
3.4.1.2 WAXS 81
3.4.1.3 N_2 BET surface area 82
3.4.2 Static adsorption studies from solution monitored using gas chromatography 82
3.4.3 Soxhlet extraction of EO adsorbed onto layered silicates 83
3.4.4 Flow micro calorimetry analysis of EO adsorption 83
3.5 Results and discussions 88
3.5.1 Characterisation substrates using physical properties 88
3.5.2 Gas chromatography adsorption studies of EO onto layered silicates 91

3.5.2.1 GC adsorption of rosewood oil onto layered silicates, and the selection of substrates 92
3.5.2.2 GC adsorption of oregano oil onto layered silicates....107
3.5.2.3 GC adsorption of manuka oil onto layered silicates....112
3.5.2.4 GC adsorption of lavender oil onto layered silicates....116
3.5.2.5 GC adsorption of geranium oil onto layered silicates\....120
3.5.2.6 GC Adsorption summary 123
3.5.3 Soxhlet extraction of EOs from layered silicates after adsorption124
3.5.4 Flow micro-calorimetry assessment of EO adsorption onto layered siliactes....125
3.5.4.1 Adsorption of EO onto Laponite® RD determined by FMC ...126
3.5.4.2 Adsorption of EOs onto Laponite® B determined by FMC 132
3.5.4.3 Adsorption of EOs onto Fulcat® 800 determined by FMC....134
3.5.4.4 FMC adsorption summary....137
3.6 Conclusions 139
CHAPTER 4....140
Organic modification of layered silicates and its effect on the adsorption of essential oils 140
Abstract 140
4.1 Introduction....140
4.1.1 Organic modification of layered silicates 141
4.1.2 Adsorption of organic molecules onto organically modified layered silicates....142
4.2 Objectives....144
4.3 Materials 145
4.3.1 Layered silicate substrates....145
4.3.2 Organic modifiers 145
4.3.3 Essential oils 145
4.3.4 Solvents 145
4.4 Experimental....146
4.4.1 Organic modification of layered silicate substrates....146

4.4.1.1 Organic modification of Laponites® 147
4.4.1.2 Organic modification of Fulcat® 800 148
4.4.2 Characterisation of organically modified substrates 148
4.4.3 Gas chromatography adsorption studies of EO onto OM substrates 152
4.4.4 Flow micro calorimetry adsorption studies of EO onto OM substrates 152
4.5 Results and discussions 153
4.5.1 Characterisation of organically modified substrates 153
4.5.1.1 Organic modification of Fulcat® 800 153
4.5.1.2 Organic modification of Laponites® 160
4.5.1.3 Organic content after organic modification of substrates 164
4.5.1.4 FTIR of OM substrates 170
4.5.1.5 Summary 182
4.5.2 Gas chromatography adsorption studies of EO onto OM substrates 183
4.5.2.1 Adsorption of EO onto OM Fulcat® 800 determined by GC ..183
4.5.2.2 Adsorption of EO onto OM Laponite® RD and OM Laponite® B determined by GC 186
4.5.2.3 Summary 189
4.5.3 Flow micro-calorimetry analysis of adsorption of EOs onto organically modified substrates 190
4.5.3.1 FMC adsorption of EO onto OM Fulcat® 800 190
4.5.3.2 FMC adsorption of EOs onto OM Laponite® RD 195
4.5.3.3 FMC adsorption of EO onto OM Laponite® B 197
4.5.3.4 Summary 200
4.6 Conclusions 201
CHAPTER 5 202
Antimicrobial polymers 202
Abstract 202
5.1 Introduction 202
5.1.1 Thermoplastics 203

5.1.2 Silicone elastomer 204
5.1.3 Solvent based paint 206
5.2 Objectives 207
5.3 Materials 208
5.3.1 Polymer samples 208
5.3.2 Culture media 208
5.3.3 Microorganisms 208
5.4 Experimental 209
5.4.1 Production of antimicrobial polymers via addition of essential oils adsorbed onto layered silicates 209
5.4.1.1 Production of silicone elastomer samples containing EO 209
5.4.1.2 Production of solvent based paint containing EO 210
5.4.1.3 Production of linear low density polyethylene samples containing EO 211
5.4.2 Antimicrobial testing of polymer samples 213
5.4.3 Controlled release of essential oils from polymer samples 214
5.5 Results and discussions 216
5.5.1 Assessment of polymer samples after addition of EO 216
5.5.1.1 Physical properties of silicone elastomer samples containing EO 216
5.5.1.2 Solvent based paint containing EO either free within the matrix or adsorbed to a substrate 217
5.5.1.3 Physical properties of linear low density polyethylene samples containing EO 218
5.5.2 Antimicrobial testing of polymer samples 224
5.5.2.1 Assessment of antimicrobial activity of silicone elastomer samples containg EO 227
5.5.2.2 Assessment of antimicrobial activity of paint samples containing EO 232
5.5.2.3 Assessment of antimicrobial activity of linear low density polyethylene samples containing EO 234
5.5.3 Assessment of controlled release behaviour of the composites 239

5.5.3.1 EO release from silicone elastomers comparison of samples containing free EO and adsorbed EO 240

5.5.3.2 EO release from paint comparison of samples containing free EO and adsorbed EO 243

5.5.3.3 EO release from linear low density polyethylene comparison of samples containing free EO and adsorbed EO 245

5.6 Conclusions 249

CHAPTER 6 250

Overall conclusions and further work 250

6.1 Conclusions 250

6.2 Further work 251

References 256

Appendices 267

List of Abbreviations

2HT2M	Di(hydrogented tallow) dimethyl ammonium chloride
a.m.u.	Atomic mass units
CBA	Columbia blood agar
CDC	Center for disease control
CEC	Cation exchange capacity
CFU	Colony forming units
CI	Confidence interval
CMC	Critical micelle concentration
CTAB	Cetyl trimethyl ammonium bromide
DRIFTS	Diffuse reflectance infrared Fourier transform spectroscopy
EO	Essential oil
EO-LRD50	Laponite® RD 50 % 2HT2M organic modification with EO adsorbed
EO-LRD100	Laponite® RD 100 % 2HT2M organic modification with EO adsorbed
F400	Fulcat® 400
F435	Fulcat® 435

F800	Fulcat® 800
Fcol	Fulacolor® XW
FIC	Fractional inhibitory concentration
FMC	Flowmicro calorimetry
FTIR	Fourier transform infrared spectroscopy
GC	Gas chromatography
GC-FID	Gas chromatography – Flame ionization detector
GC-MS	Gas chromatography – Mass spectrometry
GO	Geranium oil
HCAI	Healthcare associated infection
HDPE	High density polyethylene
HPA	Health Protection Agency
HTV	High temperature vulcanisation
LB	Laponite® B
LDPE	Low density polyethylene
LLDPE	Linear low density polyethylene
LLDPE + EO	Linear low density polyethylene containing free essential oil

LLDPE + LRD50 2HT2M	Linear low density polyethylene containing Laponite® RD 50% 2HT2M organic modification
LLDPE + (LRD50 2HT2M + EO)	Linear low density polyethylene containing Laponite® RD 50% 2HT2M organic modification with essential oil pre adsorbed
LLDPE + (LRD100 2HT2M + EO)	Linear low density polyethylene containing Laponite® RD 50% 2HT2M organic modification with essential oil pre adsorbed
LRD	Laponite® RD
LRD50	Laponite® RD with 50% 2HT2M organic modification
LRD100	Laponite® RD with 50% 2HT2M organic modification
LO	Lavender oil
MBC	Minimum bactericidal concentration
MIC	Minimum inhibitory concentration
MMT	Montmorillonite
MO	Manuka oil
MRSA	Methicillin resistant *Staphylococcus aureus*
MSSA	Methicillin susceptible *Staphylococcus aureus*
MSD	Mass selective detector

MTP	Microtitre plate
N/A	Not applicable
NI	Nosocomial infection
NINSS	Nosocomial infection national surveillance service
Na-MMT	Montmorillonite with sodium counter cations
OM	Organically modified
OMLS	Organically modified layered silicate
OO	Oregano oil
Paint + EO	Paint containing free essential oil
Paint + LRD50 2HT2M	Paint containing Laponite® RD 50% 2HT2M organic modification
Paint + (LRD50 2HT2M + EO)	Paint containing Laponite® RD 50% 2HT2M organic modification with essential oil pre adsorbed
Paint + (LRD100 2HT2M + EO)	Paint containing Laponite® RD 50% 2HT2M organic modification with essential oil pre adsorbed
PHMB	Poly hexamethylene biguanide
quats	Quaternary ammonium surfactant compounds
RI	Refractive index

RO	Rosewood oil
RTV	Room temperature vulcanisation
SE	Silicone elastomer
SE + EO	Silicone elastomer containing free essential oil
SE + LRD50 2HT2M	Silicone elastomer containing Laponite® RD 50% 2HT2M organic modification
SE + (LRD50 2HT2M + EO)	Silicone elastomer containing Laponite® RD 50% 2HT2M organic modification with essential oil pre adsorbed
SE + (LRD100 2HT2M + EO)	Paint containing Laponite® RD 50% 2HT2M organic modification with essential oil pre adsorbed
SEM	Scanning electron microscopy
SSI	Surgical site infection
T_g	Glass transition temperature
TGA	Thermo gravimetric analysis
TSST	Toxic shock syndrome toxin
TTC	Triphenyl tetrazolium chloride
UM	Unmodified
XRD	X-ray diffraction

WAXS	Wide angle x-ray scattering

List of Tables

Chapter 2

Table 2.1	Representation of the methods in Section 2.4.4 and 2.4.6	32
Table 2.2	EO concentration ranges used in EO blend + biocide, as described in section 2.2.7, against the three test bacteria. The ranges were made up of halving dilutions. * For EO blend and chlorhexidine test against *P. aeruginosa* M+L range = 2.5 to 0.156%, L+G range = 5 to 0.313 % and RW+G range = 5 to 0.313%.	33
Table 2.3	Synthetic biocide concentration ranges used in EO blend + biocide tests, as described in 2.2.7, against the three test bacteria. Demonstrating the starting concentrations used for checkerboard methods.	34
Table 2.4	Temperature programmes for the individual EO GC-MS analysis.	36
Table 2.5	MIC and MBC data from MTP assays demonstrating the antimicrobial efficacy of the EO against the test bacteria. Demonstrating that none of the EO tested were effective at less than 2 % against all three test bacteria. Standard deviations given in parentheses.	37

Table 2.6 Results from oil combination assays demonstrating the improved activity achieved for OO blends. Numbers in brackets are the combined concentrations of the oils. For MRSA and *P. aeruginosa* all samples that were tested for MBC exhibited growth, bactericidal values were not available. Average standard deviations for each oil: *A. baumannii* OO±0.05, RO±0.17, MO±0.07, LO±0, GO±0.12, MRSA (OO±0.03, RO±0.07, MO±0.06, LO±0.27, GO±0.03, *P. aeruginosa* OO±0.08. RO±0.13, MO±0.09, LO±0.02, GO±0.15). * FIC value with a 95 % CI range that lies within the assigned FIC boundary. 42

Table 2.7 MIC and MBC data from MTP assays demonstrating the antimicrobial activity of the biocides/antibiotics against the test bacteria before addition of EO blends. Demonstrating triclosan as the least effective of the biocides tested. Standard deviations are given in parentheses where appropriate. 45

Table 2.8 MIC and MBC results from Ciprofloxacin and EO blend combination testing. Demonstrating the antimicrobial activity against *A. baumannii* and the lack of an increase in efficacy. Standard deviations were given in parentheses, for the MBC data the standard deviations were ±0. * FIC value with a 95 % CI range that lies within the assigned FIC boundary. 47

Table 2.9 MIC and MBC data from combination testing of EO blends and chlorhexidine, demonstrating the negative effect on efficacy against *A. baumannii* and *P. aeruginosa*, and the lack of a positive effect on MRSA (for the FIC indices ind = indifferent, ant = antagonistic. Standard deviations for all data were 0. All FIC values had a 95 % CI range that lay within the assigned FIC boundary. 51

Table 2.10 MIC and MBC data from combination testing of EO blends and triclosan (for the FIC indices syn=synergistic, add=additive, ind=indifferent). Demonstrating the positive effect on efficacy against *A.baumannii* and the negative effect on efficacy against MRSA. Standard deviations given in parentheses, for MRSA data MIC and MBC standard deviations were 0. * FIC value with a 95 % CI range that lies within the assigned FIC boundary. 53

Table 2.11 MIC and MBC data from combination testing of EO blends and PHMB, demonstrating the reduction in EO blend and PHMB concentration required for MIC and MBC as a result (for the FIC indices syn = synergistic, ind = indifferent). Standard deviations for all data were 0. All FIC values had a 95 % CI range that lay within the assigned FIC boundary. 55

Table 2.12 Summary of the molecular features present on the essential oil molecules. Demonstrating the differences in chemical makeup of the oils, with RO containing the highest number of molecules with polar functional groups, and MO containing the lowest number of molecules with polar functional groups. 65

Chapter 3

Table 3.1 Summary details of substrates with coding. 79

Table 3.2 Surface area and d-spacing of layered silicate substrates to be used in adsorption studies. Demonstrating the differences in the physical properties of the six substrates, which may affect their adsorption characteristics. 88

Table 3.3 Percentage reduction of the oregano oil (OO) molecules analysed (from initial 1.25 % solution), after adsorption onto montmorillonite materials. Demonstrating the level of adsorption of each molecule which comprised greater than 1 % of the molecular make up of OO. 96

Table 3.4 Percentage reduction of the oregano oil (OO) molecules analysed (from initial 1.25 % solution), after adsorption onto montmorillonite materials (text in red indicates an increase in concentration of molecule after adsorption. The Substrate which gave the overall highest level of adsorption is highlighted in green and the substrate which gave the lowest level of adsorption is highlighted in red). Demonstrating the level of adsorption of each molecule which comprised greater than 1 % of the molecular make up of OO. 108

Table 3.5 Percentage reduction of the manuka oil (MO) components analysed (from initial 1.25 % solution), after adsorption onto layered silicate materials (text in red indicates an increase in concentration of molecule after adsorption. The substrate which gave the highest level of adsorption is highlighted in green, the substrate which gave the lowest level of adsorption is highlighted in red). Demonstrating the level of adsorption of each molecule which comprised greater than 1 % of the molecular make up of MO. 113

Table 3.6 Percentage reduction of the lavender oil molecules analysed (from initial 1.25 % (m/v) solution), after adsorption onto layered silicate materials (text in red indicates an increase in concentration of molecule after adsorption. The Substrate which gave the overall highest level of adsorption is highlighted in green and the substrate which gave the lowest level of adsorption is highlighted in red). Demonstrating the level of adsorption of each molecule which comprised greater than 1 % of the molecular make up of LO. 118

Table 3.7 Percentage reduction of the geranium oil (GO) molecules analysed (from initial 1.25 % solution), after adsorption onto the aluminosilicates (text in red indicates an increase in concentration of molecule after adsorption. The Substrate which gave the overall highest level of adsorption is highlighted in green and the substrate which gave the lowest level of adsorption is highlighted in red). Demonstrating the level of adsorption of each molecule which comprised greater than 1 % of the molecular make up of GO. 121

Chapter 4

Table 4.1 Constant values for; cation exchange capacity and percentage solids of the substrates, and median molecular weight of the modifiers. These values were used in Equation 4.1. 147

Chapter 5

Table 5.1 Masses required of silicone, substrate and EO to produce the SE samples for antimicrobial and controlled release analysis. 210

Table 5.2 Masses of paint, substrate and EO required for each paint formulation for antimicrobial and controlled release testing. 211

Table 5.3 Required masses of LLDPE, substrate and EO for each polymer formulation used in the antimicrobial assays, and controlled release studies. 212

List of Figures

Chapter 1

Figure 1.1	Structure of a Gram-positive bacterial cell wall. Demonstrating the thick peptidoglycan layer.	3
Figure 1.2	Structure of a Gram-negative bacterial cell wall. Demonstrationg the thin peptidoglycan layer and the outer membrane. The outer membrane acts as a barrier making Gram-negative cells often more resistant to bactericidal agents such as antibiotics, digestive enzymes and heavy metals.	4
Figure 1.3	Chemical structure of single isoprene unit.	5
Figure 1.4	Chemical structure of acyclic terpines (a) β-mycrene, (b) β-farnesene.	5
Figure 1.5	Chemical structure of cyclic terpines (a) limonene, (b) germacrene D.	5
Figure 1.6	Chemical structure of linalool.	5
Figure 1.7	Chemical structure of EO phenolic molecules (a) calamenene, (b) thymol.	6
Figure 1.8	Indus Valley distillation apparatus used to obtain oils from plant matter.	7
Figure 1.9	Schematic representation of smectite structure. Demonstrating how the stacking of the platelets creates the basal space.	10

Figure 1.10 Smectite silica sheet. Demonstrating the 3D structure of the silica tetrahedrons. 10

Figure 1.11 Smectite structure. Demonstrating the 3D structure of the tetrahedral silicate layers and the octahedral alumina sheets. As well as the gallery produced by stacking of the smectite platelets. 11

Chapter 2

Figure 2.1 96 Well Microtitre plate. Demonstrating the well layout. 26

Figure 2.2 Graphical representation of method described in 2.4.5, where each oil has had a starting concentration of 2.5 % (v/v). 28

Figure 2.3 MTP assay against *A. baumannii* columns 1-3 lavender oil, columns 5-7 geranium oil, columns 9-11 manuka oil, columns 4 and 8 are blank for spacing column 12 contains negative and positive controls. Demonstrating the use of TTC for rapid determination of MIC well, where the deep red colour indicated cell growth. 38

Figure 2.4 The major components of rosewood oil (RO) as determined by GC-MS. The numbers in red are the % composition of each component. The information on the x-axis is the retention times and chemical name of each component. Linalool was the major component of RO comprising 89.73 %. The graph uses a $\log_4$ scale where the x-axis crosses the y-axis at 1. A linear scale would result in the difference between the low percentage components being indistinguishable due to the size of the linalool bar. 58

Figure 2.5 Graph displaying the major components of oregano oil (OO) The numbers in red are the % composition of each component. The x-axis labels the retention times and chemical name of each component. Demonstrating which molecules comprised the majority of the oil. The graph uses a $\log_4$ scale where the x-axis crosses the y-axis at 1. A linear scale would result in the difference between the low percentage components being indistinguishable due to the size of the carvacrol bar. 59

Figure 2.6 Graph displaying the major components of lavender oil (LO) The numbers in red are the % composition of each component. The x-axis labels the retention times and chemical name of each component. Demonstrating which molecules comprised the majority of the oil. 632

Figure 2.7 Graph displaying the major components of geranium oil (GO) The numbers in red are the % composition of each component. The x-axis labels the retention times and chemical name of each component. Demonstrating which molecules comprised the majority of the oil. The graph uses a $\log_2$ scale where the x-axis crosses the y-axis at 1. A linear scale would result in the difference between the low percentage components being indistinguishable due to the size of the citronellol and geraniol bars. 63

Figure 2.8 Graph displaying the major components of manuka oil (MO) The numbers in red are the % composition of each component. The x-axis labels the retention times and chemical name of each component. Demonstrating which molecules comprised the majority of the oil. 64

Chapter 3

Figure 3.1	Representation of Lewis and Brønsted acid sites in the tetrahedral silicate layer of montmorillonite. Demonstrating where the acidity of MMTs originates from.	70
Figure 3.2	Schematic representation of MMT after acid treatment with alumina removed from the edges of the platelets exposing the inner silica surface.	71
Figure 3.3	Diagrammatical representation of drifts cell, (a) IR beam from source, (b) focusing mirrors, (c) sample, (d) refocused beam to detector.	74
Figure 3.4	Diffraction of x-rays within a crystalline structure, used to determine the distance between platelets of the layered silicates.	75
Figure 3.5	Diagram of FMC cell.	76
Figure 3.6	Typical FMC output measured by the thermistors showing: A_1) thermal response peaks evolved from a change in enthalpy; and A_2) thermal calibration peaks.	85
Figure 3.7	Differential refractometer plots showing the adsorbing probe, non-adsorbing probe, their overlay and subtraction plot resulting from subtraction of the non-adsorbing probe from the adsorbing probe data. The peak area of the subtraction plot (PA_e) is used in Equation 3.3. T_0 = start time, t_1 = syringe switch-over time and t_2 = as solute reaches differential refractometer.	87

Figure 3.8	FTIR spectra of dried MMT (a) Laponite® RD, (b) Laponite® B, (c) Fulcat® 435, (d) Fulcat® 400, (e) Fulacolor®, and (f) Fulcat® 800. Demonstrating the characteristic bond vibrations of each substrate.	89
Figure 3.9	FTIR spectra of EO (a) Manuka, (b) Oregano, (c) Rosewood, (d) Geranium, and (e) Lavender. Demonstrating the characteristic bond vibrations for each of the five oils.	90
Figure 3.10	Figure 3.10: (i) Extract from chromatograph of RO at 0.4 % (m/v), (ii) RO after adsorption onto F435, (iii) RO after adsorption onto LRD. For (i) and (iii) Paks assigned as follows: (a) limonene (b) eucalyptol (c) *trans*-linalool oxide (d) *cis*-linalool oxide (e) linalool (f) dodecane (internal standard) (g) α-terpineol. For (ii) peaks were assigned as (a) limonene (b) eucalyptol (c) *cis*-linalool oxide and (d) dodecane. Initial concentrations for (ii) and (iii) were 1.25 % m/v.	93
Figure 3.11	Calibration curve for α-terpineol fraction of RO demonstrating the relationship between oil concentration and the experimentally obtained peak area of molecules in the oils. The equation of the line fit was rearranged to give the concentration of x.	95
Figure 3.12	Conversion of linalool to α-terpineol (a) linalool (b) intermediate suggested by Bedoukian (c) α-terpineol.	97
Figure 3.13	Proposed mechanism for conversion of linalool to limonene under the acidified clay environment.	98
Figure 3.14	Chemical structure of eucalyptol. Demonstrating the double ring structure.	99

Figure 3.15 FTIR spectra of (a) Rosewood oil (RO) and (b) F400 after RO adsorption. Demonstrating the presence of RO peaks on the F400 spectra. 100

Figure 3.16 FTIR spectra of RO adsorbed onto (a) F400, (b) F435, (c) Fcol, displaying reduction of peak at approximately 1400 cm^{-1}. 101

Figure 3.17 FTIR spectrum of RO adsorbed onto LB, * central peak which was not observed on adsorption of RO onto natural and acid treated natural aluminosilicates (F400, Fcol and F435). 102

Figure 3.18 C–H stretching region in DRIFTS spectra for RO before and after adsorption (a) RO, (b) RO on LB, (c) RO on F800, and (d) RO on LRD. The vertical lines mark the centre of the peaks at 2858 cm^{-1}, 2925 cm^{-1} and 29700 cm^{-1} before adsorption, highlighting the shifts due to adsorption. 103

Figure 3.19 (a) *trans* conformation of linalool (CH_3 to R_2), (b) and (c) *gauche* conformations of linalool. Where R_1 is $CHCH_2$ and R_2 is $CH_2CHC(CH_3)_2$ 104

Figure 3.20 Peaks in the 1300 – 1500 cm^{-1} range for RO before and after adsorption (a) RO, (b) RO on LB, (c) RO on F800, and (d) RO on LRD. Demonstrating the presence of the central peak and the shift to higher wavenumbers for all three peaks (highlighted using dotted lines). 105

Figure 3.21 Demonstrating that there was no real difference in the adsorption performance of the three substrates when standard deviations were taken into account. 107

Figure 3.22	Chemical structure of β caryophyllene.	108
Figure 3.23	(a) α-caryophyllene (* donates carbon atoms that could undergo cyclisation to form β-caryophyllene) (b) caryophyllene oxide with ketone group that could be lost to form β-caryophyllene.	109
Figure 3.24	Levels of adsorption of OO onto layered silicate substrates estimated via GC. Demonstrating that LB provided the highest overall level of adsorption.	110
Figure 3.25	Peaks in the range 3000 to 2800 after adsorption of OO onto the aluminosilicates (a) OO, (b) F800 + OO, (c) LB + OO, and (d) LRD + OO. The vertical lines mark the centre of the peaks at 2869 cm^{-1}, 2938 cm^{-1} and 2960 cm^{-1} before adsorption, highlighting the shifts due to adsorption.	111
Figure 3.26	Chemical structure of (a) cadina-1,4-diene (b) *cis*-calamenene.	112
Figure 3.27	Levels of adsorption of MO onto layered silicate substrates estimated via GC. Demonstrating that there was little difference between the substrates in levels of adsorption when standard deviation was taken in to account.	114
Figure 3.28	Levels of adsorption of LO onto layered silicate substrates estimated via GC. LB gave the highest overall level of adsorption with F800 gave the lowest level of adsorption.	118
Figure 3.29	Levels of adsorption of GO onto layered silicate substrates estimated via GC. Demonstrating that LB gave the highest overall level of adsorption and F800 gave the lowest.	122

Figure 3.30 Extract from chromatograph obtained after extraction of F435 adsorbed rosewood oil (a) limonene peak (b) eucalyptol peak (c) *trans*-linalool oxide (d) *cis*-linalool oxide (e) dodecane (internal standard) (f) α-terpineol. Demonstrating the lack of a large linalool peak (normally seen 0.5 min after *cis*-linalool oxide in the extraction liquor of F435. 125

Figure 3.31 (a) Heat of adsorption and desorption of EO onto LRD in joules per gram of substrate (b) Mass of adsorption and desorption of EO onto LRD in milligrams per gram of substrate (c) Heat of adsorption and desorption of EO onto LRD in joules per gram of oil adsorbed. Demonstrating the overall level of adsorption achieved for each EO via FMC, and the strength of attachment of the EO molecules to the LRD surface. 128

Figure 3.32 (a) Heat of adsorption and desorption of EO onto LB in joules per gram of substrate (b) Mass of adsorption and desorption of EO onto LB in milligrams per gram of substrate (c) Heat of adsorption and desorption of EO onto LB in joules per gram of oil adsorbed. Demonstrating the overall level of adsorption achieved for each EO via FMC, and the strength of attachment of the EO molecules to the LB surface. 133

Figure 3.33 (a) Heat of adsorption and desorption of EO onto F800 in joules per gram of substrate. (b) Mass of adsorption and desorption of EO onto F800 in milligrams per gram of substrate. (c) Heat of adsorption and desorption of EO onto F800 in joules per gram of oil adsorbed. Demonstrating the overall level of adsorption achieved for each EO via FMC, and the strength of attachment of the EO molecules to the F800 surface. 136

Chapter 4

Figure 4.1	TGA trace of layered silicate before organic modification (a) Percentage mass loss plotted against time, (b) derivative of mass loss which aids the identification of the start and end of each stage of mass loss.	150
Figure 4.2	TGA trace of organically modified layered silicate (a) Percentage mass loss plotted against time, (b) derivative of mass loss which aids the identification of the start and end of each stage of mass loss.	151
Figure 4.3	The effect of OM of F800 with 2HT2M via the dry mix method on (a) N_2 BET surface area, (b) d-spacing of platelets, and (c) percentage mineral oil absorption. Demonstrating a reduction in oil absorption, an increase in d-spacing and a reduction in surface area as a result of OM.	155
Figure 4.4	The effect of OM of F800 with 2HT2M and CTAB via the wet mix method on (a) N_2 BET surface area, (b) d-spacing of platelets, and (c) percentage mineral oil absorption. Demonstrating how increasing the level of OM reduced surface area and oil adsorption, at 50% 2HT2M OM there was an increase in d-spacing of F800.	157
Figure 4.5	The effect of OM of LRD with 2HT2M via dry mix method on (a) N_2 BET surface area, (b) d-spacing of platelets, and (c) percentage mineral oil absorption. Demonstrating how increasing the level of OM affected the physical properties of the substrate.	161

Figure 4.6 The effect of OM of LB with 2HT2M via dry mix method on (a) N_2 BET surface area, (b) d-spacing of platelets, and (c) percentage mineral oil absorption. Demonstrating the reduced surface area of LB as a result of OM, and the increase in oil absorption and d-spacing. 163

Figure 4.7 Amount of organic modifier present on LB after modification with 2HT2M. The total length of the bar represents the overall surfactant level whilst the blue portion represents the level of bound surfactant and the red bar represents the level of unbound surfactant. An increase in both bound and unbound 2HT2M was observed with increasing OM. 165

Figure 4.8 Amount of organic modifier present on LRD after modification with 2HT2M. The total length of the bar represents the overall surfactant level whilst the blue portion represents the level of bound surfactant and the red bar represents the level of unbound surfactant. Demonstrating the increase in organic material with increasing OM. 166

Figure 4.9 Amount of organic modifier present on F800 after modification with 2HT2M via a dry mix method. The total length of the bar represents the overall surfactant level whilst the blue portion represents the level of bound surfactant and the red bar represents the level of unbound surfactant. Demonstrating the increase in organic material present of F800 with increasing OM. 167

Figure 4.10 Amount of organic modifier present on F800 after modification with 2HT2M via a wet mix method. Bound fraction represents 2HT2M molecules which were successfully underwent ion exchange. Unbound fraction represents 2HT2M molecules which did not undergo ion exchange but were adsorbed onto the surface of the platelets. Demonstrating the increase in organic material present of F800 with increasing OM. 169

Figure 4.11 Amount of organic modifier present on F800 after modification with CTAB via a wet mix method. Bound fraction represents CTAB molecules which were successfully underwent ion exchange. Unbound fraction represents CTAB molecules which did not undergo ion exchange but were adsorbed onto the surface of the platelets. Demonstrating the lack of change in organic level with increasing OM, which indicated that the amount of bound surfactant had reached a limiting level at 50 % OM. 170

Figure 4.12 DRIFTS spectra of LB organically modified (OM) with 2HT2M at (a) Unmodified, (b) 50 % CEC, (c) 75 % CEC, (d) 100 % CEC. Demonstrating the presence of C-H stretch vibrations in the range 2800-3000 cm^{-1} as a result of OM. 171

Figure 4.13 Data obtained from DRIFTS and XRD respectively plotted as a function of OM of LB (a) $A_{(C-H)S}/A_{(Si-O)}$, (b) d-spacing of platelets. Demonstrating the effect of increasing 2HT2M OM on the d-spacing of LB platelets, and the level of carbohydrate present on LB. 173

Figure 4.14 (a) surfactant alkyl tails arranged as a monolayer between platelets, (b) surfactant alkyl tails with vertical arrangement between platelets. 174

Figure 4.15 Data obtained from DRIFTS and XRD respectively plotted as a function of OM of LRD (a) $A_{(C-H)s}/A_{(Si-O)}$, (b) d-spacing of platelets. Demonstrating the increased d-spacing and carbohydrate level on LRD as a result of increasing 2HT2M OM. 175

Figure 4.16 FTIR spectra of F800 OM with CTAB at (a) Unmodified, (b) 50 % CEC, (c) 75 % CEC, (d) 100 % CEC. Demonstrating the presence of C-H stretch vibrations in the range 2800-3000 cm^{-1} as a result of OM. 176

Figure 4.17 Data obtained from DRIFTS and XRD respectively plotted as a function of OM of F800 with CTAB; (a) $A_{(C-H)s}/A_{(Si-O)}$, (b) d-spacing of platelets. Demonstrating the increase in carbohydrate level as a result of CTAB OM and the lack of effect OM had on the d-spacing of F800. 177

Figure 4.18 DRIFTS spectra of F800 OM with 2HT2M (wet) at (a) Unmodified, (b) 50 % CEC, (c) 75 % CEC, (d) 100 % CEC. Demonstrating the presence of C-H stretch vibrations in the range 2800-3000 cm^{-1} as a result of OM. 179

Figure 4.19 Data obtained from DRIFTS and XRD respectively plotted as a function of OM of F800 with 2HT2M using a wet mixing method and F800 with 2HT2M using a dry mixing method; (a) $A_{(C-H)s}/A_{(Si-O)}$, (b) d-spacing of platelets.
Demonstrating the effect of increasing 2HT2M OM on the d-spacing of F800 platelets, and the level of carbohydrate present on F800. 180

Figure 4.20	Comparison between mass of adsorption achieved for unmodified (UM) and CTAB modified F800. Demonstrating the decrease in adsorption at 50 % OM for RO and MO, followed by increased adsorption with increasing OM, OO adsorption was increased at all three levels of OM over UM.	183
Figure 4.21	Comparison between mass of adsorption achieved for UM and 2HT2M modified (wet method) F800. Demonstrating the reduction in adsorption of RO and MO at 50% OM, OO adsorption was unaffected by OM.	185
Figure 4.22	Comparison between mass of adsorption achieved for UM and 2HT2M modified (dry method) F800. Demonstrating that overall OM resulted in a decrease in the adsorption of the three EO.	186
Figure 4.23	Comparison between mass of adsorption onto UM and 2HT2M modified LRD. Demonstrating the general pattern for a reduction in adsorption of EO with 50 % OM in comparison to the unmodified LRD. Followed by an increase in adsorption with increasing OM.	187
Figure 4.24	Figure 4.24: Comparison between mass of adsorption onto unmodified and 2HT2M modified LB. Demonstrating the initial reduction in adsorption as a result of 50 % OM followed by a gradual increase with increasing OM.	188

Figure 4.25 Effect of OM of F800 with 2HT2M using a dry mixing method on adsorption, comparison between unmodified (0 %) and modified at 50 % and 75 % CEC (a) Enthalpy of adsorption and desorption in joules per gram of substrate. (b) Mass of adsorption and desorption in milligrams per gram of substrate. B – Blockage of cell due to gel formation therefore data not obtained. Demonstrating the reduction in the mass of EO adsorbed as a result of OM in comparison to unmodified F800. 192

Figure 4.26 Effect of OM of F800 with CTAB using wet mixing method on adsorption, comparison between unmodified (0 %) and modified at 50 % and 75 % CEC (a) Enthalpy of adsorption and desorption in joules per gram of substrate. (b) Mass of adsorption and desorption in milligrams per gram of substrate. Demonstrating a reduction in mass of OO and RO adsorbed at 50 % OM, followed by an increase in mass adsorbed at 75 %. 193

Figure 4.27 Effect of OM of LRD with 2HT2M on adsorption, comparison between unmodified (0 %) and modified at 50 % and 75 % CEC (a) Enthalpy of adsorption and desorption in joules per gram of substrate. (b) Mass of adsorption and desorption in milligrams per gram of substrate. Demonstrating the reduction in mass of adsorption, and increase in strength of adsorption, as a result of organic modification. 196

Figure 4.28 Effect of OM of LB with 2HT2M on adsorption. Comparison between unmodified (0 %) and modified at 50 % and 75 % CEC (a) Enthalpy of adsorption and desorption in joules per gram of substrate. (b) Mass of adsorption and desorption in milligrams per gram of substrate. Demonstrating a decrease in mass of adsorption as a result of OM in most cases, coupled to weaker strength of adsorption. 199

Chapter 5

Figure 5.1 Skeletal representation of polyethylene (PE) showing one repeating unit. 203

Figure 5.2 Reaction scheme for an RTV-2 SE addition cure system, demonstrating cross linking of polymer chains via a catalyst to create the solid polymer matrix. 205

Figure 5.3 Flexural test data for LLDPE samples ahowing the affect of addition of organically modified LRD with and without EO on flexural modulus. Demonstrating the increased stiffness of the LLDPE as a result of organic modification; explained by the increased interaction between the LRD platelets and the polymer matrix. 219

Figure 5.4 WAXS data for (a) LRD, (b) LRD50, and (c) EO-LRD50. Showing the effect of OM and EO adsorption on the position and shape of the (001) reflection (*) and (110) reflection (**). Demonstrating the increased d-spacing as a result of organic modification, resulting in the (001) reflection shifting to lower angles. 221

Figure 5.5 WAXS data for (a) LRD, (b) LRD100, and (c) EO-LRD100. Showing the effect of OM and EO adsorption on the position and shape of the (001) reflection (*) and (110) reflection (**). Demonstrating the increase in d-spacing of LRD with organic modification, and the further increase as a result of EO adsorption, as the (001) reflection shifts to lower angles. 222

Figure 5.6 WAXS data for LLDPE based composites containing 10 % (m/m) of (a) LRD50, (b) LRD50+EO, (c) LRD100, (d) LRD100+EO, (e) 3.3 % (m/m) EO. Demonstrating the increased d-spacing of the Laponite® as a result of interaction with the polymer matrix. 223

Figure 5.7 Antimicrobial testing of SE against MRSA, demonstrating the successful conferment of antimicrobial activity to the SE after addition of the EO antimicrobial. The graph also highlights the increased efficacy obtained by adsorbing the EO onto LRD. LRD50 = Laponite® RD 50 % CEC 2HT2M, LRD50 + EO = Laponite® RD 50 % CEC 2HT2M with EO blend adsorbed, LRD100 + EO = Laponite® RD 100 % CEC 2HT2M with EO blend adsorbed. 228

Figure 5.8 Antimicrobial testing of SE against *A. baumannii*. LRD50 = Laponite® RD 50 % CEC 2HT2M, LRD50 + EO = Laponite® RD 50 % CEC 2HT2M with EO blend adsorbed, LRD100 + EO = Laponite® RD 100 % CEC 2HT2M with EO blend adsorbed. Demonstrating the antimicrobial effect of adding EO's to SE, and the improvement in efficacy obtained by adsorbing the EO's onto an organically modified substrate prior to addition. 230

Figure 5.9 Antimicrobial testing of paint samples against MRSA. LRD50 = Laponite® RD 50 % CEC 2HT2M, LRD50 + EO = Laponite® RD 50 % CEC 2HT2M with EO blend adsorbed, LRD100 + EO = Laponite® RD 100 % CEC 2HT2M with EO blend adsorbed. 233

Figure 5.10 Antimicrobial testing of LLDPE samples against MRSA. LRD50 = Laponite® RD 50 % CEC 2HT2M, LRD50 + EO = Laponite® RD 50 % CEC 2HT2M with EO blend adsorbed, LRD100 + EO = Laponite® RD 100 % CEC 2HT2M with EO blend adsorbed. Demonstrating the antimicrobial activity of LLDPE when treated with the EO blend, and the reduction in efficacy caused by adsorption of the EO onto LRD50 before addition to LLDPE. 235

Figure 5.11 Antimicrobial testing of LLDPE samples against *A. baumannii*. LRD50 = Laponite® RD 50 % CEC 2HT2M, LRD50 + EO = Laponite® RD 50 % CEC 2HT2M with EO blend adsorbed, LRD100 + EO = Laponite® RD 100 % CEC 2HT2M with EO blend adsorbed. Demonstrating the antimicrobial effect obtained when EO's are added to LLDPE and the reduction in efficacy caused by adsorption onto LRD50 prior to addition. 237

Figure 5.12 EO molecules detected from SE + EO samples after heating to 50 ℃. Displaying the lack of retention of EO antimicrobial when added directly to the SE matrix. Inset full scale displaying data for cavacrol at 0 days. 241

Figure 5.13 EO molecules detected from SE + (LRD50 + EO) samples after heating to 50 ℃. Displaying the impr oved retention of carvacrol n provided by adsorption of the EO antimicrobial to LRD50. Inset full scale showing data for carvacrol at 0 days. 242

Figure 5.14 Positive control sample results for paint samples containing EO, showing level of EO molecules determined via headspace. Demonstrating the difference in EO molecule levels between samples containing the EO antimicrobial free within the paint, and samples where the EO antimicrobial was adsorbed onto LRD50. 243

Figure 5.15 EO molecules detected from LLDPE + EO samples after heating to 50 ℃. Demonstrating the level of EO molecule retention achieved when the EO blend is added free into the polymer matrix. Inset at full scale showing complete linalool and carvacrol bars at day 0. 245

Figure 5.16 EO molecules detected from LLDPE + (LRD50-EO) samples after heating to 50 ℃, demonstrating the improved level of retention of EO molecules after heating, in comparison to LLDPE + EO (Figure 5.15). Inset displays full scale for day 0 carvacrol data. 247

CHAPTER 1

Introduction

The primary objective of this thesis was to investigate the potential for the use of natural antimicrobials to confer antimicrobial properties to polymer materials. It was envisaged that any antimicrobial polymers successfully produced could be used in healthcare environments as an aide to combating the spread of healthcare associated infections. Polymers produced may also have applications in other areas such as paints and sealants for bathrooms which resist the build up of mould. The potential for layered silicate materials to be used as reservoirs for the antimicrobial to prolong retention within polymer materials was also investigated.

1.1 Healthcare associated infections

Healthcare associated infections (HCAI) are defined by the Centers for Disease Control (CDC) as infections that are acquired in the healthcare facility where there is no evidence that the infection was present, or incubating, at the time of admission. There are thirteen main categories of HCAI: Surgical wound infections, primary bloodstream infections, pneumonia, urinary tract infections, bone and joint infections, cardiovascular system infections, central nervous system infections, eye, ear, nose, throat, and mouth infections, gastrointestinal system infections, lower respiratory tract infections, reproductive tract infections, skin and soft tissue infections, and systemic infections [1]. HCAI are a significant problem facing the healthcare industry world-wide. Recent data from the Healthcare Protection Agency (HPA) for England and Wales reported approximately 23,000 cases of HCAI caused by either MRSA or *Clostridium difficile* in the period between April 2010 and March 2011 [2, 3], and in 2008 there were approximately 4000 cases of *Pseudomonas spp.* infection [4]. In addition in the period from April 2006 and March 2011 there were 6326 surgical site infections (SSI) reported by NHS hospitals in England [5]. In 2010 a study of 506 patients admitted to the Acute Medical Department at Odense University Hospital in Denmark found that approximately 11 % of patients acquired an

HCAI [6]. A report published in 2007 by the CDC estimated, from data supplied by The National Nosocomial Infections Surveillance System, the National Hospital Discharge Survey and the American Hospital Association Survey, that in 2002 1.7 million patients across the United States of America contracted an HCAI [7].

HCAI incur huge costs both economically (to patient and healthcare facility), and sociologically: Plowman *et al.,* reported in 2001, that in the UK an HCAI resulted in a length of stay that was on average approximately three times longer than that of a patient with no HCAI (ranging from an extra 2 days for blood stream infections, to 38 days for patients with multiple infections). HCAI lead to an average increased treatment cost of over £3000 (£1300 for urinary tract infections to £9100 for multiple infections). The total national burden due to HCAI being estimated at £930 million [8]. A more recent study conducted in 2005 by Coello *et al.* (2005), used data from Nosocomial Infection National Surveillance Service (NINSS) to calculate that the additional cost of a SSI ranged from £959 to £6103, and contraction of an HCAI resulted in an increased length of stay ranging from 3 to 21 days depending on type of surgery [9]. In the USA, Kilgore *et al.* (2008), studied over 1 million hospital admissions and found that on average the increase in length of stay was 5.74 days at an extra cost of $7826 [10].

Sanchez-Velazquez *et al.* (2006), explored the effect of acquiring a HCAI on organ failure and mortality rates. Cardiovascular, respiratory, haematological, renal, neurological and hepatic organ failures were studied: with the exception of renal and haematological failures, the presence of a HCAI caused an increase in frequency and length of organ failure. With respect to mortality, they found a 11.7 % increase in hospital patients with a HCAI, and a 16.3 % increase in intensive care unit patients with a HCAI [11].

1.2 Microbiology and the structure of bacterial cells

Bacteria are unicellular organisms that are too small to be seen with the human eye (cell diameter range approximately 0.5 µm - 20 µm), and therefore fall under the classification of microorganisms. Bacterial cells are prokaryotic meaning that there is no nuclear membrane surrounding the genetic information

of the cell. There are three main shapes of bacterial cell, *bacillus* (rod shaped), *coccus* (spherical or oval in shape) and *spiral* which have a curved or corkscrew appearance. All bacterial cells have an inner phospholipids bi layer membrane encased in a peptidoglycan cell wall and they reproduce by binary fission (where a cell will divide into two equal cells) [12]. Bacteria are separated into two groups differentiated by their reaction to specific dyes. In 1884 the Danish scientist Hans Christian Gram discovered that certain bacterial cells retained a purple dye when washed with alcohol, whilst in others the dye was washed away. Bacteria which retain the dye are referred to as Gram-positive and bacteria which do not retain the dye are referred to as Gram-negative, the difference between the two types of bacteria lies in the make-up of the cell wall.
Gram-positive bacteria have a rigid cell wall which ranges between 30nm - 100 nm thick. Its composition is primarily peptidoglycan (Figure 1.1). The peptidoglycan grows with new layers being formed on the inside of the cell wall, next to the cell membrane, with the oldest layers at the outer edge. Gram positive cell walls also contain teicholic acids which provide rigidity, and act as cell growth regulators [13].

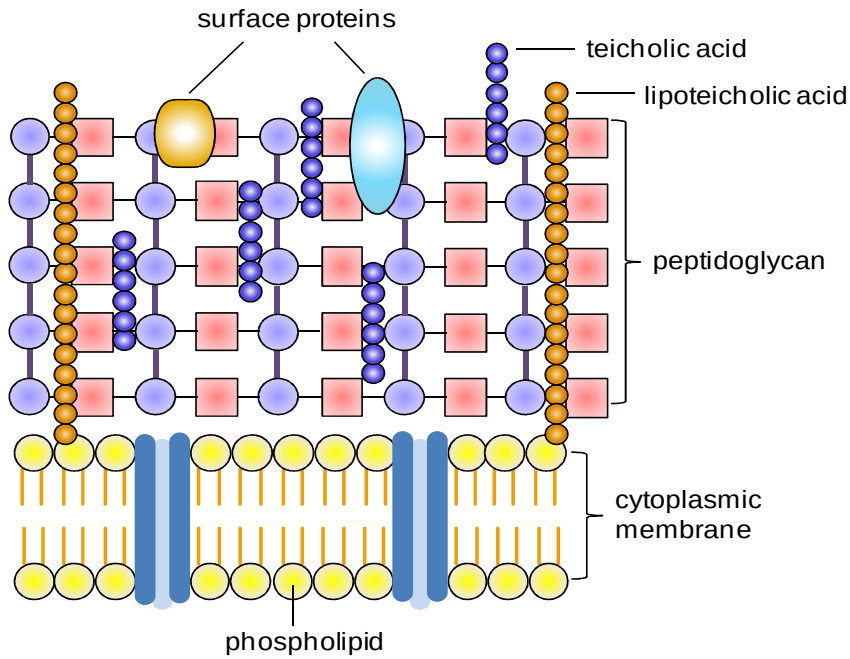

Figure 1.1: Structure of a Gram-positive bacterial cell wall. Demonstrating the thick peptidoglycan layer and teicholic acids [14].

Gram-negative bacteria in contrast have a thin peptidoglycan layer which in some cases may be a monolayer (thus causing cell wall to be more susceptible

to rupture than in Gram-positive bacteria). Surrounding the peptidoglycan layer is an outer membrane (Figure 1.2), and in-between the peptidoglycan layer and the cell membrane is the periplasmic gel. The outer membrane is a lipid bi-layer, comprising of a phospholipid internal layer and a lipopolysacharide outer layer.

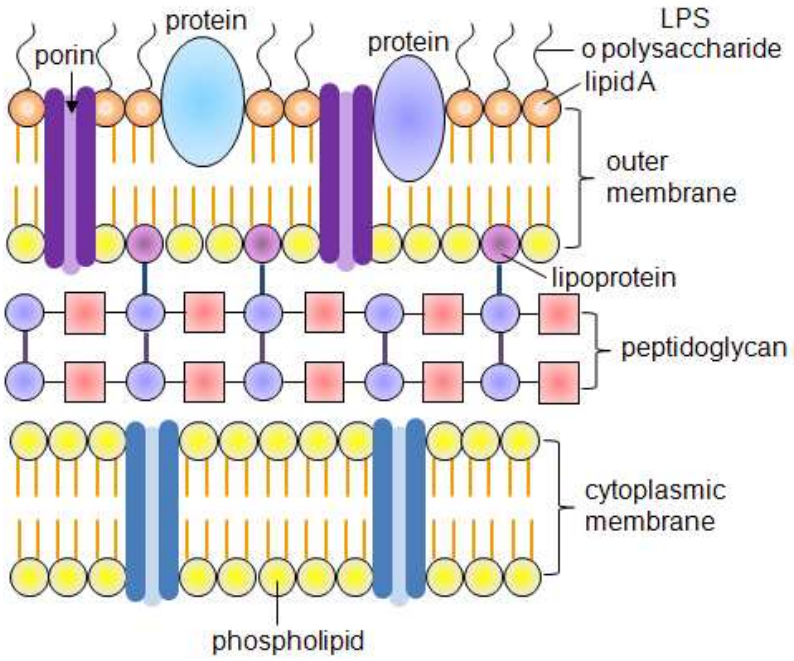

Figure 1.2: Structure of a Gram-negative bacterial cell wall [15]. Demonstrationg the thin peptidoglycan layer and the outer membrane. The outer membrane acts as a barrier making Gram-negative cells often more resistant to bactericidal agents such as antibiotics, digestive enzymes and heavy metals[12, 13].

The bacteria used in this study are discussed in detail in Section 2.1.2.

1.3 Chemical makeup of essential oils and their historical uses

Essential oils (EO) are volatile oils responsible for many of the fragrances produced by plants. They can be extracted from the plant material by a variety of different methods, including supercritical CO_2 extraction, hydro and steam distillation and solvent extraction [16]. EO are a complex mixture of chemicals, for example lavender oil contains around 60 different chemicals [17].
The majority of the chemicals that make up EO are based around repeating isoprene (Figure 1.3) units and are called terpenes.

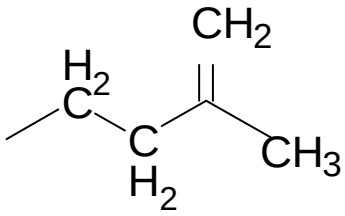

Figure 1.3: Chemical structure of single isoprene unit.

The majority of terpenes found in EO are either monoterpenes (two isoprene units) or sesquiterpines (three isoprene units), and they can arrange as either straight chain (Figure 1.4), or cyclic molecules (Figure 1.5) [18].

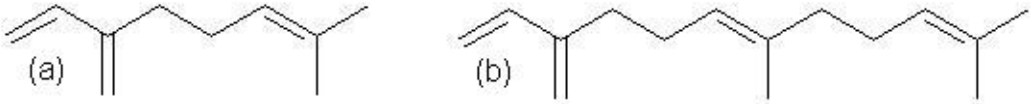

Figure 1.4: Chemical structure of acyclic terpines (a) β-mycrene, (b) β-farnesene.

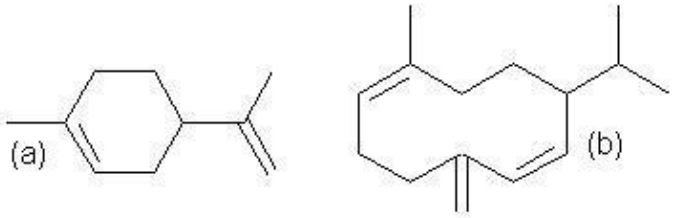

Figure 1.5: Chemical structure of cyclic terpines (a) limonene, (b) germacrene D.

As well as the basic terpenes, there are many examples with functional groups such as oxygen (alcohols, ketones, aldehydes, and esters), nitrogen and in rare cases sulphur, one of the more common of these being linalool (Figure 1.6).

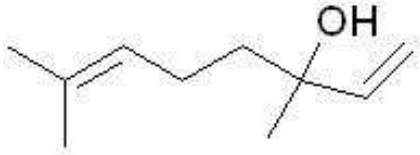

Figure 1.6: Chemical structure of linalool.

As well as terpene compounds there are also a variety of different phenol compounds, such as calamenene in manuka oil and thymol in oregano oil (Figure 1.7).

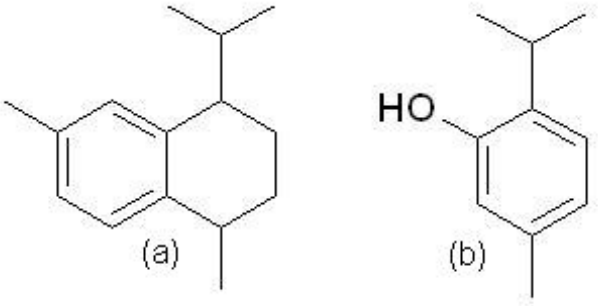

Figure 1.7: Chemical structure of EO phenolic molecules (a) calamenene, (b) thymol.

There is anecdotal evidence of EO being used throughout history for their healing properties, as well as their fragrances. Adams et al. (2009), studied European documentation from the 16th to 18th centuries and found over 60 different plant and herbal remedies (many of which using plant extracts) that were used to treat rheumatic disorders, some of which dated back as far as ancient Greece. Modern studies of many of the oils obtained from the plants used in the traditional remedies have shown some anti-inflammatory effect, giving support to the traditional uses [19]. An archaeological expedition to Pakistan in the 1970s found a vessel (Figure 1.8) for producing fragrant waters which was designed to collect and condense the vapours produced from boiling plant material dating back approximately 5000 years to the Indus Valley civilisation [17].

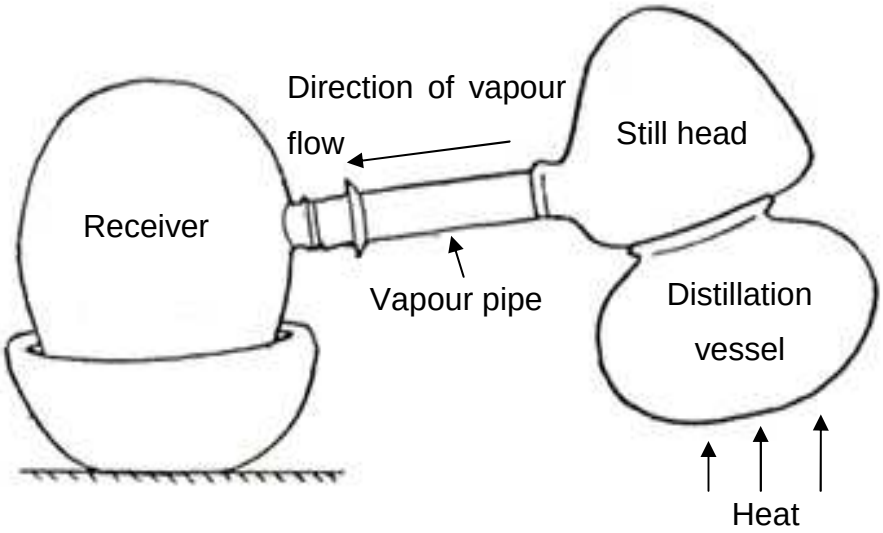

Figure 1.8: Indus Valley distillation apparatus used to obtain oils from plant matter [17].

Up until the middle of the 20th century much of the scientific literature on EO concentrated on analysis and exploration of their constituent components. Since then scientists have become increasingly interested in the effects of EO on organisms. Studies have focused on a wide range of applications, for example Yoon *et al.* (2009), have shown that a variety of citrus based essential oils have a repellent effect on cockroaches [20]. Whilst Lis-Balchin *et al.* (1997), have studied the effect of a number of different EO on smooth and skeletal muscle: in skeletal muscle they found that depending on which oil they used, the twitch response of a rats diaphragm could be either increased or decreased, or they could induce muscle contracture with and without inhibition of the twitch response. In smooth muscle they found that certain oils caused a spasmogenic response whilst others caused the same response followed by a reduction in field-stimulated contractions [17]. The health benefits of EO have also been investigated; Melo *et al*. (2011), investigated the effect of carvacrol (a constituent of oregano oil) on mice during stress tests. They found that it had a similar effect on the immobility of mice as a well known antidepressant drug, suggesting carvacrol has antidepressant like properties [21]. EO of *Juniperus* has been found to aid the speed of wound healing; the presence of chemicals with anti-inflammatory and antioxidant properties may be responsible for this activity [22].

The antimicrobial activities of EOs are well known and are discussed in Chapter 2.

1.3.1 Controlled release of essential oils to prolong their effects

The antimicrobial activity of EO could potentially be utilised to help reduce the numbers of pathogenic microbes in healthcare environments if they were applied to or incorporated into surfaces. As the oils are volatile, direct application would be ineffective as they would evaporate and lose their activity relatively rapidly. Chao *et al.* (2005), showed that after 60 minutes, activity against airborne microbes was dramatically reduced [23]. Encapsulation of the EO and provision of a controlled release mechanism would extend the length of time over which they were effective. Research into the encapsulation of EO focuses on using organic media. Maji *et al.* (2007), used gelatin to encapsulate *Zanthoxylum limonella* oil: the gelatin surrounded the oil in coacervates which were then cross linked using gluteraldehyde. They were able to achieve a maximum encapsulation efficiency of 98 % by varying the proportions of the three components, with a release rate of 60 % of the oil over 70 hours. The best release rate obtained was 90 % oil release over 70 hours, with an encapsulation efficiency of 78 % [24].

Parris *et al.* (2005), demonstrated the ability of zein nanospheres to encapsulate oregano, red thyme, and cassia oils. This was achieved by adding the oil and zien to 85 % ethanol and dispersing with high speed mixing into water containing 0.01 % silicone fluid. The solution containing the encapsulated oil particles was lyophilized to obtain a dry powder. Release rates in phosphate buffered saline (PBS), and PBS with 24 % ethanol, ranged from 60-80 % over 50 hours depending on the EO [25]. Kiawchaoon and Yoksan (2011) encapsulated carvacrol within chitosan-nano particles and achieved controlled release rates of 23 % over 30 days in pH 7 solution [26]. Paula *et al*. (2011), also investigated the encapsulation of EO in chitosan. Using chitosan beads and chitosan-cashew gum beads, they found that addition of the cashew gum significantly increased the level of controlled release with 37 % released over 24 h relative to 67 % for the chitosan beads on their own [27].

In most of the cases discussed above the rate of release of the EOs was over a number of hours. This time scale for the release of the EOs would not be suitable for an antimicrobial polymer containing EOs as the antimicrobial activity would only last a matter of days. The chitosan nano particles did show prolonged controlled release with less than 25% lost over a period of 30 days.

The controlled release materials used in this project would need to achieve similar or better levels of controlled release in order for a long lasting antimicrobial polymer to be produced.

The above encapsulation methods could be used to create sprays to treat surfaces; however regular applications would be required to maintain efficiency. Incorporation of organic encapsulated EO into a thermoplastic would be problematic due to the fragility of the organic capsule towards the high temperature (typically 200 to 300 ℃) and high shear encountered during melt processing of such materials. Organic encapsulation media may also respond poorly to being in organic media such as paint solvents and binders.

An inorganic encapsulation media would be preferable as it would give added stability and could potentially withstand the processing temperatures of common thermoplastics. Furthermore, an inorganic encapsulation approach will be more resistant to solvents found in paint formulations. There has been little reported in literature on the adsorption of EO onto inorganic media for encapsulation and controlled release. Giménez *et al.* (2012), have shown that the use of sepiolite results in controlled release of clove oil from gelatin-egg white films. This was achieved by *in situ* addition of clove oil and sepiolite during the formation of the films, resulting in an improvement of antimicrobial and antioxidant activity with respect to films containing clove oil only [28].

1.4 Physical and chemical structure of smectite minerals

Smectites are natural hydrous aluminium silicate clays with a general Si to Al ratio of 2:1. They are made up of repeating layers of an octahedral sheet (alumina) with a silica sheet on either side. The layers formed are continuous in the a and b directions and stacked one above the other in the c direction [29] (Figure 1.9). Smectites characteristically swell when immersed in water or any other liquid with polar molecules.

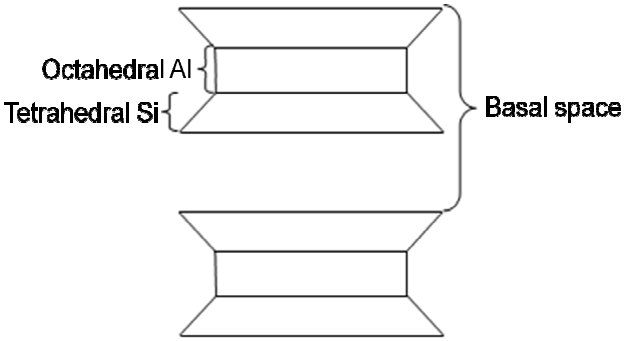

Figure 1.9: Schematic representation of smectite structure. Demonstrating how the stacking of the platelets creates the basal space.

The silica sheets are made up of tetrahedral units where each silicon atom is surrounded by 4 oxygen atoms; with the apex of each tetrahedron pointing towards the central alumina sheet (Figure 1.10).

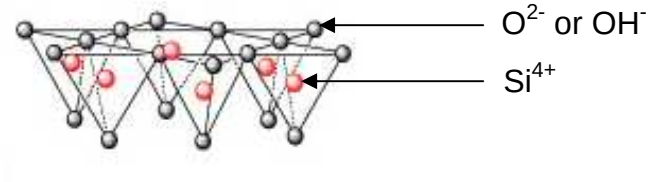

Figure 1.10: Smectite silica sheet [30]. Demonstrating the 3D structure of the silica tetrahedrons.

The octahedral alumina sheets share the oxygen atoms at the tip of the tetrahedra. Hydroxyl ions sit in between the oxygen atoms at the apex of the tetrahedra to balance the charge on the structure, giving a theoretical composition of $(OH)_4Si_8Al_4O_{20}.nH_2O$.

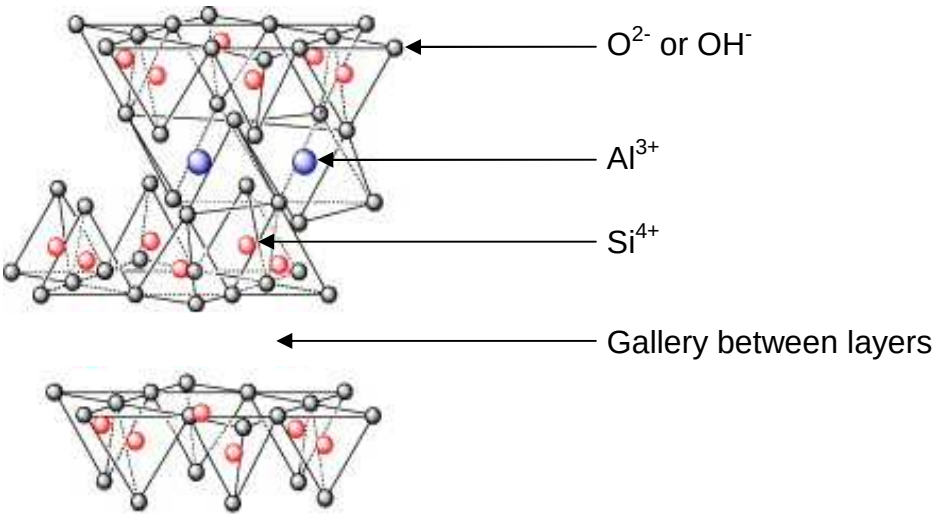

Figure 1.11: Smectite structure [30]. Demonstrating the 3D structure of the tetrahedral silicate layers and the octahedral alumina sheets. As well as the gallery produced by stacking of the smectite platelets.

Between each layer of the mineral structure, there are small gaps or galleries (Figure 1.11). Small molecules can be adsorbed into the galleries. When the galleries are empty the distance between the bottom of one mineral sheet and the bottom of the sheet below (basal spacing) is 0.96 nm. When molecules (for example water) are adsorbed into the spaces the basal spacing increases and the material swells. This property makes it attractive as a potential encapsulation medium for the EO.

In smectites, the metallic ions Al^{3+} and Si^{4+} can be partially replaced by other ions in the soil. In the tetrahedral sheet up to 15 % of the Si^{4+} ions can be replaced by Al^{3+} ions. In the octahedral sheet the Al^{3+} ions can be replaced by a number of different cations each one giving rise to a different smectite mineral. Saponite is the term used to describe minerals where the octahedral Al^{3+} is completely replaced by Mg^{2+}, and a proportion of the tetrahedral Si^{4+} is replaced by Al^{3+} [31]. Nontronite is a ferric iron silicate where the octahedral Al^{3+} is replaced by Fe^{3+}, as with saponite a small amount of Si^{4+} is replaced by Al^{3+} [23]. Hectorite contains no Al^{3+} in its structure with the octahedral layer being predominantly composed of Mg^{2+} with the charge on the structure resulting from small quantities of Li^+ giving the overall structure $[Li_{0.67}Mg_{5.34}Si_8O_{20}(OH)_4]^{0.67}$ [32]. In each of these minerals there is an overall negative charge within the layers, as a result of the replacement of some Si^{4+} with metal ions of lower

charge, which is balanced by cations held within the galleries between the layers (usually Na^+).

The sodium ions in the structure are important because they can undergo ion exchange. This allows the tailoring of the properties of the galleries of the material to specific needs. For example, in their natural form the galleries of smectites are polar and will readily adsorb other polar materials such as water. However, the high polarity is undesirable for the adsorption of organic material. By replacing the sodium ions with quaternary ammonium cations (which have one or more long aliphatic tail) the galleries of the substrate can be made more hydrophobic and therefore more receptive to organic material.

Smectite materials have found a range of different uses including acid catalysis, molecular sieves, sorption of heavy metal waste, and the modification of polymer properties such as tensile strength and flame retardancy [33-36]. The use of smectite minerals for adsorption of organic molecules (such as those found in EO) is widely reported in literature, detailed examples are given in Chapter 3 Section 3.1.2.

1.5 Thesis methodology

This project was broken down into a number of key areas to enable the fulfilment of the primary aims.

The first stage of the project was to identify a suitable antimicrobial agent which displayed activity against a number of different bacteria. Essential oils (EO) were initially tested individually against selected bacteria, however it was found that none of the EO provided suitable activity.

The next stage was to analyse blends of EO; from this work seven blends were identified which provided suitable antimicrobial activity. The effect of adding synthetic biocides to the EO blends was also investigated in order to determine whether the antimicrobial activity could be further increased.

The final stage of this work, presented in Chapter 2, was to analyse the chemical composition of the EOs used, in order to identify the more active

molecules, in an antimicrobial context, in the EO. In addition, awareness of the EO composition enabled prediction of the adsorption characteristics of the EO components on to the inorganic layered silicate substrates.

Having selected a suitable antimicrobial, the next stage, (Chapter 3), focused on the most suitable way in which to add the antimicrobial to the polymer materials, in order to promote sustained antimicrobial activity. The high volatility of EOs precludes addition of free EO to polymers, as the molecular components would evaporate out of the material too rapidly. It was hypothesised that encapsulation of the EOs within a material before addition to polymers could provide controlled release, thereby preventing rapid loss of antimicrobial activity. As polymer melt processing techniques can involve harsh conditions (i.e. high temperature and pressure), inorganic encapsulation media were selected as they would afford greater protection to the EO than organic media such as yeast cells. Six layered silicate substrates were selected, from the Rockwood Additives product portfolio, as potential encapsulation materials. In order to assess the suitability of the substrates as encapsulation materials, solution adsorption studies were carried out using gas chromatography (GC) and flow micro-calorimetry (FMC). The GC study provided information relating to; how adsorption onto the substrates affected the individual EO molecules, which EO molecules were adsorbed to the highest levels, and estimation of the overall adsorption levels. The FMC data provided information relating to; the strength of adsorption of the EOs onto the substrates and the overall level of adsorption achieved.

The adsorption results obtained suggested that three of the layered silicates showed potential as adsorption substrates for the EO based antimicrobials. The layered silicates were hydrophilic and it was proposed that this may hinder the adsorption of EOs as they are comprised mainly of molecules with dominant hydrocarbon (i.e. hydrophobic) character. Organic modification (OM) of the three selected layered silicates was undertaken. The organic modifiers were quaternary ammonium compounds featuring long alkyl chains, which were expected to increase the organophilic character of the substrates. EO adsorption on to the OM substrates was then assessed, using the same methods employed in Chapter 3; thus it was possible to determine what effect

OM had on the mass of EO adsorbed and the strength of attachment of the EO molecules to the layered silicates. Using the data obtained, the substrate which provided the best adsorption properties was selected for use as the encapsulation medium for the EO antimicrobial. This work is presented in Chapter 4.

The final stage of the project (Chapter 5) was to incorporate the EO antimicrobial into polymer materials. This was done using a room temperature curing silicone elastomer, a thermoplastic and a solvent based paint; samples of each polymer containing either the EO antimicrobial (identified in Chapter 2) free within the polymer, or the EO antimicrobial pre-adsorbed onto the best performing layered silicate (identified in Chapter 4). The antimicrobial efficacy of the EO treated polymers against the same bacteria used in Chapter 2 was assessed, in order to determine; (a) whether the antimicrobial properties of the EOs could be conferred to the polymers, and (b) whether the antimicrobial properties of the EOs were affected by adsorption onto the layered silicates. The retention of the molecular components of the EO antimicrobial within the polymer materials was assessed using headspace gas chromatography. This was done in order to investigate the effect of adsorption of the EO antimicrobial onto the layered silicate on the release of the molecular components of the EO from the polymers. In addition this work aided the understanding of the differences in antimicrobial efficacy between the polymers containing free EO and the polymers containing pre-adsorbed EO. Insight in to the mechanism of controlled release was acquired by studying the dispersion of the layered silicate platelets in the thermoplastic.

CHAPTER 2

Antimicrobial screening of essential oils and biocides

Abstract

Essential oils (EO) have been widely studied for their antimicrobial activity; this study assesses the use of EOs as a broad spectrum antimicrobial for combating healthcare associated infection (HCAI) pathogens. Manuka (MO), oregano (OO), rosewood (RO), lavender (LO) and geranium (GO) oils were examined, as individual oils and oil blends, against methicillin resistant *Staphylococcus aureus*, *Pseudomonas aeruginosa*, and *Acinetobacter baumannii* for antimicrobial efficacy using micro broth dilution and checkerboard micro broth dilution methods. Individually manuka oil and oregano oil gave the highest level of antimicrobial performance; however none of the oils were effective against all three bacteria at the required concentrations. A blend of oregano oil and rosewood oil in a 3:1 ratio gave the highest level of antimicrobial performance at a combined minimum inhibitory concentration (MIC) of less than 0.6 %. The addition of synthetic biocides and antibiotics to the EO blends to increase antimicrobial activity was studied; and the addition of polyhexamethylene biguanide (PHMB) was found to have a beneficial effect, reducing both the concentration of EO blend and of PHMB required for inhibition of growth. Gas chromatography-mass spectrometry (GC-MS) was used to identify the molecular components of the oils and provide insight into the antimicrobial activity achieved.

2.1 Introduction

The first stage of this study was to select a range of essential oils (EO) and EO blends which had broad spectrum antimicrobial activity.

2.1.1 Antimicrobial activity of essential oils

Certain EO have been shown to inhibit the growth of pathogenic microbes, including some of the more common HCAI causing bacteria.

In 1999, Hammer *et al*., looked at the effects of 52 different EO and plant extracts on pathogenic bacteria, finding that only six oils within the set showed no inhibition of the test bacteria at the highest concentration (2 % (v/v)). Vetiver oil inhibited *Staphylococcus aureus* at a concentration of 0.008 % (v/v), and lemongrass, oregano, and bay oils inhibited all 10 bacteria tested [37]. The antimicrobial effects of EO are not limited to bacteria; El-Mougy *et al.* (2009), studied the effect of carnation, caraway, and thyme oils against *Alternaria solani* a fungus responsible for early blight in potatoes. In lab tests it was found that carnation oil at concentrations of 1 % (v/v) completely inhibited growth of the fungus, while caraway and thyme caused an 80 % reduction in growth at the same concentration. The oils were also tested under field conditions; when applied as a spray to a potato crop they reduced the incidence of early blight by approximately 30 %. A commercially available fungicide (Ridomil MZ 72 WP) gave only a 14 % reduction [16].

Many EOs are only toxic to certain groups of microbes, for example myrrh will inhibit the growth of *Staphylococcus aureus* at 0.5 % concentration, however, a fourfold increase in concentration has no significant effect on the growth of *Candida albicans* and *Pseudomonas aeruginosa* [37]. Blends of EO have been shown to exhibit synergistic biocidal activity against certain microbes. Synergism denotes that the activity of the EO combination is greater than the summed activity of the individual oils. Edwards-Jones *et al.* (2004), found when combining tea-tree oil with, patchouli, lavender, geranium or Citricidal™ oils, the inhibitory effects against *Staphylococcus aureus* (Oxford) were almost doubled, relative to the individual oils [38].

The mechanisms for the antimicrobial activity are not yet completely understood. It has been shown that lipophilic compounds (such as the hydrocarbon molecules of EOs) can build up in the cell membrane of the bacterial cells [39]. As a result the membrane is weakened and the integrity of the cell membrane breaks down resulting in cell lysis [40]. Certain EO molecules such as carvacrol have also been shown to have a destabilising effect on the outer lipopolysaccharide membrane of Gram negative bacteria [41]. The oxygenated terpene based molecules have been shown to contribute the majority of this antimicrobial activity [42]. However, nonoxygenated compounds such as β-pinene have been shown to inhibit the respiration of

microbial cells via disruption of the electron transport chain within mitochondria [43]. Therefore, the antimicrobial activity of Eos is likely to be a combination of effects as a result of the complex molecular makeup of the oils [44].

For the purposes of this study the antimicrobial activity of the EOs used was assessed using two definitions. The minimum inhibitory concentration (MIC) was determined, which was the concentration of EO required to prevent the test bacteria from growing. The minimum bactericidal concentration (MBC) was also determined, which was the concentration of EO required to cause cell death of the test bacteria.
Previous research has shown that EO can have a skin sensitising effect at high concentrations, and that this effect increased as the oil is aged with in air. Due to this we decided that the EO antimicrobial developed in this project should be active at lower than 2 % (v/v) [45].

2.1.1.1 Essential oils used in this study

Geranium oil is isolated from plants of the genus *Pelargonium* and is most commonly produced in Réunion, Algeria, Egypt and Morocco. Its composition is generally dominated by geraniol and citronellol, which usually account for more than 50 % of the oil [46]. It is used by alternative practitioners as an antidepressant, and there is some scientific evidence reported that supports claims of antidepressant activity [47]. Geranium oil also has well known antimicrobial properties [48, 49]

Lavender oil is native to the Mediterranean, and was introduced to most of Europe by the Romans. It is very versatile and has been used in a range of application including; analgesic, antidepressant, bactericidal, and decongestant. Lavender oil has a complex composition which includes; linalyl, geranyl, geraniol, linalool, limonene, caryophyllene, and pinenes present as active components [46]. The antimicrobial activity of Lavender oil has been scientifically confirmed [50].

Manuka oil is obtained from the shrub *Leptospermum scoparium* which is native to New Zealand, its primary components are caryophyllene, geraniol, pinene,

linalool, humulene and leptospermone. It is referred to as being an excellent antiseptic for use on skin, however, repeated use can result in drying of the skin [46]. Literature reports show manuka oil to have antimicrobial [51] as well as an insecticidal activity [52].

Oregano oil is isolated from the plant *Oreganum vulgare*, which is native to the Mediterranean [46]. Thymol and carvacrol are the most abundant molecules present in the oil, and account for approximately 70 – 80 % of total peak area as determined by GC-FID [53]. Oregano oil has strong antimicrobial properties [51, 54], and has also been shown to cause cell death in human cancerous cells [55]. In addition there is evidence that oregano oil can be effective in reducing intestinal inflammation [56].

Rosewood oil is isolated from *Aniba rosaeodora* and its composition is primarily linalool (80 – 97 %), with small amounts of terpineol, nerol and geraniol [46]. In addition to antimicrobial activity [57], rosewood oil has also been shown to exhibit anxiolytic, sedative and anticonvulsant properties [58].

2.1.2 Bacteria used in this study

Three bacteria were selected as challenges for screening the antimicrobial activity of the EO. All three bacteria selected are responsible for causing HCAI, and they are discussed below.

2.1.2.1 Methicillin resistant Staphylococcus aureus

Methicillin resistant *Staphylococcus aureus* (MRSA) are strains of *S. aureus* which have developed resistance to the antibiotic methicillin and were first found in the 1960s [59]. MRSA are gram positive cocci, about 0.5-1 µm in diameter, they are considered to be opportunistic pathogens. *S. aureus* is one of the more common and important hospital pathogens responsible for HCAI, and is amongst the more common causes of surgical wound infections, pneumonia and blood infections [60]. It can cause osteomyelitis, septicaemia and abscesses, but is more commonly found in superficial skin conditions [61]. Due to the associated antibiotic resistance, MRSA infections are difficult to treat

and reports have suggested that MRSA infection gives an almost 50 % higher mortality rate than infection with methicillin susceptible *Staphylococcus aureus* (MSSA) infection [62]. The manufacture of surfaces which can reduce numbers of MRSA would help to reduce the number of associated HCAIs. Therefore MRSA was selected as the model gram positive bacteria for challenging the EO based antimicrobials developed in this section of the study.

2.1.2.2 Pseudomonas aeruginosa

Pseudomonas aeruginosa (*P. aeruginosa*) is a gram-negative bacillus with cell dimensions of 0.5-0.8 µm by 1.5-3.0 µm. Almost all strains of *P. aerugniosa* are motile via a single polar flagellum. *P. aeruginosa* can grow well at a range of different temperatures (25-37 ℃) and is resistant to high concentrations of salt, dyes, weak antiseptics and most commonly used antibiotics [61]. These characteristics allow it to survive well in many environments resulting in prolific transfer and contamination. The Health Protection Agency (HPA) describes *P. aeruginosa* as an opportunistic pathogen which can cause a wide range of infections, particularly amongst the immunocompromised [63]. In a recent study *P. aeruginosa* accounted for approximately 93 % of all identified *Pseudomonas spp*. infections reported in UK healthcare facilities [4]. The high numbers of HCAI caused by *P. aeruginosa* make it a good target for any technology aimed at reducing the incidence of HCAI. Infections caused by *P. aeruginosa* are often found with catheter devices. If the EO antimicrobial developed in this study could effectively inhibit growth of *P. aeruginosa*, and be incorporated into the polymeric material used for catheters, it could help reduce the number of patients contracting a catheter associated HCAI.

2.1.2.3 Acinetobacter baumannii

Acinetobacter baumannii (*A. baumannii*) are defined as gram-negative, catalase-positive, oxidase-negative, non-motile, non-fermenting coccobacilli. It has gained clinical significance over the last 15 years due to its ability to up-regulate or acquire resistance to antibiotics [64]. According to recent statistics, *A. baumannii* is the third most common bacteria responsible for ventilator associated pneumonia in hospitals in the United Stated of America [65]. *A.*

baumannii is a pathogen that is transmitted among hospital patients [66], transmission may be hindered by antimicrobial surfaces and materials.

2.1.3 Gas chromatography-mass spectrometry

Gas chromatography-mass spectrometry (GC-MS) is a combination of two techniques, and is used to analyse mixtures of chemicals. The first part of the analysis isolates the individual molecular components of the sample. In gas chromatography (GC), the chemical mixture is injected into an inert carrier gas (often helium), which is known as the mobile phase. The mobile phase and the mixture then passes through a stationary phase in the form of the GC column. The latter is a long tube containing the stationary phase, which consists of chemically receptive particles. The components in the mixture interact with the particles (at different rates) as they pass through the column containing this stationary phase. Molecules which have weaker interactions with the column particle surface will elute out of the column first, whilst molecules which interact strongly with the particles will take longer to pass though the stationary phase, and elute from the column later. In this way the molecular components are separated out. Further separation can be achieved by adjusting the temperature, with low boiling point molecules eluting faster at low temperature and high boiling point molecules eluting faster at high temperatures. Once it has passed through the stationary phase the molecule is fed into a detector, which creates an electronic signal; the greater abundance of a molecule the larger the signal. The signal is plotted on a linear time graph with abundance on the y-axis and time on the x-axis. The area of the peak generated by the signal is a measure of the amount of molecule detected and can be rationalised by using an internal standard of known concentration.

Whilst the GC allows for the determination of the number of molecular components and their abundance, the mass spectrometer can detect the chemical makeup of the molecule thus allowing it to be identified. Once the molecules have passed though the GC they are fed into the electron ionisation mass detector (of the mass spectrometer (MS)). Here they are bombarded with electrons, breaking them into ionised fragments of the original molecule. The ionised fragments are passed through a magnet which focuses them onto a detector; by varying the strength of the magnet fragments of differing molecular

mass can be focused onto the detector. The detector generates a signal for each fragment which is plotted on a graph of molecular mass on the x-axis and abundance on the y-axis. This graph is the mass spectrum of the molecule, a mass spectrum of a molecule is often unique, and by comparing the mass spectrum of an unknown to a database it is possible to identify the molecule [67].

By combining these two techniques it was possible to identify the molecular components of the EO used in this study as well as the abundance of each molecule in the oil.

2.2 Objectives

- Select a range of EO, and EO blends, that possess broad spectrum antimicrobial activity.
- Enhance the antimicrobial activity of the EO blends by combining them with antibiotics and synthetic antimicrobials.
- Determine the chemical composition of the EOs tested for antimicrobial activity.
- Identify the factors contributing to the differing levels of antimicrobial activity between the EOs.

2.3 Materials

2.3.1 Culture media

Columbia agar (Oxoid CM0331, Basingstoke, UK) was made as manufacturer's instructions, autoclaved at 121 ℃ for 15 minutes, cooled to 50 ℃ after which 5 % (v/v) horse blood (TCS:UK) was added and poured in 20 ml volumes into triple vent petri dishes (SLS select). Nutrient agar (Oxoid CM0003, Basingstoke, UK) made as manufacturer's instructions, autoclaved at 121 ℃ for 15 minutes, cooled to 50 ℃ and poured into 20 ml volumes into triple vent peti dishes. All agar plates were stored at 4 ℃, after 3 weeks any unused plates were discarded.

Nutrient Broth (Oxoid CM0001, Basingstoke, UK) made as manufacturer's instructions, autoclaved at 121 ℃ for 15 minutes, then cooled to 25 ℃. Peptone Water (Oxoid CM0009, Basingstoke, UK) made as manufacturer's instructions, autoclaved at 121 ℃ for 15 minutes, then cooled to 25 ℃.

2.3.2 Microorganisms

The test bacteria used for antimicrobial assays with the EO and biocides were; Methicillin resistant *Staphylococcus aureus* (MRSA) 16 (TSST) (clinical isolate), *Pseudomonas aeruginosa* NCTC 6749, and *Acinetobacter baumannii* NCTC 12156.

2.3.3 Essential oils and biocides

Geranium bourbon (*Pelargonium graveolens L'Her*.), rosewood (*Aniba rosaeodora var*. *amazonica Ducke*), lavender english folgate (*Lavandula angustifolia Mill*.), origanum (*Origanum vulgare L*.), manuka (*Leptospermum scoparium*) Forster & Forster, grape seed oil (*Vitis vinifera L*.) were obtained from Essentially oils Ltd. (Chipping Norton, UK). All oils were stored away from sunlight. Sterility was checked periodically by streaking onto a nutrient agar plate and incubating for 24h.

The EO were diluted to the required concentrations (% (v/v)) using grape seed oil. The solutions made up were at concentrations three times higher than those required in the micro titre plate wells.

The antimicrobial agents used were Triclosan (Irgasan from Fluka, UK), Chlorhexidine (Sigma-aldrich, UK), Polyhexamethylene Biguanide (PHMB) (ARCH chemicals, Manchester, UK), and Ciprofloxacin (Adatab from Mast Diagnostics, Merseyside, UK).

A stock solution of triclosan 40 % (m/v) was made using grape seed oil. All triclosan solutions used were made up by further dilutions of the stock solution using grape seed oil.

A stock solution of chlorhexidine 0.01 % (m/v) was made in sterile distilled water (SDW). All chlorhexidine solutions were made up by further dilutions of the stock solution using SDW.

PHMB was obtained as a 20 % (m/v) stock solution. All PHMB solutions used were made up by dilutions of the stock solution with SDW.

Ciprofloxacin adatabs were made up as per manufacturer's instructions to obtain a 2.4×10^{-3} % (m/v) stock solution in SDW. All ciprofloxacin solutions were made up by further dilutions of the stock solution using SDW.

2.3.4 Solvents

Heptane CHROMASOLV®, for HPLC, ≥99 % (Sigma Aldrich, UK) was used as the EO solvent for the GC-MS analysis of the EO (Section 2.4.8). Dodecane *ReagentPlus*®, ≥99 % (Sigma Aldrich, UK)

2.4 Experimental

2.4.1 Sub culturing microorganisms

A fresh subculture of all microorganisms was prepared weekly by streaking onto a fresh agar plate (Columbia blood agar (CBA) for *Acinetobacter baumannii*, and nutrient agar for MRSA 16 and *Pseudomonas aeruginosa*) and incubating the plate at 37 ℃ for 24 hours in air.

2.4.2 Preparation of overnight broth

A sterile loop was used to remove one colony from the agar plate, and inoculated into sterile broth and incubated for 18 hours at 37 ℃.

2.4.3 Estimation of bacterial numbers

An overnight broth culture (100 µl) was added to sterile saline solution (900 µl) to create a 10^{-1} dilution. Serial 10 fold dilutions were undertaken to generate a dilution series from 10^{-1} to 10^{-8}. Three drops (10 µl) from each dilution was added to the surface of a dried agar plate. This was allowed to dry onto the surface and incubated at 37 ℃ for 24 hours.

The dilution where each 10 µl drop contained 10-30 individual colonies was used to estimate the colony forming units (CFU). The average number of colonies from the three drops was multiplied by 100 to obtain the CFU in 1 ml. This value was divided by the dilution factor to determine CFU/ml of original broth culture.

2.4.4 Minimum inhibitory concentration and minimum bactericidal concentration of essential oils

Using a 96 well micro titre plate (MTP)(Figure 2.1) wells A1 to H1 were filled, using an auto pipette, with sterile double strength nutrient broth (75 µl) containing 0.15 % (m/v) metabolic dye triphenyl tetrazolium chloride (TTC) (Sigma Aldrich, UK) and 1.5 % (m/v) tween 20 (Sigma Aldrich, UK). 75 µl of the EO at the desired concentration was added to appropriate wells (well A1 contained the highest concentration and H1 contained the lowest

concentration). The EO was thoroughly mixed using an auto pipette by removing and reinjecting a 100 µl volume 8 times. An overnight broth culture of the target bacterium in nutrient broth, diluted to at $1x10^6$ CFU using sterile nutrient broth, was added to each well (75 µl). The MTP was covered, using lids supplied by the manufacturer, and placed in an incubator at 37 ℃ for 24 h. After 24 h the plates were inspected for growth, which was indicated by the red colour produced by the TTC metabolic dye when it was enzymatically reduced to triphenyl formazan. The minimum inhibitory concentration (MIC) well was taken to be the first well which displayed no sign of red colouration.

The minimum bactericidal concentrations (MBC) were determined by removing 10 µl volumes, using an auto pipette, from each well which showed no growth in the MIC test and sub-culturing onto agar. The 10 µl drops were allowed to dry into the agar and the agar plates were then incubated at 37 ℃ for 24 h. The first concentration which produced no growth from the 10 µl drop was taken to be the MBC.

For the MIC testing the concentrations in the MTP wells of each oil used were 5, 2.5, 1.25, 0.625, 0.3125, 0.156, 0.078 and 0.039 %.

A summary of the formulations described in the above section is presented (Table 2.1).

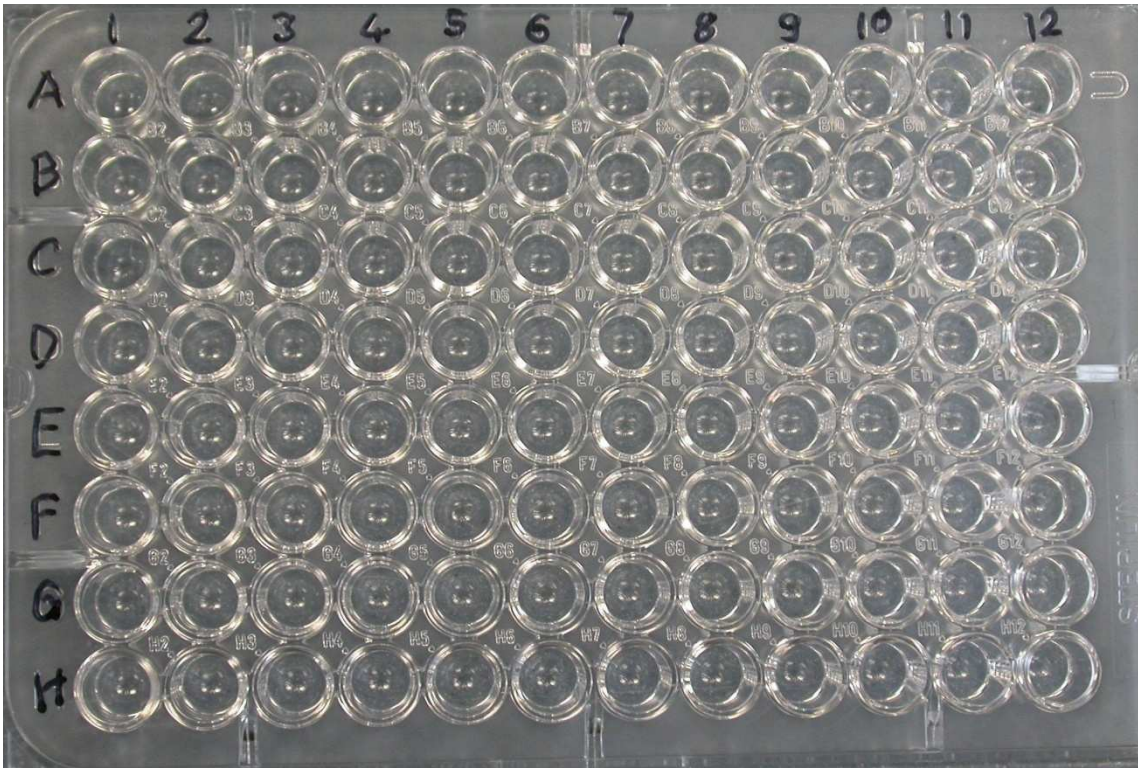

Figure 2.1: 96 Well Microtitre plate. Demonstrating the well layout.

All experiments were carried out in triplicate and the MIC and MBC values quoted were the mean of the three replicates.

2.4.5 Oil blend MIC and MBC screening

On a MTP, an 8x8 grid (A1 to H8) had double strength nutrient broth (150 µl) containing 0.15 % (m/v) TTC and 1.5 % (m/v) tween 20 (viscous liquid, Sigma Aldrich, UK) added to each well. To wells A2 to A8, the first oil to be tested (75 µl) was added at the required concentrations. The contents of the wells were thoroughly mixed and then 75 µl was transferred from each well in row A to the corresponding well in row B, using a multi-channel pipette. This process was repeated from B to C, C to D etc. until all rows contained a volume of oil. From row H, 75 µl of the contents were removed and discarded. To wells B1 to H1 the second oil to be tested (75 µl) was added at the required concentrations. The contents of the wells were mixed thoroughly and transferred from column 1 to the corresponding well in column 2. This process was repeated across the MTP until all the columns up to 8 contained a volume of oil 2. From column 8, 75 µl of the contents was removed and discarded. A graphical representation of this method is given (Figure 2.2). Each well was then inoculated with an overnight broth culture of the bacterium to be tested (75 µl) at $1x10^6$ CFU. The MTP was covered and incubated at 37 ℃ for 24 h. The well in which the MIC was observed was taken to be the well containing the lowest concentration of a particular oil that exhibited no microbial growth. The experiments were carried out in triplicate and the quoted MIC and MBC values were the mean of the three replicates

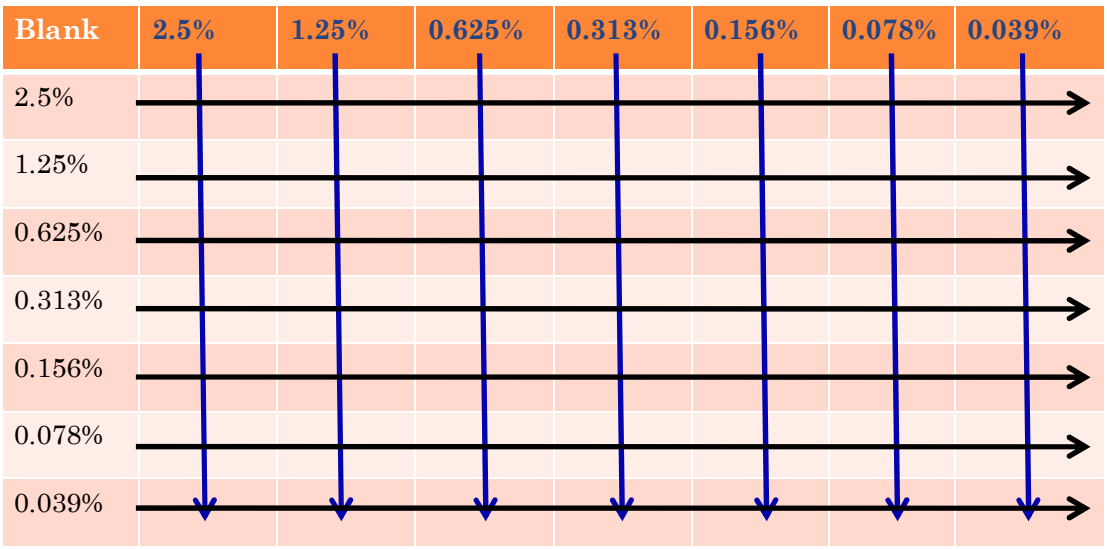

Figure 2.2: Graphical representation of method described in 2.4.5, where each oil has had a starting concentration of 2.5 % (v/v).

The level of synergistic activity was assessed using fractional inhibitory concentration (FIC) calculations:

FIC = A+B where $A = \frac{MIC\ X\ in\ combination}{MIC\ X\ individually}$

$B = \frac{MIC\ Y\ in\ combination}{MIC\ Y\ individually}$

where X is the first EO and Y is the second EO.

If		FIC ≤ 0.5	the relationship is synergistic.
If	0.5 <	FIC ≤ 1.0	the relationship is additive.
If	1.0 <	FIC ≤ 4.0	the relationship is indifferent.
If		FIC > 4.0	the relationship is antagonistic.

Synergism was defined as a positive interaction between the two antimicrobials such that the combined effect of the two antimicrobials was significantly greater than the expected result. Antagonism was defined as a negative interaction between the two antimicrobials such that the combined effect of the two antimicrobials was significantly less than expected. An additive relationship occurred when the sum of the separate effects was the same as the effect of EOs used in combination. Indifference indicated that the effect of the EOs in

combination was the same as that of the most potent of those EOs used individually [68].

The FIC values reported were the median FIC from three replicates. Analysis of variance (AnOVar) tests were carried out using Minitab (Minitab, Inc. Pennsylvania) on the FICs obtained for each experiment, and used to determine whether the 95 % confidence interval (CI) range was within the FIC boundary which described the median FIC. If this was the case then the FIC value could be said to lie within that boundary with a confidence of 95 %.
The MBC were determined using the same approach as in Section 2.4.4.

2.4.6 Individual synthetic biocide MIC and MBC screening

Chlorhexidine and PHMB were tested against the three test microbes using the same method as in described in Section 2.4.4. Ciprofloxacin was tested against *A. baumannii* and *P. aeruginosa* using the same method as described in Section 2.4.4. MRSA was not tested as it is known to be resistant to ciprofloxacin.

For chlorhexidine, the concentrations (% m/m) tested against the microbes were:

1. $3.3x10^{-3}$ %
2. $2.5x10^{-3}$ %
3. $1.25x10^{-3}$ %
4. $6.25x10^{-4}$ %
5. $3.13x10^{-4}$ %
6. $1.56\ x10^{-4}$ %
7. $7.8\ x10^{-5}$%
8. $3.9\ x10^{-5}$ %

For PHMB the concentrations (% v/v) tested against the microbes were:

1. $7x10^{-3}$ %
2. $6x10^{-3}$ %
3. $5x10^{-3}$ %
4. $4x10^{-3}$ %
5. $3x10^{-3}$ %
6. $2x10^{-3}$ %
7. $1x10^{-3}$ %
8. $5\ x10^{-4}$ %

For ciprofloxacin the concentrations (% m/v) tested against the microbes were:

1. $2.66x10^{-4}$ %
2. $2.33x10^{-4}$ %
3. $2x10^{-4}$ %
4. $1.66x10^{-4}$ %
5. $1.33x10^{-4}$ %
6. $1x10^{-4}$ %
7. $6.6x10^{-5}$ %
8. $3.3x10^{-5}$ %

At high concentrations the triclosan became insoluble; this necessitated a modification to the method described in Section 2.4.4. Instead of using equal volumes of biocide, nutrient broth, and broth culture (each 75 µl), 108.75 µl of double strength nutrient broth, and biocide were added to each well. The well was then inoculated with 7.5 µl of broth culture. In Section 2.4.4 the stock solutions were three times the strength of the final concentration in the MTP well. The modification made here allowed the stock solution of triclosan to be made up to twice the concentration required in the MTP well. Therefore the problem with triclosan solubility at high concentrations was resolved. As the broth culture volume had been reduced by a factor of 10, the CFU of the culture was increased by a factor of 10 from 10^6 to 10^7. The MTP well concentrations for triclosan against each bacterium are given below.

For *P. aeruginosa* the triclosan concentrations (% m/v) tested were:

1. 20 %
2. 15 %
3. 10 %
4. 5 %
5. 2.5 %
6. 1.25 %
7. 0.625 %
8. 0.313 %

For *A. baumannii* the triclosan concentrations (% m/v) tested were:

1. 5 %
2. 4 %
3. 2 %
4. 1 %
5. 0.5 %
6. 0.25 %
7. 0.125 %
8. 0.0625 %.

Against MRSA the method from Section 2.4.4 was used to test for the triclosan MIC.

The triclosan concentrations (% m/v) tested against MRSA were:

1. $2.5x10^{-1}$ %
2. $1.25x10^{-1}$ %
3. $6.25x10^{-2}$ %
4. $3.13x10^{-2}$ %
5. $1.56x10^{-2}$ %
6. $7.8x10^{-3}$ %
7. $3.9x10^{-}3$ %
8. $1.95\ x10^{-3}$ %

All experiments were carried out in triplicate and the MIC and MBC values reported were the mean of the three replicates.

MBC for all tests in Section 2.4.6 were carried out as described in Section 2.4.4

A summary of the formulations described in the above section is presented in Table 2.1.

2.4.7 Biocide and essential oil blend MIC and MBC screening

To test the effect of combining the EO blends with the synthetic biocides the method described in Section 2.4.5 was used, with the modification that a 6x6 grid was used instead of an 8x8 grid. This was done to save time and materials, as it had been observed in the previous experiments that the two outermost rows and columns (those that contained the lowest concentrations) always displayed growth.

The first test biocide was added to wells A2 to A6 at the required concentrations, with the highest concentration in A2 and the lowest concentration in A6. The EO blend was added to wells B1 to F1 at the required concentration, with the highest concentration in B1 and the lowest concentration in F1. The EO concentrations used for the tests are shown in Table 2.2. The biocide concentrations for the test are shown in Table 2.3.

The EO blends were made up in a 1 to 1 ratio, and then diluted using grape seed oil.

All experiments were carried out in triplicate and the MIC and MBC values reported were the mean of the three replicates.

FIC values were calculated as described in Section 2.4.5 to assess the effect of combining the EO blends with biocides. The FIC values reported were the median value of three replicates and AnOVa tests were used (Section 2.4.5) to calculate the 95 % confidence interval range.

MBC for all tests in Section 2.4.7 were carried out as described in Section 2.4.4.

Table 2.1: Representation of the methods in Section 2.4.4 and 2.4.6

Biocide concentration (for all microbes unless stated) (% w/v)	Volume of double strength nutrient broth containing TTC and Tween 20 (µl)	Volume (µl) of broth culture	Concentration (CFU) of Broth culture	Volume of biocide (µl)	Total volume in MTP well (µl)
Essential oils 5 to 0.039 % (doubling dilutions)	75	75	10^6	75	225
Triclosan Against *P. aeruginosa* 20, 15, 10, 5, 2.5, 1.25, 0.625 and 0.313 Against *A. baumannii* 5, 4, 2, 1, 0.5, 0.25, 0.125 and 0.0625	108.75	7.5	10^7	108.75	225
Triclosan Against MRSA $2.5x10^{-1}$, $1.25x10^{-1}$, $6.25x10^{-2}$, $3.13x10^{-2}$, $1.56x10^{-2}$, $7.8x10^{-3}$, $3.9x10^{-3}$ and $1.95 x10^{-3}$	75	75	10^6	75	225
Chlorhexidene $3.3x10^{-3}$, $2.5x10^{-3}$ to $3.9x10^{-5}$ (doubling dilutions)	75	75	10^6	75	225
PHMB $7x10^{-3}$, $6x10^{-3}$, $5x10^{-3}$, $4x10^{-3}$, $3x10^{-3}$, $2x10^{-3}$, $1x10^{-3}$, $5x10^{-4}$	75	75	10^6	75	225
Ciprofloxacin $2.66x10^{-4}$, $2.33x10^{-4}$, $2x10^{-4}$, $1.66x10^{-4}$, $1.33x10^{-4}$, $1x10^{-4}$, $6.6x10^{-5}$, $3.3x10^{-5}$	75	75	10^6	75	225

Table 2.2: EO concentration ranges used in EO blend + biocide, as described in Section 2.2.7, against the three test bacteria. The ranges were made up of halving dilutions. *For EO blend and chlorhexidine test against *P. aeruginosa* the chlorhexidine ranges used with; Manuka+Lavender = 2.5 to 0.156%, Lavender+Geranium range = 5 to 0.313 % and Rosewood+Geranium range = 5 to 0.313 %.

	A. baumannii	MRSA	**P. aeruginosa*
Oregano + Rosewood % (v/v)	0.625 to 0.039	2.5 to 0.156	2.5 to 0.156
Oregano + Manuka % (v/v)	0.625 to 0.039	2.5 to 0.156	2.5 to 0.156
Manuka + Rosewood % (v/v)	2.5 to 0.156	2.5 to 0.156	2.5 to 0.156
Manuka + Lavender % (v/v)	2.5 to 0.156	2.5 to 0.156	0.625 to 0.039
Manuka + Geranium % (v/v)	1.25 to 0.078	2.5 to 0.156	2.5 to 0.156
Lavender + Geranium % (v/v)	5 to 0.313	5 to 0.313	2.5 to 0.156
Rosewood + geranium % (v/v)	2.5 to 0.156	5 to 0.313	2.5 to 0.156

Table 2.3: Synthetic biocide concentration ranges used in EO blend + biocide tests, as described in 2.2.7, against the three test bacteria. Demonstrating the starting concentrations used for checkerboard methods.

	A. baumannii	MRSA	*P. aeruginosa*
Chlorhexidine % (m/m)	$1.25x10^{-3}$, $6.25x10^{-4}$, $3.13x10^{-4}$, $1.56x10^{-4}$, to $7.81x10^{-4}$	$3.5x10^{-3}$, $2.5x10^{-3}$, $1.25x10^{-3}$, $6.25x10^{-4}$, $3.13x10^{-4}$	$3.5x10^{-3}$, $2.5x10^{-3}$, $1.25x10^{-3}$, $6.25x10^{-4}$, $3.13x10^{-4}$
PHMB % (v/v)	$4x10^{-3}$, $2x10^{-3}$, $1x10^{-3}$, $5x10^{-4}$, $2.5x10^{-4}$	$4x10^{-3}$, $2x10^{-3}$, $1x10^{-3}$, $5x10^{-4}$, $2.5x10^{-4}$	$9x10^{-3}$, $8x10^{-3}$, $6x10^{-3}$, $4x10^{-3}$, $2x10^{-3}$
Ciprofloxacin % (m/v)	$2.66x10^{-4}$, $1.33x10^{-4}$, $6.65x10^{-5}$, $3.33x10^{-5}$, $1.66x10^{-5}$	N/A	N/A
Triclosan % (m/v)	1, 0.75, 0.5, 0.25, 0.125	1, 0.75, 0.5, 0.25, 0.125	N/A

2.4.8 Gas chromatography mass spectrometry analysis of essential oils

GC-MS analysis of the five individual EO was performed using an HP 5890 series 2 GC connected to 5972 series mass selective detector (MSD) (Hewlett Packard co., Palo Alto, USA).

For each of the oils, a 1000 ppm solution in heptane was prepared. As this concentration is too strong for the MSD, the sample was injected using a split of 20 to 1; meaning that for every 1 part that reaches the detector 19 parts go to waste. Therefore, the concentration reaching the detector was now at a manageable level and saturation was avoided. Helium, at a flow rate of 1 ml/min, was used as the carrier gas. The injection volume was 1 µl.

To allow GC runs to be completed within a reasonable timescale, a temperature programme was used. The initial oven temperature was 60 ℃ for 3 min, then increased at 4 ℃/min to 230 ℃ and held for 22 min . After running the oils though the programme, it was determined that a number of peaks came off around 110 ℃. The method was edited so there was a n initial temperature ramp from 60 ℃ to 112 ℃ at a rate of 4 ℃/min, fo llowed by a second temperature ramp from 112 ℃ to 230 ℃ at a rate of 10 ℃/min. For each oil the hold times at 112 ℃ and 230 ℃ were modified using trial and error to obtain the best peak separation in the shortest run time. The individual temperature programmes for each oil are given in Table 2.4.

The injector and detector temperatures were 275 ℃ and 250 ℃ respectively. Other MSD conditions were as follows: ionisation energy, 70 eV; mass range, 50 to 550 atomic mass units (a.m.u.); scanning rate 1.53 scans/s. Peaks were positively identified using a Wiley 275 mass spectral database.

Table 2.4: Temperature programmes for the individual EO GC-MS analysis.

Oil	Hold t_{60} (min)	Ramp 60-112 (℃/min)	Hold t_{112} (min)	Ramp 112-230 (℃/min)	Hold t_{230}	Total run time (min)
Rosewood	3	4	14	10	10	51.8
Oregano	3	4	27	10	15	69.8
Manuka	3	4	16	10	10	53.8
Lavender	3	4	20	10	15	62.8
Geranium	3	4	26	10	15	68.8

2.5 Results and discussions

2.5.1 MIC and MBC screening of individual essential oils

Each of the five oils (manuka oil (MO), geranium oil (GO), lavender oil (LO), oregano oil (OO) and rosewood oil (RO)) were tested for antimicrobial efficiency against *Acinetobacter baumannii, Pseudomonas aeruginosa* and Methicillin Resistant *Staphylococcus aureus (*MRSA*).* The MIC and MBC data are presented (Table 2.5). An image taken of the MTP assay of lavender geranium and manuka oils against *A. baumannii* is given (Figure 2.3).

Table 2.5: MIC and MBC data from MTP assays demonstrating the antimicrobial efficacy of the EO against the test bacteria. Demonstrating that none of the EO tested were effective at less than 2 % against all three test bacteria. Standard deviations given in parentheses.

EO type	*Pseudomonas aeruginosa*		*Acinetobacter baumannii*		MRSA	
	MIC (%)	**MBC (%)**	**MIC (%)**	**MBC (%)**	**MIC (%)**	**MBC (%)**
MO	4.20 (1.4)	> 5.00	0.31 (0)	0.31 (0)	1.25 (0)	> 5.00
GO	2.50 (0)	4.20 (1.4)	1.25 (0)	1.25 (0)	5.00 (0)	5.00 (0)
LO	5.00 (0)	> 5.00	0.83 (0.36)	1.66 (0.72)	>5.00	> 5.00
OO	2.50 (0)	> 5.00	0.31 (0)	0.31 (0)	1.25 (0)	2.50 (0)
RO	5.00 (0)	> 5.00	1.25 (0)	1.25 (0)	5.00 (0)	> 5.00

Of the five oils tested oregano exhibited the strongest antimicrobial effect, giving the lowest MIC for each of the test bacteria. Lavender and rosewood were the least effective, with lavender failing to inhibit growth of MRSA at a concentration of 5 %.

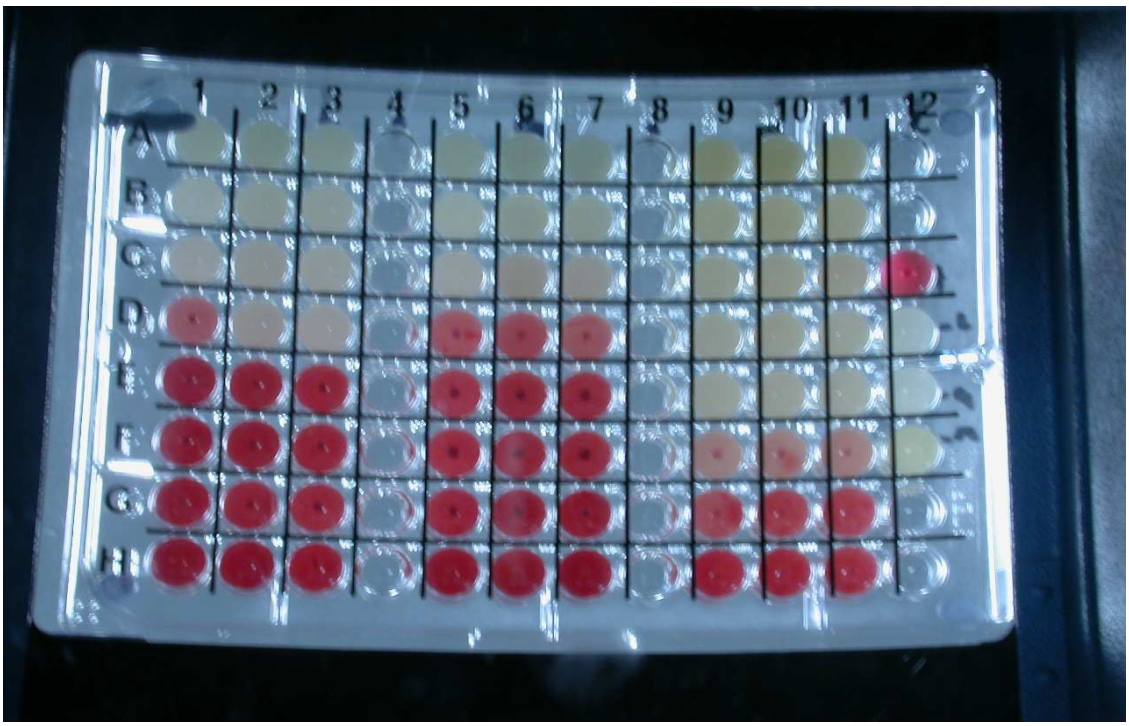

Figure 2.3: MTP assay against *A. baumannii* columns 1-3 lavender oil, columns 5-7 geranium oil, columns 9-11 manuka oil, columns 4 and 8 are blank for spacing column 12 contains negative and positive controls. Demonstrating the use of TTC for rapid determination of MIC well, where the deep red colour indicated cell growth.

Of the three bacteria tested *Pseudomonas aeruginosa* showed the strongest resistance to the oils; it was initially proposed that the outer lipopolysaccharide membrane acted as a barrier to EO attack. *Acinetobacter baumannii* showed the least resistance to the oils, with growth inhibited at concentrations of less than 2 % for each of the oils. The low resistance of *A. baumannii* (which is also a gram negative organism) to the EOs suggests that the lipopolysaccharide outer membrane was not providing barrier properties. Therefore another mechanism of protection must be behind the high EO resistance of *P. aeruginosa*. Studies by Cox and Markham indicated that addition of the protonophore carbonyl cyanide *m*-chlorophenylhydrazone resulted in increased susceptibility of *P. aeruginosa* to EO. It is therefore highly likely that ATP-dependent efflux was responsible for the tolerance of *P. aeruginosa* to EO [41]. This suggests that the EO molecules are able to pass through the outer lipopolysaccharide membrane, explaining the susceptibility of *A. baumannii* to

EO attack. However, in the case of *P. aeruginosa* they are removed by a transporter mediated process, therefore damage to the bacterial cell is prevented. The MIC values found for lavender oil and oregano oil against *A. baumannii* and *P. aeruginosa* correlate well with those found in the literature, with Hammer (1999) obtaining an MIC of 1 % for *A. baumannii*, and > 2 % for *P. aeruginosa* compared to 0.833 % and 5 %, respectively [37]. The MICs of geranium oil and rosewood oil against *P. aeruginosa* (2.5 and 5 % respectively) also matched earlier reported studies in which both oils were found to have an MIC of > 2 %. The values obtained from geranium oil and rosewood oil against *A. baumannii* did not match those found in literature, with Hammer (1999) reporting MIC values of 0.25 % and 0.12 %, respectively [37], which are much lower than those found in this study. Literature values for the five oils against MRSA were not available; however Hammer obtained MIC values for geranium oil (0.25 %), lavender oil (1.00 %), oregano oil (0.12 %), and rosewood oil (2.50 %) against methicillin susceptible *Staphylococcus aureus* (MSSA). In this study the values obtained for MRSA were all considerably higher, with values of 5.00, 5.00, 1.25, and 5.00 % being obtained, respectively. There are a number of possible reasons for the discrepancies between the literature MIC values and those obtained in this study. Firstly, Hammer used an agar dilution method whilst a broth dilution method was used in this study; therefore the availability of the EO molecules to the bacterial cells will be different. Secondly, previous research has shown that the antimicrobial effect of EO can be affected by the climatic and environmental conditions (e.g. average rainfall and soil acidity) in which the plants are grown, as well as the time of day at which the plants used to produce the oil were harvested. These aspects can affect the chemical composition of the oil obtained [69-71], resulting in different batches of the same oil having different levels of antimicrobial activity. It is conceivable that the quality of the oil used may also have an effect on the antimicrobial activity. In addition to these factors, different strains of bacteria may have differing characteristics which may cause them to have varying resistance to an antimicrobial. EOs are known to have various chemotypes which produce different chemical compositions of the EO [72, 73], Hammer did not include the chemotype of the oils used in their study. If the EO used in this study were of a different chemotype to those used by Hammer this could also explain the differences in antimicrobial activity observed.

The aim was to identify an EO antimicrobial that was effective against the three test organisms at less than 2 % (v/v). The MIC data displayed above show that none of the five oils would be suitable if used individually as they all require a concentration of > 2 % (v/v) to inhibit at least one of the bacteria used.
In order to obtain an antimicrobial that was effective at concentrations below 2 % (v/v), blends of the oils were tested for synergism.

2.5.2 MIC and MBC screening of oil blends

Using the method described in Section 2.4.5, the five oils were tested for their effectiveness in blends. The blends were tested against the same three bacteria that were used for the individual MIC tests, and the effectiveness of the blends was determined by calculating the fractional inhibitory concentration (FIC). Blends were said to be synergistic if they had an FIC of ≤ 0.50, an FIC of between 0.99 and 0.50 showed an additive relationship. If the blend had an FIC of between 3.99 and 1.00, the relationship was indifferent and an FIC ≥ 4 showed the relationship to be antagonistic. The results of the oil combination tests are displayed (Table 2.6).

Oil blends containing oregano oil were the most effective against *A. baumannii,* with three of them (oregano oil + rosewood oil, oregano oil + geranium oil, and oregano oil + lavender oil) having a median FIC value in the synergistic range. The relationship between the oils in the three blends could not be said to be truly synergistic as the 95 % CI ranges crossed the boundary between synergistic and additive behaviour. Therefore, despite the median FIC being synergistic it could not be ruled out that the relationship was additive. However, oregano oil + rosewood oil, and oregano oil + lavender oil were the most effective at inhibiting the growth *A. baumannii*, with both combinations inhibiting growth at a combined oil level of 0.142 % (v/v). This represented a drop in comparison to the concentration of the individual oils required to inhibit growth (oregano = 0.31, rosewood = 1.25 and lavender = 0.83). Blends containing manuka oil were the least effective, with all four blends providing an indifferent FIC value (with 95 % CI lying within the indifferent range). Therefore, there was no benefit to using these blends against *A. baumannii* in comparison to the individual oils. The best bactericidal effect was given by oregano oil + geranium

oil, and oregano oil + lavender oil, which killed all bacteria at 0.24 % (v/v) concentration. From the results it was determined that, although a number of the blends provided a reduced level of oil to inhibit growth in comparison to the individual oils, as there were no blends where the 95 % CI for the FIC was within the synergistic range none of the oil blends statistically provided a synergistic relationship. Despite not providing a significant improvement in the concentration of oil required to inhibit growth the three blends with synergistic median FICs did require a reduction in the overall amount of oil required. The reduced amount of oil required would reduce the cost of the antimicrobial and therefore it would still be of benefit to use one of oregano + rosewood, oregano + geranium or oregano + lavender over the individual EOs.

Oil blends containing lavender oil were the least effective against MRSA, with rosewood oil + lavender oil and oregano oil + lavender oil failing to inhibit growth at the highest concentration tested (1.4 % (v/v)). Blends containing lavender oil could not be analysed for synergy as the MIC test for the individual oil (Table 2.5) did not yield an MIC. All of the other blends exhibited a synergistic relationship with oregano oil + geranium oil giving the best results, inhibiting growth at a concentration of 0.14 % (v/v). In addition to the median FICs being synergistic the 95 % CI ranges for all of the blends fell within the boundary for synergism. Therefore, it was determined that by blending the oils a significant reduction in the concentration of oil required to inhibit the growth of MRSA could be achieved.

Minimum bactericidal concentration values were not obtainable as all samples taken from, and subsequently plated on agar, exhibited growth after 24 h incubation. The latter observations therefore indicated bacteriostatic properties with no bactericidal action being observed.

Of the three blends that required a reduced oil concentration to inhibit the growth of *A. baumannii* in comparison to the individual EOs, oregano + lavender would not be suitable for use against MRSA as no MIC was obtained. For the other two blends, synergistic behaviour was reported against MRSA resulting in a reduction in the level of oil required for inhibition.

Table 2.6: Results from oil combination assays demonstrating the improved activity achieved for OO blends. Numbers in brackets are the combined concentrations of the oils. For MRSA and *P. aeruginosa* all samples that were tested for MBC exhibited growth, bactericidal values were not available. Average standard deviations for each oil: *A. baumannii* OO±0.05, RO±0.17, MO±0.07, LO±0, GO±0.12, MRSA (OO±0.03, RO±0.07, MO±0.06, LO±0.27, GO±0.03, *P. aeruginosa* OO±0.08. RO±0.13, MO±0.09, LO±0.02, GO±0.15). * FIC value with a 95 % CI range that lie within the assigned FIC boundary.

Oil blend	*Acinetobacter baumannii*			MRSA			*Pseudomonas aeruginosa*		
	MIC (%)	MBC (%)	FIC	MIC (%)	MBC (%)	FIC	MIC (%)	MBC (%)	FIC
Oregano+Rosewood	0.11 + 0.03 (0.142)	0.12 + 0.42 (0.54)	0.37 Synergistic	0.14 + 0.15 (0.29)	N/A	0.15 Synergistic*	0.42 + 0.12 (0.54)	N/A	0.19 Synergistic*
Oregano+Manuka	0.33 + 0.06 (0.39)	0.19 + 0.92 (1.12)	1.25 Indifferent*	0.15 + 0.14 (0.29)	N/A	0.23 Synergistic*	0.37 + 0.83 (1.20)	N/A	0.25 Synergistic*
Oregano+Geranium	0.10 + 0.13 (0.24)	0.10 + 0.13 (0.24)	0.43 Synergistic	0.09 +0.05 (0.14)	N/A	0.05 Synergistic*	1.1 + 1.6 (2.78)	N/A	1.1 Indifferent
Oregano+Lavender	0.11 + 0.03 (0.142)	0.10 + 0.13 (0.24)	0.39 Synergistic	N/A	N/A	N/A	N/A	N/A	N/A
Rosewood+Manuka	0.37 + 0.83 (1.20)	0.92 + 0.55 (1.48)	2.97 Indifferent*	0.15 + 0.14 (0.29)	N/A	0.14 Synergistic*	0.37 + 0.83 (1.20)	N/A	0.27 Synergistic*
Rosewood+Geranium	0.37 + 0.83 (1.20)	0.92 + 0.55 (1.48)	0.96 Additive*	0.18 +0.42 (0.60)	N/A	0.12 Synergistic*	0.37 + 0.83 (1.20)	N/A	0.41 Synergistic
Rosewood+Lavender	0.37 + 0.83 (1.20)	0.37 + 0.83 (1.20)	1.3 Indifferent*	N/A	N/A	N/A	1.1 + 1.6 (2.78)	N/A	0.54 Additive
Manuka+Geranium	0.31 + 0.27 (0.58)	0.37 + 0.83 (1.20)	1.22 Indifferent*	0.15 + 0.14 (0.29)	N/A	0.15 Synergistic"	0.93 + 0.55 (1.48)	N/A	0.44 Synergistic
Manuka+Lavender	0.37 + 0.83 (1.20)	0.37 + 0.83 (1.20)	2.19 Indifferent	0.18 + 0.42 (0.60)	N/A	N/A	0.33 + 0.06 (0.39)	N/A	0.09 Synergistic*
Lavender+Geranium	0.37 + 0.83 (1.20)	0.37 + 0.83 (1.20)	1.11 Indifferent*	0.28 + 0.46 (0.74)	N/A	N/A	0.37 + 0.83 (1.20)	N/A	0.41 Synergistic

As with MRSA, the blend of oregano + geranium failed to inhibit the growth of *P. aeruginosa* at all of the concentrations tested. This confirmed that despite exhibiting good efficacy against *A. baumannii* the blend of oregano + geranium would not be a suitable antimicrobial for the purposes of this work. The nine remaining blends all resulted in a reduction in the concentrations, of the constituent EOs, required for the inhibition of *P. aeruginosa* in comparison to the individual EOs.

The blends oregano + rosewood, oregano + manuka, rosewood and manuka and manuka and lavender all yielded a synergistic median FIC, together with FIC 95 % CI ranges that lay within the range for synergism. The median FICs for rosewood + manuka, rosewood + geranium, and rosewood + lavender were synergistic, and the median FIC for lavender and geranium was additive. For all four blends the 95 % CI spanned the boundary between synergistic and additive behaviour. Therefore, it cannot be said with certainty that the median FIC was a true measure of the interaction between the EOs. As a result despite the reduction in concentration of EO required for inhibition these four blends were determined to be less effective than the blends of oregano + rosewood, oregano and manuka, and rosewood and geranium.

The blend of oregano and geranium had an indifferent median FIC with a 95 % CI range of 0.97 to 1.22. As the CI range spanned the threshold between additive and indifferent behaviour it could not be said with certainty that the relationship was indifferent. However, the total amount of oil required for inhibition was 2.78 %(v/v), this was above the concentration of EO at which sensitisation of skin can occur (2 %) and was therefore deemed unsuitable for use in this work.

The blend of oregano + rosewood was shown to be the most effective of all the EO blends tested. It provided a significant increase in antimicrobial activity against both MRSA and *P. aeruginosa* in comparison to the oils individually. While it did not provide significant improvement for *A. baumannii* the blend did provide the highest antimicrobial activity of all the blends against *A. baumannii* as well as reducing the overall concentration of oil required in comparison to the individual oils.

As a result of the EO blend testing three of the blends were rejected as antimicrobials. Rosewood + lavender failed to inhibit the growth of MRSA, and

oregano + lavender failed to inhibit the growth of MRSA and *P. aeruginosa*. Oregano + geranium was also not suitable as the concentration required to inhibit *P. aeruginosa* was greater than 2 %(v/v). The seven other blends were selected to be studied in combination with synthetic biocides, to investigate whether the concentration of EO required for antimicrobial activity could be further reduced.

Due to the fact that very little research has been done into this area, it is not fully understood why some oil blends display synergy whilst others do not. Perhaps by analysing the GC-MS data of the individual oils and comparing them to the GC-MS profiles of the EO blends, it may be possible to detect any changes that may occur in the oils after blending. This could lead to a theory as to why some blends display synergism and others display antagonism. This was outside the scope of this project. However, it was an area that may be assessed in work that leads on from this project.

2.5.3 MIC and MBC screening of individual synthetic biocides

The three synthetic biocides (chlorhexidine, triclosan, and polyhexamethylene biguanide (PHMB)) and an antibiotic (ciprofloxacin) were tested for their individual effectiveness against the three test bacteria. The results of the MIC and MBC test are displayed (Table 2.7).

Table 2.7: MIC and MBC data from MTP assays demonstrating the antimicrobial activity of the biocides/antibiotics against the test bacteria before addition of EO blends. Demonstrating triclosan as the least effective of the biocides tested. Standard deviations are given in parentheses where appropriate.

	Pseudomonas aeruginosa		*Acinetobacter baumannii*		MRSA	
	MIC (%)	**MBC (%)**	**MIC (%)**	**MBC (%)**	**MIC (%)**	**MBC (%)**
Ciprofloxacin	$1.33x10^{-4}$ (0)	$>2.3x10^{-4}$	$1x10^{-4}$ (0)	$>2.3x10^{-4}$	N/A	N/A
Chlorhexidine	$1.25x10^{-3}$ (0)	$2.5x10^{-3}$ (0)	$3.13x10^{-4}$ (0)	$6.25x10^{-4}$ (0)	$1.25x10^{-3}$ (0)	$2.5x10^{-3}$ (0)
Triclosan	15 (0)	15 (0)	0.5 (0)	0.5 (0)	0.125 (0)	0.125 (0)
PHMB	$4x10^{-3}$ (0)	$7x10^{-3}$ (0)	$1x10^{-3}$ (0)	$2x10^{-3}$ (0)	$1x10^{-3}$ (0)	$5x10^{-3}$ (0)

Ciprofloxacin showed good levels of inhibition against *P. aeruginosa* and *A. baumannii*. However it was not bactericidal at any of the concentrations tested. It had no effect on MRSA at any of the concentrations tested (up to $2.4x10^{-3}$ %). The isolate of MRSA used can be said to be resistant to ciprofloxacin as this value is much higher than literature values for the MIC ($6x10^{-6}$ %) [74].

Chlorhexidine successfully inhibited all three microbes. As well as showing good levels of growth inhibition, it also exhibited good bactericidal activity at concentrations double that required to inhibit growth. When compared to ciprofloxacin, against *P. aeruginosa* it was approximately ten times less

effective, and against *A. baumannii* it was approximately five times less effective.

PHMB inhibited the growth of all three microbes as well as causing cell death. For *P. aeruginosa* and *A. baumannii*, the bactericidal concentration was approximately double the inhibitory concentration. For MRSA, the MBC was five times greater than the MIC. Triclosan was the least effective of the biocides tested, performing particularly poorly against *P. aeruginosa* with an MIC of 15 %. The experimental MIC values obtained for chlorhexidine and ciprofloxacin compare well to the values found in the literature. Previous studies reported ciprofloxacin MIC's of $2x10^{-4}$ % and $5x10^{-5}$ % for *P. aeruginosa* and *A. baumannii* respectively [75, 76]. For chlorhexidine the literature values were $1x10^{-4}$ % for MRSA, $2.5x10^{-3}$ % for *P. aeruginosa* and $3.2x10^{-3}$ % for *A. baumannii* [75, 77].

The MIC values obtained for triclosan in this study were higher than those reported in the literature, with Lambert reporting MICs of $9x10^{-7}$ % and 0.05 % for MRSA and *P. aeruginosa* respectively [75]. The reason for this large difference in values could be due to the dilution method used for triclosan. In this study the, triclosan was dissolved in grape seed oil, and the triclosan/grape seed oil solution was then used in the broth dilution assays. As an organic liquid, grape seed oil had a poor miscibility in the polar broth, thus in an attempt to aid the miscibility the surfactant tween 20 was used as an emulsifier. Despite the use of an emulsifying agent, complete miscibility was not obtained. It is highly probable that this factor was related to the high MIC values obtained for triclosan in this study. Under the conditions of the latter, transfer of the triclosan to the broth containing the bacteria may well have been hindered.

Grape seed oil was used to dilute the triclosan as it was the solvent used for the EOs and it was envisaged that using the same solvent for both would be helpful in the biocide and EO blend combination assays. In order to improve the availability of the triclosan to the bacterial cells a solvent with a higher miscibility in water, such as glycerine, could be used.

2.5.4 MIC and MBC screening of biocide and essential oil blend combinations

The seven EO blends selected in Section 2.5.2 were tested in combination with the biocides from Section 2.5.3 in an attempt to further improve the activity of the oils. The EO blends were made up in 50:50 ratios of the component oils to keep the test as simple as possible. The results from the combination tests are shown in Table 2.8 (Ciprofloxacin), Table 2.9 (chlorhexidine), Table 2.10 (triclosan) and Table 2.11 (PHMB).

Table 2.8: MIC and MBC results from Ciprofloxacin and EO blend combination testing. Demonstrating the antimicrobial activity against *A. baumannii* and the lack of an increase in efficacy. Standard deviations were given in parentheses, for the MBC data the standard deviations were ±0.). * FIC value with a 95 % CI range that lies within the assigned FIC boundary.

	MIC (%)	MBC (%)
LO+GO + Ciprofloxacin	$0.185(\pm0.05) + 6.8\times10^{-5}(\pm2\times10^{-5})$ FIC 1.04 - indifferent	$1.6 + 5.9\times10^{-5}$
RO+GO + Ciprofloxacin	$0.83(\pm0) + 5.9\times10^{-5}(\pm0)$ FIC 2.21 – indifferent*	N/A
OO+MO + Ciprofloxacin	$>0.21 + 5.9\times10^{-5}$	N/A
OO+RO + Ciprofloxacin	$>0.21 + 5.9\times10^{-5}$	N/A
MO+GO + Ciprofloxacin	$>0.42 + 5.9\times10^{-5}$	N/A
MO+RO + Ciprofloxacin	$0.83(\pm0.23) + 5.9\times10^{-5}(\pm6.9\times10^{-6})$ FIC 2.21 – indifferent*	$0.83 + 5.9\times10^{-5}$
MO+LO + Ciprofloxacin	$0.83(\pm0.23) + 5.9\times10^{-5}(\pm6.9\times10^{-6})$ FIC 2.21 – indifferent*	N/A

The lavender + geranium blend combination with ciprofloxacin (Table 2.8) resulted in a reduction in the concentrations of oil (1.2 to 0.18 %(v/v)) and ciprofloxacin ($1x10^{-4}$ to $6.8x10^{-5}$ %(m/v)) required to inhibit the growth of *A. baumannii*. The median FIC obtained for the blend was indifferent at 1.04, with the 95 % CI range crossing the boundary between indifferent and additive behaviour. This indicated that although there was a reduction in concentration required the increase in activity was not significant in comparison to the EO blend and ciprofloxacin individually. For manuka + rosewood, rosewood + geranium and manuka + lavender, combinations with ciprofloxacin produced an indifferent median FIC with a 95 % CI range within the indifferent FIC boundaries. Therefore, despite all three combinations resulting in a reduction in concentration required for EO blend and ciprofloxacin, the improvement in activity was not significant. The other three EO blends did not yield MIC as there was microbial growth at all concentrations tested. In the case of manuka oil + geranium oil and oregano oil + manuka oil the highest oil concentration used in the EO / ciprofloxacin test was slightly lower than the MIC for the EO blend, 0.42 to 0.58 for manuka oil + geranium oil and 0.21 to 0.39 for oregano oil + manuka oil. These tests should be repeated using higher oil concentrations to determine if the addition of ciprofloxacin has a positive or negative effect on the EO blends. For oregano oil + rosewood oil the amount of EO blend required for inhibition was found to be higher than 0.21 %. This is higher than the value obtained for the EO blend on its own (0.14 %) suggesting that ciprofloxacin has a negative effect on the activity of oregano oil + rosewood oil on *A. baumannii.* Further testing needs to be conducted in order to analyse the effect of ciprofloxacin on the activities of the seven EO blends on MRSA and *P. aeruginosa.* Due to the subsequent analysis with PHMB (Table 2.11), and the improvement in antimicrobial activity of the EO and PHMB as a result of combination, it was determined that PHMB would be the biocide to be used in any further combination work. Therefore, analysis with MRSA and *P. aeruginosa* was not completed as part of this project).

There was a no improvement in antimicrobial activity observed as a result of the addition of ciprofloxacin to the EO blends against *A. baumannii*, in the cases where results were obtained. Taking into account the positive results obtained later with PHMB it was decided that it would not be a suitable use of time to

reassess the blends of manuka + geranium and oregano + manuka at higher concentrations with ciprofloxacin for antimicrobial activity.

Against *A. baumannii* (Table 2.9), five of the EO blends tested in combination with chlorhexidine (manuka + lavender, manuka + rosewood, manuka + geranium, manuka + oregano and oregano + rosewood) had median FIC of greater than 4. Therefore, the relationship between the oil blends and chlorhexidine was antagonistic meaning the combinations caused a significant reduction in activity compared to the constituent antimicrobials individually (95 % CI ranges also fell within the antagonistic range). This was as a result of the increase in concentration of chlorhexidine required to inhibit growth. In the combinations with manuka + oregano and oregano + rosewood there was a greater than 6 fold increase in the concentration of chlorhexidine in comparison to chlorhexidine individually.

The two remaining blends (rosewood + geranium and lavender + geranium) exhibited an indifferent relationship, which indicated that the combination of EO blend and chlorhexidine only provided antimicrobial activity equal to that of the constituent antimicrobials as individuals.

Five of the EO blends did exhibit a reduction in inhibition concentration as a result of being used in combination with chlorhexidine. However, this did not provide a significantly better antimicrobial as the same antimicrobial effect could be achieved by using chlorhexidine individually at concentrations lower than those in the combinations.

Four of the EO blend chlorhexidine combinations (manuka + lavender, manuka + rosewood, manuka + geranium and manuka + oregano) exhibited no significant improvement in antimicrobial activity against MRSA. The FIC values for all four of the blends were indifferent with 95 % CI ranges which were within the FIC range for indifference. The three remaining EO blend chlorhexidine combinations had median FIC values in the additive range. Therefore, the combinations could be said to provide some improvement in the activity of the constituent antimicrobials but not to a level that could be considered significant.

Against *P. aeruginosa* all combinations of chlorhexidine and the EO blends did not inhibit growth. For four of the oil blends (oregano oil + manuka oil, lavender

oil + geranium oil, rosewood oil + geranium oil and manuka oil + geranium oil) the highest concentration of oil tested was lower than the MIC obtained from the EO combination testing. (As a result of the good results subsequently obtained with PHMB, it was determined that for the purposes of this work, repeating the *P. aeruginosa* tests at higher concentrations would not be necessary). In addition the MRSA and *A. baumannii* testing had already indicated that combining the EO blends with chlorhexidine did not provide a significant improvement in the activities of both antimicrobials. Therefore, there would be no benefit to using a combination of EO blend and chlorhexidine over either the EO blends or chlorhexidine on their own.

Table 2.9: MIC and MBC data from combination testing of EO blends and chlorhexidine, demonstrating the negative effect on efficacy against *A. baumannii* and *P. aeruginosa*, and the lack of a positive effect on MRSA (for the FIC indices ind = indifferent, ant = antagonistic. Standard deviations for all data were 0. All FIC values had a 95 % CI range that lay within the assigned FIC boundary.

	Acinetobacter baumannii		MRSA		*Pseudomonas aeruginosa*	
	MIC (%)	MBC (%)	MIC (%)	MBC (%)	MIC (%)	MBC (%)
MO+LO + Chlorhexidine	$0.83 + 7.78 \times 10^{-4}$ FIC 4.19 - ant	$0.83 + 7.78 \times 10^{-4}$	$0.83 + 2.78 \times 10^{-4}$ FIC 2.59 - ind	$0.83 + 2.78 \times 10^{-4}$	$>1.6 + 7.7 \times 10^{-4}$	N/A
MO+RO + Chlorhexidine	$0.83 + 7.78 \times 10^{-4}$ FIC 4.19 - ant	N/A	$0.13 + 2.31 \times 10^{-4}$ FIC 1.07 - ind	$0.83 + 2.78 \times 10^{-4}$	$>1.6 + 7.7 \times 10^{-4}$	N/A
MO+GO + Chlorhexidine	$0.83 + 7.78 \times 10^{-4}$ FIC 5.37 - ant	N/A	$0.27 + 2.31 \times 10^{-4}$ FIC 2.04 - ind	$0.83 + 2.78 \times 10^{-4}$	$>0.83 + 7.7 \times 10^{-4}$	N/A
MO+OO + Chlorhexidine	$0.27 + 8.15 \times 10^{-4}$ FIC 5.26 - ant	$0.83 + 7.78 \times 10^{-4}$	$0.42 + 2.78 \times 10^{-4}$ FIC 3.12 - ind	$0.42 + 2.78 \times 10^{-4}$	$>0.83 + 7.7 \times 10^{-4}$	N/A
OO+RO + Chlorhexidine	$0.27 + 8.15 \times 10^{-4}$ FIC 8.33 - ant	$0.83 + 7.78 \times 10^{-4}$	$0.13 + 2.31 \times 10^{-4}$ FIC 1.00 - add	$0.13 + 2.31 \times 10^{-4}$	$>0.83 + 7.7 \times 10^{-4}$	N/A
RO+GO + Chlorhexidine	$0.55 + 8.15 \times 10^{-4}$ FIC 3.67 - ind	$1.6 + 7.78 \times 10^{-4}$	$0.185 + 1.46 \times 10^{-4}$ FIC 0.96 - add	$0.185 + 1.46 \times 10^{-4}$	$>0.83 + 7.7 \times 10^{-4}$	N/A
LO+GO + Chlorhexidine	$0.185 + 5.49 \times 10^{-4}$ FIC 2.11 - ind	$1.6 + 7.78 \times 10^{-4}$	$0.185 + 1.46 \times 10^{-4}$ FIC 0.65 - add	$0.185 + 1.46 \times 10^{-4}$	$>0.83 + 7.7 \times 10^{-4}$	N/A

By combining the EO blends with triclosan (Table 2.10), it was possible to reduce the concentration of both antimicrobials required for the inhibition of *A. baumannii* in comparison to their individual MICs. The best effect was observed for blends of manuka + lavender and manuka + rosewood. In both cases the concentration of EO blend was reduced from 1.200 % to 0.031 % (v/v) and the concentration of triclosan was reduced from 0.50 to 0.19 % (m/v). The median FICs obtained indicated a synergistic relationship. However, due to the large standard deviation (0.03) for the EO blend concentrations the 95 % CI ranges spanned the threshold of synergistic and additive behaviour. Therefore, it could not be said with confidence that the relationship was synergistic resulting in a significant improvement in the antimicrobial activity. The blend of lavender + geranium in combination with triclosan had an FIC of 0.75 and a 95 % CI range that lay within the range 0.5 to 1. This indicated that both antimicrobials had an improved activity in combination, but that the improvement over the individual MICs was not large enough to be significant. The four other blends had FIC's that were either indifferent or additive with a 95 % CI range that crossed the threshold of additive and indifferent behaviour. Therefore, there was no evidence to suggest that the combinations of rosewood + geranium, oregano + rosewood, manuka + oregano and manuka + geranium with triclosan resulted in any improvement in antimicrobial effectiveness.

In combination testing of triclosan and the EO blends against MRSA only three of the triclosan EO blends inhibited growth at the concentrations tested (manuka + lavender, manuka + rosewood and manuka + oregano). Of these three blends two showed a reduction in concentration of both the EO blend and triclosan required to inhibit growth (manuka oil + oregano oil reduced from 0.6 to 0.27 % and manuka oil + lavender oil reduced from 0.29 to 0.14 %, triclosan reduced from 0.5 to 0.24 and 0.22 % respectively). The FIC values for both combinations were found to be in the indifferent range. Therefore, despite the reduction in concentrations required of the antimicrobials the increase in antimicrobial activity was not significantly different. The blend of manuka + rosewood required an increased oil concentration (0.29 to 0.42 %). This resulted in an FIC value in the antagonistic range, indicating that combination with triclosan had a significant negative effect on the antimicrobial activity. Of the four blends which did not yield MIC's, three were tested at concentrations

higher than the MIC's obtained for the EO blends on their own. Oregano oil and rosewood oil showed an increase from 0.29 % (without triclosan) to > 0.42 % (with triclosan), rosewood oil + geranium oil and lavender oil + geranium oil showed increases from 0.6 % to > 0.83 % and 0.74 % to greater than 0.83 % respectively. The manuka oil + geranium oil blend showed no inhibitory effect up to 0.21 %, which is slightly lower than the EO blend MIC of 0.29 %.

Table 2.10: MIC and MBC data from combination testing of EO blends and triclosan (for the FIC indices syn=synergistic, add=additive, ind=indifferent). Demonstrating the positive effect on efficacy against *A.baumannii* and the negative effect on efficacy against MRSA. Standard deviations given in parentheses, for MRSA data MIC and MBC standard deviations were 0.). * FIC value with a 95 % CI range that lies within the assigned FIC boundary.

	Acinetobacter baumannii		MRSA	
	MIC (%)	MBC (%)	MIC (%)	MBC (%)
MO+LO + Triclosan	$3.1x10^{-2}$(0.03)+0.19(0.03) FIC 0.44 - syn	$9.3x10^{-2}$(0.1) + 0.24(0.01)	0.27+0.24 FIC 2.99 – ind*	0.27+0.24
MO+RO + Triclosan	$3.1x10^{-2}$(0.03)+0.19(0.03) FIC 0.44 - syn	$9.3x10^{-2}$(0.1) + 0.24(0.01)	0.42+0.22 FIC 4.66 ant*	0.42+0.22
MO+GO + Triclosan	0.14(0.15)+0.24(0.01) FIC 0.89 - add	0.42(0)+0.22(0)	>0.21+0.22	N/A
MO+OO + Triclosan	0.21(0)+0.22(0) FIC 2.51 – ind*	0.21(0)+0.22(0)	0.14+0.24 FIC 2.88 – ind*	0.14+0.24
OO+RO + Triclosan	$6.94x10^{-2}$(0.07)+0.24(0.01) FIC 1.96 – ind*	0.21(0)+0.22(0)	>0.42+0.22	N/A
RO+GO + Triclosan	0.27(0)+0.24(0) FIC 1 - add	0.27(0)+0.24(0)	>0.83+0.22	N/A
LO+GO + Triclosan	0.19(0)+0.19(0) FIC 0.75 – add*	0.19(0)+0.19(0)	>0.83+0.22	N/A

As the triclosan had had a negative effect on at least four of the blends tested against MRSA it was decided that it was not an effective biocide to combine with the EO blends. For this reason testing of the EO blends with triclosan

against *P. aeruginosa* and testing of manuka + geranium blend at higher concentrations were not undertaken.

The combination testing of PHMB with the EO blends (Table 2.11) against *A. baumannii* gave positive results. All seven of the blends tested exhibited reductions in the concentration of oil required to inhibit growth. The biggest reduction was for manuka oil + lavender oil, with the MIC falling from 1.2 % to 0.031 % (a reduction of approximately 97 %). The lowest reduction was observed for oregano oil + rosewood oil, with the MIC falling from 0.14 % to 0.069 %. In addition the required concentration of PHMB was also reduced for all combinations from $1x10^{-3}$ % to concentrations in the region of $5x10^{-5}$. The blend of oregano + rosewood had an indifferent FIC value (1.53). Therefore, the increase in antimicrobial activity for the constituents of this combinations was not deemed to be significant. The other six EO blend + PHMB combinations had synergistic FIC values with 95 % CI ranges well within the range for synergism. This indicated that the reduction in concentrations of the antimicrobials required for inhibition represented a significant increase in antimicrobial activity.

The combination of PHMB with the EO blends brought about large reductions in the amount of EO blend required to inhibit growth of MRSA relative to the EO blends on their own. The largest reduction in EO blend concentration required for inhibition was observed with the manuka oil and lavender oil blend, with MIC falling from 0.6 % to 0.031 % (a reduction of approximately 95 %).

PHMB / EO blend mixtures also had a positive effect against *P. aeruginosa*; the concentration of oil required to inhibit growth was greatly reduced. The greatest reduction in MIC was observed for manuka oil + geranium oil and lavender oil + geranium oil blends; in the latter cases a 99 % reduction in MIC was observed, relative to the blends alone.

The FIC values for all combinations against MRSA and *P. aeruginosa* were in the synergistic range; with 95 % CI ranges that were within the boundary for synergism. Therefore, the reduced concentrations required for inhibition represented a significant increase in the antimicrobial activity for both the EO blends and PHMB.

Table 2.11: MIC and MBC data from combination testing of EO blends and PHMB, demonstrating the reduction in EO blend and PHMB concentration required for MIC and MBC as a result (for the FIC indices syn = synergistic, ind = indifferent). Standard deviations for all data were 0. All FIC values had a 95 % CI range that lay within the assigned FIC boundary.

	Acinetobacter baumannii		MRSA		*Pseudomonas aeruginosa*	
	MIC (%)	MBC (%)	MIC (%)	MBC (%)	MIC (%)	MBC (%)
MO+LO + PHMB	$3.1x10^{-2} + 2.7x10^{-5}$ FIC 0.09 - syn	$3.1x10^{-2} + 2.7x10^{-5}$	$3.1x10^{-2} + 2.7x10^{-5}$ FIC 0.15 - syn	$0.28 + 7.4x10^{-5}$	$1.3x10^{-3} + 1.8x10^{-5}$ FIC 0.42 - syn	$1.3x10^{-3} + 1.8x10^{-5}$
MO+RO + PHMB	$9.3x10^{-2} + 4.7x10^{-5}$ FIC 0.24 - syn	$0.27 + 7.4x10^{-5}$	$3.1x10^{-2} + 2.7x10^{-5}$ FIC 0.26 - syn	$3.1x10^{-2} + 2.7x10^{-5}$	$5.1x10^{-3} + 1.8x10^{-5}$ FIC 0.01 - syn	$5.1x10^{-3} + 1.8x10^{-5}$
MO+GO + PHMB	$4.6x10^{-2} + 4.7x10^{-5}$ FIC 0.21 - syn	$4.6x10^{-2} + 4.7x10^{-5}$	$3.1x10^{-2} + 2.7x10^{-5}$ FIC 0.26 - syn	$0.19 + 4.7x10^{-5}$	$5.1x10^{-3} + 1.8x10^{-5}$ FIC 0.01 - syn	$5.1x10^{-3} + 1.8x10^{-5}$
MO+OO + PHMB	$2.3x10^{-2} + 4.7x10^{-5}$ FIC 0.49 - syn	$2.3x10^{-2} + 4.7x10^{-5}$	$3.1x10^{-2} + 2.7x10^{-5}$ FIC 0.26 - syn	$9.3x10^{-2} + 4.7x10^{-5}$	$5.1x10^{-3} + 1.8x10^{-5}$ FIC 0.01 - syn	$5.1x10^{-3} + 1.8x10^{-5}$
OO+RO + PHMB	$6.9x10^{-2} + 7.4x10^{-5}$ FIC 1.53 - ind	$0.21 + 8.8x10^{-5}$	$3.1x10^{-2} + 2.7x10^{-5}$ FIC 0.26 - syn	$3.1x10^{-2} + 2.7x10^{-5}$	$5.1x10^{-3} + 1.8x10^{-5}$ FIC 0.03 - syn	$5.1x10^{-3} + 1.8x10^{-5}$
RO+GO + PHMB	$9.3x10^{-2} + 4.7x10^{-5}$ FIC 0.24 - syn	$9.3x10^{-2} + 4.7x10^{-5}$	$6.2x10^{-2} + 2.7x10^{-5}$ FIC 0.27 - syn	$6.2x10^{-2} + 2.7x10^{-5}$	$5.1x10^{-3} + 1.8x10^{-5}$ FIC 0.01 - syn	$1x10^{-2} + 5.4x10^{-5}$
LO+GO + PHMB	$9.3x10^{-2} + 1.6x10^{-5}$ FIC 0.20 - syn	$9.3x10^{-2} + 4.7x10^{-5}$	$6.2x10^{-2} + 2.7x10^{-5}$ FIC 0.21 - syn	$0.19 + 4.7x10^{-5}$	$3.9x10^{-3} + 3.5x10^{-5}$ FIC 0.02 - syn	$3.9x10^{-6} + 3.5x10^{-6}$

For the EO blend/PHMB combinations it appeared that the concentration of PHMB was an important factor, especially for MRSA and *P. aeruginosa*. For MRSA the required PHMB MIC was the same for 7 of the combinations tested and for *P. aeruginosa* the required MIC was the same for 6 of the combinations tested. Comparing the MIC of PHMB against MRSA and *P. aeruginosa* with the concentration of PHMB in the EO biocide blends suggests that addition of the EO blends boosted the activity of PHMB as well as PHMB increasing the activity of the EO. Against MRSA, the amount of PHMB required fell from $1x10^{-3}$ % to $2.7x10^{-4}$ % (v/v) for all seven of the blends. Against *P. aeruginosa* the concentration of PHMB was reduced from $4x10^{-3}$ % to $1.8x10^{-4}$ % (v/v) for six of the seven blends with a greater reduction for the blend with lavender oil + geranium oil ($4x10^{-3}$ to $3.5x10^{-5}$ % (v/v)).

The strong positive relationship between PHMB and the oils was possibly due to the modes of actions of the compounds. It is believed that EO act on the cell membrane increasing the permeability of the cell [78]. PHMB acts on the cell membrane and also on the DNA of the cell [79]. For PHMB to act on the cell DNA it needs to enter the cell, this process could be facilitated by the damage caused to the cell membrane by the EO allowing the PHMB to act faster on the cell thus reducing the concentration required to cause cell death. In addition, it is possible that the EO molecules and the PHMB were acting on different components of the cell membrane resulting in a more rapid degradation of the membrane integrity, thus the point at which the cell membrane was damaged sufficiently to result in cell death was reached more rapidly.

2.5.6 Gas chromatography - mass spectroscopy analysis of the chemical makeup of essential oils

The five EO were analysed using Gas chromatography - mass spectroscopy (GC-MS) in order to determine the relative levels, and retention times of the major components. The definition of a major component in this study was one which comprised more than 1 % of the oil.

The rosewood oil used in this study was comprised of eighteen major compounds (Figure 2.4). The most abundant molecule is linalool which accounts for almost 90 % of the oil. Only five other components account for more than 1 % of the oil, these were: limonene, eucalyptol, *cis*- and *trans*-linalool oxides and α-terpineol. Linalool has been shown to have antimicrobial properties [80, 81] and is therefore likely to be largely responsible for the antimicrobial activity of rosewood oil.

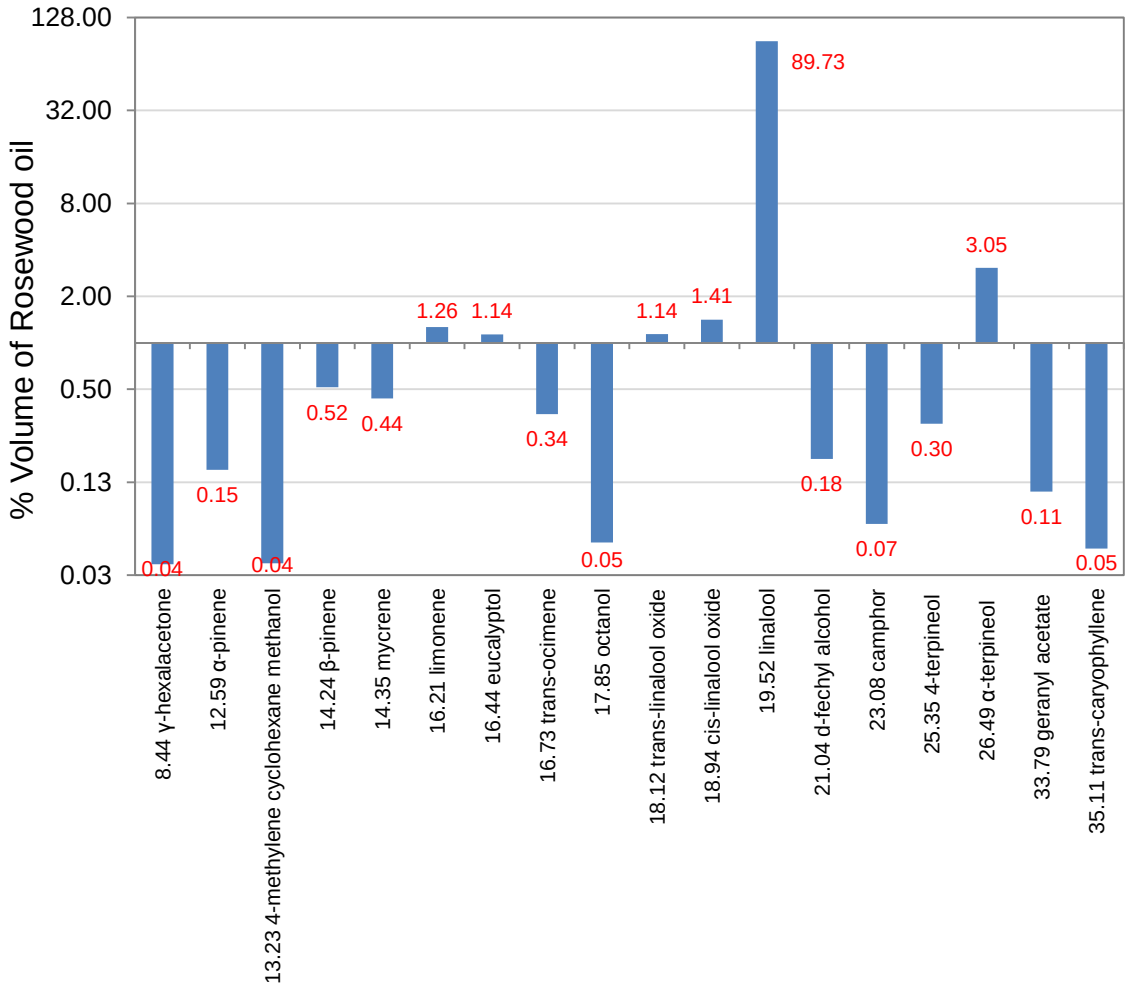

Figure 2.4: The major components of rosewood oil (RO) as determined by GC-MS. The numbers in red are the % composition of each component. The information on the x-axis is the retention times and chemical name of each component. Linalool was the major component of RO comprising 89.73 %. The graph uses a $\log_4$ scale where the x-axis crosses the y-axis at 1. A linear scale would result in the difference between the low percentage components being indistinguishable due to the size of the linalool bar.

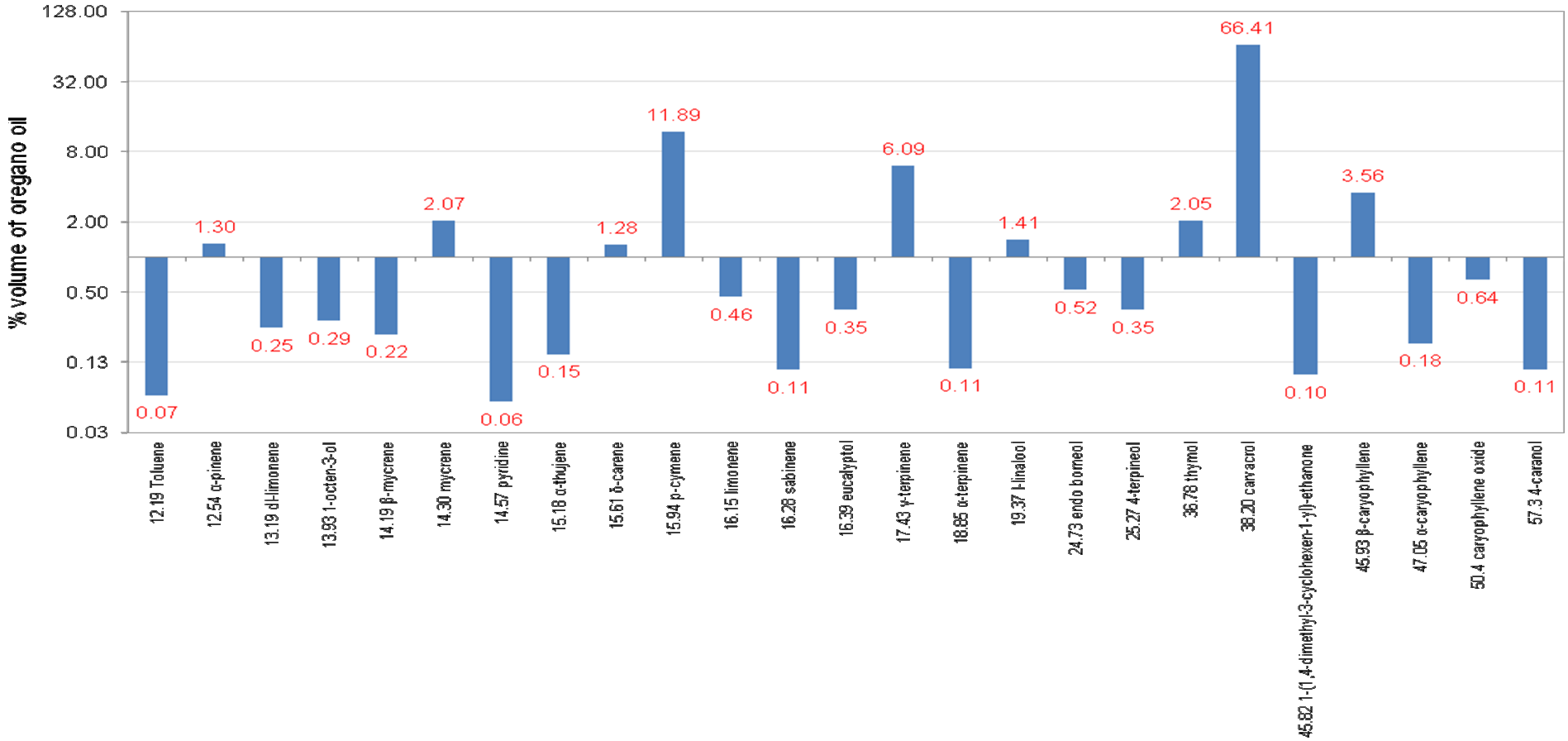

Figure 2.5: Graph displaying the major components of oregano oil (OO) The numbers in red are the % composition of each component. The x-axis labels the retention times and chemical name of each component. Demonstrating which molecules comprised the majority of the oil. The graph uses a $\log_4$ scale where the x-axis crosses the y-axis at 1. A linear scale would result in the difference between the low percentage components being indistinguishable due to the size of the carvacrol bar.

There were 25 major components of oregano oil observed in the GC-MS data (Figure 2.5). Carvacrol was the most abundant molecule comprising approximately 66 % of the oil. There are eight other molecules which account for more than 1 % of the oil: α-pinene, mycrene, δ-carene, p-cymene, γ-terpinene, l-linalool, thymol and β-caryophyllene. The high level of carvacrol present in oregano oil suggests a reason for the observed level of toxicity against *P. aeruginosa* in Section 2.5.1. Carvacrol has been shown to act on the outer lipopolysaccharide membrane of gram-negative bacteria [41], therefore the efflux mechanism which provides protection against other EO molecules would be negated.

GS-MS data revealed that there were 24 major components of lavender oil (LO) (Figure 2.6). Unlike oregano oil and rosewood oil, there is no dominant molecular component in lavender oil. Instead linalool and linalyl acetate comprise approximately 65 % of the oil. In comparison to oregano oil and rosewood oil, there are also far more molecules (15 in fact) that account for at least 1 % of the oil.

The proportion of each of the 25 major components of geranium oil (GO) was determined (Figure 2.7). Approximately 68 % of the oil is comprised of three molecules, linalool (17 %), R citronellal (27 %) and geraniol (24 %). There were seven other molecules that comprise more than 1 % of the oil, the most abundant of these are l-menthone, citronellyl formate, β-bourbonene and methyl benzoate.

Manuka oil (MO) was the most complex of the five oils used with 35 major components (Figure 2.8). Of the 35 molecules, 15 account for at least 1 % of the total volume of the oil, with four making up 10 % or more [isoledene (10.5 %), β-selinene (10.2 %), *cis*-calamenene (18.5 %) and cadina-1,4-diene (13 %)].

In Section 2.4.4, it was reported that manuka and oregano oils showed the highest levels of antimicrobial activity. Lavender, geranium and rosewood oils showed similar levels of activity to each other and were much less active than manuka and oregano. From the GC-MS, analysis it can be seen that the major

components of geranium oil, rosewood oil and lavender oil were similar in structure. All of the molecules for these oils which accounted for at least 10 % of the oil's composition were straight chain monoterpenes, with a single oxygen atom, either in the form of an alcohol or aldehyde. The exception to this was linalyl acetate, which is the acetate ester of linalool and therefore has two oxygen atoms.

The major molecular components in oregano oil and manuka oil had significantly different structure to those of the other three oils. The two major components of oregano oil were benzene based molecules which differ only in term of an alcohol group present on carvacrol (66 %), but absent on para-cymene (11.89 %). Manuka oil also featured major components which were cyclic; in this case, however, they were bicyclic molecules. Three of the four major molecular components of manuka oil were naphthalene based (2 fused phenyl rings), the fourth (isoledene) was a tricyclic molecule composed of 3, 5, and 7 membered rings. None of the major molecules of manuka oil had any oxygen based functional groups.

The mechanism of action of EO molecules against bacterial cells has been investigated in recent years. Studies have shown that the hydrophobic EO molecules accumulate in the cell membrane due to their attraction to the hydrophobic lipid tails of the phospholipid bi layer [39]. The accumulation of EO molecules in the cell membrane leads to structural instability, creating holes which release cell constituents and eventually breakdown of the membrane resulting in cell death [40]. The mode of action of EO provides an explanation for the higher susceptibility of the bacteria tested in Section 2.5.2 to manuka and oregano oil. Cyclical molecules would occupy more space in the phospholipid bi layer, compared to the straight chain molecules in lavender, geranium and rosewood, resulting in fewer molecules required to destroy the structural integrity of the bacterial cell.

As rosewood oil was the least complex of the oils, it was selected for use in the initial stages of the adsorption studies to determine which of the inorganic substrates might be the most effective at encapsulating the oils. Once the initial screening had been carried out, the best performing substrates were selected for adsorption studies with all of the oils.

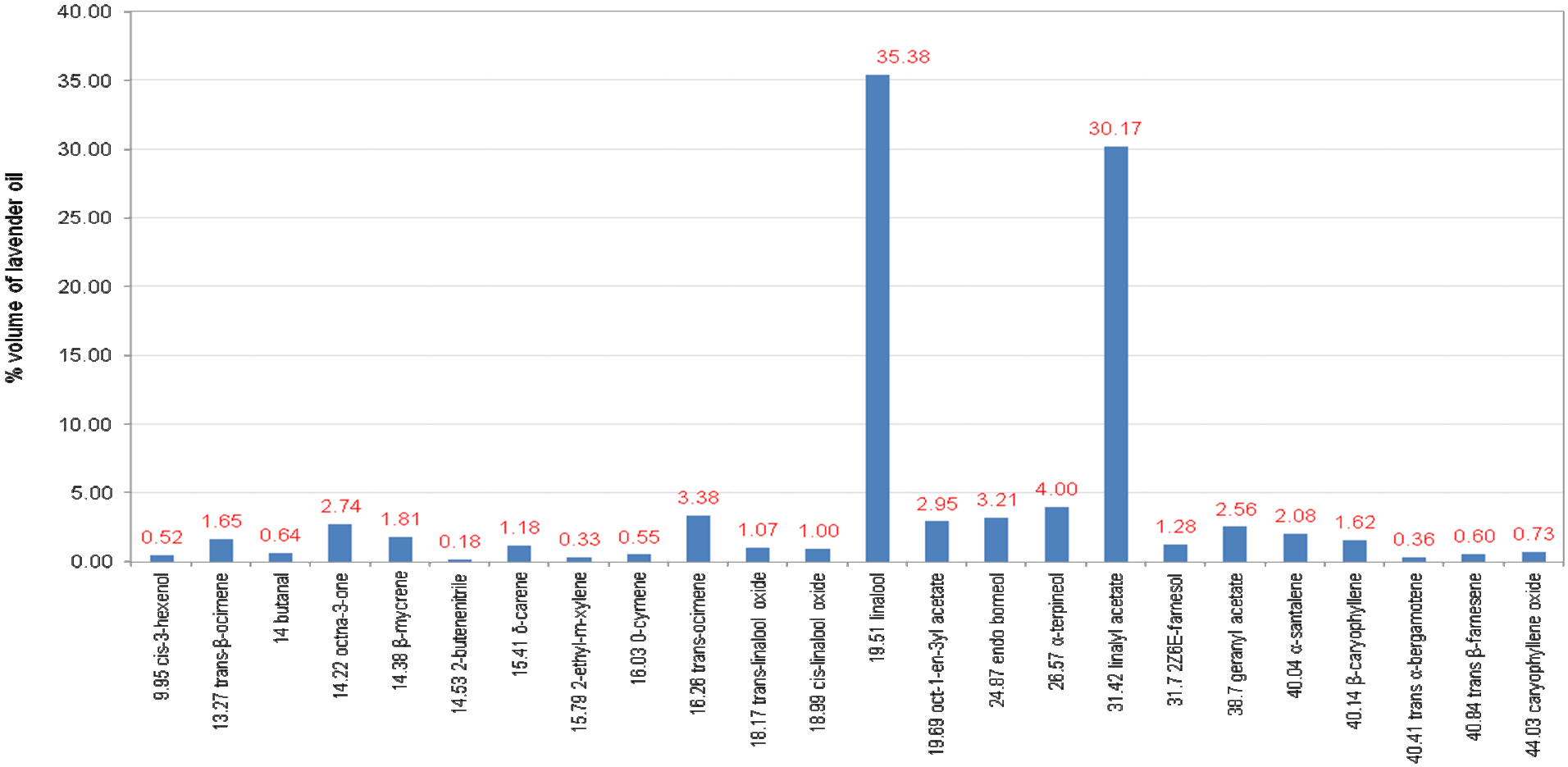

Figure 2.6: Graph displaying the major components of lavender oil (LO) The numbers in red are the % composition of each component. The x-axis labels the retention times and chemical name of each component. Demonstrating which molecules comprised the majority of the oil.

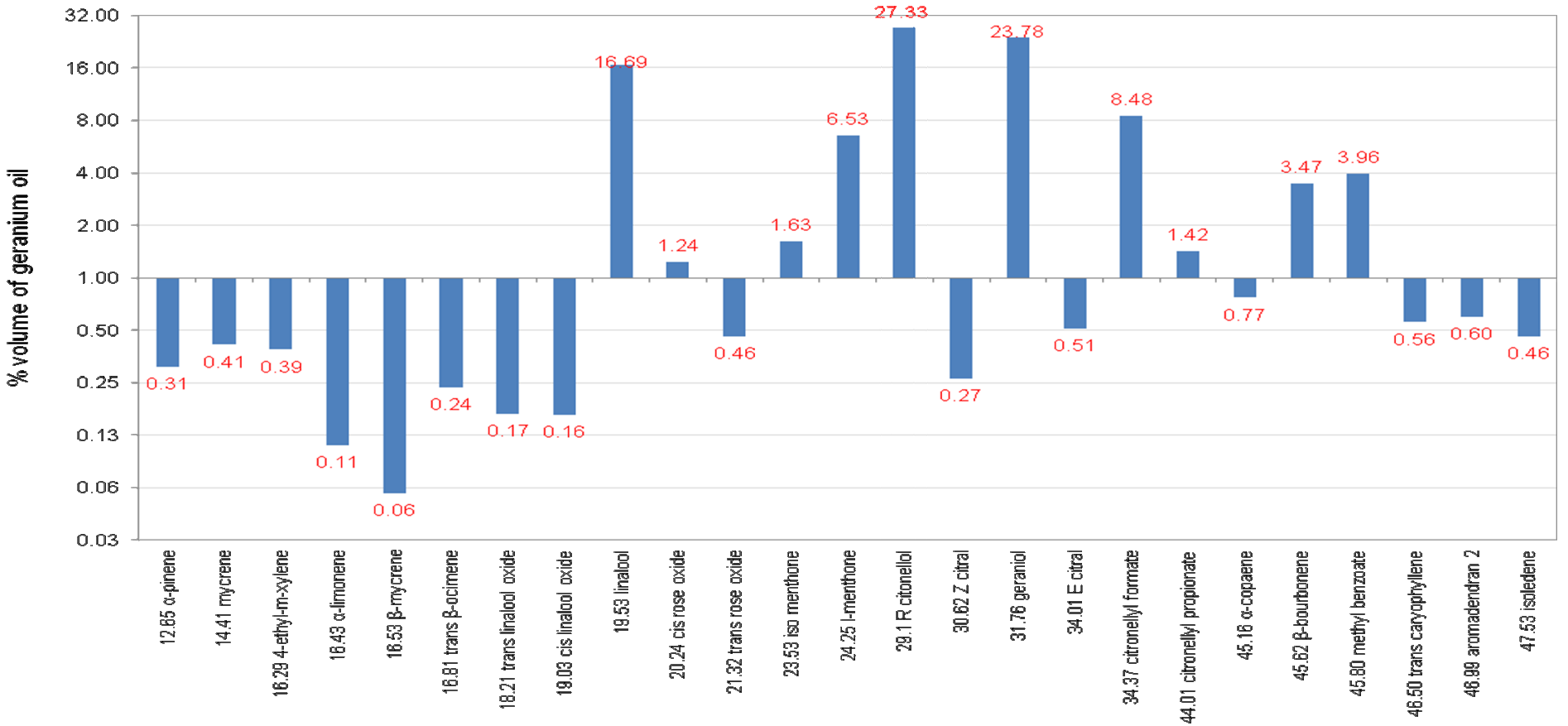

Figure 2.7: Graph displaying the major components of geranium oil (GO) The numbers in red are the % composition of each component. The x-axis labels the retention times and chemical name of each component. Demonstrating which molecules comprised the majority of the oil. The graph uses a $\log_2$ scale where the x-axis crosses the y-axis at 1. A linear scale would result in the difference between the low percentage components being indistinguishable due to the size of the citronellol and geraniol bars.

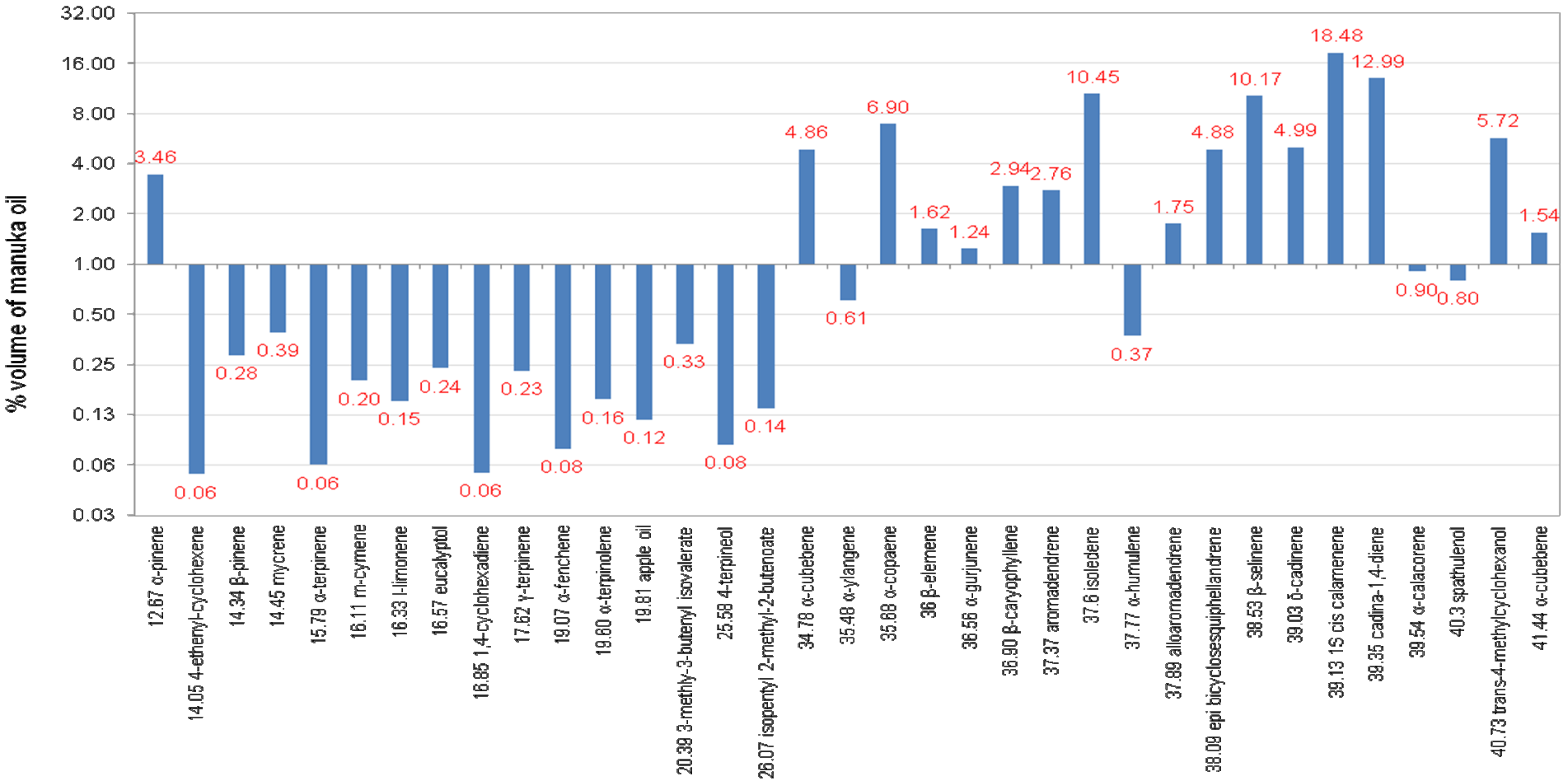

Figure 2.8: Graph displaying the major components of manuka oil (MO) The numbers in red are the % composition of each component. The x-axis labels the retention times and chemical name of each component. Demonstrating which molecules comprised the majority of the oil.

Using the data obtained via GC for the EOs a list of most common molecular features of the component molecules of the oils was comprised and summarised (Table 2.12).

Table 2.12: Summary of the molecular features present on the essential oil molecules. Demonstrating the differences in chemical makeup of the oils, with RO containing the highest number of molecules with polar functional groups, and MO containing the lowest number of molecules with polar functional groups.

Essential Oil	Polar functional groups		Conjugated double bonds		Double bonds only	
	No.	% of oil	No.	% of oil	No.	% of oil
RO	12	96.90	2	0.78	4	1.98
OO	11	72.29	6	14.36	8	12.10
LO	14	92.63	4	1.10	7	6.28
GO	14	83.87	6	8.22	4	5.24
MO	7	7.41	8	25.81	20	67.24

Rosewood oil and lavender oil were almost entirely comprised of molecules containing polar functional groups. It was speculated that this may prove to be beneficial for adsorption onto the layered silicate substrates which are hydrophilic in nature. Conversely the low proportion of polar functional groups present in manuka oil may have a limiting effect on the mass of EO which can be adsorbed onto the substrates.

2.6 Conclusions

- Five EO were selected as antimicrobials; oregano, manuka, rosewood, lavender and geranium.
- Manuka oil and oregano oil exhibited the highest level of antimicrobial activity against the three test micro organisms, this effect may be due to the presence of a high number of cyclic molecules. The latter were speculated to cause greater damage to the cell membranes than linear molecules.
- Blending of the EO enabled the identification of seven blends which displayed a reduction in the overall level of oil required for antimicrobial activity in comparison to the individual oils. All seven of the blends successfully inhibit bacterial growth at total oil levels of less than 2 % (v/v). However, none of the blends exhibited full synergism against all three of the test bacteria. The blend of oregano oil and rosewood oil in a 3:1 ratio gave in the best level of antimicrobial activity.
- Addition of PHMB to the seven EO blends resulted in a positive effect on antimicrobial activity against all three test micro organisms. Thus addition of PHMB to a polymer material containing EO blends could increase the antimicrobial activity of the formulation.
- Lavender, geranium and rosewood oils exhibited similarities in chemical composition, with all three being comprised mainly of straight chain terpene molecules. In contrast manuka and oregano oils were comprised mainly of cyclic molecules, oregano oil molecules were predominantly monocyclic and manuka oil molecules were predominantly bicyclic.
- The larger cyclic molecules in manuka and oregano oil are likely to be a significant factor in their greater antimicrobial activity compared to lavender, rosewood and geranium oils.

CHAPTER 3

Adsorption of essential oils onto layered silicate substrates

Abstract

This study assessed the suitability of layered silicate substrates as adsorption media for an antimicrobial EO blend, in order to develop a controlled release mechanism for the EO. Three montmorillonites (MMT), a natural/synthetic hybrid MMT and two synthetic layered silicates were selected as potential adsorption materials. Gas chromatography (GC) and flow micro-calorimetry (FMC) were used to follow the static and dynamic adsorption of the EOs from heptane respectively. The GC adsorption studies allowed the effect of adsorption on the individual molecular components of the oils to be determined, while FMC allowed the determination of the overall level of adsorption and the strength of adsorption of the oil. The MMTs were found to degrade some of the important molecules in the EO and were therefore deemed to be unsuitable. The synthetic layered silicates provided the highest levels of adsorption in both the GC and FMC studies, achieving up to 170 $mg.g^{-1}$ adsorption, without the degradation effects shown by the natural MMTs. The synthetic layered silicates also gave the highest strength of adsorption which resulted in a greater controlled release effect as the molecular components take longer to desorb.

3.1 Introduction

Incorporation of an essential oil (EO) based antimicrobial directly into polymer materials is unlikely to prove beneficial, as EO are highly volatile and will bloom to the surface and rapidly volatise out of the polymer, resulting in a loss of antimicrobial activity. Adsorption of the EO onto a porous material such as montmorillonite before addition to the polymers may provide a reservoir of the EO and therefore enable a controlled release.

3.1.1 Montmorillonite structure

Montmorillonites are part of the smectite family of minerals (Section 1.4), and exhibit large surface area due to the galleries between the platelets, making them ideal adsorbents.

In montmorillonite (MMT) for every five Al^{3+} ions in the octahedral sheet there is one Mg^{2+} ion, giving the general composition $[(Al_{4-x}Mg_x)Si_8O_{20}(OH_4)]$ where x is ⅔. Because the magnesium ions have a lower charge (+2) than the aluminium (+3) there is a charge imbalance on the material. To address this, cations usually Na^+, are adsorbed onto the external and internal surfaces of the material to make the overall charge neutral thus giving the general formula $Na_x[(Al_{2-x}Mg_x)Si_4O_{10}(OH_2)]$.

3.1.2 Adsorption of organic material onto montmorillonite

The high surface area of MMT materials, resulting from their layered structure makes them an ideal adsorbent. The adsorption properties of MMT are well documented in the scientific literature, with many examples of adsorption of organic material some of which are reported below.

Gianotti *et al.* (2008) [82], examined the adsorption of 2,4,6-trichloroanaline (2,4,6-TCA) and 4-chlorophenol (4-CP) by Na-MMT from a reference soil mixture. They found that individually 10 mg g^{-1} of 2,4,6-TCA and 5.8 mg g^{-1} of 4-CP was adsorbed into the structure of the clay. When adsorption took place from a mixture of 2,4,6-TCP and 4-CP the amounts adsorbed were 3.1 and 1.2 mg g^{-1} respectively. Desorption characteristics were also investigated, 2,4,6-TCA was not desorbed, 2-CP was released in varying amounts depending on the leaching agent. The maximum desorption occurred in hydro-organic solutions.

Parolo *et al*. (2012) [83], measured the uptake of the antibiotic tetracycline on Ca^+MMT by following the reduction in concentration to tetracycline from solution. They found that the presence of Ca^+ ions in the pores of MMT had a significant effect on the process of adsorption. With no Ca^+ present adsorption was highest at low pH, however with Ca^+ present adsorption was highest at pH > 5. In general the presence of Ca^+ was found to be beneficial to adsorption of tetracycline.

Giménez *et al.* (2012) [28], reported improved retention of clove oil within gelatin-egg white films with the addition sepiolite, indicating adsorption of the oil onto silicate materials. However they did not publish any in depth studies analysing the adsorption of the clove oil onto sepiolite. The author has been unable to find any work which specifically monitors the adsorption of EO onto MMT materials reported in literature.

3.1.3 Desorption of material from montmorillonite

Allowing material to desorb off after adsorption will be a vital property for any material used in this study, as the antimicrobial EO blend will need to be available if it is to have any effect. Desorption of organic material from MMT has been less extensively studied than adsorption.

Sannino *et al.* (1999) [84], studied the adsorption of simazine (a herbicide) onto MMT and hydroxy aluminum coated MMT (aMMT) in order to obtain deeper insight in to the understanding of how pesticides build up in soil. As part of this study they also examined the desorption of simazine from MMT materials in order to assess how much of the pesticide adsorbed in soil may be released back into the wider environment. They found that only negligible quantities desorbed from unmodified MMT over a 24 h period, whilst in some cases aMMT gave rise to more rapid desoprtion over the 24 h period.

Wang *et al.* (2005), analysed the desorption of 2,4,6-trichlorophenol (2,4,6-TCP) from MMT into a 0.01 M KCl solution with 100 µg mL^{-1} NaN_3. They found that the 2,4,6-TCP desorbed in a biphasic fashion with an initial fast release of 2,4,6-TCP followed by an increasingly slower release as the desorption proceeded [85].

Kim *et al.* (2005) [86], used MMT organically modified with hexadecyltrimethylammonium (HDTMA) to adsorb 2,4-dichlorophenyl (2,4-DCP) and 2,4,5-trichlorophenol (2,4,5-TCP). They then studied desorption of both compounds from the HDTMA-MMT under controlled pH (4.85 and 9.15). For 2,4-DCP adsorbed at pH 4.85 desorption was more effective at pH 4.85 (K_F = 2.83 (mg/g)/(mg/L)^{NF}) than at pH 9.15 (K_F = 0.78 (mg/g)/(mg/L)^{NF}). The same was true for 2,4-DCP adsorbed at pH 9.15 with K_F values of 2.70 and 0.83 at pH 4.85 and 9.15 respectively, and 2,4,5-TCP adsorbed at pH 4.85 with K_F values of 20.17 and 2.39 at pH 4.85 and 9.15 respectively. Desorption of 2,4,5-TCP

adsorbed at pH 9.15 did not differ substantially depending on pH with K_F values of 3.88 and 3.12 at pH 4.85 and 9.15.

3.1.4 Adsorption substrate materials

3.1.4.1 Naturally derived substrates from montmorillonites

The substrates derived from natural MMT used in this thesis can be further divided into three groups depending on the processing conditions of the material; group 1 included Fulcat® 400 and Fulcat® 435, group 2 contained Fulacolor® XW and group 3 contained Fulcat® 800.

Fulcat® 400 is defined by Rockwood Additives Ltd. as a refined natural MMT clay catalyst and adsorbent with a moderate surface area [87], Fulcat® 400 contains Lewis and Brønsted acid sites resulting from the replacement of Si with Al in the tetrahedral silicate sheet (Figure 3.1).

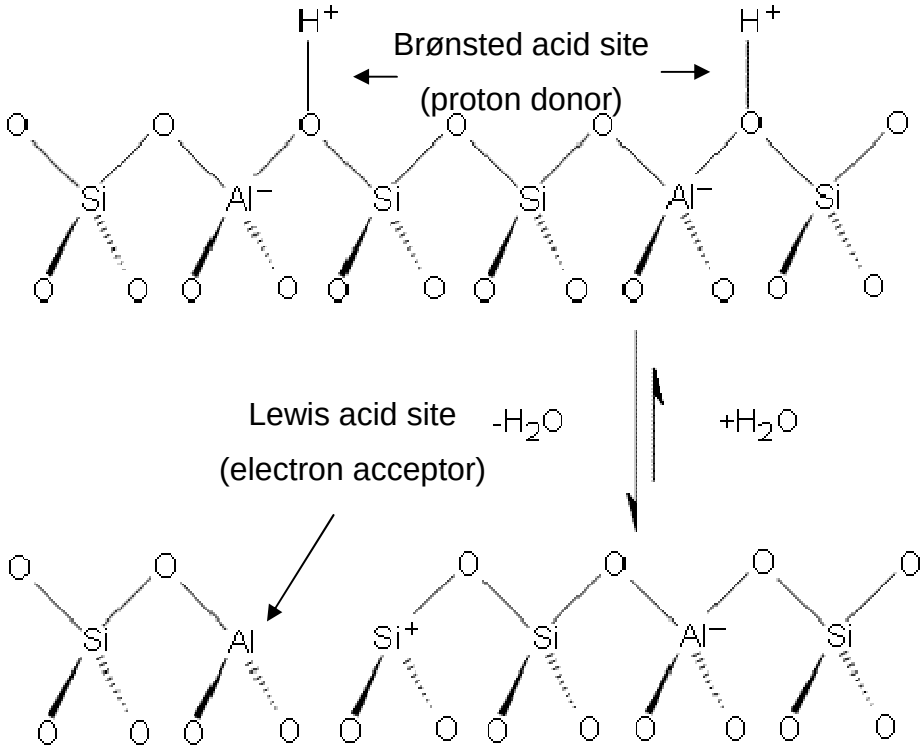

Figure 3.1: Representation of Lewis and Brønsted acid sites in the tetrahedral silicate layer of montmorillonite [88]. Demonstrating where the acidity of MMTs originates from.

The Lewis and Brønsted acid sites in the structure of the Fulcat® 400 provide these MMTs with their catalytic properties.

Fulcat® 435 is also defined as a natural MMT clay catalyst and adsorbent [89]. Iit differs from Fulcat® 400 in that it has been acid activated using sulphuric acid. Acid activation of the clay has a number of effects; the acid leaches the metal ions from the octahedral layer of the clay structure while leaving the Si tetrahedral layer intact [90]. This has the effect of increasing the surface area of the material by exposing the side of the tetrahedral sheet which is normally bound to the octahedral metal ions (Figure 3.2).

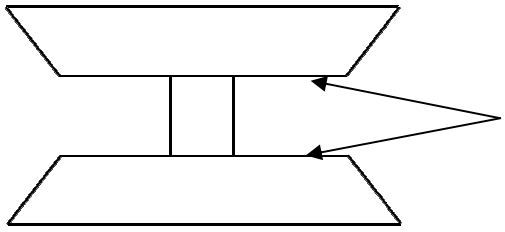

Figure 3.2: Schematic representation of MMT after acid treatment with alumina removed from the edges of the platelets exposing the inner silica surface.

Increasing the surface area will result in an increase in the number of adsorption sites and could therefore have a beneficial effect on adsorption. The increase in surface area resulting from acid activation of Fulcat® was large with Fulcat® 400 having a surface area of 80 $m^2.g^{-1}$ and Fulcat® 435 having a surface area of 350 $m^2.g^{-1}$ [87, 89]. Acid activation also has an effect on the acidity of the MMT, resulting in a 2 % wt. solution of Fulcat® 435 having a pH of 3.5 compared to 8.5 for Fulcat® 400 [87, 89]. The increase in activity is a result of two factors; during the acid treatment the counter cations in the pores of the MMT are exchanged with H^+ from the acid [91], there is also an increase in the number of Brønsted acid sites associated with structural OH groups [92].

Fulacolor® XW, like Fulcat® 435, is a natural MMT which has been acid activated with sulphuric acid, it has a surface area of 285 $m^2.g^{-1}$ (placing it in between the Fulcat® substrates) and a 2 % wt. solution gives a pH of 3.5. Fulacolor® is predominantly used as a colour developer for carbonless systems [93].

Fulcat® 800 is a development product of Rockwood Additives Ltd. which is defined as a chemically modified natural/synthetic hybrid MMT. No details were been provided regarding its structure / morphology.

3.1.4.2 Synthetic layered silicates; Laponites®

The two synthetic layered silicates provided by Rockwood Additives Ltd. were from their range of Laponite® materials, which are defined by Rockwood Additives Ltd. as layered silicate colloids manufactured from naturally occurring inorganic mineral sources [94]. Laponites® differ from natural MMT in a number of key ways, most notably chemical composition, particle size and particle size distribution. Natural MMT are aluminosilicates, with a basic structure of octahedral alumina sheets sandwiched between two silica sheets, in Laponites® the central octahedral sheet is comprised of Mg^{2+} ions instead of Al^{3+} ions. The two Laponites® used in this study were Laponite® B and Laponite® RD and they have the empirical formulae:

Laponite B $Na_{0.7}^{+}$ $[(Si_8Mg_{5.5}Li_{0.3})O_{20}(OH_{2.5})F_{1.5}]^{0.7-}$

Laponite RD $Na_{0.7}^{+}$ $[(Si_8Mg_{5.5}Li_{0.3})O_{20}(OH_4)]^{0.7-}$

The difference in formulae result from different reaction conditions where Laponite® B is produced using HF results in some of the structural OH^- being replaced by F^-. The Li^+ in the structure perform the same function as Mg^{2+} in MMT, resulting in a charge imbalance across the structure which is balanced with the Na^+ counter ions. Laponites® have a small particle size (25 nm) [94] compared to MMT platelets which can be up to 1000 nm across [95]. As well as a much smaller particle size Laponite® particles are uniform in shape and size while MMT particles can range from 10 nm to 1000 nm [95]. The small uniform particle size results in a much higher surface area for Laponites® (373 and 412 $m^2.g^{-1}$ for RD and B respectively) compared to 80 $m^2.g^{-1}$ for the natural MMT, Fulcat® 400.

3.1.5 Analytical techniques

The specific techniques used for the characterisation of layered silicates and the analysis of EO adsorption onto said silicates.

3.1.5.1 Fourier transform infrared spectroscopy

In Fourier transform infrared spectroscopy (FTIR) a beam of light in the infrared (IR) region of the electromagnetic spectrum is passed though a sample (the sample is diluted with KBr and commonly pressed into a disc). Certain wavelengths of the IR beam are absorbed by the chemical bonds in the sample because the frequency of the IR radiation matches that of certain vibration modes of the bonds. IR frequencies that do not coincide with bond vibration modes are transmitted straight through the sample to a detector. Once the beam hits the detector it is analysed using the Fourier transform mathematical operation which produces a spectrum of the wavelengths absorbed. The wavelength of absorption of bonds in a specific chemical group is unique, always producing the same peak, and therefore the FTIR spectrum can be used to determine the chemical makeup of a sample. In addition changes in the chemical environment of a bond can result in shifting and/or broadening of the resultant peak; due to this FTIR can be used to analyse interactions between molecules and substrates. For example, hydrogen bonding of a C=O of an adsorbate molecule to an H–O group of the substrate, will result in a weakening of the original C=O bond causing it to absorb energy at a slightly lower, resulting in the FTIR peak shifting to lower energy. The H-O vibrations will also be attenuated / shifted as a result of the interaction.

3.1.5.2 Diffuse reflectance infrared Fourier transform spectroscopy

Diffuse reflectance infrared Fourier transform spectroscopy (DRIFTS) is a specific type of FTIR which enables the use of a powdered sample rather than having to press samples into KBr discs. The powdered sample is diluted with KBr and placed in a DRIFTS cell, the IR beam is focused at the centre of the sample to be analysed and radiation is adsorbed at specific wavelengths in the

same way as traditional FTIR. The reflected IR radiation is focused using an elliptical mirror back into a beam which is passed into a detector for analysis. A diagrammatical representation of a DRIFTS cell is shown (Figure 3.3).

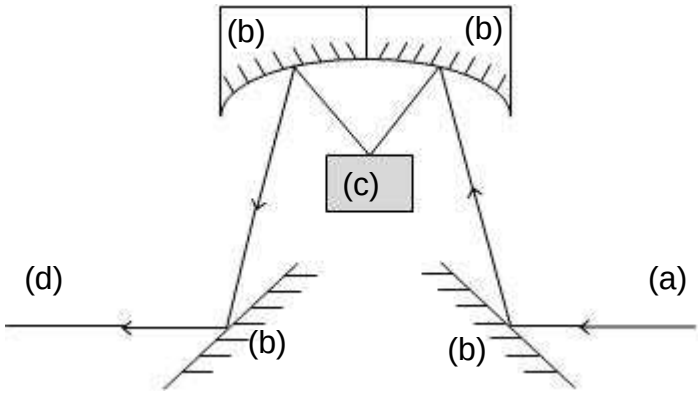

Figure 3.3: Diagrammatical representation of drifts cell, (a) IR beam from source, (b) focusing mirrors, (c) sample, (d) refocused beam to detector.

The advantage of DRIFTS over standard FTIR methods is that it eliminates the need for grinding and preparation, thus removing the risk of modifying the chemical nature of the sample before analysis. In addition, in comparison to transmission IR, DRIFTS is more surface specific as a result of a significant proportion of low end glancing angle reflections through filler layers [96].

3.1.5.3 Wide angle X-ray scattering

Wide angle X-ray scattering (WAXS) is an analysis technique which is commonly used for the determination of the structure of a material. When X-rays are passed through a material they are diffracted by the atoms in the structure (scattering centres). If the scattering points are disordered such as in an amorphous, material the waves will be refracted in all directions resulting in destructive and constructive interference. The latter will occur at a distribution of random angles of incidence in an amorphous material. If the scattering centres are in an ordered arrangement (such as in the crystalline structures) then constructive and destructive interference occurs at sharply defined angles of incidence (Figure 3.4).

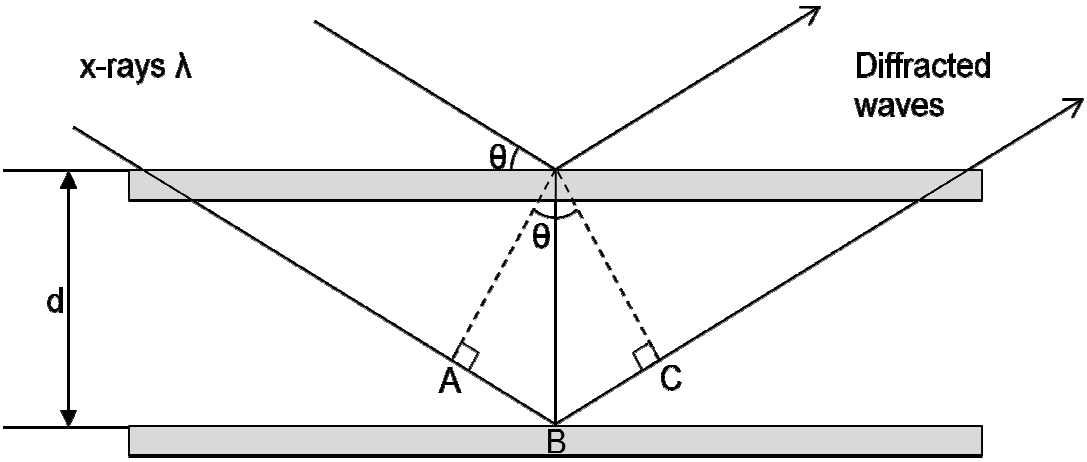

Figure 3.4: Diffraction of x-rays within a crystalline structure, used to determine the distance between platelets of the layered silicates.

These waves can be detected and used to determine the spacing between planes of electron density (scattering planes). If the distance AB+BC is equal to a whole number of wavelengths (i.e. AB+BC = nλ) then constructive interference will occur and the Bragg equation (Equation 3.1) can be used to determine the distance between the two crystalline planes;

Equation 3.1: $2d\sin\theta = n\lambda$

Where θ is the angle of refraction, d is the distance between the planes, λ is the x-ray wavelength and n is an integer.

3.1.5.4 Flow micro-calorimetry

Flow micro-calorimetry (FMC) is a technique which can be used to calculate the enthalpies of adsorption/desorption of a probe (from solution) on to a substrate [97, 98]. Under continuous flow, a solvent containing a dissolved probe molecule (the solution) is passed through a cell containing a known mass of the adsorption substrate. As the solution passes over the substrate any chemical interactions between the probe and the substrate will result in minute changes in temperature which are measured using thermistors. Once the solution has passed through the cell it is fed into a differential refractometer, which measures the changes in the refractive index which are proportional to the concentration

of the probe. A diagrammatic representation of an FMC cell is presented (Figure 3.5).

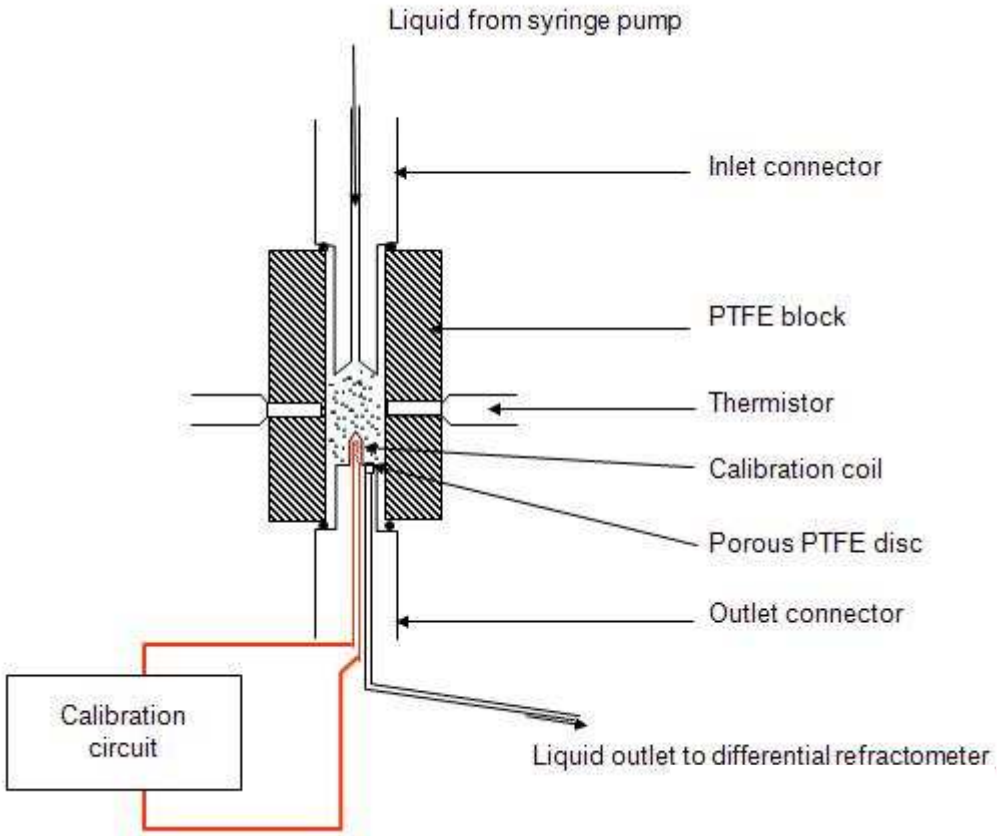

Figure 3.5: Diagram of FMC cell.

The FMC used in this study was a Microscal© 3Vi, this apparatus utilises two pairs of thermistors, two of which are in direct contact with the cell, There are other reference thermistors, which are buried deep within the walls of the cell. The thermistors are in a Wheatstone bridge arrangement and can detect temperature changes as small as 10^{-5} ℃. The bridge circuit outputs its signal to an A/D converter within a chromatography data station. A Waters© 410 differential refractometer is connected downstream from the cell and detects changes in probe concentration, and outputs the data to the chromatography data station. A computer running chromatography software records the data from both apparatus as a function of time. (Details of the equipment and software used were given in Section 3.4.4).

Initially the pure carrier solvent (heptane) is passed through the cell, this serves two purposes; firstly to remove any water molecules loosely bound to the substrate and secondly to allow an equilibrium between the solvent and the

substrate to form (indicated by a constant signal from the bridge amplifier). Once equilibrium has been reached, the flow of pure solvent is replaced by a solution of the adsorption probe (diluted to a known concentration in the initial solvent). As this passes through the cell and over the substrate the probe molecules adsorb to the surface of the substrate displacing the heptane molecules, resulting in the evolution of heat measured by the thermistors. Downstream, the differential refractometer measures the change in RI from the pure heptane to the probe solution. The longer it takes for the RI to increase to that of the probe solution the greater is the level of adsorption of the probe on the substrate. The flow of probe solution continues until equilibrium is reached for both heat and RI index measurements.

Once the equilibrium of adsorption has been reached, the desorption process is observed by switching the flow of solution through the FMC back to pure solvent. As the probe molecules desorb from the substrate into the solvent, a decrease in temperature occurs and is measured by the FMC. The differential refractometer measures the change in RI from that of the probe solution back down to the pure solvent. This process continues until equilibrium is once again reached.

3.2 Objectives

- Identification of a substrate that will be suitable for use as a reservoir of the antimicrobial EO blend selected in Section 2.4.5. It is anticipated that the substrate will provide protection to the EO during melt blending with the polymers and then control the release of the EO and thus prolong any antimicrobial activity.
- Investigate the ability of layered silicate materials to adsorb the molecular components of essential oils.
- As some of the acid treated clays in particular contain acid catalytic sites, a secondary objective was to investigate whether adsorption of the EO has any effect on the chemical makeup of the oils.

3.3 Materials

3.3.1 Layered silicate substrates

Rockwood Additives Ltd. (Moorfield Road Widnes, Lancashire, WA8 3AA, UK) provided six porous minerals for use as adsorption substrates which are summarised below in Table 3.1. From henceforth, the coding system shown below in Table 3.1 was used to identify the substrates.

Table 3.1: Summary details of substrates with coding.

Substrate	Coding	Comment
Fulcat® 400	F400	Natural aluminosilicate
Fulcat® 435	F435	Natural aluminosilicate which have been acid treated in order to partially exfoliate the pores and increase the surface area.
Fulcat® 800	F800	Chemically modified aluminosilicate (development product).
Fulacolor®	Fcol	Natural aluminosilicate which have been acid treated in order to partially exfoliate the pores and increase the surface area.
Laponite® RD	LRD	Synthetic magnesium silicate made without the presence of hydrogen fluoride.
Laponite® B	LB	Synthetic magnesium silicate made in the presence of hydrogen fluoride.

3.3.2 Essential oils

Vide supra Section 2.3.3

3.3.3 Solvents

Heptane CHROMASOLV®, for HPLC, ≥99 % (Sigma-aldrich, UK) was used as the EO solvent for all adsorption studies (Sections 3.4.2 and 3.4.4). Dodecane ReagentPlus®, ≥99 % (Sigma-aldrich, UK) was used as the internal standard (IS) for all gas chromatography adsorption studies (Section 3.4.2). Hexane CHROMASOLV®, for HPLC, ≥97.0 % (GC) (Sigma-aldrich, UK) was used as the IS for all headspace controlled release studies (Section .4.3)

3.4 Experimental

3.4.1 Characterisation of substrates

3.4.1.1 Fourier transform infra red spectroscopy of layered silicate substrates and essential oils.

The substrate recovered from the filtration in Section 3.4.2 was analysed in powder form using Diffuse Reflectance Fourier Transform Infrared spectroscopy (DRIFTS). A Thermo Nicolet Nexus FT-IR spectrometer (Thermo Fisher Scientific, Waltham USA) was fitted with a Spectra-Tech DRIFTS cell (Thermo Fisher Scientific, Waltham USA). Samples were diluted to 5 % (m/m) with finely ground KBr. Care was taken not to grind the sample with the KBr; the sample was gently folded into the ground KBr using a spatula. The KBr diluted sample was loaded into the DRIFTS cell and analysed between 4000 and 500 cm^{-1} wavenumbers. Spectra were made up of 164 co-added scans at a resolution of 4 cm^{-1}. The used background was the pure KBr. The sample compartment and beam path was purged with H_2O and CO_2 free air to remove any peaks resulting from CO_2 and atmospheric H_2O. The FTIR spectrum obtained was compared to spectra for the un-modified dried substrate and the EO on its own to determine whether any of the EO peaks were present in the adsorbed substrate.

The EO were analysed using FTIR by placing a drop of the pure oil between 2 KBr plates, the plates were then mounted in a holder in the spectrometer, and analysed between 4000 and 500 cm^{-1} wavenumbers. Spectra were made up of 32 co-added scans at a resolution of 4 cm^{-1}. The background used was the KBr plates with no sample.

3.4.1.2 WAXS

WAXS powder diffraction was undertaken using a Philips PW 1730 (Philips, UK), a Cu-Kα tube was used at an anode voltage and current of 50 kV 40 mA respectively. The conditions were are follows: start angle 1.5°, end angle 35.5° degrees, step size 0.010 degrees, counting time 1 s, temperature 25 ℃. Data

was recorded and process using Diffrac AT software (Bruker AXS, Coventry UK).

3.4.1.3 N_2 BET surface area

Multi-point BET surface area determination was carried out on the substrates using a Tristar II 3020 BET analyser (Micrometrics, Norcross USA), the data were processed and plotted using Tristar confirm™ software (Micrometrics, Norcross USA). Samples were degassed by cooling under vacuum, then to heating 60℃ under vacuum overnight in preparation for analysis.
BET surface area was determined from a five point N_2 adsorption isotherm. The absolute pressures used were 50.0; 87.5; 125; 162.5; 200.0 mmHg.

3.4.2 Static adsorption studies from solution monitored using gas chromatography

Calibration curves for the key molecular components of the five major components of the EO were set up by running GC analysis of each oil at 0.05, 0.1, 0.15, 0.2, 0.25, 0.3, 0.35, and 0.4 % (m/v) in heptane. The peak areas of each molecule were ratioed against the peak area of an internal standard and plotted against percentage (m/v) in order to obtain the calibration plot. The data points were fitted using linear regression analysis, and the regression equation was then used to calculate the percentage (m/v) of the molecule remaining in the solution after adsorption onto a substrate.
In a 100 ml bottle with a PTFE seal lid, the substrate to be analysed (5 g) was added to heptane (100 ml) spiked with dodecane (1.25 %) as an internal standard (IS), and the chosen EO (1.25 g) was then added. A magnetic stirrer bead was placed in the heptane solution and the bottle was sealed. The mixture was stirred for 18 h at room temperature. After stirring, the substrate was filtered off from the supernatant liquor using Buchner filtration. The recovered substrate was then allowed to dry at room temperature. The substrate was then analysed using DRIFTS (Section 3.4.1.1). After filtration the supernatant liquor (25 ml) was centrifuged at 4000 rpm for 10 minutes using a Hermle Z200A (Cambridge Biosystems, UK) (relative centrifugal force, 1700*g*), to deposit any

fine particles remaining, and the resultant liquid was decanted into a small glass vial.

The supernatant liquor was analysed using a HP 5890 Series 2 GC (Hewlett Packard, UK) in order to determine the concentration of molecular components (identified in Section 2.5.6) after adsorption. By taking the ratio of the peak area of a particular component molecule to the peak area of the IS and inputting it into the relevant calibration equation, it was possible to obtain the percentage (m/v) of the molecule in the supernatant liquor after adsorption. This value was then compared to the equivalent value for the molecule in a 1.25 % (m/v) solution in order to determine the level of reduction of the molecule due to adsorption. From the latter the level of adsorption of that component onto the substrate was calculated. The calibration graphs are displayed in Appendix 1.

The GC adsorption experiments were carried out in triplicate and the total mass of adsorption reported was the mean of the three replicates.

3.4.3 Soxhlet extraction of EO adsorbed onto layered silicates

Extraction studies were undertaken on some of the substrates recovered after filtration, as the GC analysis of the supernatant liquor only gave a measure of the reduction of the EO components from the solvent. Extraction studies were used to help confirm that the EO molecules have been adsorbed onto the substrates. Selected samples isolated from the adsorption flasks were Soxhlet extracted with heptane. The Soxhlet apparatus was lagged with glass wool (Acros organics, UK) and the mass of sample was approximately 4 g. The total extraction time was 16 hours, completed as two 8 hour sessions. The extract solution was analysed using GC (Section 3.4.2).

3.4.4 Flow micro calorimetry analysis of EO adsorption

A Microscal® model 3Vi flow microcalorimeter (Microscal Limited, 79 Southern Row, London W10 5AL, UK) was connected downstream to a Waters® 410 differential refractometer (Millipore, Watford UK) as described in Section 3.1.7. Using a PerkinElmer® Nelson 970 series data station, the data from the two

instruments was collected and analysed using PerkinElmer® Totalchrom v6.3.1 (PerkinElmer, Cambridge UK). In order to maintain constant temperature conditions the FMC cell was extensively insulated, and enclosed in an insulated sealed box at 22 ± 0.5 ℃. This was done to reduce the possibility of errors caused by fluctuations in room temperature.

A graduated ignition tube was used to measure out the correct volume of MMT substrate to fill the FMC cell (0.15 cm^3), and the mass recorded. The substrate was then transferred into the FMC cell using a purpose made metal funnel.

As the FMC thermal data gives a measure of the displacement of solvent molecules from the surface of the substrate with the probe (EO) molecules it was important to use a solvent that would have as little interaction with the substrate as possible. n-Heptane was used as it is a non-polar solvent and should therefore interact relatively weakly with the polar surface of the MMT. The probe (in this case individual EO) (75 ± 5 mg) was dissolved in heptane (25 ml accurately measured in a volumetric flask) (dried twice over a molecular sieve (4A mesh, Acros Organics, UK)) to create a 0.3% (m/v) solution. The probe solution was then transferred to a 20 ml glass syringe which was labelled as syringe 2. A second syringe was filled with heptane and labelled as syringe 1.

The substrate sample in the FMC was equilibrated in heptane from syringe 1 overnight at a flow rate of 0.4 $cm^3\ h^{-1}$. After equilibration the heptane flow rate was increase to 4 $cm^3\ h^{-1}$. Once FMC and differential refractometer readings had settled to a baseline, the inlet was switched from syringe 1 to syringe 2 (flow rate 4 $cm^3\ h^{-1}$) allowing adsorption of the probe to take place. After adsorption equilibrium was reached, two thermal calibration peaks were generated. The inlet was then switched back to syringe 1 (containing heptane) in order for desorption to take place, after attainment of equilibrium the run was terminated. Five calibration peaks for the differential refractometer were then obtained using a 20 µl calibration loop.

The thermal data produces a peak, either positive (exothermic) for adsorption or negative (endothermic) for desorption. The peak areas are proportional to the

energy change associated with adsorption and desorption. The peak obtained can be converted to a value for enthalpy via the thermal calibration peaks which are generated via passage of a known quantity of electrical power through a length of resistance wire integrated in to the cell outlet. The calibration peak area is proportional to the known amount of energy released in to the cell, and can therefore be used to calculate the enthalpy of adsorption/desorption via use of Equation 3.2.

Equation 3.2: $$Heat\ of\ reaction\ (J) = \frac{A_1}{A_2} \times P \times t$$

Where A_1 is the experimentally derived peak area, A_2 is the calibration peak area, P is the power (mW) supplied to the thermistors during calibration, and t is the time (s) power was supplied to the thermistors.

An example of the data obtained from the FMC cell is given (Figure 3.6).

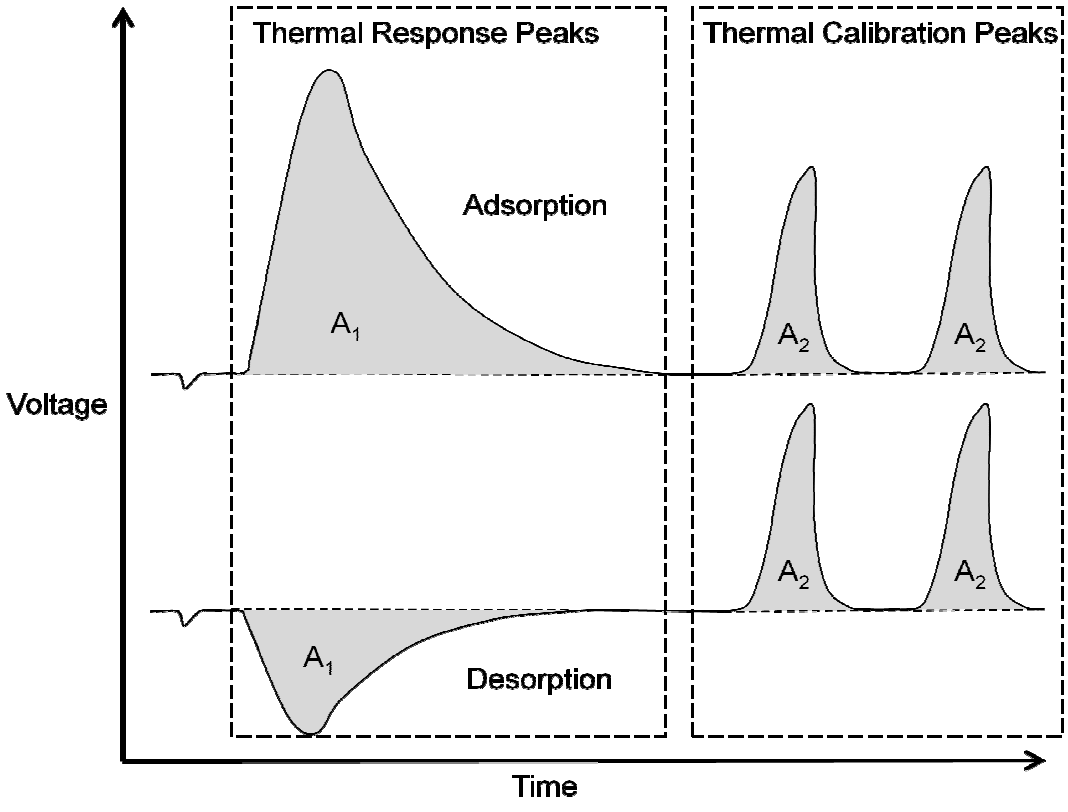

Figure 3.6: Typical FMC output measured by the thermistors showing: A_1) thermal response peaks evolved from a change in enthalpy; and A_2) thermal calibration peaks [99].

In order to calculate the mass of probe adsorbed and desorbed, data for a non-adsorbing probe were obtained. Decahydronaphthalene (anhydrous ≥ 99 % Sigma Aldrich, UK) was used as the non adsorbing probe due to its high refractive index and weak interaction with the substrates used. Using PerkinElmer Totalchrom software, the adsorbing probe data and non-adsorbing probe data were aligned using the time markers (solvent to solution switch over spike) in the thermal data. The non-adsorbing data were then subtracted from the adsorbing data, resulting in a negative peak. The area of the negative peak was proportional to the mass of probe adsorbed and the latter was then calculated using the average of the differential refractometer calibration peaks using Equation 3.3.

Equation 3.3: $$Mass\ adsorbed\ /\ desorbed\ (g) = \left(\frac{PA_e}{PA_c}\right) \times \left\langle \left\langle m_p \times 40 \right\rangle \times V_1 \right\rangle$$

Where: PA_e refers to the experimentally determined peak area, PA_c refers to the average calibration peak area, m_p refers to the mass of adsorbing probe (approximately 0.075 g) and V_l refers to the loop volume (2×10^{-5} L). The mass of probe used was in 25 ml of solvent, in order to convert to the equivalent mass of probe in 1 L the mass of probe was multiplied by 40.

Desorption was calculated using the same method with the exception that the adsorbing probe data and non adsorbing probe data were aligned using the solution to solvent switching spikes in the thermal data. After subtraction of the non-adsorbing probe data from the adsorbing probe data a positive peak was obtained.

An example of data obtained from the differential refractometer is given (Figure 3.7).

FMC adsorption studies were carried out in duplicate and the masses and energies of adsorption and desorption reported were the mean of the two replicates.

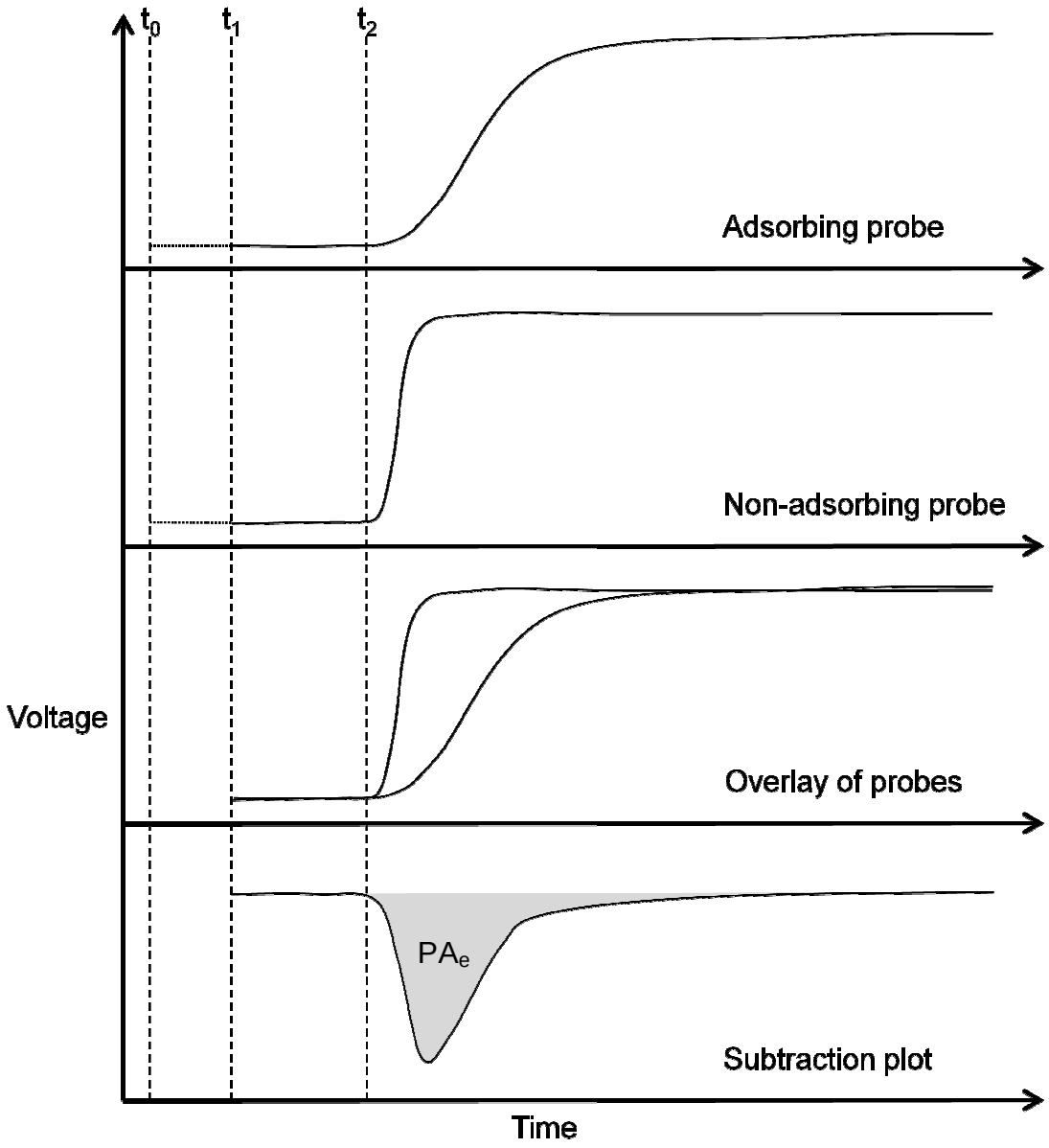

Figure 3.7: Differential refractometer plots showing the adsorbing probe, non-adsorbing probe, their overlay and subtraction plot resulting from subtraction of the non-adsorbing probe from the adsorbing probe data. The peak area of the subtraction plot (PA_e) is used in Equation 3.3. T_0 = start time, t_1 = syringe switch-over time and t_2 = as solute reaches differential refractometer [99].

3.5 Results and discussions

3.5.1 Characterisation substrates using physical properties

The surface area of the layered silicate substrates, determined using N_2 BET adsorption and the d-spacing of the platelets, determined by WAXS were demonstrated (Table 3.2).

Table 3.2: Surface area and d-spacing of layered silicate substrates to be used in adsorption studies. Demonstrating the differences in the physical properties of the six substrates, which may affect their adsorption characteristics.

Substrate	Surface area ($m^2.g^{-1}$)	d-spacing (nm)
F400	80	1.54
F435	326	1.56
Fcol	285	1.58
F800	374	1.29
LRD	373	1.32
LB	412	1.29

The higher surface area of F800 and the Laponites®, if accessible to the molecules, may provide a greater number of adsorption sites for the EO molecules, leading to a higher mass of adsorption. However, the smaller d-spacing and therefore smaller interlayer spacing (distance between platelets) may restrict the entry of the EO molecules into the galleries of F800 LRD and LB. The EOs were comprised of hydrocarbons, the typical width of a hydrocarbon unit (CH_3) was 0.4 nm [100]. Therefore, to accommodate the EO molecules within the galleries of the substrates the interlayer space (d-spacing minus platelet thickness) would need to be 0.4 nm or greater. The typical width of a platelet is 0.94 nm [101], therefore the interlayer spacing of F800 and LB (0.35 nm) would be too small to accommodate the EO molecules. The interlayer space of LRD (0.38 nm) would also not be wide enough to accommodate a hydrocarbon chain such as those found commonly in EO molecules.

The substrates were prepared for DRIFTS analysis by drying them at 120 ℃ for 24 hours to remove any water adsorbed to the surface. They were then analysed using DRIFTS (Figure 3.8) as described in Section 3.4.1.1.

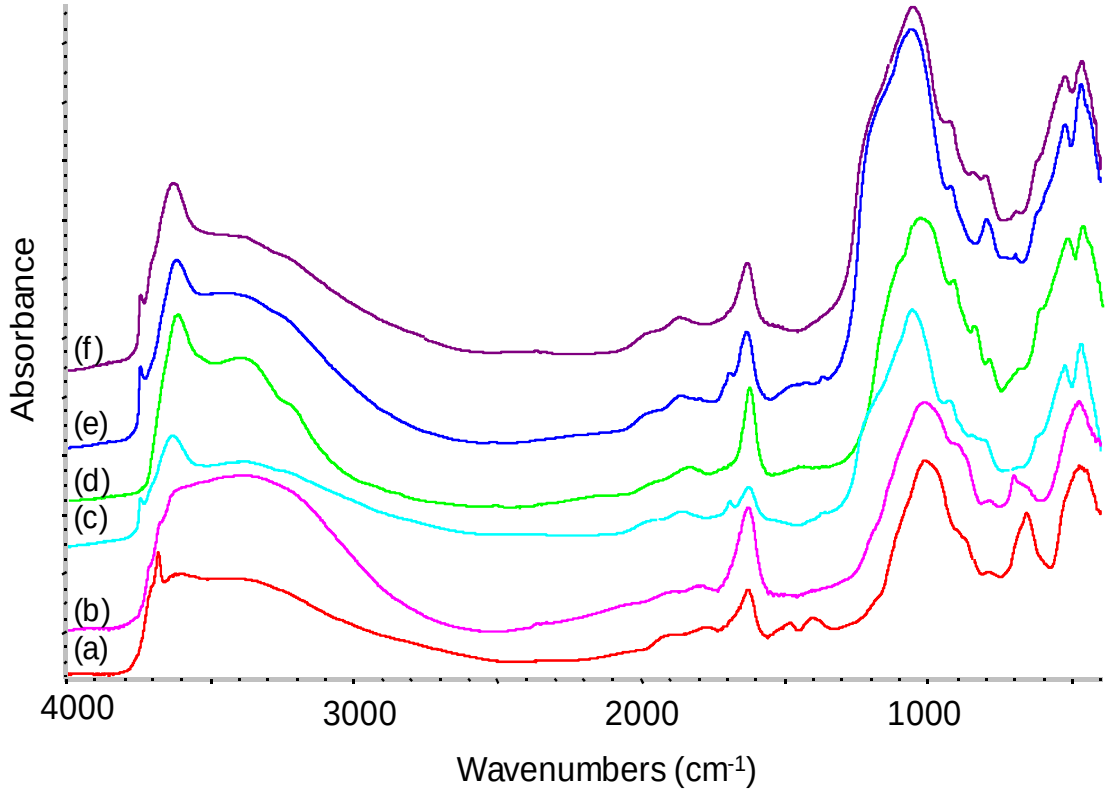

Figure 3.8: FTIR spectra of dried MMT (a) Laponite® RD, (b) Laponite® B, (c) Fulcat® 435, (d) Fulcat® 400, (e) Fulacolor®, and (f) Fulcat® 800. Demonstrating the characteristic bond vibrations of each substrate.

The FTIR spectra obtained for the MMT followed the same basic pattern for all five substrates. The broad peak between 3500 cm^{-1} and 3000 cm^{-1} can be attributed to the silanol (Si–OH) groups in the substrate structures. The sharp peak present at approximately 3700 – 3750 cm^{-1} can be assigned to isolated silanol groups within the layered silicate structures. This peak is significant as hydrogen bonding of EO molecules to accessible isolated silanol groups would lead to the disappearance of these absorption bands due the silanols no longer being isolated. For all five silicate substrates, there is a peak at approximately 1650 cm^{-1} which corresponds to O–H bending in molecular water. The presence of this peak shows that despite drying the silicates still retained water within the pores / layers. At 1100 cm^{-1} there is a broad intense peak which can be attributed to the Si–O–Si bonds in the MMT structure. On the down slope of the

Si–O–Si for (c), (d), (e), (f) there is a peak at approximately 920 cm^{-1} which is an OH deformation characteristic of Al–Al–OH This peak is not present in the spectra for (a) and (b) as the Laponite® layered silicates do not have any alumina present in their structure [102]. The peak at 840 cm^{-1} present for (c), (d), (e), (f) was attributed to Al–Mg–OH [102] and was also not present in (a) and (b) due to the Laponites lack of alumina in the structure. The broad peak at approximately 800 cm^{-1} for the two Laponite® spectra (a) and (b) was attributed to the Mg–Mg–OH bonds in the octahedral layer of the structure.

The EO were analysed using FTIR by placing a drop of the pure oil between 2 KBr plates, the spectra obtained are demonstrated (Figure 3.9).

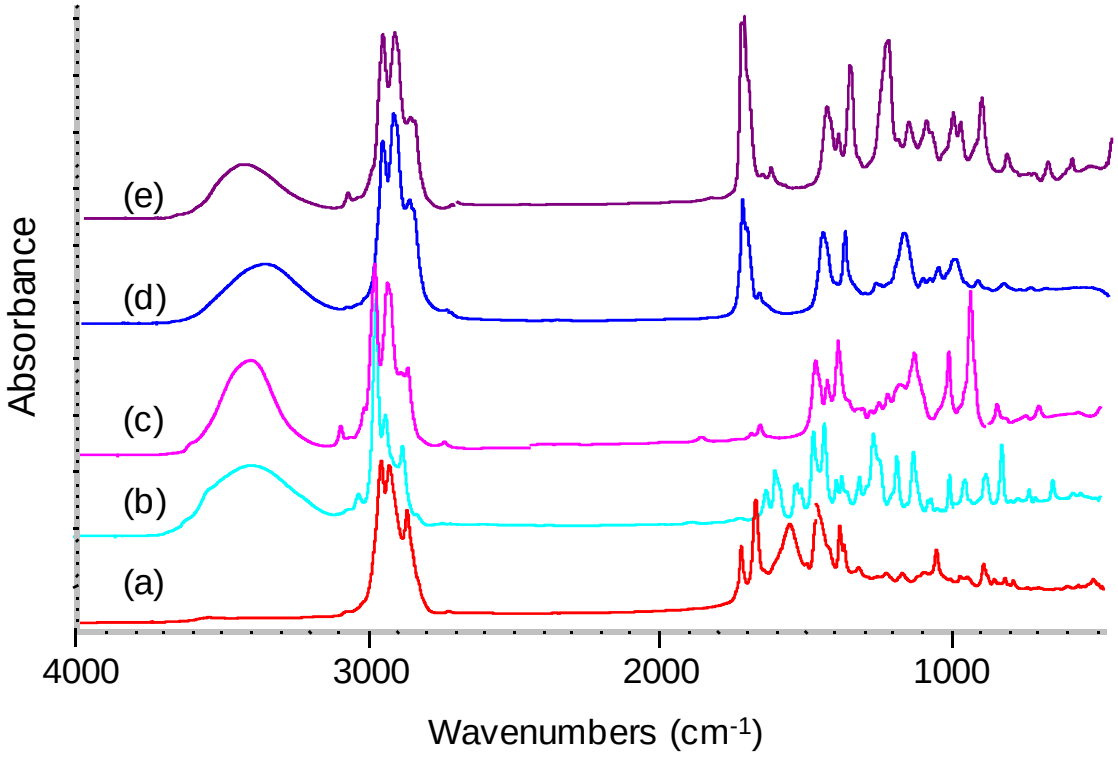

Figure 3.9: FTIR spectra of EO (a) Manuka, (b) Oregano, (c) Rosewood, (d) Geranium, and (e) Lavender. Demonstrating the characteristic bond vibrations for each of the five oils.

As with the MMT samples, the EO FTIR spectra displayed some common characteristics. At approximately 3500 cm^{-1} there was a broad peak visible in spectra of four of the oils which can be assigned to hydrogen bonded O-H stretching. This peak was not present in manuka oil which is due to the low concentration of –OH functional molecules in this EO relative to the other oils.

All five of the oils exhibited aromatic and alkenic C–H=C–H stretch vibrations; manuka oil demonstrated two weak peaks at 3075 cm^{-1} and 3113 cm^{-1}, oregano oil showed weak peaks at 3090 cm^{-1} and 3054 cm^{-1} one more intense peak at 3020, rosewood oil demonstrated two weak peaks at 3007 cm^{-1} and 3054 cm^{-1} plus one more intense peak at 3085 cm^{-1}, geranium oil had weak peaks at 3050 cm^{-1} and 3085 cm^{-1}, and lavender oil showed weak peaks at 3006 cm^{-1} and 3084 cm^{-1} and a more intense peak at 3087 cm^{-1}. Any shifting of the C–H=C–H vibrations would give insight into the mode of adsorption of the EO molecules onto the substrates, and to whether the pi electrons in the double bond were involved in adsorption. Each oil exhibited three peaks in the range 3000-2800 cm^{-1}, which were attributed to the C–H stretch vibration of the aliphatic CH_2 bonds in the EO molecules. These peaks should be the most obvious indicator of adsorption of EO on to the substrates as they appear at tail end of the hydrogen bonded Si-OH peak, and will not be masked by any large MMT peaks. Geranium oil, lavender oil and manuka oil all exhibited carbonyl stretching absorption peaks at 1700 cm^{-1} which was most intense for lavender oil. The carbonyl bands may be obscured by absorption bands originating from the substrates. Between 1500 and 1300 cm^{-1} there were a number of peaks present for each of the oils, ranging from two for geranium oil to five for manuka oil, attributed to the C–H bending of the aliphatic CH_2 groups, and C–O–H bending. These peaks fall in a region where there were no peaks present in the MMT spectra and therefore should be visible on a spectrum of an MMT with adsorbed EO. A large number of the EO peaks are present below 1100 cm^{-1}; these peaks were masked by the intense Si–O–Si peaks present in the MMT spectra and therefore were not be able to be used as evidence for adsorption of the EO onto the substrates.

3.5.2 Gas chromatography adsorption studies of EO onto layered silicates

Adsorption of the five essential oils (EO) analysed for antimicrobial activity in Section 2.5.1 onto the six layered silicate substrates was initially investigated using gas GC. The use of GC was primarily to determine which components of the EO were adsorbed, and to confirm that no new molecules were created during adsorption onto the substrates. The latter would indicate catalytic

damage of the EO molecules arising from contact with Brønsted and Lewis acid sites on the modified substrates (see Section 3.1.4.1).

3.5.2.1 GC adsorption of rosewood oil onto layered silicates, and the selection of substrates

Layered silicates have been shown to be able to adsorb organic material such as oils (see Section 3.1.2). The majority of work examining adsorption of organic materials onto layered silicates has focused on materials made up of a single molecule. This type of work enables the use of simple techniques such as UV-Vis spectroscopy [103, 104], as a single peak can be attributed to the molecule being adsorbed. Changes in intensity of that peak can be used to calculate the level of adsorption. With EO, being a mixture of a multitude of components, these methods are not suitable as a single peak cannot be representative of the EO as a whole.

Chromatograms from GC have an individual peak for each molecular component of the oil. By monitoring the effect of adsorption on each molecule and combining the results it was possible to acquire insight into how adsorption affected each individual molecule, as well as obtain an overall level of adsorption of the EO onto the substrate.

As stated in Section 2.5.6, the initial screening of substrates for adsorption characteristics was carried out using rosewood oil (RO). All six of the substrates provided by Rockwood Additives were analysed and substrates that gave the highest levels of adsorption of rosewood oil were to be selected for further adsorption studies using all of the EO described in Section 2.5.6. In order to restrict the volume of data, only molecules which comprised greater than 1 % of the total of the EO were analysed for adsorption. For rosewood oil, the molecules analysed were: limonene, eucalyptol, *trans*-linalool oxide, *cis*-linalool oxide, linalool and α-terpineol.

Comparison of the chromatograms of supernatant liquors from adsorption onto the acid treated montmorillonite F435 (Figure 3.10ii) with that of rosewood oil in heptane (Figure 3.10i) showed an apparent reduction in a number of the major peaks of the oil. The peaks for *trans*-linalool oxide, linalool, and α-terpineol were reduced to such a level that they were immeasurable using GC. Similar patterns were observed following adsorption of rosewood oil onto the natural

aluminosilicate F400 and the acid treated aluminosilicate, Fcol (data not shown).

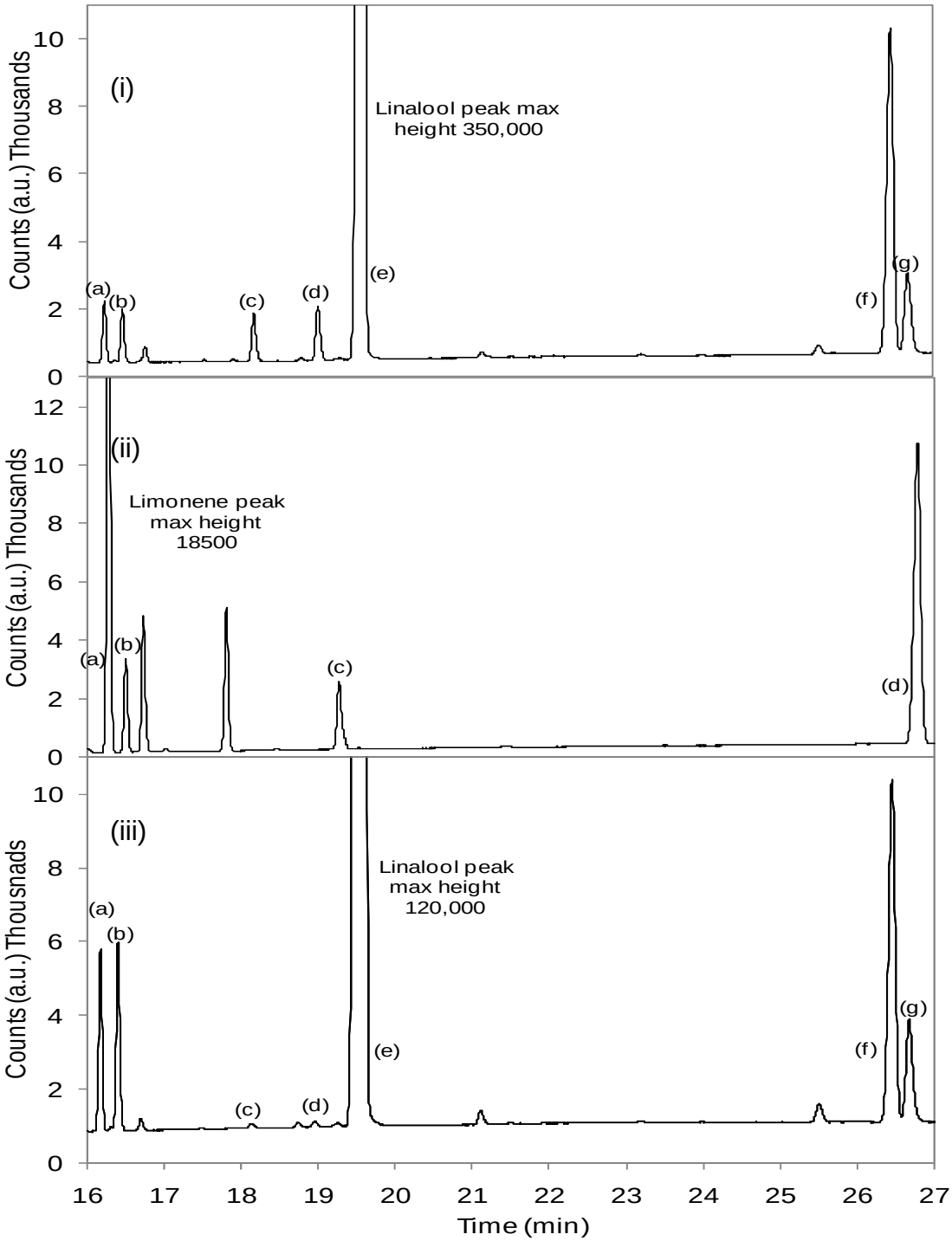

Figure 3.10: (i) Extract from chromatograph of RO at 0.4 % (m/v), (ii) RO after adsorption onto F435, (iii) RO after adsorption onto LRD. For (i) and (iii) Paks assigned as follows: (a) limonene (b) eucalyptol (c) *trans*-linalool oxide (d) *cis*-linalool oxide (e) linalool (f) dodecane (internal standard) (g) α-terpineol. For (ii) peaks were assigned as (a) limonene (b) eucalyptol (c) *cis*-linalool oxide and (d) dodecane. Initial concentrations for (ii) and (iii) were 1.25 % m/v.

In addition to a large reduction in intensity of several peaks, it was also observed that the ratio of limonene peak to eucalyptol peak had been affected, changing from almost 1:1 to almost 3:1 for all of the natural alumina silicates. It was initially proposed that this may be due the eucalyptol being adsorbed to a greater extent than the limonene. The data from the calibration graphs would be used to confirm this, by analysing the remaining proportion of each of the molecules in the liquor reclaimed after the adsorption study (Table 3.3).

The synthetic and chemically modified layered silicate materials (Laponite® RD (LRD), Laponite® B (LB) and Fulcat® 800 (F800)) gave a different pattern of results relative to the natural MMT. Figure 3.10(iii) shows the chromatogram obtained from the liquor reclaimed after adsorption of rosewood oil onto LRD. In contrast to equivalent data obtained from adsorption on to the natural and modified natural MMTs, the linalool and α-terpineol peaks were not completely removed. Both linalool oxide isomers were significantly reduced, this compares favourably with the behaviour of the natural and modified natural MMTs where the peak for the *trans*-isomer was removed from the chromatogram but the *cis*-isomer still had a significant peak. The final difference between the natural and modified natural MMTs and the synthetic/chemically modified layered silicates was the ratio of the limonene and eucalyptol peaks. As shown above, after adsorption onto the natural MMT, the ratio of limonene to eucalyptol changed from 1:1 to 3:1 for F435 and Fcol and 7:1 for F400, whilst for the synthetic/chemically modified layered silicates the ratio of the two molecules was kept much more constant, remaining around 1:1. Two reasons for this difference were proposed: either the synthetic/chemically modified layered silicates gave a more even level of adsorption of the two molecules and thus maintained the ratio, or during the adsorption process of rosewood oil onto the natural MMT there was a reaction occurring which resulted in limonene being produced.

It was possible that the apparently greater level of adsorption achieved from the natural MMT was due to the Brønsted and Lewis acidic sites at the surface, which may promote hydrogen bonding of oxygenated species to the surface of the MMT; the latter are found in many EO molecules. The acid treatment of the natural aluminosilicate to give F435 and Fcol would increase the number of acidic sites on the surface potentially increasing this effect; the exposure of

more of the silicate surface after acid treatment may also contribute to higher adsorption as there would be more available adsorption sites.

Using the calibration curves exemplified (Figure 3.11) (see Section 3.4.2) it was possible to determine the extent of reduction of each of the major molecules of rosewood oil after adsorption onto the MMT materials. The results obtained using the calibration curves are displayed (Table 3.3).

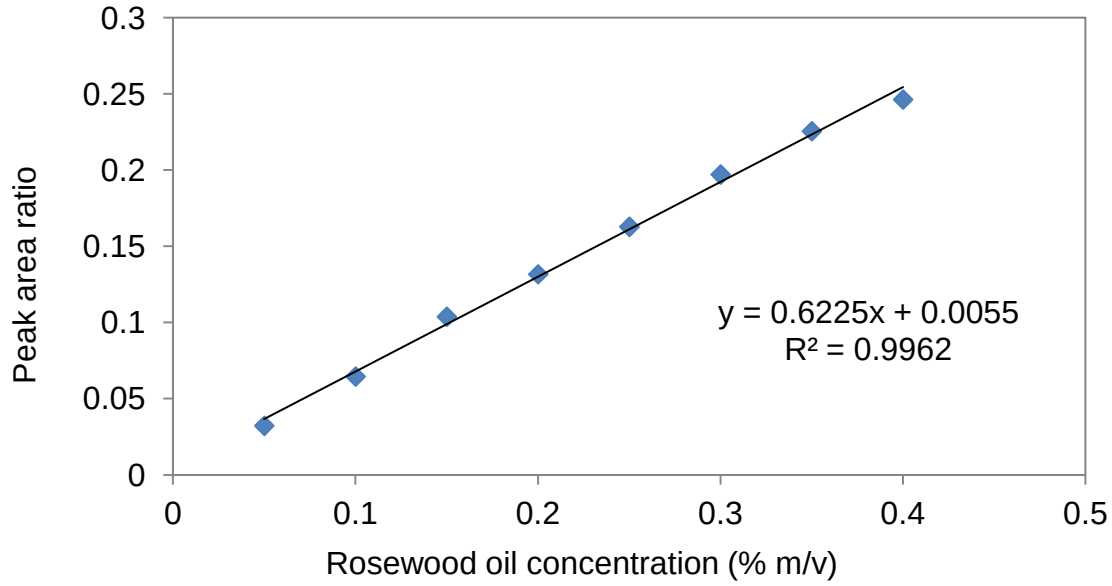

Figure 3.11: Calibration curve for α-terpineol fraction of RO demonstrating the relationship between oil concentration and the experimentally obtained peak area of molecules in the oils. The equation of the line fit was rearranged to give the concentration of x.

Analysis of the GC data using the calibration curves resulted in a greater understanding of what was happening during the adsorption of rosewood oil onto the layered silicate substrates. The natural and modified natural aluminosilicates showed the highest overall reduction of EO molecules in the liquor (F400 73 %, F435 93 % and Fcol 93 %). However, there were anomalies observed for a number of the molecules after adsorption onto these substrates. For all three, it was found that after adsorption, the amount of limonene in the liquor was higher than expected, considering the initial rosewood oil concentration of 1.25 %. For F400, the concentration of limonene was approximately 600 % higher and it was also found that eucalyptol, *cis*-linalool oxide and α-terpineol were present in concentrations higher than would be found, considering the initial rosewood oil concentration of 1.25 % (m/v).

Table 3.3: Percentage reduction of the oregano oil (OO) molecules analysed (from initial 1.25 % solution), after adsorption onto montmorillonite materials. Demonstrating the level of adsorption of each molecule which comprised greater than 1 % of the molecular make up of OO.

EO molecular component	LRD		LB		F800		F400		F435		Fcol	
	% after adsorption	% reduction	% after adsorption	% reduction	% after adsorption	% reduction	% after adsorption	% reduction	% after adsorption	% reduction	% after adsorption	% reduction
limonene	0.95	24.40	1.10	12.00	1.17	6.40	9.27	-641.60	3.28	-162.40	3.63	-190.40
eucalyptol	1.31	-4.80	1.38	-10.40	1.18	5.60	1.30	-4.00	1.05	16.00	0.95	24.00
trans linalool oxide	0.03	97.84	0.07	94.72	0.09	92.46	0.05	96.00	0.00	100.00	0.00	100.00
cis linalool oxide	0.04	96.64	0.12	90.08	0.15	88.16	3.29	-163.20	0.55	56.00	0.33	73.60
linalool	0.76	39.20	0.78	37.44	0.82	34.48	0.03	97.60	0.00	100.00	0.00	100.00
α-terpineol	0.48	61.52	0.60	51.84	0.48	61.52	2.45	-96.00	0.00	100.00	0.02	98.40
Combined		40		38		35		75		93		93

As well as the increase in concentration of a number of molecules, it was also observed that *trans*-linalool oxide, linalool, and in the case of F435 and Fcol, α-terpineol, had been almost completely removed from the liquor. It was hypothesised that the acid sites of the natural and modified natural aluminosilicates may be acting as catalysts and degrading or modifying the EO molecules that showed the highest reduction. Conversion of some of these molecules via catalysis could explain the high concentrations of limonene observed. It may be possible that a cyclisation of linalool was taking place resulting in the production of limonene.

The cyclisation of linalool is a 6-exo-tet reaction and therefore would be favoured by Baldwin's rules. The catalytic conversion of linalool to α-terpineol under acidic conditions has been reported in the literature [105]. The reaction mechanism for conversion of linalool to α-terpineol is not fully understood; but it has been suggested that it occurs via an intermediate (Figure 3.12) [106].

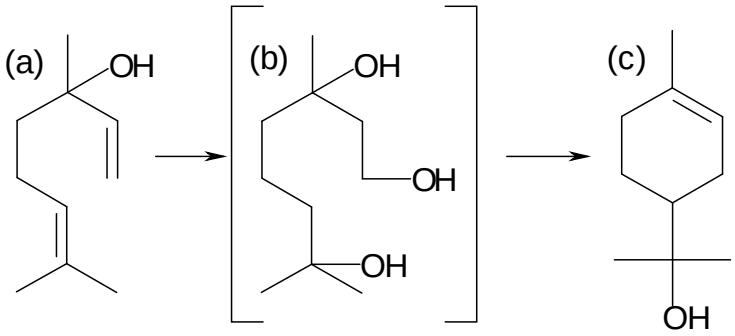

Figure 3.12: Conversion of linalool to α-terpineol (a) linalool (b) intermediate suggested by Bedoukian (c) α-terpineol.

The proposed intermediate (Figure 3.12) would require an excess of OH to be present in order to form the two extra alcohol bonds. During adsorption of linalool onto the natural MMT, there may not be sufficient OH present to allow the formation of α-terpineol in this way. Due to the lack of available OH, present it is possible that the cyclisation of linalool, catalysed by the acid sites, would result in the production of limonene; a mechanism for this reaction was proposed (Figure 3.13). If the latter mechanism was correct then water would be formed as a by-product. If low levels of water are formed they most probably would adsorb onto the hydrophilic surface of the substrates, though if a large number of linalool molecules were converted to limonene, then the build up of

water molecules may result in there being sufficient OH present to allow the reaction to proceed via the mechanism proposed (Figure 3.14). This may explain the increase in concentration of both limonene and α-terpineol that was observed during adsorption of rosewood oil onto F400. The lower level of limonene produced during adsorption of rosewood oil onto F435 and Fcol may be related to there being insufficient water released to enable the formation of α-terpineol.

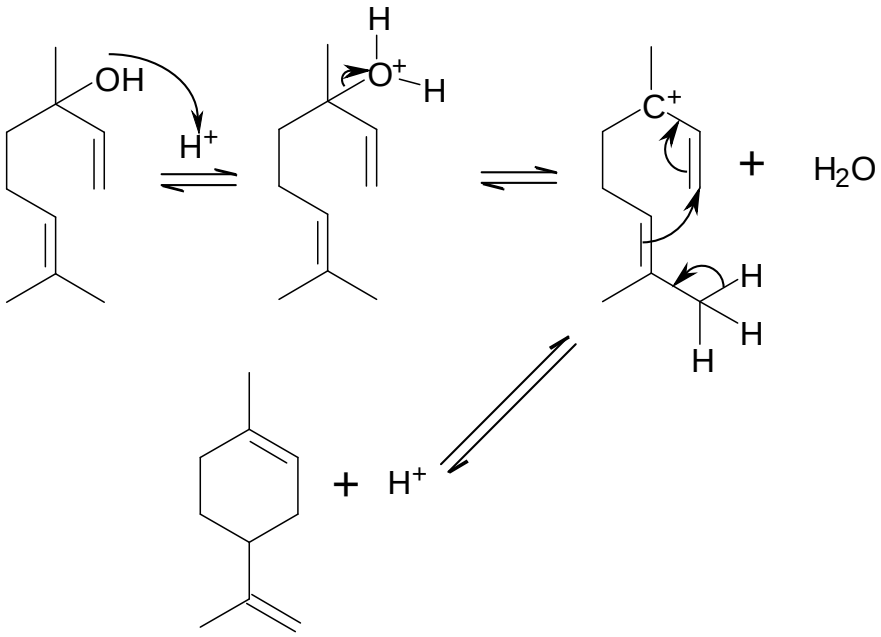

Figure 3.13: Proposed mechanism for conversion of linalool to limonene under the acidified clay environment.

Analysis of the individual levels of total oil adsorption showed that the synthetic/chemically modified layered silicates (the Laponites® and Fulcat® 800) showed lower overall levels of adsorption relative to the natural aluminosilicates: (LRD 40 % (reduction of oil from liquor), LB 38 % and F800 35 %). However, it was also observed that in the former case there was little evidence of increased concentration of any of the EO molecules after adsorption, therefore the catalytic effect proposed for the natural Aluminosilicates was not occurring in the case of the synthetic/chemically modified layered silicates. It was also observed that limonene and eucalyptol were adsorbed to a lower level than the other four molecules analysed. The surface of the aluminosilicate is relatively hydrophilic, and it is possible that the polar OH functional group present on the linalool oxide isomers, linalool and α-

terpineol aided their adsorption onto the substrates. The low level of adsorption of limonene can be attributed in part to the lack of a polar functional group and the non-polar characteristics of the molecule. The low level of adsorption of eucalyptol can be attributed to a number of factors. Eucalyptol has a ketone functional group which is less polar than the OH functional group therefore the attraction to the hydrophilic environment of the aluminosilicates will be lower compared with the rosewood oil molecules bearing an OH group. Eucalyptol also has a double ring structure (Figure 3.14) which is bulkier than the straight chain or single ring structures which restricts its entry into the galleries of the synthetic/chemically modified layered silicates. This is supported by the fact that the acid treated aluminosilicate (in which the alumina layer has been leached out exposing more of the silica surface resulting in a larger area for adsorption) give a higher level of adsorption of eucalyptol than the LRD, LB and F800.

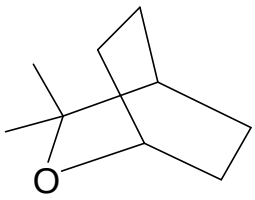

Figure 3.14: Chemical structure of eucalyptol. Demonstrating the double ring structure.

DRIFTS analysis of the rosewood oil adsorbed onto natural aluminosilicates (Figure 3.15) added further evidence to support the idea that the substrates were having a negative effect on the oil.

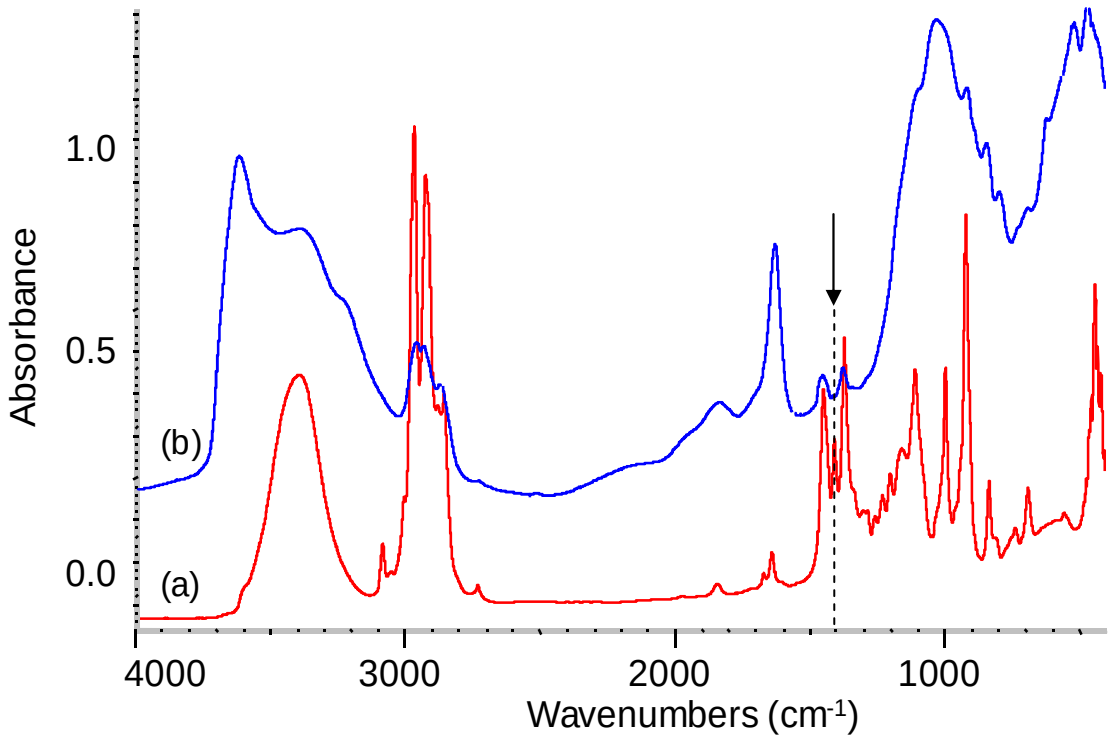

Figure 3.15: FTIR spectra of (a) Rosewood oil (RO) and (b) F400 after RO adsorption. Demonstrating the presence of RO peaks on the F400 spectra.

It can be clearly seen that after adsorption onto F400, one of the three prominent peaks in the 1500 to 1300 cm^{-1} range of rosewood oil was not present. This trend was also true for the acid modified natural aluminosilicate (Figure 3.15). The central peak (approximately. 1400 cm^{-1}) of the three rosewood oil peaks (Figure 3.16) has been significantly reduced in relation to the other two peaks following adsorption of rosewood oil onto F400. The same peak was not present in the spectra for F435 and Fcol, suggesting even greater damage had occured to the oil with adsorption onto the latter two substrates. If the degradation of linalool was due to acid catalysis, then the greater number of acid sites on the F435 and Fcol due to acid treatment would explain why those two substrates resulted in a larger reduction of the peak than F400.

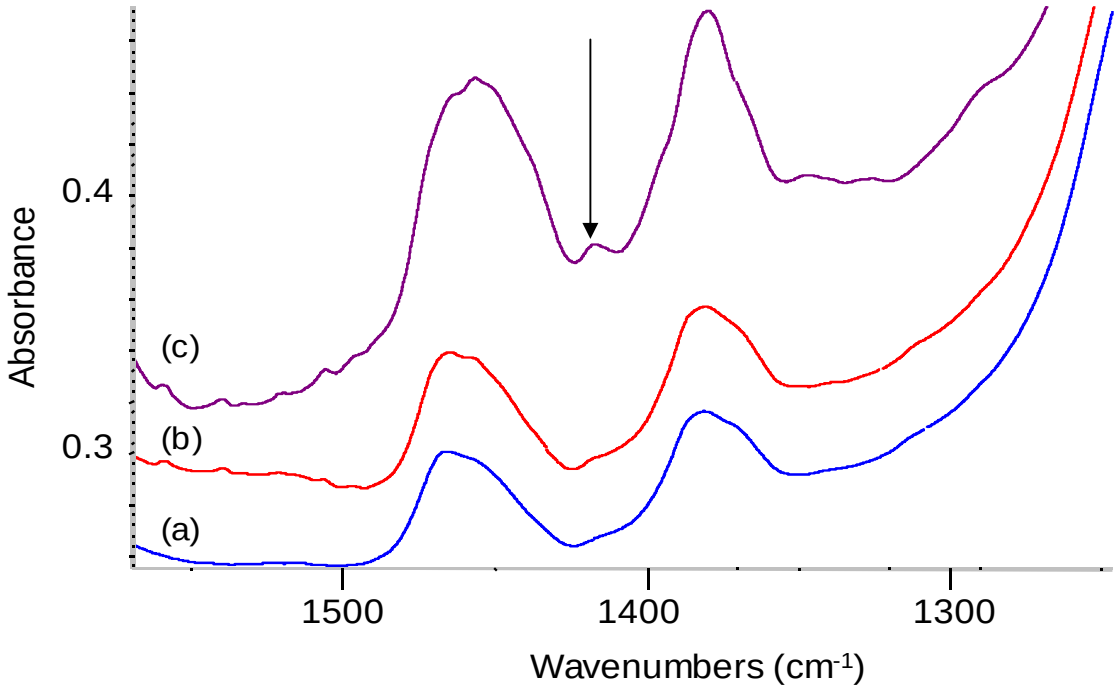

Figure 3.16: FTIR spectra of RO adsorbed onto (a) F400, (b) F435, (c) Fcol, displaying reduction of peak at approximately 1400 cm^{-1}.

It is proposed that the central peak is attributed to the tertiary C–O–H bond present in linalool. The removal of the OH group from linalool as a result of the cyclisation reaction proposed (Figure 3.13), forming limonene, would account for the loss of this absorption.

In contrast after adsorption of rosewood oil onto the synthetic/chemically modified aluminosilicate substrates, the central peak of the three is still clearly visible. This can be demonstrated (Figure 3.17) for LB and was also evident in the case of rosewood oil adsorption on LRD and F800. This was to be expected as the GC data did not suggest that rosewood oil had been modified after adsorption. This IR evidence showing that the natural and acid treated natural aluminosilicates degraded the linalool whilst the synthetic/chemically modified counterparts did not. This added further weight to the conclusion that the natural/acid treated natural aluminosilicates would not make suitable adsorption media for the EO.

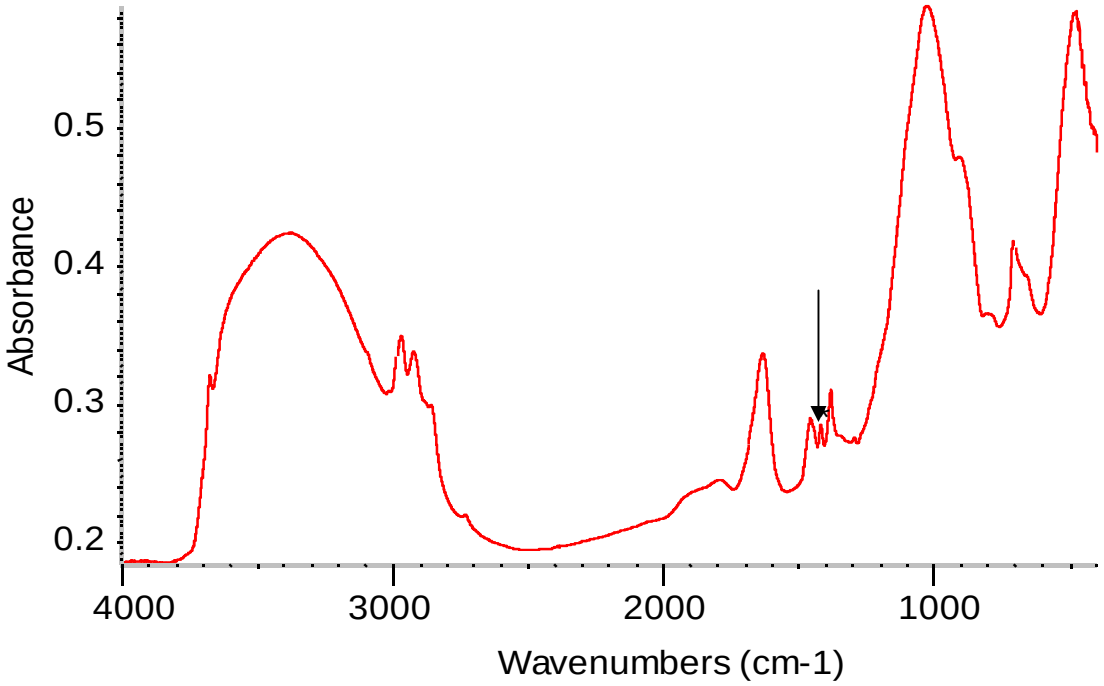

Figure 3.17: FTIR spectrum of RO adsorbed onto LB, * central peak which was not observed on adsorption of RO onto natural and acid treated natural aluminosilicates (F400, Fcol and F435).

Whilst the FTIR spectra of rosewood oil adsorbed on to LB, LRD and F800 did not show any evidence of damage to the rosewood oil, they did reveal a number of subtle changes to the rosewood oil peaks which gave an insight into the mode of adsorption of the oil components onto the substrate. The C–H stretch vibrations in the 3000 cm^{-1} – 2800 cm^{-1} range, and the alkeninc and aromatic C–H stretch vibrations (3000 cm^{-1} – 3100 cm^{-1}) for rosewood oil before and after adsorption onto the MMT substrates were compared to demonstrate this change (Figure 3.18).

After adsorption two of the three alkenic/aromatic C–H stretches were visible, corresponding to the 3007 cm^{-1} and 3085 cm^{-1} vibrations observed in the pure oil. Adsorption onto the substrates resulted in both peaks shifting to higher wavenumbers, indicating that the alkenic/aromatic C–H bond had been shortened and were therefore vibrating at a higher frequency. The shortening of the C–H bond was as a result of the pi electrons interacting with the surface silanols. The pi electrons were therefore withdrawn from the double bond causing the carbon atom to become slightly electron deficient, and thus drawing the electron density from the C–H bond towards the carbon, shortening the bond. This provided evidence of adsorption of the rosewood oil molecules to the

substrates via the double bonds in the EO molecules, and suggests that there may be multipoint adsorption of some molecules as OH groups on the EO component molecules will adsorb via hydrogen bonding to the substrate silanols.

After adsorption the peaks in the range 3000 cm^{-1} – 2800 cm^{-1} exhibited two changes (i) the peaks broadened slightly and (ii) the peaks shifted to higher wavenumbers. The first effect was due to differing bond energies of the C–H stretches; hydrogen bonding between oxygenated functional groups on the EO molecules and silanol groups on the layered silicates resulted in electron density being drawn to the from the carbon atom which affected its electron density. The change in electron density has an effect on the atoms bonded to the carbon resulting in shorter C–H bonds for the carbon atom and neighbouring carbon atoms. The change in length of C–H bonds would result in a different vibration frequency compared to analogous C–H bond in the molecule resulting in a broadening of the corresponding IR absorption peak. A shortening of the C–H bonds also results in the shift to higher wavelengths observed (Figure 3.18).

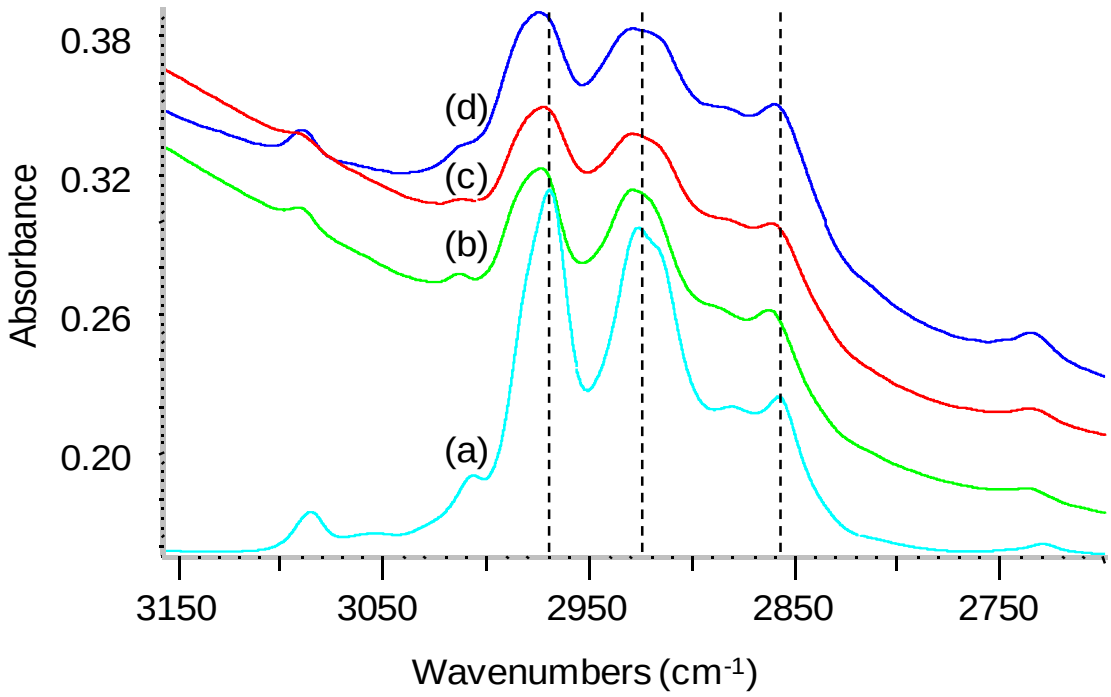

Figure 3.18: C–H stretching region in DRIFTS spectra for RO before and after adsorption (a) RO, (b) RO on LB, (c) RO on F800, and (d) RO on LRD. The vertical lines mark the centre of the peaks at 2858 cm^{-1}, 2925 cm^{-1} and 29700 cm^{-1} before adsorption, highlighting the shifts due to adsorption.

In addition, the shift to higher frequencies could be explained by molecules switching from trans conformers to gauche conformers [107, 108], due to the restricted space in the pores of the substrates. An example of this is demonstrated for the linalool CH_3 attached to the alcohol carbon (Figure 3.19).

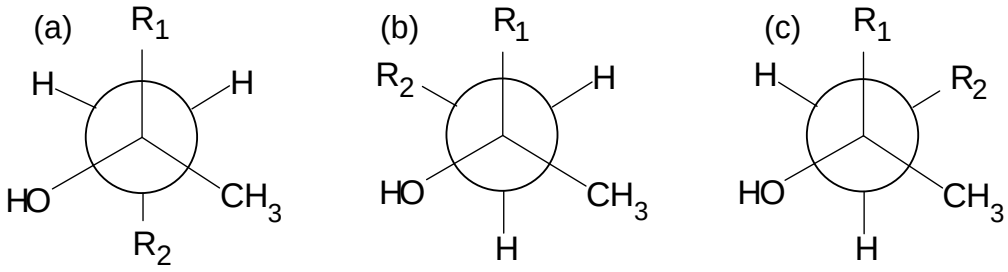

Figure 3.19: (a) *trans* conformation of linalool (CH_3 to R_2), (b) and (c) *gauche* conformations of linalool. Where R_1 is $CHCH_2$ and R_2 is $CH_2CHC(CH_3)_2$

The peaks observed between 1500 and 1300 cm^{-1} exhibited the same shift to higher frequencies as was seen for the C–H stretches in the 2800 to 3000 cm^{-1} range (Figure 3.20). The only peak to exhibit broadening was the peak at the highest frequency (approximately 1450 cm^{-1}) attributable to the C–H bend of the methylene groups present in the rosewood oil molecules.

The lack of broadening for the peaks at approximately 1410 cm^{-1} and 1375 cm^{-1} was due to the peaks corresponding to carbons with a single functional group (C–O–H and C–H respectively), as there is only one bond vibration interaction with the surface of the silicate substrates does not result in a differing of bond energies.

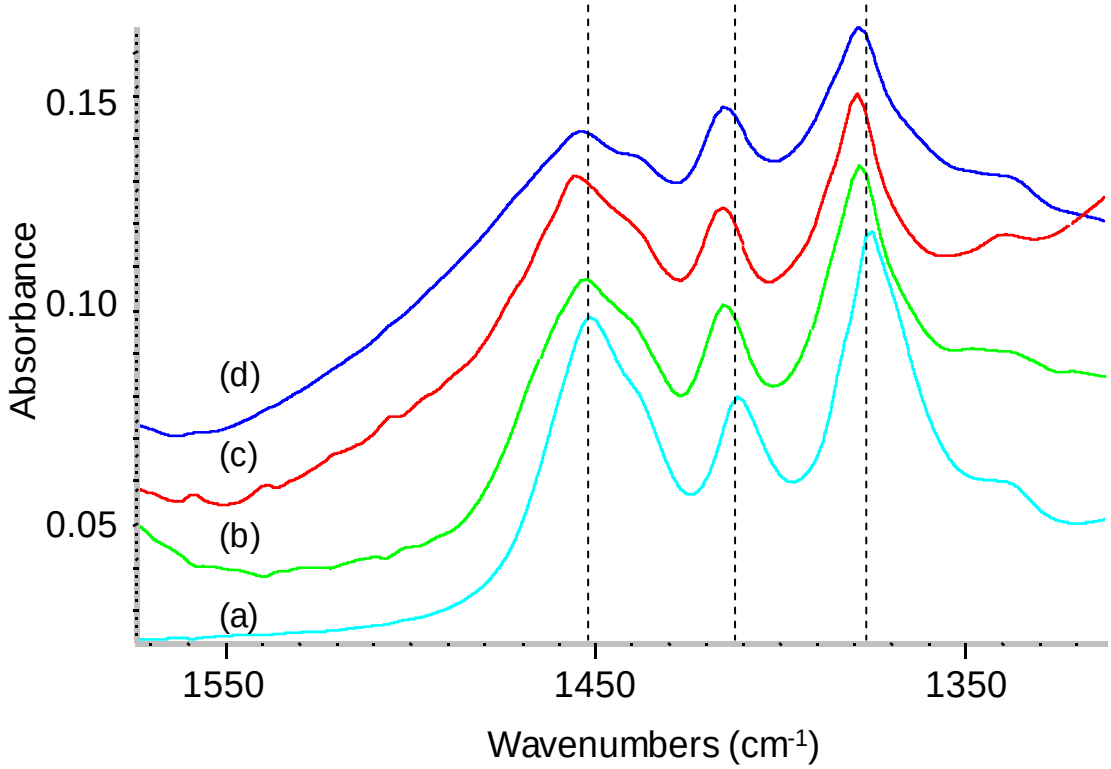

Figure 3.20: Peaks in the 1300 – 1500 cm^{-1} range for RO before and after adsorption (a) RO, (b) RO on LB, (c) RO on F800, and (d) RO on LRD. Demonstrating the presence of the central peak and the shift to higher wavenumbers for all three peaks (highlighted using dotted lines).

Soxhlet extraction of selected substrates recovered after adsorption (Section 3.5.3) enabled accurate determination of which molecules from the EO had been adsorbed. Molecules which were not recoverable through extraction were taken to be the molecules which had been damaged or converted by the substrates.

The synthetic/chemically modified layered silicates (LRD, LB and F800), did not show the same evidence of damage to the EO molecules as the natural MMT. Instead of a large increase in the amount of limonene present in the supernatant liquor there was a slight reduction. Adsorption onto LRD and LB did show a slight increase in the amount of eucalyptol (4.8 and 10.4 % respectively). In this case however, the level of increase was small relative to the levels of adsorption of the other molecules and it is unlikely that the slight increase in eucalyptol would result in a major modification of rosewood oil after adsorption. As the increase corresponded to an increase in eucalyptol from 1.14 % of the overall oil to 1.19 % and 1.26 % respectively, when taking into account

the lack of evidence of damage to linalool (which comprises 90 % of the oil) these are very small changes.
Of the three synthetic/chemically modified layered silicates LRD showed the highest overall levels of adsorption (40 % (reduction of oil from liquor)), as well as giving the highest individual level of adsorption for the major component of rosewood oil linalool (39.2 % (reduction of oil from liquor)).

The results obtained from the adsorption of rosewood oil onto the layered silicate substrates showed that the natural MMT materials would not be suitable for adsorption due to the damage to the major molecular components. Linalool has been shown to have significant antimicrobial properties, resulting in the inhibition of growth of bacteria at less than 2000 ppm [81], with rosewood oil comprised of 90 % (m/m) linalool, arguably any material that causes damage to linalool would adversely affect the antimicrobial activity of rosewood oil after adsorption. In contrast LRD, LB and F800 all showed good levels of adsorption for rosewood oil without the evidence for significant modification of the oils molecular make up. Taking this into account the natural and acid treated aluminosilicates were deemed unsuitable as adsorption substrates and were therefore not analysed in depth for adsorption of the other four oils. All further adsorption studies were carried out only using LB, LRD and F800. Using the adsorption data for the individual rosewood oil molecules (Table 3.2), the percentage of oil adsorbed from the supernatant liquor it was possible to calculate the percentage adsorption of the total oil onto the substrates. The total adsorption of rosewood oil onto the Laponites® and F800 is displayed as milligrams of oil adsorbed per gram of layered silicate (Figure 3.21). From the data displayed it was possible to determine that while LRD achieved the best levels of adsorption, the difference in levels of adsorption between the three substrates was small. F800 achieved 88.2 $mg.g^{-1}$ adsorption and LRD achieving 99.5 $mg.g^{-1}$ adsorption. The error bars for all three substrates, displaying the standard deviations, overlap and therefore the differences in adsorption were unlikely to be significant.

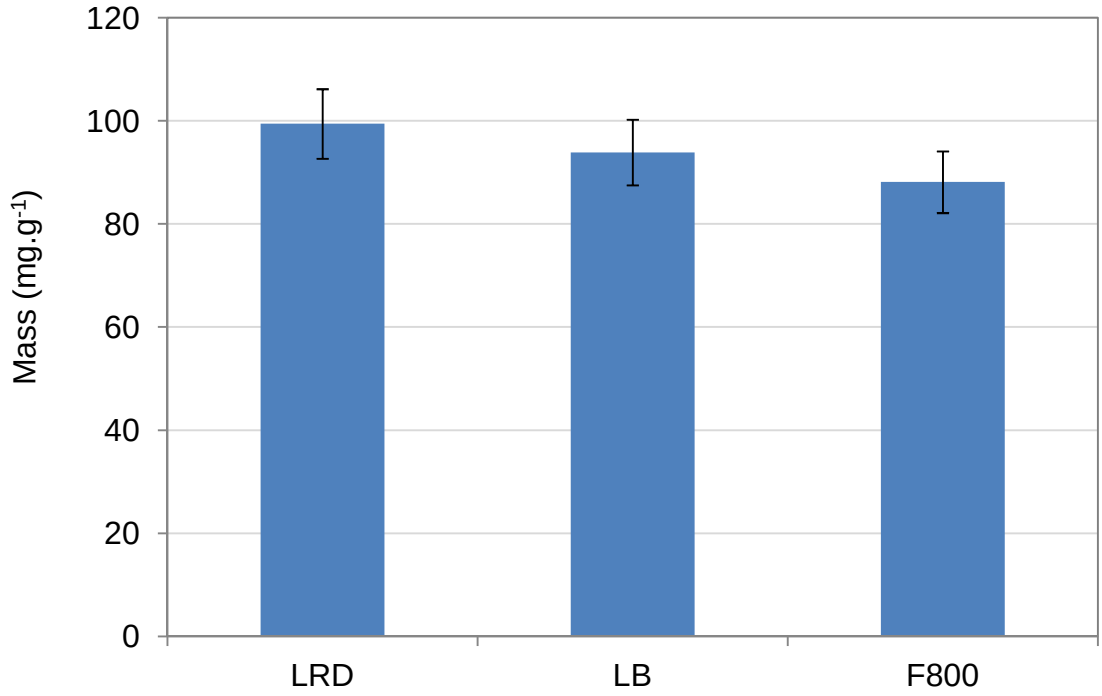

Figure 3.21: Levels of adsorption of RO onto layered silicate substrates estimated via GC. Demonstrating that there was no real difference in the adsorption performance of the three substrates when standard deviations were taken into account.

3.5.2.2 GC adsorption of oregano oil onto layered silicates

As the EO blend that was selected for best activity was a mix of oregano oil and rosewood oil, oregano oil was selected as the next oil to be analysed for adsorption. The adsorption results for the major components of oregano oil onto the Laponites® and Fulcat 800® as determined by GC are displayed (Table 3.4). As with rosewood oil, the molecular components of oregano oil with hydrophilic functional groups showed a greater percentage reduction after adsorption than the non-polar molecules which were comprised entirely of carbon and hydrogen.

The greatest reduction observed for a non-polar (hydrocarbon) EO component was with adsorption of mycrene onto LRD (approximately 28.6 %). Whilst the highest level of adsorption exhibited was linalool (86 %) on LB, the high adsorption activity was due to the polar nature of the molecule. In general the EO components bearing polar functional groups gave higher levels of adsorption. There was just one exception to this which was thymol onto LB.

After adsorption onto all three of the substrates there was an increase in the level of β-caryophyllene (Figure 3.22) present in the supernatant liquor, with the greatest level of increase observed after adsorption onto LRD.

Table 3.4: Percentage reduction of the oregano oil (OO) molecules analysed (from initial 1.25 % solution), after adsorption onto montmorillonite materials (text in red indicates an increase in concentration of molecule after adsorption. The Substrate which gave the overall highest level of adsorption is highlighted in green and the substrate which gave the lowest level of adsorption is highlighted in red). Demonstrating the level of adsorption of each molecule which comprised greater than 1 % of the molecular make up of OO.

EO molecular component	LRD		LB		F800	
	% after adsorption	% adsorption	% after adsorption	% adsorption	% after adsorption	% adsorption
α-pinene	1.02	27.66	1.23	12.77	1.16	17.73
mycrene	1.00	28.57	1.16	17.14	1.08	22.86
δ-4-carene	0.89	13.59	1.04	-0.97	1.02	0.97
p-cymene	1.18	25.79	1.33	16.35	1.31	17.61
γ-terpinene	0.94	8.74	1.01	1.94	1.02	0.97
l-linalool	0.39	73.65	0.21	85.81	0.40	72.97
thymol	1.02	38.55	1.23	25.90	1.11	33.13
carvacrol	0.79	44.37	0.64	54.93	0.85	40.14
β-caryophyllene	1.31	-24.76	1.12	-6.67	1.14	-8.57
Combined		35.13		40.55		30.93

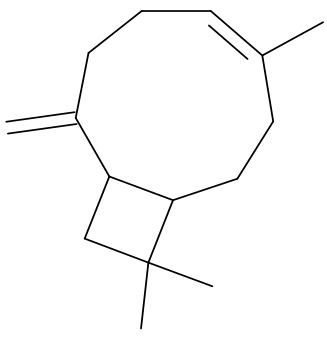

Figure 3.22: Chemical structure of β caryophyllene.

It was possible that the increase in the level of β-caryophyllene could have resulted from caryophyllene oxide (Figure 3.23) molecules undergoing reduction, resulting in removal of the keytone group, or a cyclisation reaction on α-caryophyllene between the carbons marked (*) in Figure 3.23.

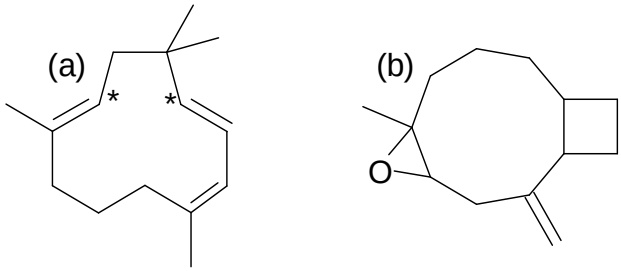

Figure 3.23: (a) α-caryophyllene (* donates carbon atoms that could undergo cyclisation to form β-caryophyllene) (b) caryophyllene oxide with ketone group that could be lost to form β-caryophyllene.

Unlike the increase in some fractions of rosewood oil after adsorption onto the natural and acid treated aluminosilicates, the increase in β-caryophyllene after adsorption of oregano oil was relatively small (a 9 % increase in a molecule comprising 3 % of the oil) . It is not likely that any of the major components of oregano oil were being converted to β-caryophyllene and therefore it should not have a significant effect on the antimicrobial activity of the EO.

Of the three substrates analysed for adsorption, LB gave the highest levels of oregano oil adsorption. As with rosewood oil, F800 gave the lowest levels of adsorption. LRD gave lower overall levels of adsorption compared to LB, however there was evidence that LRD was better at adsorbing the non-polar components of oregano oil (on average about 10 % greater reduction after adsorption than LB). This observation suggests that the environment within the pore structure of LRD was less hydrophilic than that of LB, and may be indicated by the lower CEC of LRD. This proposition appeared to be supported, since for two of the three alcohol molecules analysed, LRD achieved approximately 10 % lower adsorption than LB. The reduced levels of adsorption for F800 compared to the Laponites® was consistent across all of the oregano oil molecules, suggesting that access to the adsorption sites was the limiting factor rather than the chemical environment of the substrate.

The mass of oregano oil adsorbed in $mg.g^{-1}$ was calculated from the percentage reduction of EO molecules in the supernantant liquor. There was a greater difference in levels of adsorption for oregano oil across the three substrates than for rosewood oil (Figure 3.24). F800 again resulted in the lowest levels of adsorption achieved (77.5 $mg.g^{-1}$) with LB achieving the highest levels of adsorption (101.5 $mg.g^{-1}$).

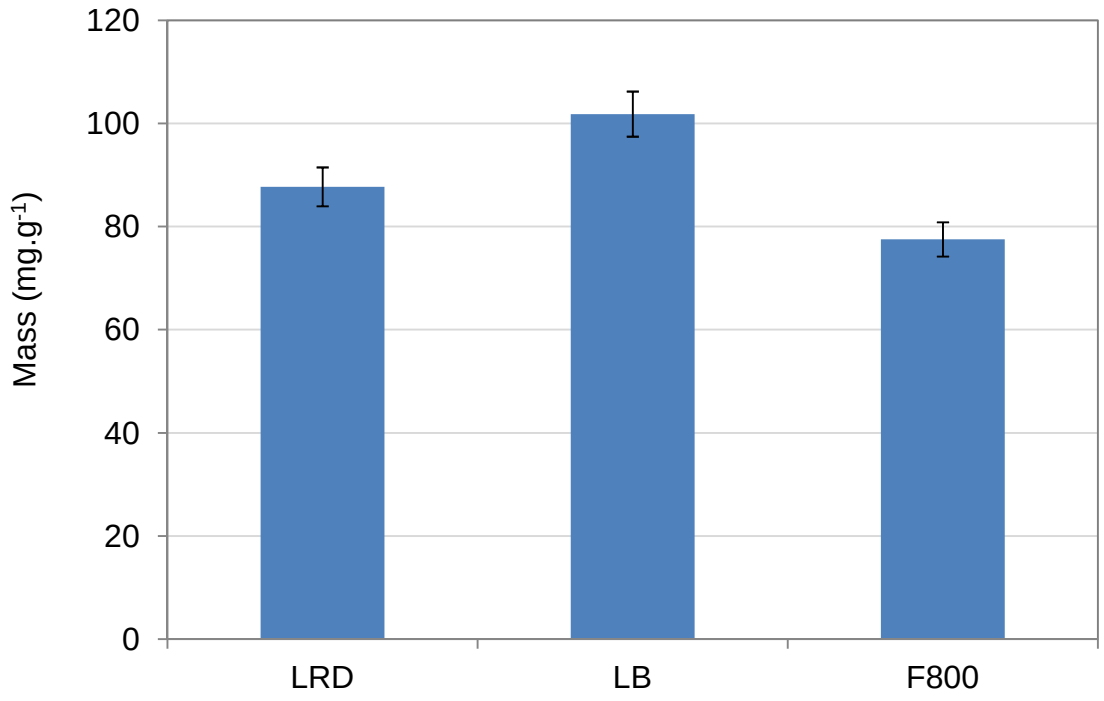

Figure 3.24: Levels of adsorption of OO onto layered silicate substrates estimated via GC. Demonstrating that LB provided the highest overall level of adsorption.

The FTIR data obtained for oregano oil after adsorption onto the substrated followed the same general pattern as that observed for rosewood oil for the peaks in the 3000 – 2800 cm^{-1} range, with peaks shifting to higher frequencies and undergoing a broadening effect. It was observed that after adsorption onto F800 the shifting effect was more pronounced than after adsorption onto the Laponite® substrates (Figure 3.25). There are two potential causes of the greater shift: (i) a greater level of conversion to gauche conformers had taken place after adsorption onto F800, (ii) adsorption onto Laponite® substrates resulted in a lesser degree of restriction of the C–H bond vibrations, allowing them to vibrate at a lower frequency. After adsorption of the three

alkenic/aromatic peaks, only the one at 3020 cm^{-1} was visible as the other two peaks were masked by the substrates large silanol peak. As with the rosewood oil peaks, (section 3.5.2.1) a shifting to higher wavenumbers was observed after adsorption onto the substrate. In contrast to rosewood oil, the extent of shifting was dependant on the adsorption substrate. The shifts were as follows: F800 3020 cm^{-1} to 3029 cm^{-1}, LB 3020 cm^{-1} to 3026 cm^{-1} and LRD 3020 cm^{-1} to 3023 cm^{-1}. This indicated that the strength of attraction of the pi electrons was stronger for F800 than the Laponite®s and that LB had a stronger attraction than LRD.

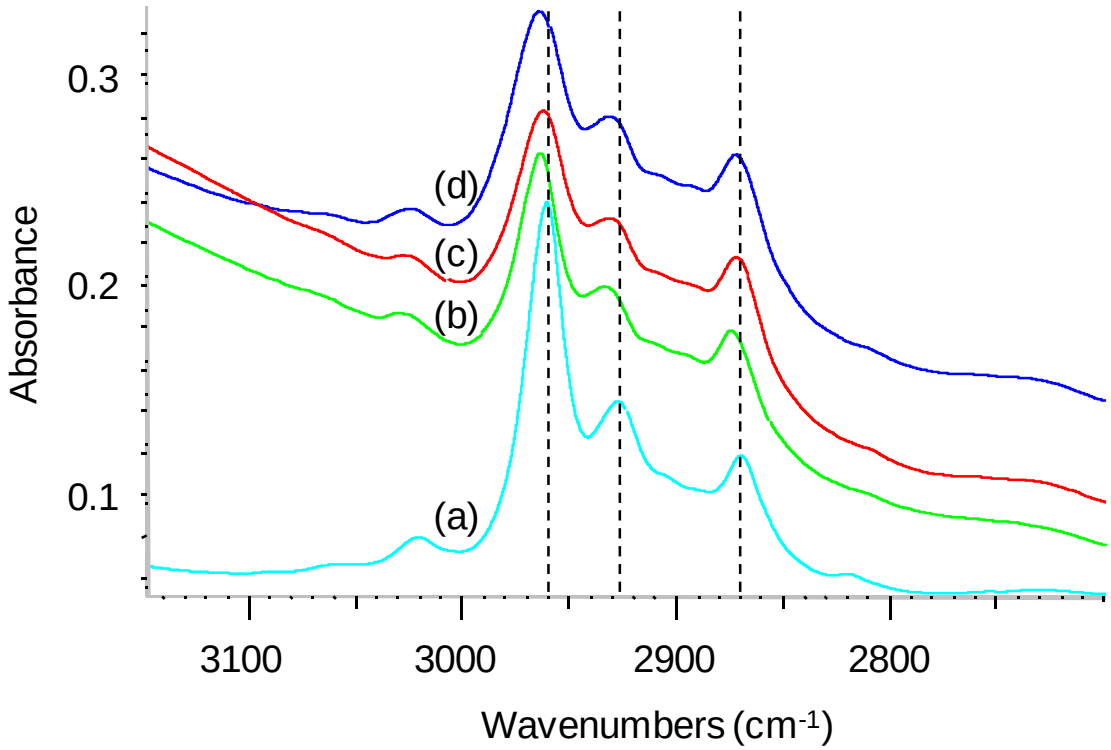

Figure 3.25: Peaks in the range 3000 to 2800 after adsorption of OO onto the aluminosilicates (a) OO, (b) F800 + OO, (c) LB + OO, and (d) LRD + OO. The vertical lines mark the centre of the peaks at 2869 cm^{-1}, 2938 cm^{-1} and 2960 cm^{-1} before adsorption, highlighting the shifts due to adsorption.

The only difference between the FTIR spectra for the adsorption of oregano oil onto the layered silicate substrates compared to the adsorption of rosewood oil was the general trend for less intense peaks after adsorption of oregano oil onto F800 in comparison to the Laponites®. This lower intensity was due to the lower mass of adsorption observed (Figure 3.24).

3.5.2.3 GC adsorption of manuka oil onto layered silicates

Data for the adsorption of selected components of manuka oil (MO) was demonstrated (Table 3.5). As manuka oil was a more complex oil than oregano oil and rosewood oil, 14 molecules were assessed for their adsorption onto the three aluminosilicates. None of the 14 molecules, which comprised more than 1 % of the manuka oil, contained any polar functional groups. It was therefore hypothesised that the levels of adsorption would be lower than those achieved for rosewood oil and oregano oil.

The levels of adsorption of manuka oil from the liquor onto the substrates were lower than those for rosewood oil and oregano oil by approximately 10 %. This was due to the more hydrophobic nature of the major components of manuka oil being less compatible with the hydrophilic silicate substrates. The majority of the molecules that account for greater than 1 % of manuka oil are bicyclic molecules, β-elemene excepted, making them larger than the monocyclic or acyclic molecules that make up the majority of oregano oil and rosewood oil. The larger molecules require more space for adsorption; this aspect will therefore limit the number of molecules that can be adsorbed onto the aluminosilicates. These factors help to explain why the level of adsorption from the liquor is lower than that achieved for the other oils. In addition to the lower levels of adsorption achieved, it was also observed that after adsorption onto each of the substrates there was an increase in concentration of molecules above the levels expected for a 1.25 % concentration solution. Adsorption of manuka oil on to both LRD and LB resulted in an increase in the concentration of cadina-1,4-diene by approximately 47 % and 69 % respectively. This is significant as cadina-1,4-diene makes up a significant proportion of manuka oil and is therefore likely to be involved in the antimicrobial activity of the EO. If the concentration of cadina-1,4-diene is increasing in the liquor, not only are other molecules being converted but also the levels of adsorption of the molecule itself must be very low. The increase of cadina-1,4-diene may arise in several ways; *cis*-calamenene has a very similar structure to cadina-1,4-dien (Figure 3.26) (possessing one extra double bond). A large proportion of *cis*-calamenene was removed from the liquor during adsorption and it is possible that some of it may have been converted.

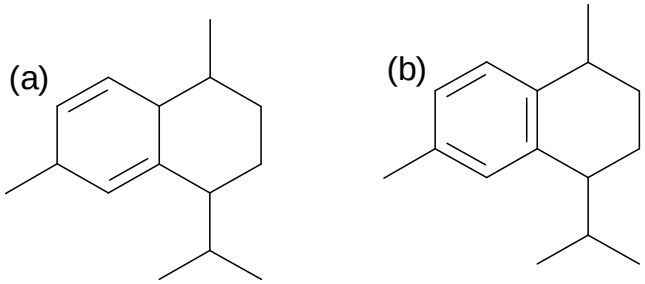

Figure 3.26: Chemical structure of (a) cadina-1,4-diene (b) *cis*-calamenene.

Table 3.5: Percentage reduction of the manuka oil (MO) components analysed (from initial 1.25 % solution), after adsorption onto layered silicate materials (text in red indicates an increase in concentration of molecule after adsorption. The substrate which gave the highest level of adsorption is highlighted in green, the substrate which gave the lowest level of adsorption is highlighted in red). Demonstrating the level of adsorption of each molecule which comprised greater than 1 % of the molecular make up of MO.

EO molecular component	LRD		LB		F800	
	% after adsorption	% adsorption	% after adsorption	% adsorption	% after adsorption	% adsorption
α-pinene	1.06	9.40	0.73	37.61	1.08	7.69
α-cubebene	0.78	38.10	0.77	38.89	0.15	88.10
α-copaene	1.06	15.87	0.98	22.22	1.00	20.63
β-elemene	0.76	36.13	0.076	93.61	0.53	55.46
α-gurjunene	1.02	22.73	0.98	25.76	0.97	26.52
β-caryophyllene	0.93	25.00	0.92	25.81	0.88	29.03
aromadendrene	1.12	9.68	1.08	12.90	1.00	19.35
isoledene	0.67	33.66	0.68	32.67	0.24	76.24
alloaromadendrene	0.37	65.09	0.45	57.55	0.91	14.15
epi-bicyclosesquiphellandrene	0.28	73.08	0.25	75.96	1.46	-40.38
β-selinene	0.59	50.83	0.70	41.67	1.09	9.17
δ-cadinene	1.10	8.33	1.27	-5.83	1.27	-5.83
cis-calamenene	0.28	78.13	0.34	73.44	1.12	12.50
cadina-1,4-diene	1.63	-46.85	1.87	-68.47	0.62	44.14
Combined		27.30		24.43		23.51

Also present in manuka oil was cada-1,4-diene, a stereoisomer of cadina-1,4-diene, which potentially could be converted during the adsorption onto the Laponites® contributing to the increased levels of cadina-1,4-diene.

After adsorption onto F800, instead of an increase in the level of cadina-1,4-diene, there was approximately a 44 % reduction. A possible reason for this difference was that F800 is an aluminosilicate and therefore will have a different chemical environment to the magnesium silicate Laponites®. Another example of the different chemical nature of the substrates affecting the adsorption characteristics comes from epi-bicyclosesquiphellandrene. For the Laponites® the reduction after adsorption was approximately 75 % where as adsorption onto F800 resulted in a 40 % increase.

The mass of oil adsorbed, calculated from the adsorption data of the oil molecules (Table 18) was demonstrated (Figure 3.27).

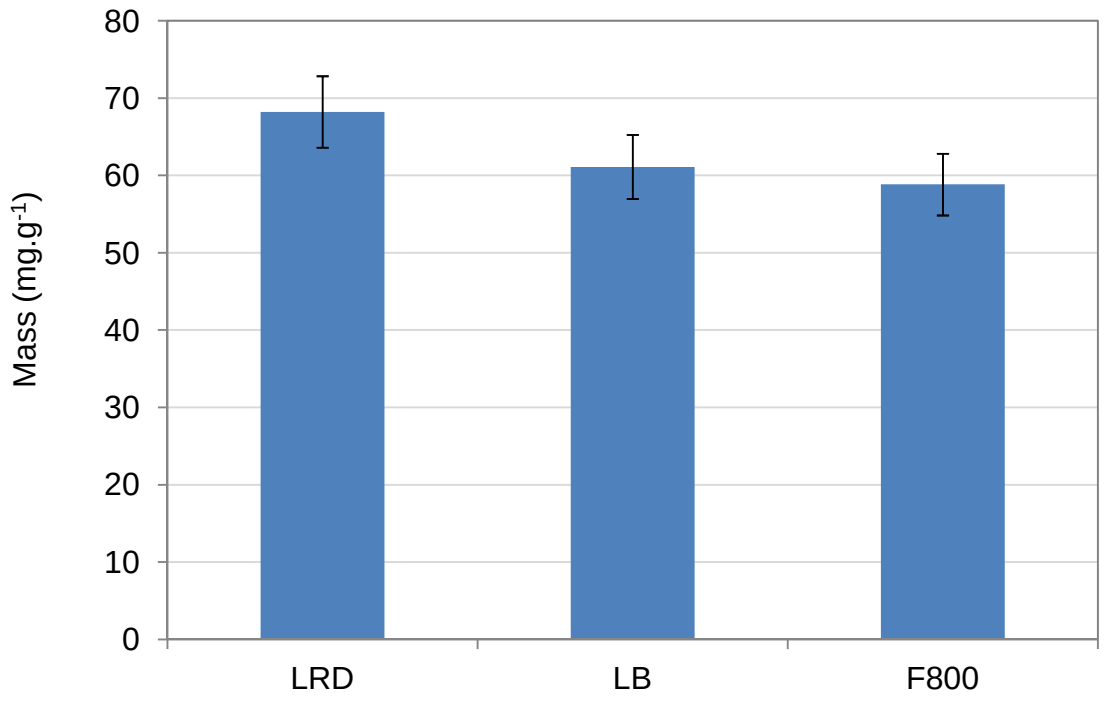

Figure 3.27: Levels of adsorption of MO onto layered silicate substrates estimated via GC. Demonstrating that there was little difference between the substrates in levels of adsorption when standard deviation was taken in to account.

The Laponites® gave higher levels of adsorption than F800; however it is important to take into account the change in makeup of the oil caused by reactive adsorption when determining which substrate performed the best.

All three of the substrates had some negative effect on the molecular make up of manuka oil. The possible negative effect caused by adsorption of manuka oil onto the Laponites® was significant as it resulted in a large increase (47 % and 68 % for LRD and LB respectively) in the level of one of the most abundant molecules (cadina-1,4-diene). This would be an issue as it is likely to significantly change the makeup of the oil and could affect the antimicrobial properties. The data also suggests that there was very little adsorption of cadina-1,4-diene which may also have a significant effect on the antimicrobial properties of the oil once it is adsorbed onto the aluminosilicates. For F800, there was less of an effect on the overall makeup of the oil as the molecule which showed an increase after adsorption was a minor component, comprising approximately 5 % (m/m) of the oil. Therefore despite F800 showing the lowest overall level of adsorption, it may well be the best substrate to use order to maintain the antimicrobial character of the EO after adsorption.

FTIR analysis of the substrates after adsorption of manuka oil showed that the peaks in the 3000 – 2800 cm^{-1} range behaved in the same way as was seen for rosewood oil. The observable manuka oil peaks in the 2000 – 1200 cm^{-1} range are discussed below. The two C–H=C–H peaks present in the oil spectrum at 3113 cm^{-1} and 3075 cm^{-1} were not visible on spectra of manuka oil adsorbed onto the substrates as they were masked by the silanol peak.

Peaks in the 1580 – 1500 cm^{-1} range (assignable to C=C–C aromatic ring stretches) showed no change in position or width after adsorption. Peaks at 1460 and 1422 cm^{-1} (methyl C–H bending vibrations) showed a shift to higher frequencies after adsorption; the shift may suggest formation of gauche conformers. The gem-dimethyl C-H bending peak at 1362 cm^{-1} (present in carvacrol, p-cymene and γ-terpinene) also underwent a shift to higher frequency after adsorption. After adsorption, the phenol OH peak (1382 cm^{-1}), of 4-terpineol, appeared to split, resulting in one peak at a slightly higher frequency and one peak at slightly lower frequency. It is possible that after adsorption, due to the restricted space, the phenolic OH was held in close proximity to the other functional groups thus creating transition dipoles.

Manuka oil exhibited two peaks between 1725 cm^{-1} and 1670 cm^{-1}. These peaks may be attributable the esters, apple oil and isopentyl 2-methyl-2-butenoate. After adsorption, the peak at 1723 cm^{-1} had shifted to a lower frequency by approximately 20 cm^{-1} indicating a high level of hydrogen bonding. The peak at 1673 cm^{-1} was no longer visible and it was possible that as a result of hydrogen bonding it has shifted to a lower energy, but was being masked by the large layered silicate peak at 1633 cm^{-1}. As with the other EO there was evidence of a change in conformation after adsorption, with peaks at 1556 cm^{-1}, 1497 cm^{-1}, 1382 cm^{-1} and 1316 cm^{-1} all shifting to higher frequencies. The peak at 1382 cm^{-1} showed significant broadening and was possibly attributable to the tertiary alcohol group present on spathulenol.

The shifting and broadening of peaks observed for manuka oil after adsorption onto the aluminosilicate substrates suggested that there had been interaction between the EO molecules and the surface of the substrates, providing evidence for adsorption of the molecular components of manuka oil.

3.5.2.4 GC adsorption of lavender oil onto layered silicates

Lavender oil (LO), like manuka oil, is a complex oil with 15 molecules comprising greater than 1 % of the oil (making it the most complex oil analysed). Unlike manuka oil there are a number of molecules containing one or more polar functional groups and only a few bicyclic molecules. This makes lavender oil more like oregano oil and rosewood oil and this was reflected in the higher levels of adsorption observed (Table 3.6).

After adsorption of lavender oil onto all three substrates, there was a significant increase in the level of β-mycrene and *trans*-ocimene. Both of these molecules can be formed from the dehydration of linalool [109]. Adsorption of lavender oil onto LB also resulted in a doubling of the level of *cis*-linalool oxide, whilst adsorption onto F800 resulted in a slight increase in the level of *cis*-linalool oxide. Working from the assumption that the majority of the increases in level of the molecules listed above originated from chemical reactions of linalool (either dehydration or oxidation), it would appear that adsorption of lavender oil onto these aluminosilicates has a negative effect. For LRD this would mean that approximately 20 % of the linalool present in the initial oil solution would have

been converted to other molecules. Therefore, instead of a 45 % level of adsorption of linalool, the value would be closer to 25 %. For LB approximately 21.5 % of the linalool had been converted, reducing the level of adsorption from 78 % to approximately 56 %. The greatest effect was on F800, with approximately 32 % of the linalool removed from the solution during adsorption being converted to other molecules, changing the level of adsorption from approximately 48 % to 16 %. Even if some of the increase in concentration of β-mycrene, *trans*-ocimene and *cis*-linalool oxide, originated from other molecules present in lavender oil, it was reasonable to assume that a large proportion of the linalool would be converted as it wass the most abundant molecule in the oil. This would result in a significant modification of the properties of the oil, potentially changing its antimicrobial properties.

As lavender oil showed low levels of antimicrobial activity (Section 2.2.4) it was not selected for use in the final antimicrobial combinations in this project, therefore the damage to the oil components during adsorption onto the aluminosilicates was not significant as far as this project was concerned. However, it is important to note that from the work carried out, none of the aluminosilicates used in this work would provide a suitable medium for the adsorption of lavender oil.

Table 3.6: Percentage reduction of the lavender oil molecules analysed (from initial 1.25 % (m/v) solution), after adsorption onto layered silicate materials (text in red indicates an increase in concentration of molecule after adsorption. The Substrate which gave the overall highest level of adsorption is highlighted in green and the substrate which gave the lowest level of adsorption is highlighted in red). Demonstrating the level of adsorption of each molecule which comprised greater than 1 % of the molecular make up of LO.

EO molecular component	LRD		LB		F800	
	% after adsorption	% reduction	% after adsorption	% reduction	% after adsorption	% reduction
Octan-3-one	0.18	84.75	0.19	83.90	0.66	44.07
β-mycrene	0.74	-208.33	0.89	-270.83	0.99	-312.50
δ-carene	1.22	4.69	1.26	1.56	1.20	6.25
trans-ocimene	1.76	-97.75	1.38	-55.06	2.40	-169.66
trans-linalool oxide	0.15	90.13	0.14	90.79	0.22	85.53
cis-linalool oxide	1.13	5.83	2.35	-95.83	1.39	-15.83
linalool	0.69	45.24	0.28	77.78	0.66	47.62
oct-1-en-3-yl acetate	0.62	53.38	0.59	55.64	0.89	33.08
endo-borneol	0.54	60.29	0.43	68.38	0.46	66.18
α-terpineol	0.53	59.54	0.71	45.80	0.46	64.89
linalyl acetate	0.36	73.72	0.16	88.32	0.34	75.18
2z 6e farnesol	0.15	86.73	0.11	90.27	0.17	84.96
geranyl acetate	0.60	55.22	0.72	46.27	1.53	-14.18
α-santalene	1.22	12.86	1.21	13.57	1.25	10.71
β-caryophyllene	1.20	-5.26	1.15	-0.88	1.20	-5.26
Combined		43.64		58.59		37.10

The mass of lavender oil adsorbed onto the aluminosilicate substrates was calculated from the values given in Table 3.6 (Figure 3.28)

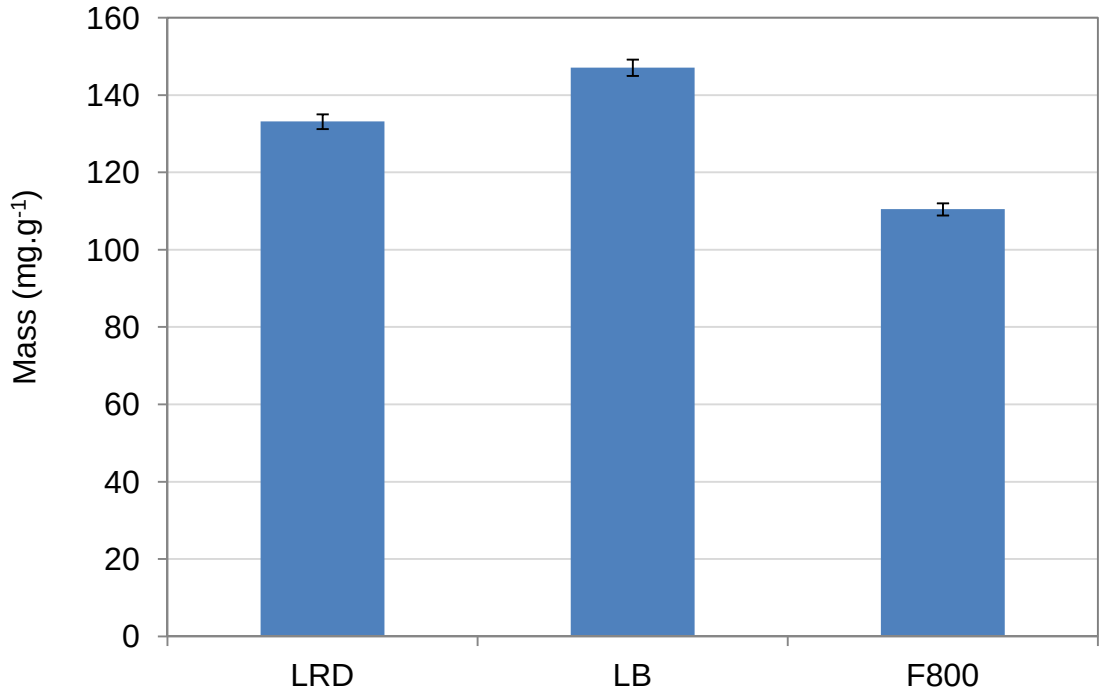

Figure 3.28: Levels of adsorption of LO onto layered silicate substrates estimated via GC. LB gave the highest overall level of adsorption with F800 gave the lowest level of adsorption.

All three of the substrates achieved good levels of adsorption for lavender oil compared to the other oils, with Fulcat® 800 at 92 $mg.g^{-1}$ and Laponite® B as high as 147 $mg.g^{-1}$. However, the changes in the chemical makeup of the oil that were evidenced (Table 3.6), meant that despite the high levels of adsorption achieved, the three substrates tested were unlikely to be suitable for adsorbing and thus acting as a reservoir for lavender oil.

FTIR analysis of the layered silicates was undertaken after adsorption of lavender oil. The peaks in the 3000 – 2800 cm^{-1} range behaved in the same way as reported previously (Section 3.5.2.1). The alkenic/aromatic peaks exhibited similar behaviour to that described for rosewood oil (Section 3.5.2.1), with shifts to higher wavenumbers observed. Due to the low intensity of the peaks, once adsorbed onto LB they were masked by the substrate silanol peak and were therefore not visible. The peak at 3087 cm^{-1} was visible after adsorption onto both F800 and LRD and exhibited a shift to approximately 3091 cm^{-1}, indicating adsorption via the lavender oil molecule double bonds to the substrates. The peak at 3006 cm^{-1} was only visible for F800 after adsorption.

Undergoing a large shift to 315.5 cm^{-1}, this was evidence of a strong interaction between the aromatic double bonds in the lavender oil molecules. Such a large shift was indicative of the molecule lying flat to the surface of the substrate.

The C=O peak present in lavender oil (attributable to linalyl acetate) at 1740 cm^{-1} exhibited a large shift to lower frequencies, approximately 1712 cm^{-1}, after adsorption onto the substrates. This supplied evidence for significant hydrogen bonding interactions and therefore demonstrated the interaction between the EO molecules and the surface of the aluminosilicates. Peaks at 1412 cm^{-1} and 1373 cm^{-1} shifted to higher frequencies thus suggesting a change in the conformation of some of the molecular components of lavender oil as a result of adsorption onto the aluminosilicates. The peak at 1451 cm^{-1}, corresponding to CH_3 bending vibrations, exhibited some broadening, resulting from a change in bond length of some of the C–H bonds contributing to the peak. Adsorption onto F800 resulted in a shift to a higher frequency, whereas adsorption onto the Laponites® resulted in a shift to lower frequencies. This difference in behaviour for the peak at 1451 cm^{-1} may be as a result of the higher level of adsorption observed for the Laponites® (especially LB). Closer packing of the EO molecules in the Laponites®, relative to F800 could result in dispersive forces lengthening the C–H bonds on groups protruding from the molecules. The longer (weaker) bond would have a lower bending frequency. In F800 with fewer molecules adsorbed, the EO molecules may be ble to shift to gauche conformations, restricting bond vibrations and resulting in the shift to a higher wavelength for the 1451 cm^{-1} peak.

3.5.2.5 GC adsorption of geranium oil onto layered silicates

Geranium oil (GO) was the final oil to be tested for adsorption onto the three aluminosilicate substrates. Like lavender oil, oregano oil and rosewood oil, geranium oil is comprised of a high proportion of molecules which have polar functional groups. Geranium oil was also similar in complexity to oregano oil and rosewood oil and has fewer than 10 molecules which comprise greater that 1 % of the oil. It was hypothesised that the latter features of geranium oil might favour high levels of adsorption of the EO molecules onto the substrates (Table 3.7). After adsorption onto the substrates there was little or no evidence of any negative modification of the oil, with only adsorption onto the F800 resulting in a

small increase (approximately 3 % (m/m)) in the level of methyl benzoate. Of the three substrates, LB showed the highest levels of adsorption, resulting in almost 60 % (m/m) of the EO components being removed from the liquor after adsorption. Of the three substrates F800 gave the lowest levels of adsorption, as was the case with the adsorption of the four other EO.

Table 3.7: Percentage reduction of the geranium oil (GO) molecules analysed (from initial 1.25 % solution), after adsorption onto the aluminosilicates (text in red indicates an increase in concentration of molecule after adsorption. The Substrate which gave the overall highest level of adsorption is highlighted in green and the substrate which gave the lowest level of adsorption is highlighted in red). Demonstrating the level of adsorption of each molecule which comprised greater than 1 % of the molecular make up of GO.

EO molecular component	LRD		LB		F800	
	% after adsorption	% adsorbed	% after adsorption	% adsorbed	% after adsorption	% adsorbed
Linalool	0.93	35.42	0.76	47.22	1.00	30.56
cis-rose oxide	1.00	33.33	1.20	20.00	1.26	16.00
iso-menthone	0.11	77.55	0.16	67.35	0.24	51.02
l-menthone	0.45	68.31	0.63	55.63	1.00	29.58
r-citronellol	0.45	66.67	0.32	76.30	0.49	63.70
geraniol	0.30	77.44	0.14	89.47	0.37	72.18
citronellyl formate	0.97	36.18	1.00	34.21	1.30	14.47
β-bourbonene	0.90	38.36	1.10	24.66	1.30	10.96
methyl benzoate	1.40	0.00	1.40	0.00	1.44	-2.86
Combined		53.33		58.99		44.28

The individual adsorption data for the geranium oil molecules was used to calculate the overall mass of adsorption of geranium oil onto the three layered silicate substrates (Figure 3.29).

The levels of adsorption achieved for geranium oil onto the substrates was high compared with the other oils, with Laponite® B achieving approximately 150 $mg.g^{-1}$. The reasons for this were likely to be related to the chemical makeup of

geranium oil. This will occur since all but one of the major components contained at least one polar functional group, which wouldl be attracted to the hydrophilic nature of the layered silicate surfaces.

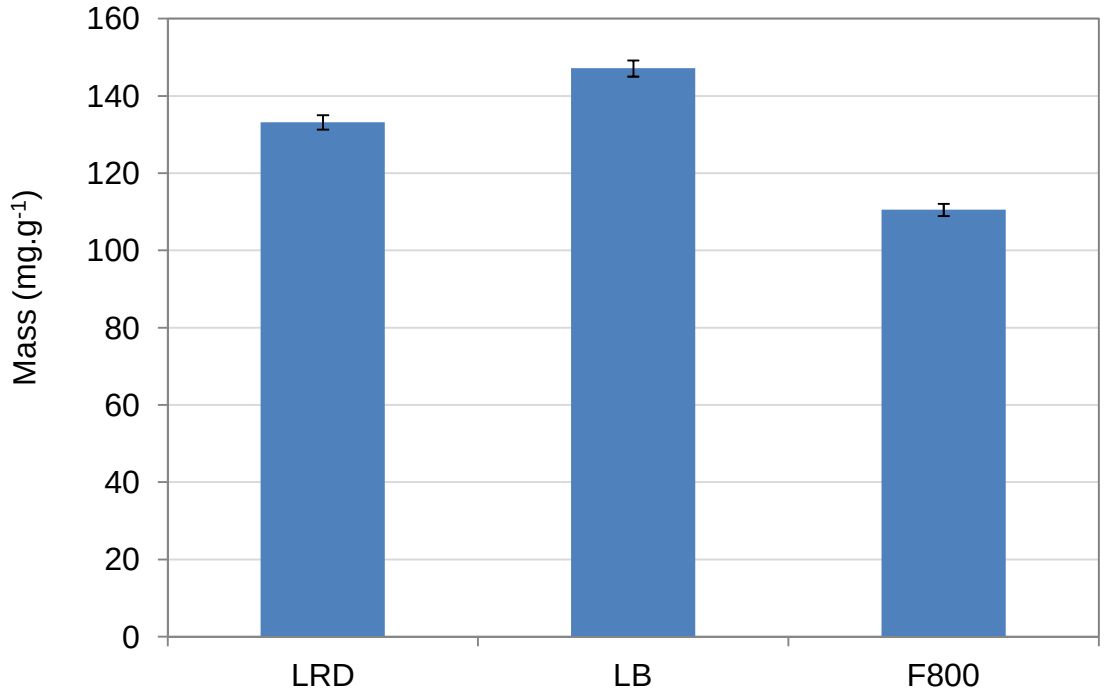

Figure 3.29: Levels of adsorption of GO onto layered silicate substrates estimated via GC. Demonstrating that LB gave the highest overall level of adsorption and F800 gave the lowest.

FTIR analysis of the layered silicates was undertaken after adsorption of geranium oil. The peaks in the 3000 – 2800 cm^{-1} range behaved in the same way as reported previously (Section 3.5.2.1). The alkenic and aromatic C–H peaks were not visible on the geranium oil-substrate spectra as they were masked by the silanol peak due to their low intensity.

Geranium oil was the least complex of the five oils analysed, in that there were only three peaks that could be analysed after adsorption in the range 1750 - 1200 cm^{-1}. The greatest effect after adsorption was observed for the aldehyde C=O peak at 1729 cm^{-1} assignable to R-citronellal. There was a significant shift to lower frequencies (approximately 1700 cm^{-1}) seen with all three substrates. This suggests that there was a high level of hydrogen bonding between the carbonyl oxygen and the hydrogen of surface silanol groups of the substrates.

3.5.2.6 GC Adsorption summary

For all five of the oils assessed F800 gave the lowest levels of adsorption, in general achieving between 10 and 20 $mg.g^{-1}$ lower adsorption than the best performing Laponite®. Of the two Laponite® substrates used, LB gave the highest levels of adsorption for three of the five oils, it adsorbed almost 50 $mg.g^{-1}$ more lavender oil than LRD. The latter achieved the highest level of adsorption for rosewood oil and manuka oil, however in both cases the level of adsorption achieved was only slightly higher than that for LB. Due to a significant increase in the concentration of a number of molecules after adsorption it is unlikely that any of the three substrates tested would be suitable for adsorption of lavender oil. After adsorption of manuka oil onto the Laponites® there was an increase in the level of cadina-1,4-diene which comprises approximately 13 % of the oil. It was therefore likely that F800 would be the most suitable substrate for adsorbing manuka oil despite it achieving the lowest level of adsorption.

Although LB achieved the highest levels of adsorption for the majority of the oils there was little difference between the two Laponites® when analysing the level of adsorption of the two oils (oregano and rosewood) which were to be used in the antimicrobial EO blend (selected using the data in Section 2.5.2). LRD gave the higher level of adsorption of rosewood oil whereas LB gave the higher level of adsorption for oregano oil. By analysing the interactions of the two oils with the Laponites® using FMC (Section 3.5.4) it may be possible to obtain greater distinction between the two substrates as to which will provide the best adsorption and desorption characteristics for use as a controlled release reservoir in the polymer formulations.

From analysing the DRIFTS data for EO adsorbed on the aluminosilicate substrates, it was clear that a significant fraction of EO molecules were retained on the substrates. By observing changes in peak shape and position, it was also possible to determine that there was a level of interaction between the EO molecules and the substrate, demonstrating that adsorption rather than just absorption into the pores took place. In particular, there was evidence for hydrogen bonding both between the oxygenated species on the EO molecules and principally the silanol groups on the aluminosilicate surfaces. There was

also evidence for adsorption of the EO onto the substrates resulting in a switch of conformation from trans to gauche in some cases.

3.5.3 Soxhlet extraction of EOs from layered silicates after adsorption

As the combined GC and FTIR (Section 3.5.2.1) results had shown evidence of the acid treated clays having a significant destructive effect on rosewood oil. Soxhlet extraction of F435 recovered after rosewood oil adsorption to allow for determination of which EO molecules had been adsorbed was carried out. If no linalool was retrievable from the F435 – RO substrate then it would be clear evidence that the natural MMT were not suitable for adsorption of one of the oils which would be present in the antimicrobial EO blend to be used.

Using heptane as the solvent the F435 recovered after adsorption of rosewood oil (Section 3.6.2) was extracted. After extraction the heptane was analysed with GC (Figure 3.30) to determine which if any rosewood oil molecules had been extracted and therefore initially adsorbed onto the F435

After adsorption of rosewood oil onto F435 no linalool was remaining in the heptane when analysed using GC (Section 3.4.2). Significantly, GC analysis of the heptane extract also showed no evidence of linalool. There was no linalool remaining in the supernatant liquor after adsorption and none was adsorbed onto the F435, thus it can be concluded that it had been chemically modified. This confirms the unsuitability of F435, and the other natural and acid treated aluminosilicates as adsorption reservoirs for the EO. All of the other major molecular components of rosewood oil were recovered from the heptane extract, showing that adsorption of the other molecular components had taken place.

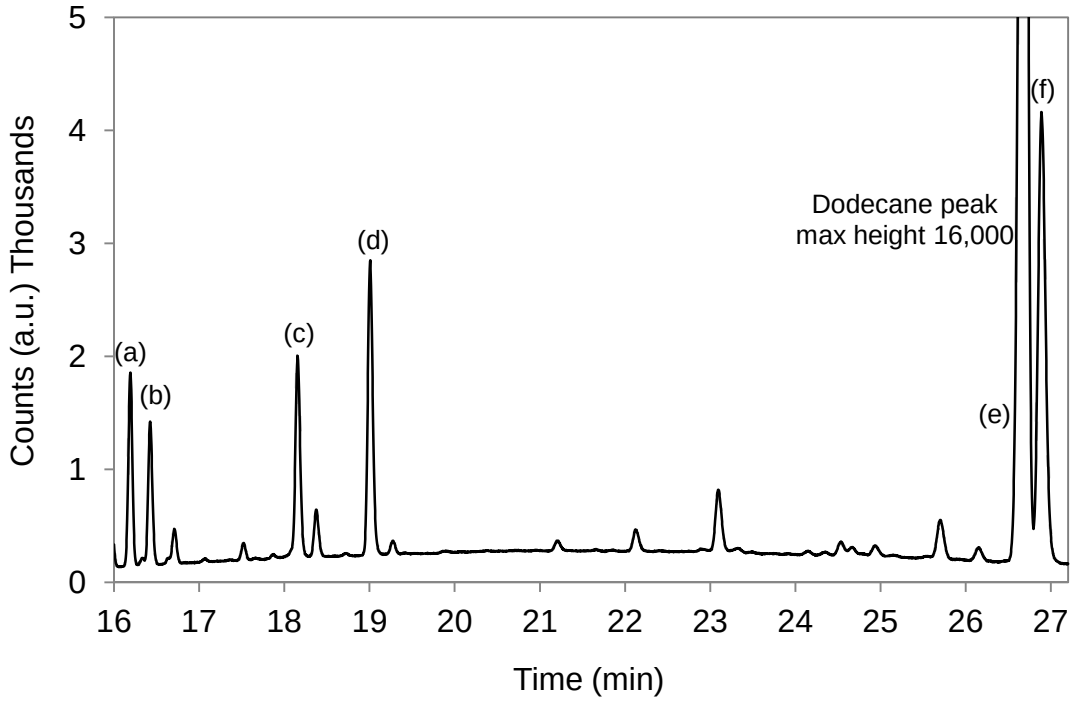

Figure 3.30: Extract from chromatograph obtained after extraction of F435 adsorbed rosewood oil (a) limonene peak (b) eucalyptol peak (c) *trans*-linalool oxide (d) *cis*-linalool oxide (e) dodecane (internal standard) (f) α-terpineol. Demonstrating the lack of a large linalool peak (normally seen 0.5 min after *cis*-linalool oxide in the extraction liquor of F435.

3.5.4 Flow micro-calorimetry assessment of EO adsorption onto layered siliactes

The GC adsorption studies enabled determination of which of the major EO components, that comprised greater than 1 % of the oil, adsorbed on to the substrates. It was considered that flow micro-calorimetry (FMC) could provide an alternative view of the adsorption process as the technique can provide insight in the strength of adsorption, and at the same time, provide data relating to the amount of EO adsorbed and desorbed. A direct comparison between the FMC and GC adsorption studies was not possible due to the significant differences in the adsorption conditions. The GC studies utilised a static system in which an equilibrium between adsorption and desorption would form. Under the FMC conditions, the concentration of EO in solution was constantly replenished by the flow of solution over the substrate, therefore equilibrium would not be achieved. This may lead to an expectation that adsorption levels

obtained via FMC would be greater than those obtained via GC. There are also other factors to consider, for example the concentration of EO used in the FMC studies was approximately 0.3 % (m/v) where as the initial concentration in GC was 1.25 % (m/v). If the strength of adsorption was weak then the higher initial concentration present in the GC studies result in a higher level of adsorption.

FMC can be a time consuming process, with a single run taking up to 8 hours, depending on the level of adsorption achieved. In order to prevent the work taking an excessive amount of instrument time, and taking account of damage to EO components caused by reactive adsorption to some of the substrates (i.e. Fcol, F400 and F435, described in Sections 3.5.2.1 and 3.5.3), the FMC study was focussed on the adsorption of the five EO onto F800, LB and LRD.

Due to the time consuming nature of the FMC runs and technical issues associated with the FMC, single replicate data has been reported in some instances which will be clearly indicated. In such cases the average error (5.25 %) will be used to represent the spread of data expected.

3.5.4.1 Adsorption of EO onto Laponite® RD determined by FMC

FMC data for Laponite® RD (LRD) (Figure 3.31) was obtained from a single replicate (with the exception of rosewood oil). The error bars displayed in for oregano oil, lavender oil, geranium oil, manuka oil (Figure 3.31) were calculated from the average error obtained from the rest of the FMC data.

Rosewood oil and lavender oil showed the most energetic adsorption per unit mass of the substrate, with a high level of retention, whilst oregano oil and manuka oil showed the strongest retention. The levels of adsorption, as measured from the differential refractometer data are reasonable estimates if most of the EO components are adsorbed. The latter would be true of rosewood oil and lavender oil, as these two oils contained a large amount of linalool (90 % and 35 % of the total oil composition respectively) and other polar components (97 % and 93 % of the total oil composition respectively). However, if an oil had a significant fraction of potentially non-adsorbing components (such as the bulky non-polar molecules found in manuka oil) could give rise to

underestimates of the level of adsorption due to the refractive index signal increasing more quickly than it would if all the EO components had adsorbed. If this was the case the levels of EO desorption would also be similarly underestimated.

The highest masses of adsorption achieved for LRD were with oregano oil and rosewood oil, whilst the lowest mass of adsorption observed was for manuka oil. The high level of adsorption for rosewood oil can be attributed to the simple make up of the oil and the fact that the major component (linalool > 90 %) was a straight chain molecule with a polar OH group. The OH group would interact with the OH groups on the surface of the LRD via hydrogen bonding, the relatively low level of desorption reflects strong adsorption which is consistent with hydrogen bonding. Adsorption of rosewood oil also resulted in a high enthalpy of adsorption adding further evidence that the linalool was hydrogen bonding to the surface OH groups present on LRD.

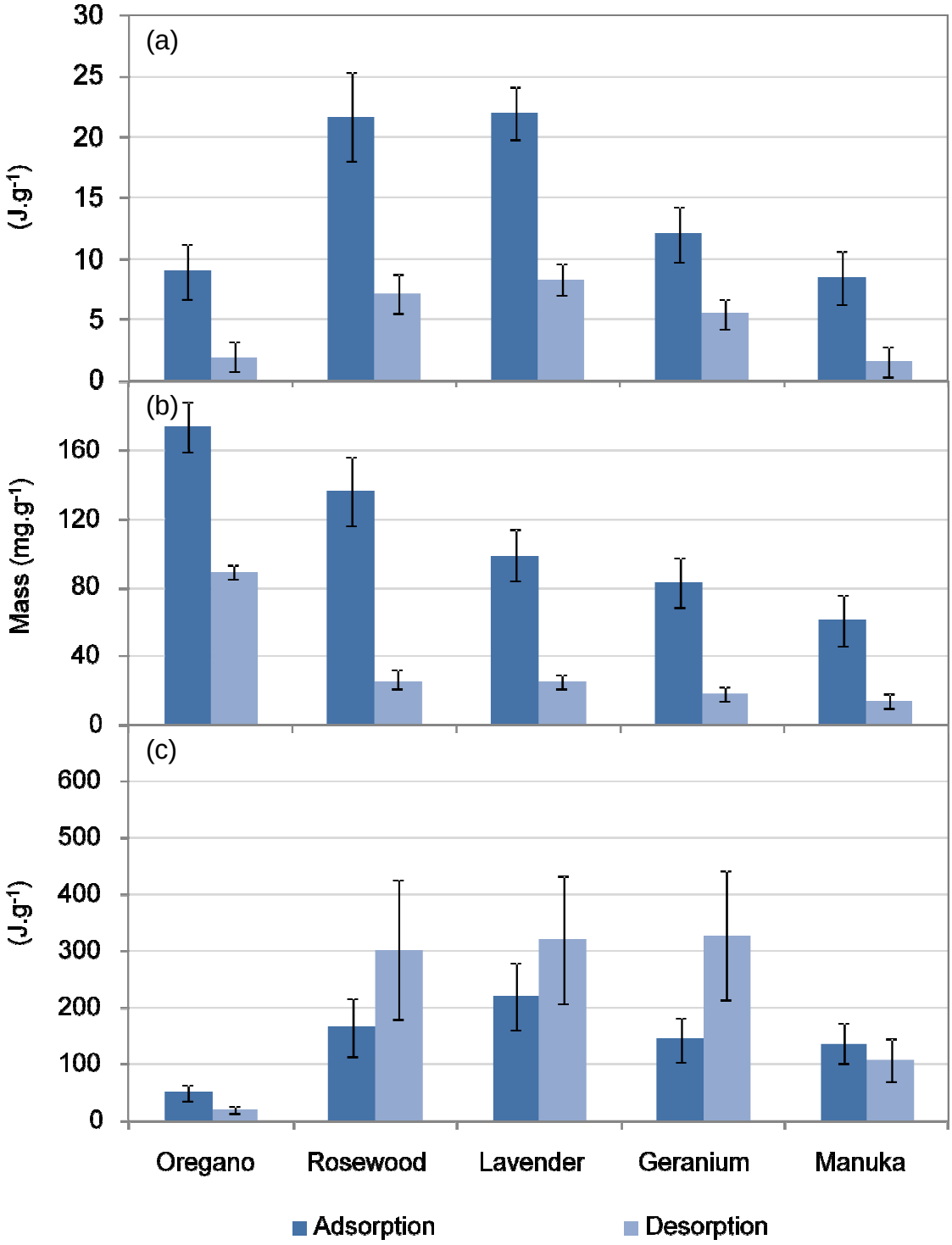

Figure 3.31: (a) Heat of adsorption and desorption of EO onto LRD in joules per gram of substrate (b) Mass of adsorption and desorption of EO onto LRD in milligrams per gram of substrate (c) Heat of adsorption and desorption of EO onto LRD in joules per gram of oil adsorbed. Demonstrating the overall level of adsorption achieved for each EO via FMC, and the strength of attachment of the EO molecules to the LRD surface.

The high mass of desorption in proportion to adsorption for oregano oil indicated weak adsorption. Oregano oil contains fewer molecules with polar functional groups than lavender oil, geranium oil and rosewood oil and therefore there would be less hydrogen bonding of the oregano oil molecules. In addition, the majority of the polar functional groups in the oregano oil molecules are in close proximity to other bulky functional groups resulting in steric hindrance and making them less available for hydrogen bonding. Adsorption of oregano oil resulted in a very low enthalpy of adsorption in comparison to the mass; this was evidence for a lack of interaction between the oregano oil molecules and the LRD surface. Molecules which were adsorbed into the galleries of the LRD but did not undergo interactions, such as hydrogen bonding, would increase the mass of adsorption recorded but have no effect on the enthalpy of adsorption. This resulted in comparatively low enthalpy of adsorption when compared to the mass of adsorption.

The lower mass of adsorption observed for lavender oil and geranium oil (relative to rosewood oil) can in part be attributed to the presence of larger molecules such as farnesol, geranyl acetate and citronellyl formate. Once adsorbed they would cover a greater area of the surface thus restricting the space for more molecules to be adsorbed. For lavender oil, the enthalpy of adsorption per gram of substrate was similar to that for rosewood oil. Therefore the enthalpy of adsorption per gram of oil adsorbed was higher for lavender oil in comparison to rosewood oil. In Section 3.5.2.4 it was observed that there was a large increase in the concentrations of a number of lavender oil molecules after adsorption. The increase in concentration was most likely due to conversion of other molecules within lavender oil. The chemical reactions taking place to do this would produce heat, which would result in an overestimation of the enthalpy of adsorption. This may explain why the enthalpy of adsorption for lavender oil per gram of oil adsorbed was higher than the value recorded for rosewood oil.

The low mass of adsorption for manuka oil was due to there being only a few polar molecules in its composition, combined with the larger molecular size of some of the bicyclic molecules. The lack of polar species together with the larger molecular size of some of the components will mitigate against prolific adsorption. Manuka oil also exhibited the lowest heat of adsorption, however the heat of adsorption per mass of oil adsorbed was equal to that of geranium

oil and higher than oregano oil. This was unexpected as the hydrophobic nature of the oil and the low mass of adsorption led to the expectation that there would be few interactions between the manuka oil molecules and the LRD surface therefore the enthalpy of adsorption would be low. It is possible the strength of attraction between the manuka oil molecules and the LRD may be as a result of pi electrons from aromatic rings and double bonds present in many of the molecules interacting with the electron deficient hydrogens of the LRD surface silanols. Multiple double bonds in the molecules may have led to more than one point of surface interaction for each molecule increasing the strength of adsorption. In Section 3.5.2.3 it was observed that there was a significant increase in the concentration of cadina-1,4-diene after adsorption onto LRD. This increase most likely came from the conversion, via chemical reactions of other similar molecules (e.g. calamenene). Heat would be evolved in such a process and therefore could explain the unexpectedly high enthalpy of adsorption per mass of manuka oil. The mass of desorption for manuka oil was relatively low compared to what would be expected. If the manuka oil molecules were not interacting with the surface of the LRD then they would be easily removable which would result in a high proportion of the adsorbed molecules being recovered through desorption. However, only 23 % of the mass of manuka oil adsorbed was able to desorb off in comparison to 50 % of the mass of oregano oil. It is possible that the mass of desorption was underestimated. In order to calculate the mass from the changes in refractive index (RI) (Section 3.4.4) calibration peaks must be obtained. These peaks are obtained using the complete oil; this is an imperfect situation as it assumes the RI of the oil desorbed from the substrate is equal to that of the oil before adsorption. Changes in the oil composition (such as the formation of cadina-1,4-diene could result in a change in the RI. In addition, if the molecules adsorbed were the lower RI molecules in the oil then during desorption the speed of reduction of RI would be faster, resulting in an underestimation of the mass of desorption. An underestimation of mass would result in an unexpectedly high enthalpy of desorption per mass of oil desorbed. The enthalpy of desorption for manuka oil was shown to be almost equal the enthalpy of adsorption (Figure 3.31c) (not what would be expected with weak adsorption). This added evidence to the speculation that the mass of manuka oil desorbed was underestimated.

The enthalpies of desorption per mass of oil adsorbed for rosewood oil, geranium oil and lavender oil were all greater than the enthalpies of adsorption. It is possible that the mass of desorption was underestimated for the three oils, due to the refractive index of the components desorbed being lower than that of the total oil. As the enthalpy calculated by FMC was not subject to the same variation as the mass (and therefore gave a more accurate value) an underestimation of mass would result in an over estimation of the enthalpy of adsorption per mass of oil.

3.5.4.2 Adsorption of EOs onto Laponite® B determined by FMC

Adsorption of the EO onto Laponite® B (LB) (Figure 3.32) resulted in a similar pattern to LRD for both enthalpy and mass. However, for all of the EO the mass of adsorption achieved was lower (by at least 20 $mg.g^{-1}$ in the case of lavender oil, and up to 90 $mg.g^{-1}$ for oregano oil). This lower adsorption was in contrast to what was observed in the GC adsorption studies (Section 3.5.2). For rosewood oil, geranium oil and manuka oil the lower level and greater reversibility of adsorption on LB relative to LRD represents weaker adsorption activity of the former substrate. The low initial concentration of EO (0.3 %) and weak adsorption would result in the LB not being able to draw as many of the EO molecules out of solution as the solution passed through the cell. In addition LB has double the CEC of LRD, meaning there are double the number of Na^+ counter ions present in LB than LRD. This will have the effect of making the galleries of LB more hydrophilic and therefore less receptive to the organic EO molecules.

The enthalpies of adsorption per mass of substrate for geranium oil, manuka oil and oregano oil were higher with LB than for LRD with lavender oil exhibiting a similar heat of adsorption. When taking into account the lower mass of adsorption achieved for these EO onto LB this resulted in a significantly higher enthalpy of adsorption per mass of oil. The major difference between the two silicates is the presence of Si–F bonds in LB replacing of some of the Si–OH bonds. In a tetrahedral $Si(OH)_3F$ arrangement the fluorine will draw electrons towards it as it was more electronegative than the hydroxyls; this will result in a polarisation of the Si-F bond making the fluorine δ^-. The fluorine will attract the δ^+ hydrogens of any hydroxyl groups on the EO molecules and the subsequent hydrogen bonding will be stronger than the oxygen to hydrogen H-bonding in LRD. This may explain the higher enthalpy of adsorption per mass of oil observed for LB in comparison to LRD.

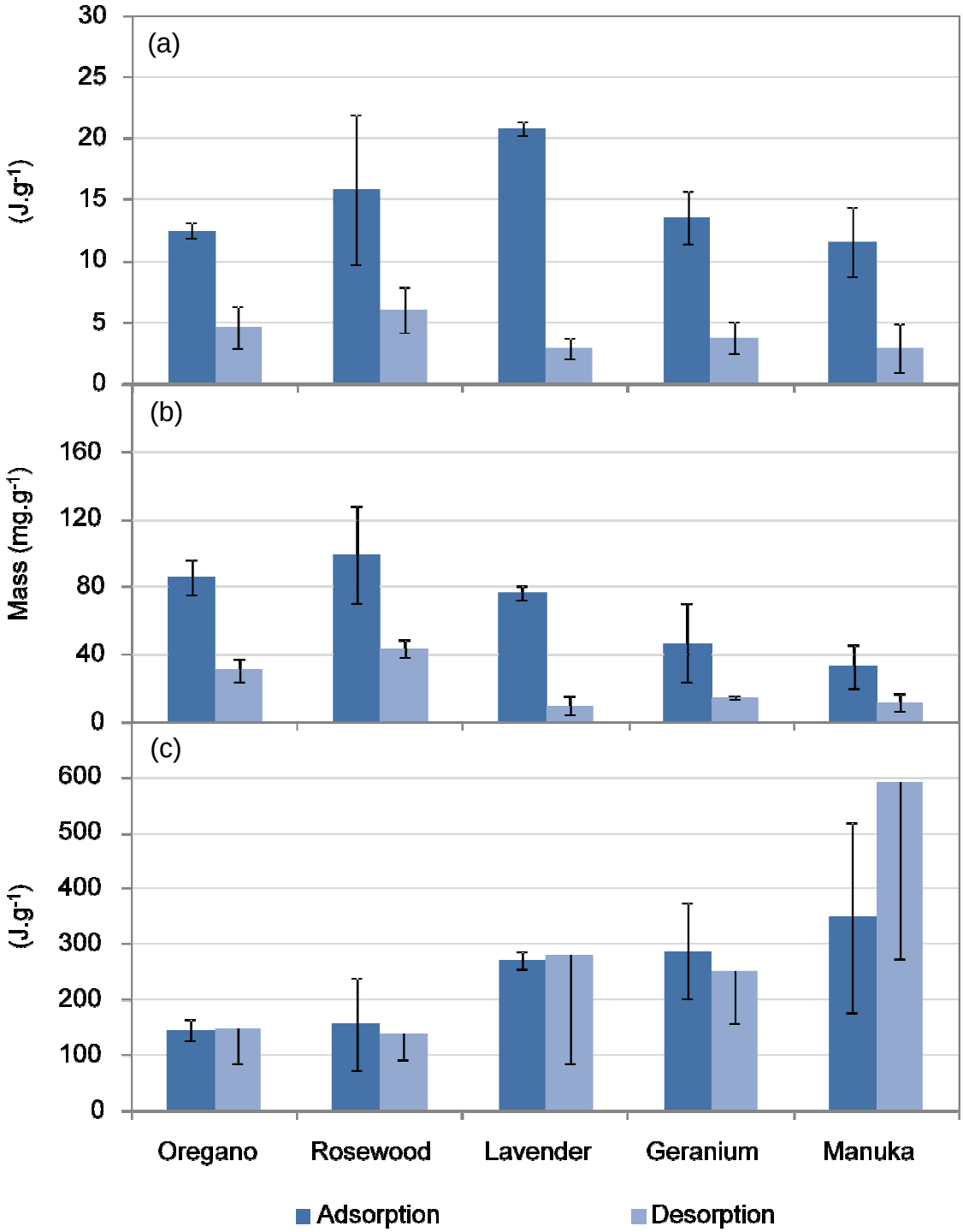

Figure 3.32: (a) Heat of adsorption and desorption of EO onto LB in joules per gram of substrate (b) Mass of adsorption and desorption of EO onto LB in milligrams per gram of substrate (c) Heat of adsorption and desorption of EO onto LB in joules per gram of oil adsorbed. Demonstrating the overall level of adsorption achieved for each EO via FMC, and the strength of attachment of the EO molecules to the LB surface.

The enthalpy of desorption per gram of oil for manuka oil was exceptionally high, as with LRD adsorption onto LB resulted in an increase in concentration of cadina-1,4-diene. It was proposed that the increase comes from modification of calamnene, where effectively a phenyl ring is converted to cyclohexadiene. Cyclohexadiene has a lower RI than benzene (1.475 compared to 1.501) [110] and therefore this conversion would result in the lowering of the RI of the adsorbed manuka oil. A lower RI during desorption would result in an underestimation of the mass of desorption which in turn would result in an overestimation of enthalpy of desorption per mass of oil. Underestimation of the mass desorbed would also result in a wider variation which was evidenced by the large observed error for manuka oil.

3.5.4.3 Adsorption of EOs onto Fulcat® 800 determined by FMC

The adsorption results obtained for Fulcat® 800 (F800) (Figure 3.33) displayed a different pattern to those obtained for the Laponite® substrates. Instead of manuka oil giving the lowest level of adsorption it was the second highest after oregano oil. This indicates that F800 was more hydrophobic than the Laponites®; this was further supported by the observation that rosewood oil gave the lowest level of adsorption for the five EO onto F800. In the case of the Laponites® rosewood oil gave some of the highest adsorption activities. A secondary reason for the higher level of adsorption observed for manuka oil may be taken from the GC adsorption data. In Section 3.6.2 it was noted that due to reactive adsorption the Laponite® substrates gave rise to an increase in concentration of some of the component molecules after adsorption. There was no way of determining which molecules were consumed in these reactions due to their concentration also being reduced by adsorption. These effects will inevitably distort the adsorption level. As FMC relies on a differential refractometer to determine the levels of adsorption/desorption, molecules which had been modified but not adsorbed would not contribute to the mass of adsorption. Therefore in the case of manuka oil the level of adsorption would appear lower than the GC values for the substrates which caused a change in the molecular makeup. F800 did not display the same evidence for damage to the manuka oil components as the Laponites®. This observation may explain

why the FMC and GC determined levels of adsorption for manuka oil were relatively close for F800.

In contrast to the mass of adsorption, the heat of adsorption for manuka oil was lower than that observed for LB and only equal to LRD. This indicates that whilst more adsorption was taking place, fewer molecules were interacting strongly with the surface of F800. The energy required for desorption of manuka oil was higher in proportion to the heat of adsorption for F800 than for the Laponite® substrates. This indicates that whilst fewer molecules are adsorbing to the surface, those that do are undergoing stronger adsorption than the molecules adsorbed to the Laponites®.

For lavender oil and rosewood oil a higher proportion of oil adsorbed was able to desorb back off of the F800 in comparison to the Laponite® substrates. This indicates that the EO molecules are less tightly held on and within the F800. It is possible that the apparently greater hydrophobicity of the F800 had resulted in fewer molecules undergoing hydrogen bonding interactions. Weaker interactions such as dispersion / induced dipole forces may also be more prevalent. If this is the case the molecules would be more freely able to desorb from F800 than the Laponites®.

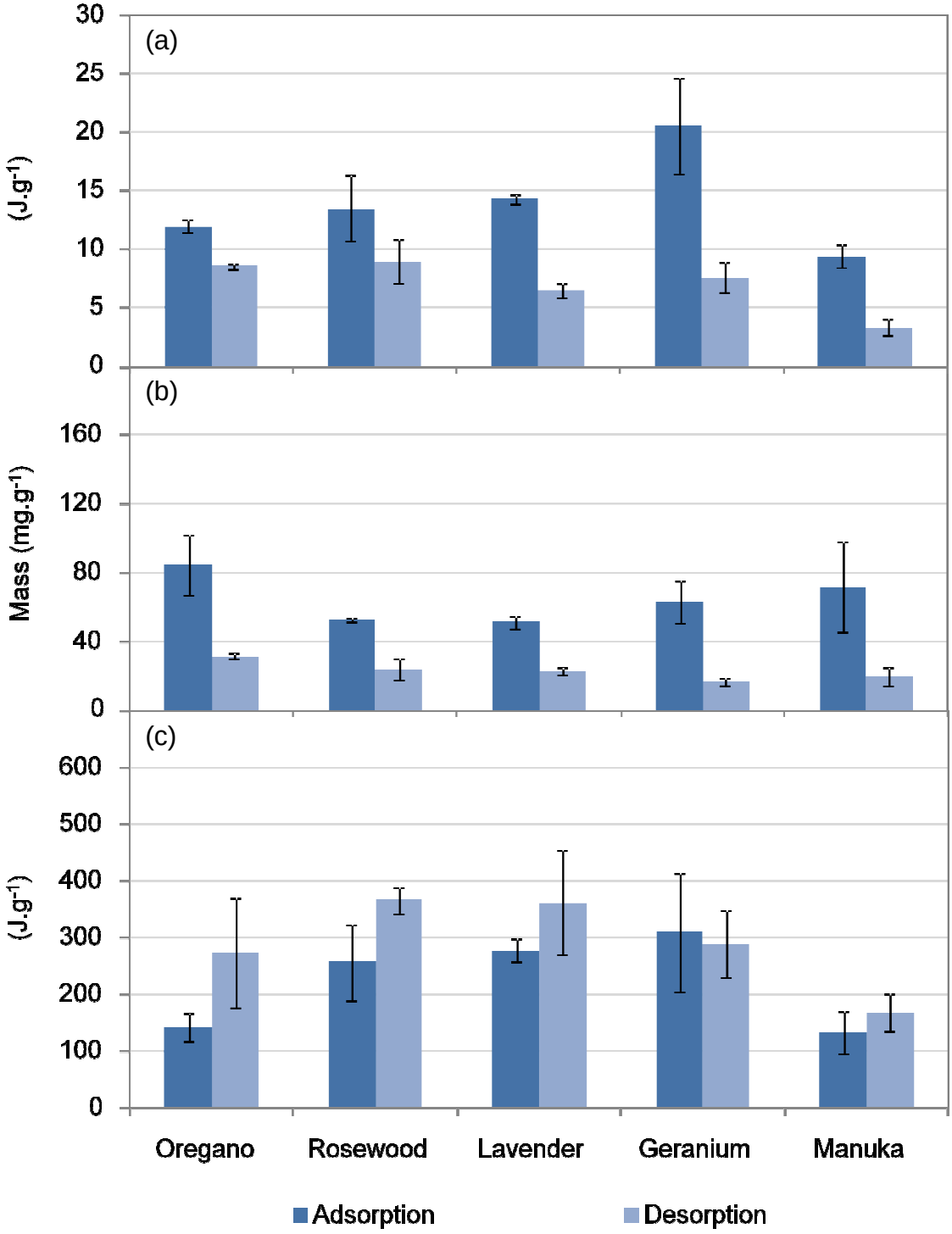

Figure 3.33: (a) Heat of adsorption and desorption of EO onto F800 in joules per gram of substrate. (b) Mass of adsorption and desorption of EO onto F800 in milligrams per gram of substrate. (c) Heat of adsorption and desorption of EO onto F800 in joules per gram of oil adsorbed. Demonstrating the overall level of adsorption achieved for each EO via FMC, and the strength of attachment of the EO molecules to the F800 surface.

The heats of adsorption observed for rosewood oil and lavender oil were lower than those observed for the Laponites®. This was due in part to the lower mass of EO molecules adsorbed by F800. The adsorption data also indicated that the F800 was less polar than the Laponites® therefore the surface would be less attractive to the polar functional groups of the molecular components of rosewood oil and lavender oil.

The enthalpy of desorption per gram of substrate for rosewood oil and lavender oil was relatively high in comparison to the mass of desorption. As a result of this the enthalpy of desorption per gram of oil desorbed was higher than the corresponding enthalpy of adsorption. As discussed in Section 3.5.4.1, the calculation of mass adsorbed relies on a calibration peak that assumes the refractive index (RI) of the material desorbing is the same as the RI of the oil before adsorption. If the oil components that desorb have a lower RI than that of the EO itself, there will be an underestimation of the mass desorbed, resulting in an overestimation of the enthalpy per gram of oil desorbed. As the adsorption data indicated that there was weak adsorption of the rosewood oil and lavender oil molecular components (exhibited by the relatively high mass of oil desorbed compared to mass adsorbed) the enthalpy of desorption per gram of oil desorbed should be low. It is possible that the mass of rosewood oil and lavender oil components desorbing has been underestimated resulting in an artificially high enthalpy of desorption per gram of oil.

Geranium oil adsorption resulted in much higher enthalpy of adsorption than was observed for adsorption onto the Laponite® substrates, despite the fact that the mass of geranium oil adsorbed was similar to the Laponites®. This indicates that a greater proportion of the geranium oil molecules adsorbed were adsorbing onto the surface of F800. The higher energy required for desorption adds further evidence for a greater number of surface interactions.

3.5.4.4 FMC adsorption summary

In general the Laponite® substrates gave higher levels of adsorption than F800, with the exception of manuka oil. F800 also yielded the lowest levels of adsorption in the GC study, therefore the data suggests that the Laponite® substrates were more suitable for the adsorption of EO and will therefore be preferable for use as a controlled release substrate in the polymer materials.

LRD gave the highest levels of adsorption (with the exception of manuka oil), however when analysing these results it was important to keep in mind that the LRD results were obtained from only one replicate, with the exception of rosewood oil which had 2 replicates.

Of the four other oils, rosewood oil and oregano oil were adsorbed to a greater level than lavender oil and geranium oil. This was significant to note as it was the reverse of what was seen with the GC adsorption (Section 3.5.2). There was a drop in the level of adsorption observed using FMC compared to GC for lavender oil and geranium oil. For geranium oil this could in part be explained by weak adsorption, resulting in the lower initial concentration of EO in the FMC study (0.3 % compared to 1.25 % for GC) restricting the amount of molecules that could be adsorbed as the solution was passed through the cell. This is particularly true of adsorption on to LB, where only approximately 20 % of the geranium oil adsorbed was retained, indicating very weak adsorption of the molecules. The relatively low level of FMC adsorption of lavender oil, relative to GC monitored adsorption, is harder to explain as the strength of adsorption appeared high (89.8 % of the lavender oil was retained on LB). As with manuka oil, significant modification of the EO composition was observed in the GC adsorption studies. Large increases in the amount of the two molecules were observed on adsorption on to LRD. Similarly noticeable increases in the levels of three molecules were observed during adsorption on to LB and F800. This indicates that reduction in the level of some molecules was due to them being converted to other species, rather than being consumed by adsorption. However, because of the limitations of the GC method (i.e. inability to distinguish between reduction of EO molecules due to adsorption and reduction due to catalytic conversion), all reductions in concentration were used to calculate the level of adsorption. The latter could lead to over-estimation of the mass adsorbed. Additionally, masses of EO adsorbed determined from the RI data, obtained from FMC, can be skewed in cases where the EO contains a significant proportion of non-adsorption active species and/or if reactions occur which change the composition. Whilst each method has its advantages and disadvantages, important insight in to the adsorption of the EOs on the substrates was nevertheless obtained.

3.6 Conclusions

- Natural and acid treated natural aluminosilicates (F400, F435 and Fcol) were found to be unsuitable for the adsorption of essential oils (EO) due to catalytic destruction of molecules which comprise a high proportion of the EOs.
- EO components with hydrophilic functional groups were adsorbed to a greater extent than molecules without hydrophilic functional groups, indicating that the hydrophilic surface of the layered silicates was more receptive to these molecules. Therefore, organically modifying the substrates may help to improve the adsorption of the EO molecules that were more organic in character by increasing the hydrophobicity of the substrates.
- GC and FMC measurements of adsorption of EO on to the substrates revealed that the Laponite® layered silicates exhibited higher levels of adsorption than F800. A higher level of EO adsorbed onto the substrates was preferable as theoretically the greater the amount of EO present the stronger the antimicrobial activity.
- FMC data indicated that the EOs were most strongly retained on LRD. The more strongly adsorbed a molecule was to the substrate the greater the energy to remove it from the surface. Therefore stronger adsorption may result in a higher level of controlled release.

CHAPTER 4

Organic modification of layered silicates and its effect on the adsorption of essential oils

Abstract

In an attempt to further increase the level of adsorption, the most adsorption active layered silicate substrates discussed in Chapter 3 were organically modified using quaternary ammonium surfactant compounds (quats). The long alky chains of the surfactant can make the chemical environment within the galleries of layered silicates more hydrophobic. Di(hydrogenated tallow) dimethyl ammonium chloride (2HT2M) and cetyl trimethyl ammonium bromide (CTAB) were used as organic modifiers (at 50 %, 75 % and 100 % of the cation exchange capacity) and the adsorption of EO onto the organically modified substrates was again assessed using GC and FMC techniques. Unfortunately during adsorption from solution, organic modification resulted in a general reduction in the mass of adsorption of the EOs onto all of the substrates. This was most likely due to block of the galleries of the substrates restricting the surface area available for adsorption.

4.1 Introduction

The layered silicate substrates have hydrophilic surfaces, this is due to two major factors which include; the surface silanol groups (mainly at the platelet edges), and the negative charge across the crystal structure and the counter cations in the galleries between the platelets [111]. A hydrophilic surface was not ideal for the adsorption of organic molecules such as the components of EOs. If the surfaces of the layered silicates could be made more hydrophobic it was hypothesised that it may be possible to further increase the level of EO adsorption.

4.1.1 Organic modification of layered silicates

One of the more important characteristics of some layered silicate materials is the ability to exchange the alkali and alkaline earth cations present within the galleries for other cations [102, 112]. The number of cations that can be exchanged is quantified using a parameter known as the cation exchange capacity (CEC) which is calculated from the quantity of negative charges within the crystal structure. The units of CEC are milliequivalents per gram of layered silicate substrate. The interchangability of cations in smectite minerals has been utilised for removal of heavy metals waste from water [113, 114]. The properties of the layered silicate can also be modified by the introduction of cations with the desired chemical properties. The use of organic salts for cation exchange was described in the early 1900's [115] and the presence of organic cations in the galleries of layered silicates has been shown to successfully convert the material from being hydrophilic to hydrophobic (or organophilic) [116, 117]. In general, quaternary ammonium surfactants with at least one long hydrocarbon chain are used for the organic modification of layered silicates. The quaternary ammonium moiety has a single positive charge, and therefore in layered silicates with Na^+ as the counteraction, it will exchange in a 1:1 ratio, quats usually have one or two alkyl tails, typically over 10 carbons in length.

Organic modification of layered silicates is widely used to improve compatibility with organic polymers, encouraging intercalation of the polymer material into the galleries of the layered silicate and promoting exfoliation [118] of the layered silicate into individual platelets. The addition of organically modified (OM) layered silicates to polymeric materials has been shown to improve the properties of the resulting composites. Such properties include mechanical and thermal (including flame retardation) and gas barrier properties [119-121].

Addition of OM layered silicates to bitumen has been shown to improve fatigue resistance and aging (with the surfactant used influencing properties). As a result, OM layered silicates could be used to increase the lifetime of asphalt [122].

4.1.2 Adsorption of organic molecules onto organically modified layered silicates

The adsorption of organic material onto OM layered silicates has been widely reported in the literature. Ake *et al.* (2003), investigated the adsorption of polycyclic aromatic hydrocarbons and pentachlorophenol from ground water onto organically modified montmorillonite (o-MMT). The o-MMT was immobilised on sand. They found that for forty contaminants found in effluent from an oil-water separator the average percentage reduction (percentage adsorbed) was 97 % (minimum 86 %, maximum >99 %). They also analysed adsorption of the same contaminants from effluent from a bioreactor, and reported the average percent reduction was 79 % [123].

Carmody *et al.* (2007), used MMT, modified with three different surfactants, as adsorbents for hydrocarbons to assess their suitability for use in oil spill remediation. The surfactants used were octadecyltrimethylammonium bromide (ODTMA), dodecyldimethylammonium bromide (DDDMA) and di(hydrogentated tallow)dimethylammonium chloride (tallow). The three o-MMTs were tested for effectiveness at adsorbing diesel, hydraulic oil, and engine oil and the results were compared against reference adsorbents. Of the three o-MMTs examined ODTMA-MMT gave the weakest performance, and DDDMA-MMT gave the best overall performance. When compared to the reference sorbents, Tallow and DDDMA-MMT gave equal or better performance whilst ODTMA-MMT had slightly reduced performance. The study not only showed the potential for o-MMT to be used as adsorbents of hydrocarbon spills but also the importance of the organically modified structure regarding adsorption capacities [124].

Akçay *et al.* (2009), studied the adsorption of the anti-inflammatory drug flurbiprofen (a phenylalkanoic compound) onto MMT modified with tetrabutylammonium (TBA) (TBA-MMT), with the aim of understanding how to use o-MMT for the effective administration of the drug. The adsorption at 25 ℃ and at 40 ℃ was studied with adsorption levels of 9 µmol g^{-1} (25 ℃) and 6.5 µmol g^{-1} (40 ℃) being observed after 200 minutes, from a solution containing 42.94 µmol L^{-1}. They concluded that TBA-MMT was an effective adsorbent for flurbiprofen due to its high adsorption capacity [125].

Researchers at the State University of New York investigated the potential for exchanging the Na^+ in an Na^+-MMT with ligands which displayed antimicrobial

activity. They were successfully able to incorporate the ligands into the galleries of natural and synthetic clay minerals (including MMT) which conferred antimicrobial activity onto the colloid particles. They also demonstrated that the modified clays could be applied to substrates (a range of fibres including cotton, natural down, nylon, polyester, wool, and fibreglass and also surface materials such as metals, glass, ceramics, and wood) via a range of processes including spraying, spreading, dipping or brushing. The antimicrobial complex could also be blended with materials such as plastics during the manufacturing process to confer antimicrobial activity to the material [126].

Zaghouane-Boudiaf and Boutahala (2011) compared the adsorption of 2,4,5-trichlorophenol onto a sodium-montmorillonite (Na-MMT), an acid treated montmorillonite (A-MMT), and a pillared montmorillonite (Al-MMT) to adsorption onto organically modified (OM) samples of the same substrates. They demonstrated that the OM Na-MMT and OM Al-MMT, outperformed the non modified samples in terms of adsorption, with 375 $mg.g^{-1}$ adsorbed onto the OM Na-MMT [127].

4.2 Objectives

- Investigate the effect of organic modification (OM) on the properties of LRD, LB and F800.
- Determine whether OM enhances the adsorption and desorption of the EO antimicrobials on the layered silicate substrates.

4.3 Materials

4.3.1 Layered silicate substrates

Vide supra Section 3.3.1

4.3.2 Organic modifiers

Organic modifiers were used to make the layered silicates more hydrophobic in an attempt to improve the levels of adsorption of the EO achieved. Di(hydrogenated tallow) dimethyl ammonium chloride (2HT2M) with approximate alkyl chain length distributions of; 65 % C18; 30 % C16 and 5 % C14, which was purchased as Arquad® 2HT-75 (AkzoNobel, UK) and Cetyl trimethyl ammonium chloride (CTAB) with an alkyl chain length distribution of C_8H_{17} to $C_{16}H_{33}$ (Acros Organics, UK) were used.

4.3.3 Essential oils

Vide supra Section 3.3.2

4.3.4 Solvents

Vide supra Section 3.3.3

4.4 Experimental

4.4.1 Organic modification of layered silicate substrates

The best performing substrates in the adsorption studies were selected for organic modification. Two different organic modifiers were used; di(hydrogenated tallow) dimethyl ammonium chloride (2HT2M) and cetyl trimethyl ammonium chloride (CTAB). Laponite® RD (LRD), Laponite® B (LB), and Fulcat® 800 (F800) were modified to increase the organophillic character of their galleries. Modification was carried out at 25, 50, 75 and 100 % of the substrate cation exchange capacities (CEC). The mass of modifier required was calculated using Equation 4.1.

Equation 4.1:

$$Mass\ organic\ modifier = \frac{CEC \times m_{mmt} \times (\%_s/100) \times M_{OM} \times (\%_e/100)}{\%_a \times 1000}$$

Where; m_{mmt} was the mass of montmorillonite material to be modified which was always 150 g, $\%_s$ was the percentage solids of the montmorillonite calculated using a moisture meter, M_{OM} was the median molecular weight of the organic modifier, $\%_e$ was the percentage exchange and was the required level of organic modification, and $\%_a$ was the percentage activity and was the activity of the organic modifier. The constant values for the substrates and organic modifiers are given (Table 4.1).

Table 4.1: Constant values for; cation exchange capacity and percentage solids of the substrates, and median molecular weight of the modifiers. These values were used in Equation 4.1.

	LRD	LB	F800	2HT2M	CTAB
CEC substrate (meq 100 g^{-1})	53.9	98.62	128.08		
% Solids	92.98	92.75	92.48		
MMW (g mol^{-1})				573.5	365.4
% activity				75	14.55

4.4.1.1 Organic modification of Laponites®

Organic modification of Laponite® samples was carried out using with 2HT2M only because CTAB modification required a wet mix method (Section 4.4.2) and recovery of the Laponite® solids would have been too time consuming due to the high volume of water required and technical difficulties when filtering the resulting gel formed at lower modification levels. The Laponite® samples were modified to levels of 50, 75 and 100 % of the CEC, Laponite® RD was also modified to 25 % CEC.

The Laponite® to be modified (150 g) was added to a 200 ml beaker, the mass of 2HT2M (pre melted in an oven at 50 ℃) required was calculated from Equation 4.1 and weighed out. The molten 2HT2M was added to the Laponite® in stages and mixed between additions using a spatula. The beaker and spatula were both heated to 50 ℃ to reduce the risk of the organic modifier solidifying when it came into contact with them. Once the total amount of 2HT2M had been added the OM Laponite® was put in an oven at 50 ℃ for 2 h to ensure it was dry. After drying the OM Laponite® was milled (using a standard food blender) and sieved to a maximum particle size of 250 µm. This work was carried out at the Rockwood additives laboratories in Widnes.

4.4.1.2 Organic modification of Fulcat® 800

OM Fulcat® 800 samples (modified to 50, 75, and 100 % of CEC) were made using 2HT2M in the same way as described in Section 4.4.1.1. In addition to the 2HT2M samples made using the dry mix method, 50, 75, and 100 % 2HT2M OM samples were made using a wet mix method described as follows: Fulcat® 800 (100 g) was added to H_2O (1000 ml) in a 4 L round bottom flask, this was heated to 60 ℃ using an isomantle and stirred. The required amount of molten 2HT2M (calculated using Equation 4.1) was then added and stirred for 30 minutes. The sample was then Buchner filtered, washed on the funnel with deionised water (until no more foam was observed when filtering) and dried at 60 ℃ for 8h. Once dry, the OM Fulcat® 800 was milled and sieved to a maximum particle size of 250 µm.

OM Fulcat® 800 samples (modified to 50, 75, and 100 % of CEC) were made using CTAB. Fulcat® 800 (100 g) was added to H_2O (1000 ml) in a 4 L round bottom flask, heated to 35 ℃ using an isomantle and stirred. The required amount of CTAB (calculated using Equation 4.1) was fully dissolved in H_2O at 35 ℃, and added to the round bottom flask and stirred for 30 minutes. The sample was then Buchner filtered, and washed on the funnel with deionised water and dried at 50 ℃ for 8h. Once dry the OM Fulcat® 800 was milled and sieved to a maximum particle size of 250 µm.

Adsorption testing for the oils (oregano (OO), manuka (MO) and rosewood (RO)) was undertaken on the OM substrates using the methods described in Sections 3.4.2 and 3.4.4.

4.4.2 Characterisation of organically modified substrates

Mineral oil absorption tests were undertaken on the unmodified and OM substrates, in order to determine the amount of mineral oil required for saturation. The latter can be considered to be relatable to the relative organophillic character of the substrates. Mineral oil was added stepwise to a known mass of layered silicate substrate using a burette; after each addition the substrate was stirred using a spatula. The layered silicate sample was taken to be saturated at the point where it formed a single clump; the increase in mass

was then used to calculate the percentage oil absorbed (mass of oil/mass of substrate).

The OM substrates were characterised using WAXS, N_2 BET adsorption and DRIFTS, *Vide supra* section 3.4.1.

Thermo gravimetric analysis (TGA) was used to calculate the organic content of the substrates after organic modification and to determine the proportion of organic modifier present that was bound to the substrate. TGA was carried out using a PerkinElmer TGA 4000 running Pyris™ AutoStepwise TGA Software. The sample (F8 5 – 15 mg, Laponite®s 20 – 60 mg) was heated to 35 ℃ in air from room temperature and this temperature was maintained for 1 min. Then, the temperature was increased to 950 ℃ at 20 ℃ mi n^{-1} and maintained at 950 ℃ for 1 min.
The percentage organic content (POC) was calculated using Equation 4.2.

Equation 4.2:

$$Percentage\ organic\ content = \frac{(Mass\ after\ free\ water\ loss - (Mass\ after\ volatile\ loss / Residue\ fraction))}{Mass\ after\ free\ water\ loss} \times 100$$

Where the residue fraction was the percentage mass remaining after the water present in the crystal lattice of the unmodified substrates had been removed.
The residue fractions for the substrates used were as follows: F800 = 0.829, LRD = 0.8869 and LB = 0.8883.
An example of a TGA trace for a layered silicate with no organic modification is given (Figure 4.1).

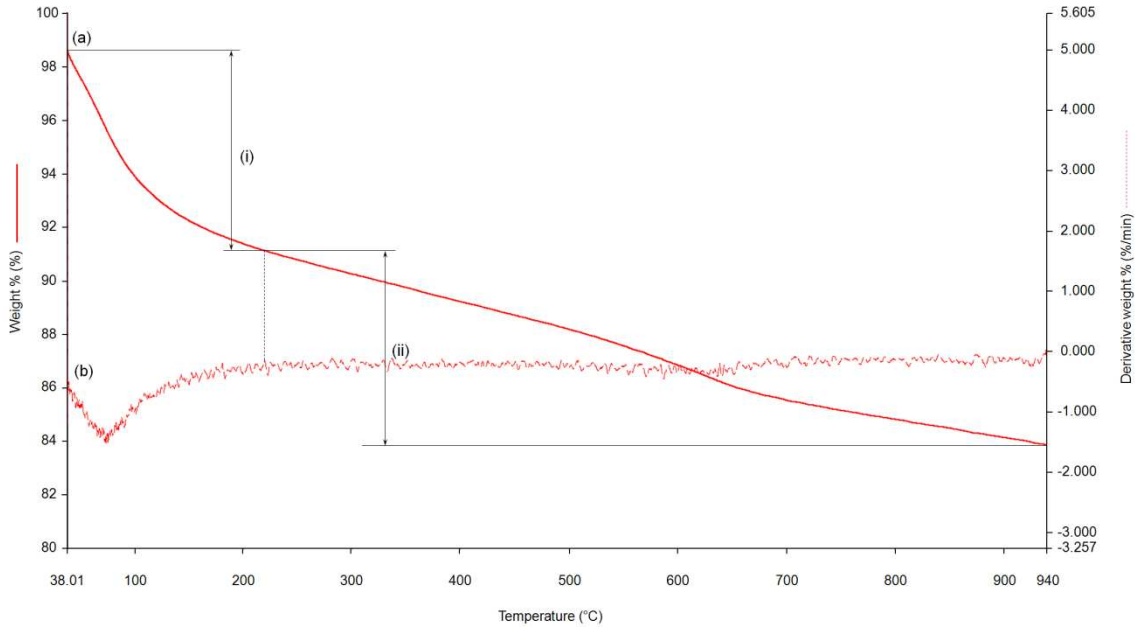

Figure 4.1: TGA trace of layered silicate before organic modification (a) Percentage mass loss plotted against time, (b) derivative of mass loss which aids the identification of the start and end of each stage of mass loss.

There were two separate instances of mass loss for the unmodified substrates marked (i) and (ii) (Figure 4.1). Mass loss (i) occurred below approximately 160 ℃ and was the loss of molecular water absorbed by the interlayer cations. Mass loss (ii) in the temperature range 160-940 ℃ is associated with the loss of structural water in the crystal lattice.

The percentage mass remaining at 940 ℃ was the sub strate crystal lattice minus water content and this was the residue fraction which was used in Equation 4.2.

A TGA trace for an organically modified layered silicate (F800 75 % 2HT2M via wet mix method) was demonstrated (Figure 4.2)

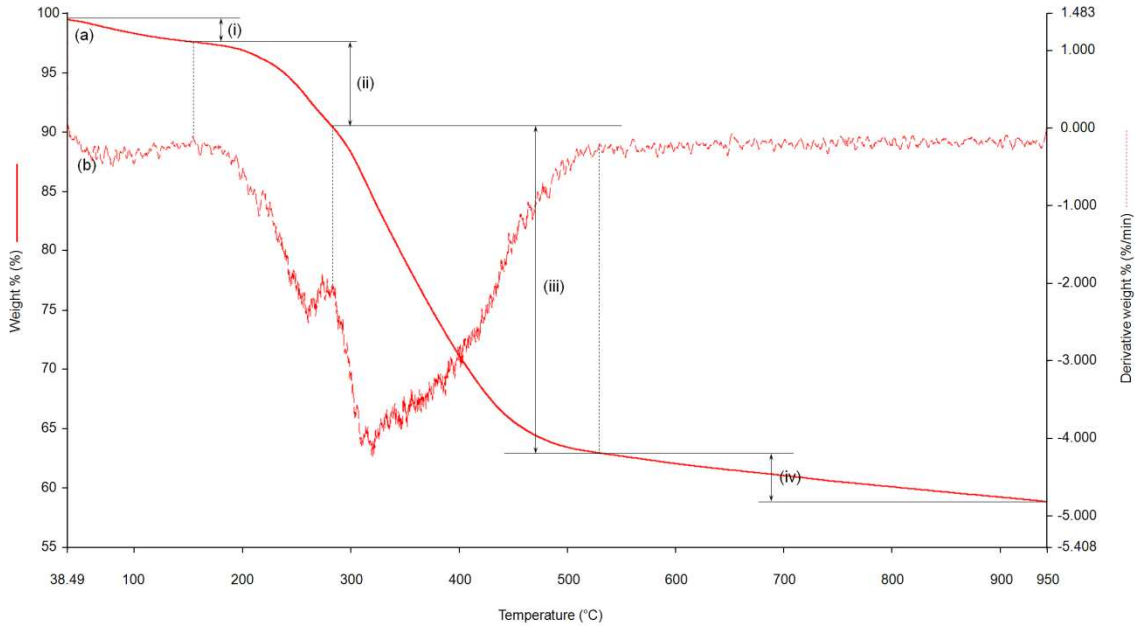

Figure 4.2: TGA trace of organically modified layered silicate (a) Percentage mass loss plotted against time, (b) derivative of mass loss which aids the identification of the start and end of each stage of mass loss.

There were four instances of mass loss from the organically modified layered silicate during the TGA heating process. For mass loss (i), as with the unmodified layered silicate occurred below 160 ℃ and was the loss of molecular water the mass remaining after mass loss (i) was the mass after free water loss used in Equation 4.2. Mass loss (ii) occurred between 160 ℃ and 300 ℃ and was the loss of the organic modifier molecules which were either unbound or loosely bound to the substrate. Mass loss (iii) occurred between 300 ℃ and 525 ℃ and was attributed to the loss of organic modifier molecules ionically bound to the substrate. Combining the mass losses (ii) and (iii) gave the total loss of organic modifier and the loss of unbound modifier at lower temperatures. This allowed for the determination of the proportion of organic modifier molecules on the layered silicate which have undergone cation exchange and were fully bound to the surface. Mass loss (iv) occurred between 525 ℃ and 950 ℃ and was attributable to the loss of structural water from the crystal lattice. The mass remaining after 950 ℃ is taken as the mass after volatile loss used in Equation 4.2.

4.4.3 Gas chromatography adsorption studies of EO onto OM substrates

Vide supra Section 3.4.2.

4.4.4 Flow micro calorimetry adsorption studies of EO onto OM substrates

Vide supra Section 3.4.4.

4.5 Results and discussions

The data obtained from the adsorption studies in Chapter 3 indicated that the layered silicate substrates could be used as an adsorption medium for the essential oils (EO). The structure of the layered silicate substrates promotes a strongly hydrophilic character, and despite the presence of hydrophilic functional groups on the EO molecules, the said molecules have an overriding organic character overall. It was proposed that organic modification (OM) of the layered silicates, using cetyl trimethyl ammonium bromide (CTAB) and di(hydrogenated tallow) dimethyl ammonium chloride (2HT2M) (see Section 4.4.1), would render the galleries more organophillic in character. It was therefore envisaged that the layered silicate galleries would be more receptive to the EO molecules and therefore a higher level of adsorption into the galleries would be obtained. Organic modification of MMT has been shown to increase the distance between the platelets (d-spacing) and in general the longer the alkyl chain of the organic modifier, the greater the increase in interlayer spacing [128]. An increase in d-spacing and hydrophobicity of the gallery environment should create more space and a more favourable environment which will increase the entry of the EO molecules into the gallery of the layered silicates.

4.5.1 Characterisation of organically modified substrates

Organically modified substrates were characterised using BET N_2 adsorption, and X-ray diffraction to investigate the effect OM had on the physical properties. The amount of mineral oil the layered silicates could absorb before and after OM was also investigated.

4.5.1.1 Organic modification of Fulcat® 800

The results for mineral oil absorption, N_2 BET surface area and d-spacing of platelets as determined by XRD for Fulcat® 800 (F800) modified with 2HT2M via the dry mix method are given (Figure 4.3).

There was a negative relationship between OM and the surface area of F800 (Figure 4.3a), with a reduction of over 300 $m^2.g^{-1}$ from unmodified to 50 % OM and further decreases with increasing OM. This was due to pores between the

silicate layers being blocked by the alkyl tails of the 2HT2M molecules, it was also possible that OM resulted in aggregation of the F800 particles.

The X-ray diffraction data (Figure 4.3b) showed a small increase in the d-spacing of the F800 platelets with 50 % OM (< 0.1 nm), and then with increasing OM there was little change in the d-spacing (1.37 nm at 50 %, 1.36 nm at 75 % and 1.38 nm at 100 %). The total increase in d-spacing was 0.09 nm; this was small in comparison to the increase in interlayer spacing observed for natural MMTs after OM. Kim *et al.* (2009) observed up to a 1.5 nm increase and Liauw *et al.* (2007) observed up to a 2.5 nm increase [129, 130]. Assuming a plate thickness of a natural Na-MMT of 0.94 nm [101] the interlayer space (i.e. the gap between the top edge of one platelet and the bottom edge of the platelet above) for F800 at all levels of OM was approximately 0.4 nm (exhibiting a 0.1 nm increase from the unmodified). The average thickness of an OM alky chain is 0.4 nm [100]. The increase in interlayer space by the approximate thickness of the 2HT2M molecule indicates that the surfactant molecules are uniformly distributed along the length of the galleries formed between platelets with the alkyl chains lying flat in a mono-layer along the surface.

The reduction of available surface area and the lack of increase in d-spacing (and therefore interlayer space) had an overall negative effect on the absorption of mineral oil (Figure 4.3c). From unmodified to 50 % OM there was a 50 % decrease in the amount of oil absorbed by the F800 (Figure 4.3a). Further modification had little effect on mineral oil adsorption.

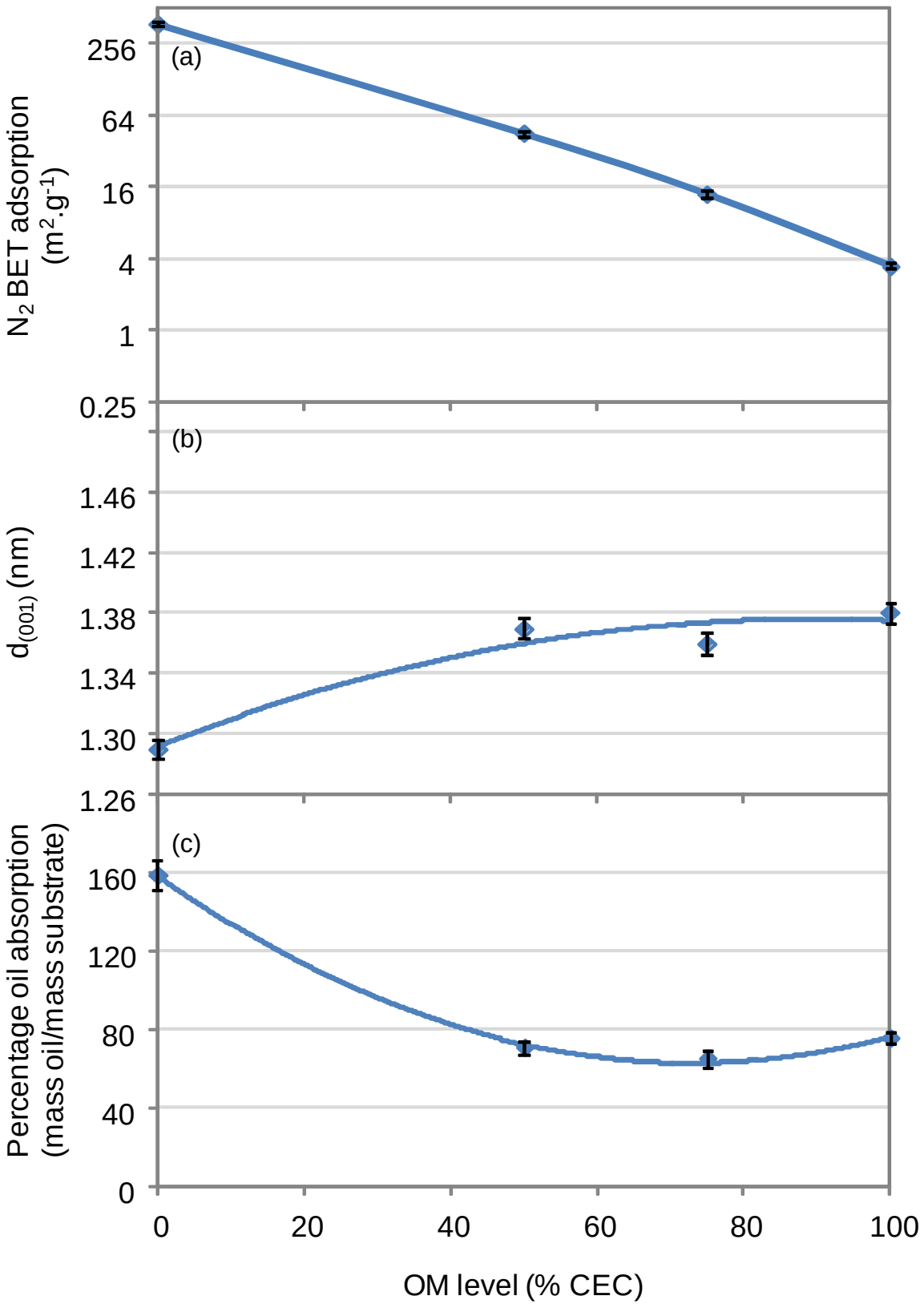

Figure 4.3: The effect of OM of F800 with 2HT2M via the dry mix method on (a) N_2 BET surface area, (b) d-spacing of platelets, and (c) percentage mineral oil absorption. Demonstrating a reduction in oil absorption, an increase in d-spacing and a reduction in surface area as a result of OM.

The CTAB organic modifier was obtained as a water soluble powder and therefore a wet mixing method was required for OM. The 2HT2M was a waxy material that could be melted to liquid at 50 ℃ and therefore did not require a wet mix method. However samples of F800 OM with 2HT2M were prepared using both the dry mixing method (Figure 4.3) and the wet mixing method (Figure 4.4), in order to allow for comparison between the dry mix and wet mix substrates. Substrates OM using the wet mixing method should in theory have more even distribution of organic modifier than substrates OM using the dry mixing method. The results from the characterisation of F800 OM with CTAB and F800 OM with 2HT2M (wet mix method) are given (Figure 4.4).

OM of F800 with 2HT2M using a wet mixing method had a similar effect on surface area as the dry mixing method modification, with 50 % OM resulting in a large decrease in surface area for both (Figure 4.4a). In contrast to the dry mixing method samples, instead of a further decrease in surface area with increasing OM the wet mixing method, samples exhibited a limiting value of surface area at 75 % modification. In the wet mixing method the substrate was washed with distilled water after modification (this was not done with dry mixing) it is possible that unbound or loosely bound surfactant may have been washed out of the F800 during this process. As there was no washing process in the dry mix method, unbound surfactant would remain in the material potentially blocking the surface for adsorption. If this was the case it may explain the lower reduction in surface area for the wet mix OM with 2HT2M compared to the dry mix OM with 2HT2M.

As with the dry mixing method for OM of F800 with 2HT2M the wet mixing method initially resulted in a small increase in d-spacing of the F800 (Figure 4.4b), increasing the interlayer space to approximately 0.4 nm which was indicative of the surfactant molecules intercalating in the galleries of the F800 and forming a monolayer at the surface. At 75 % and 100 % OM, the d-spacing of the platelets was approximately equal to that of the unmodified substrate. As a result the interlayer spacing was below 0.4 nm, the latter would be observed when the surfactant is adsorbed as a horizontal monolayer in the galleries. The critical micelle concentration for the 2HT2M used in this study was $4x10^{-4}$ $mol.L^{-1}$ [131], the concentrations of 2HT2M during O9M were $7.9x10^{-2}$, $1.2x10^{-1}$ and $1.6x10^{-1}$ $mol.L^{-1}$ for 50, 75 and 100 % CEC OM respectively.

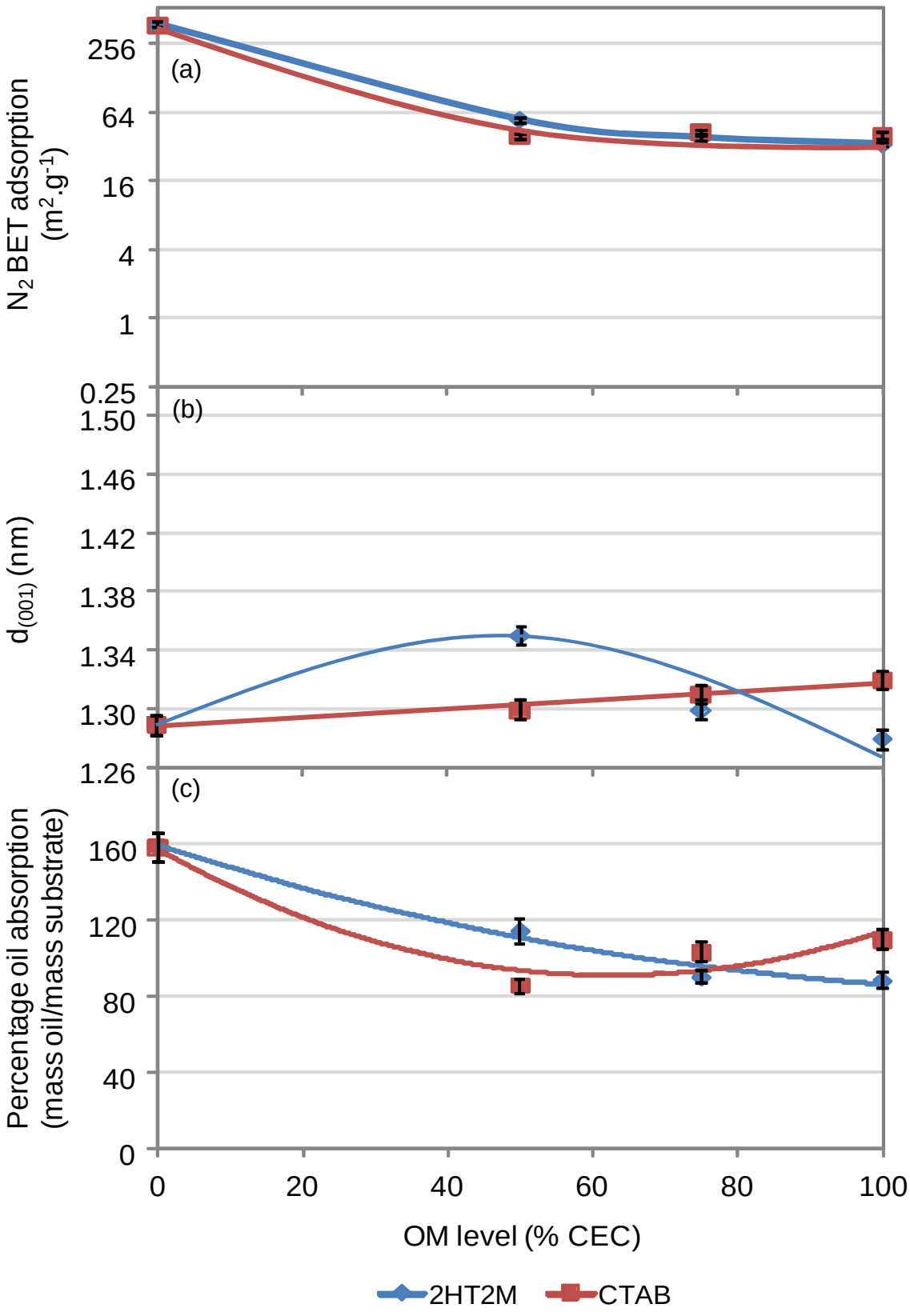

Figure 4.4: The effect of OM of F800 with 2HT2M and CTAB via the wet mix method on (a) N_2 BET surface area, (b) d-spacing of platelets, and (c) percentage mineral oil absorption. Demonstrating how increasing the level of OM reduced surface area and oil adsorption, at 50% 2HT2M OM there was an increase in d-spacing of F800.

It was possible that at the higher surfactant concentrations for 75 and 100 % OM, more micelles were formed resulting in a greater likelihood that the entrances of the pores of the substrate would become blocked by the micelles. Blockage of the pore entrances would prevent further surfactant molecules from intercalating between the platelets of the F800. Therefore entry of surfactant molecules in to the F800 galleries at concentrations needed for 75 and 100 % OM was hindered by blockage of the pore entrances by surfactant micelles. This effect therefore provides an explanation for the perceived reduction in d-spacing from 50 % OM to 75 % OM.

OM of F800 with 2HT2M (wet mixing method) resulted in a decrease in absorption of the mineral oil (Figure 4.4c), following a similar pattern to that observed for the dry mixing method material. The reduction in absorption was not as severe for the wet mixed materials as the dry mixed materials, as discussed with surface area; this may be due to unbound surfactant in the dry mixed samples that was absent in the wet mixing method materials.

As with the 2HT2M samples, modification of F800 with CTAB resulted in a large reduction in surface area from unmodified to 50 % OM (273 $m^2.g^{-1}$ to 40 $m^2.g^{-1}$), further increases in the dosage of CTAB resulted in a slight increase in the available surface area (Figure 4.4a).

Following the pattern of OM with 2HT2M there was little change in d-spacing of the F800 platelets (Figure 4.4b) with increasing level of 2HT2M (a 0.01 nm increase was observed for every incremental level of surfactant added).

The reduction in surface area and lack of increase in interlayer space resulted in a large decrease in the absorption of mineral oil for 50 % OM F800 in comparison to the unmodified F800 (Figure 4.4c). In contrast to the 2HT2M modified F800 increasing the level of CTAB OM from 50 % resulted in an increase in mineral oil absorption (Figure 4.4a). CTAB molecules only have one long alkyl chain, whereas 2HT2M has two, the two chains on 2HT2M would occupy more space than the single chain on CTAB resulting in more space available on the CTAB F800 for absorption.

The X-ray diffraction data (Figure 4.4b) gave the most significant information on the F800 OM substrates. There was no increase in the d-spacing observed at any level of OM resulting in the interlayer space remaining at approximately 0.3

nm. This was significant as the alky chains, at 0.4 nm in thickness, would not be able to fit in the space between the platelets and therefore it is evidence that no surfactant molecules were present in the galleries, i.e. no intercalation occurred. The solution of CTAB used for OM was 0.41 $mol.L^{-1}$, the critical micelle concentration for CTAB is $9.2x10^{-4}$ $mol.l^{-1}$ [132], formation of micelles is likely to limit the amount of adsorption that occurs. There is a dynamic equilibrium between the amount of surfactant in micelles and the amount in solution. Only strong adsorption of the surfactant would result in a shift in the equilibrium. It can also be appreciated that adsorption of micelles could lead to blockage of the pores and adsorption would be limited to the pore entrances and the edge planes of the F800 particles.

4.5.1.2 Organic modification of Laponites®

The Laponite® substrates were OM with 2HT2M using a dry mix method only. This was due to Laponites forming a gel upon dispersion in water making isolation of the dry OM Laponite® very laborious. The data obtained from characterisation of Laponite® RD (LRD) is shown (Figure 4.5).

As with the Fulcat® substrates, OM resulted in a decrease in surface area for LRD (Figure 4.5a), however the decrease in surface area from unmodified to 50 % OM was not as large (277 $m^2.g^{-1}$ approximately 74 % reduction) in comparison with F800 (329 $m^2.g^{-1}$ approximately 88 % reduction). This indicated that there may not have been as much blockage of the pores between platelets in the case of LRD.

The XRD data for LRD (Figure 4.5b) provided evidence of the Laponites® being affected differently by OM than F800. From unmodified to 50 % OM there was a 0.1 nm increase in the d-spacing followed by a 0.09 nm increase to 75 % OM. This result means that the total increase in d-spacing was more than twice the largest increase seen for F800. The latter has much larger particles than Laponite® and if the surfactant was adsorbed only around the edges on the platelets in F800 then a situation might occur where in the middle of the platelets the d-spacing did not change, but the edges were fanned out. As XRD takes an average of d-spacing across the material this would result in the observed d-spacing not displaying much change (though peak broadening may be detectable). As Laponite® platelets are much smaller, it would be easier for the surfactant molecules to adsorb in the central regions of the platelet resulting in a greater likelihood of the distance between platelets being increased. The d-spacing values for all three OM levels were high enough for the interlayer spacing between the platelets to be at least 0.4 nm. The latter is the minimum spacing required to accommodate the alkyl chains of the 2HT2M in a horizontal (parallel to basal surface) orientation. Therefore it is likely that intercalation of the surfactant molecules within the gallery had taken place and that the distribution of surfactant molecules was fairly uniform across the platelet surface.

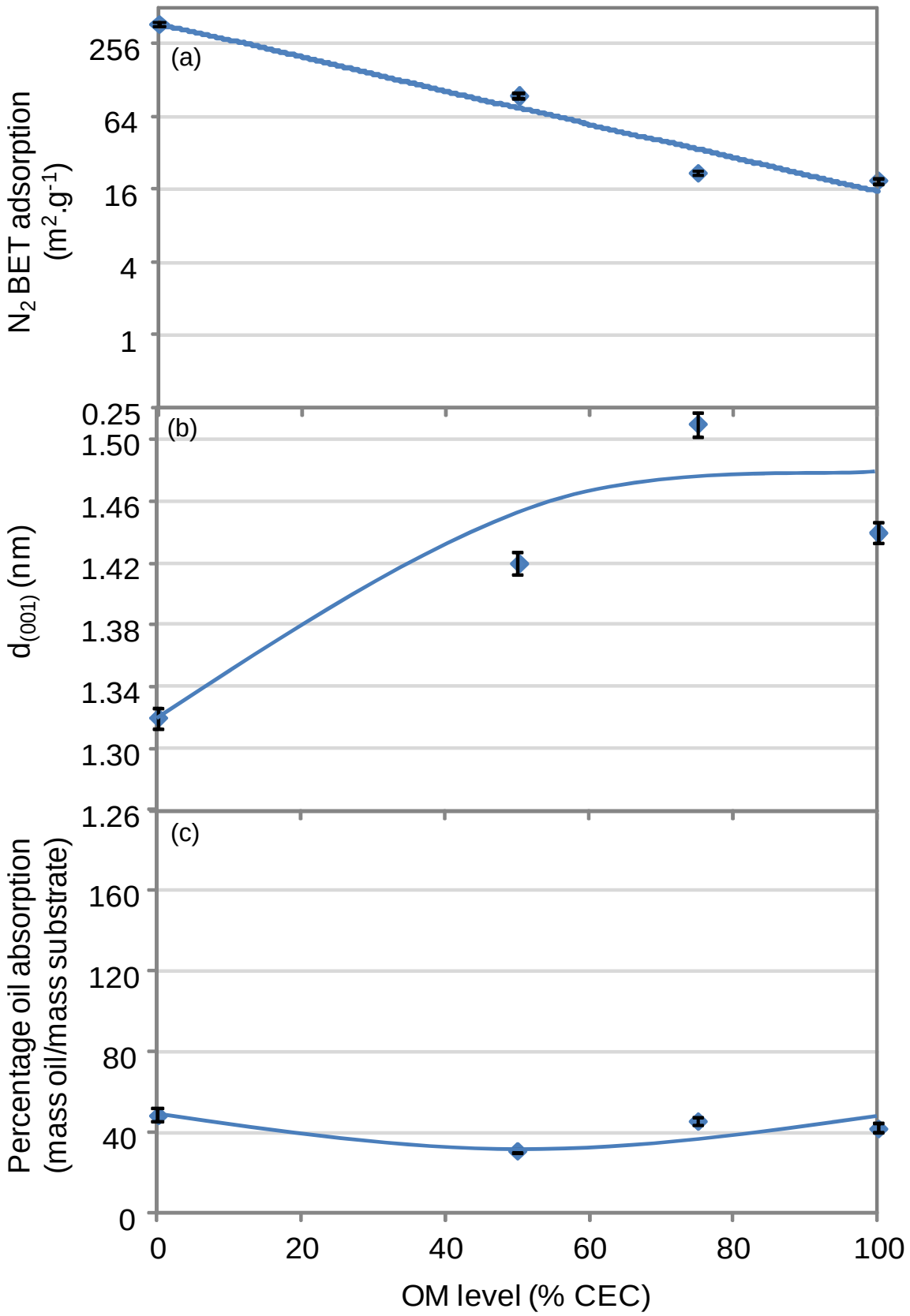

Figure 4.5: The effect of OM of LRD with 2HT2M via dry mix method on (a) N_2 BET surface area, (b) d-spacing of platelets, and (c) percentage mineral oil absorption. Demonstrating how increasing the level of OM affected the physical properties of the substrate.

At 50 % OM there was a decrease in the amount of mineral oil absorption (Figure 4.5c), this is most likely attributable to the loss of surface area observed with the OM. Increasing the OM to 75 % resulted in an increase in mineral oil adsorption back to the levels achieved by the unmodified Laponite®. The further increase in organic character coupled with the larger space between the platelets may have contributed to this increased ability to absorb.

The characterisation data for Laponite® B (LB) is displayed (Figure 4.6), and it revealed a number of differences between the behaviours of LRD and LB. The general trend for surface area (Figure 4.6a) was the same as that observed for LRD; however the effect of OM on surface area was more pronounced. The unmodified LB had the highest surface area of the three substrates (412 $m^2.g^{-1}$), after 50 % OM this had been reduced to 17.6 $m^2.g^{-1}$, and at 75 % and 100 % OM the surface area was measured at less than 0.5 $m^2.g^{-1}$. The reason for the difference between the two Laponites® was explained determining at the amount of OM required to achieve the desired level of modification. LB required twice as much modifier as LRD to achieve the same level of cation exchange, 0.61 $mmol.g^{-1}$ for 100 % OM compared to 0.3 $mmol.g^{-1}$, despite the initial surface areas being similar. This resulted in there being almost twice as much 2HT2M on the surface of LB in comparison to LRD.

The effect of OM on the d-spacing of the LB platelets (Figure 4.6b) was similar to that of LRD with a total increase in interlayer spacing of 0.17 nm, providing the required space for intercalation of the surfactant molecules within the galleries.

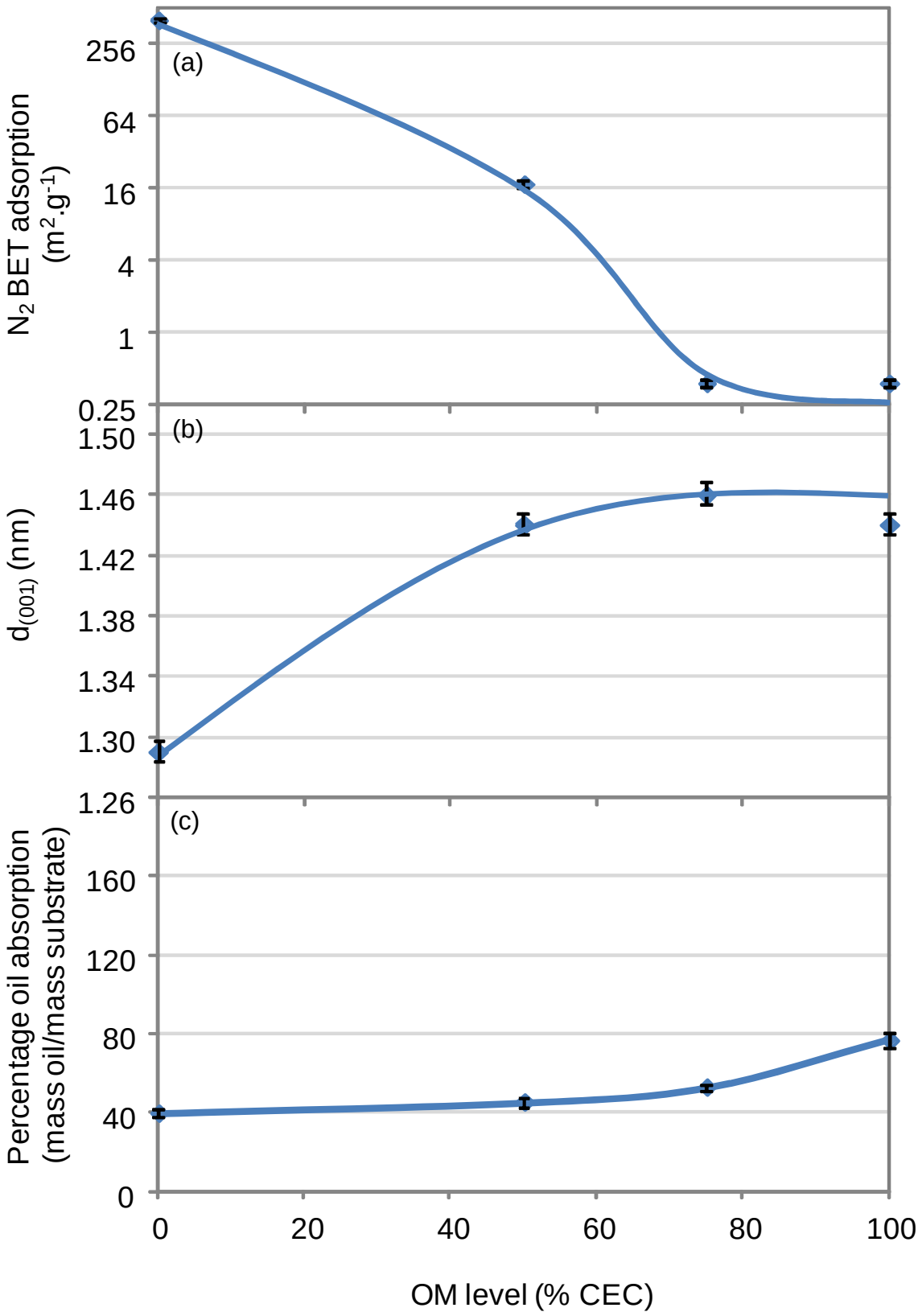

Figure 4.6: The effect of OM of LB with 2HT2M via dry mix method on (a) N_2 BET surface area, (b) d-spacing of platelets, and (c) percentage mineral oil absorption. Demonstrating the reduced surface area of LB as a result of OM, and the increase in oil absorption and d-spacing.

There was a large difference between LB and LRD in their behaviour during the mineral oil absorption test (Figure 4.6c). Initially LB required less oil to reach its saturation point. This can be explained by considering the cation exchange capacities (CEC) of the two substrates. As LB required twice as much organic modifier to achieve the same level of cation exchange it had double the CEC of LRD, this meant that LB had twice as many cations within its galleries as LRD. The effect of this would be to make LB more hydrophilic than LRD explaining the reduced capacity for the organic mineral oil. For 50 % and 75 %, OM there were slight increases in the level of mineral oil absorption, increasing the level of OM to 100 % resulted in a large increase in absorption, this appears to be in contradiction with the surface area data. It is possible that the OM caused the LB platelets to aggregate resulting in a low available surface area. The presence of the mineral oil may have caused these aggregates to break up exposing more of the platelets surface and therefore aiding absorption.

4.5.1.3 Organic content after organic modification of substrates

Thermal gravimetric analysis (TGA) was used to determine level of organic modifier (surfactant) that was actually added to the substrates. Previous studies [133] have shown that in some cases the relative levels of relatively weakly bound and relatively strongly bound surfactants can be resolved via use of the derivative mass loss data. The strongly bound surfactant is attributed to molecules bound to the substrate surface via ionic interactions; the weakly bound surfactant is attributed to bonding to other surfactant molecules. From here-after relatively weakly bound surfactant will be classified as unbound and the relatively strongly bound surfactant will be classified as bound. The bound surfactant is evolved from the sample at a higher temperature than the unbound (see Section 4.4.2). The unbound surfactant may also be simply physically adsorbed at the platelet edges, on the exterior surface of aggregates of platelets and also, in some cases within the galleries, between bound molecules.

A graphical representation of the data obtained from the TGA analysis of LB at the three levels of organic modification with 2HT2M undertaken in this study was demonstrated (Figure 4.7).

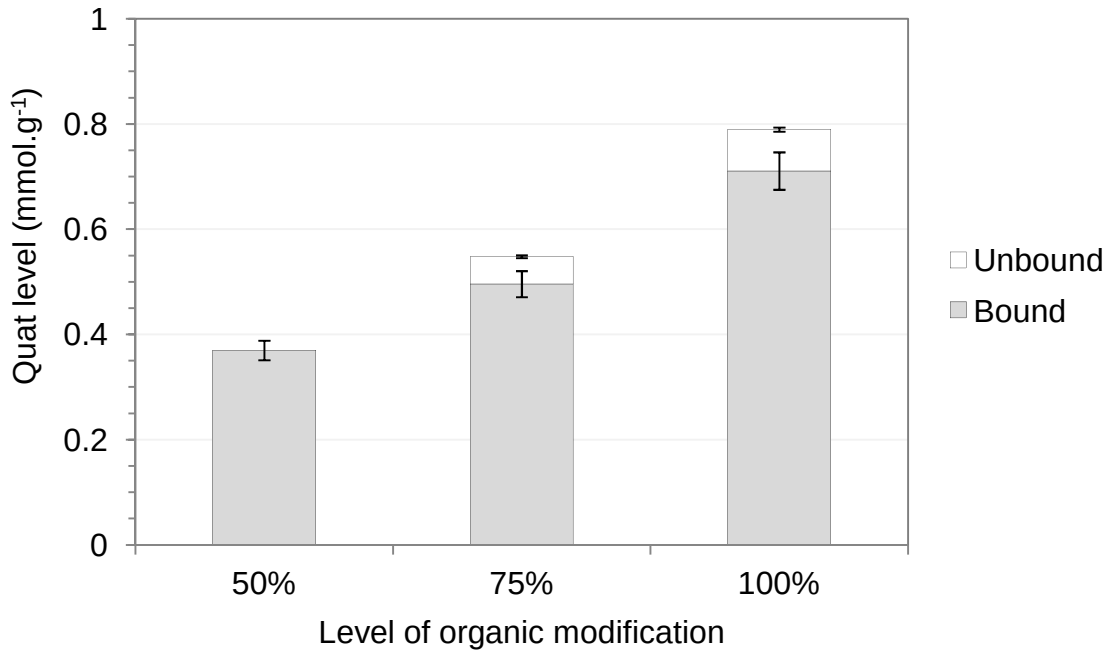

Figure 4.7: Amount of organic modifier present on LB after modification with 2HT2M. The total length of the bar represents the overall surfactant level whilst the grey portion represents the level of bound surfactant and the white bar represents the level of unbound surfactant. An increase in both bound and unbound 2HT2M was observed with increasing OM.

At 50 % OM, all of the 2HT2M molecules present on LB were bound to the surface of the platelets. The experimentally derived 2HT2M level was slightly higher (0.37 mmol.g^{-1}) than the initial amount of 2HT2M added (0.26 mmol.g^{-1}. During the milling and sieving process there were considerable losses of the LB powder. If the majority of the losses were of LB with little or no OM present this may explain why the 2HT2M level obtained via TGA was higher than the initial 2HT2M level added. At 75 % OM there was an increase in the level of 2HT2M bound to the surface of the LB. It was also observed that some of the 2HT2M present on the LB (approximately 9 %) was less strongly bound or unbound indicating that it may not have undergone ion exchange and was instead weakly adsorbed to the surface. This indicates that while there were still ion exchange sites available on the LB they may be less accessible (further into the galleries between the platelets) to the 2HT2M molecules. This would result in it being easier for the molecules to adsorb to areas around the platelet surface where there were spaces between the regions of negative charge. There was a further

increase in the mass of 2HT2M present on the LB at 100 % organic modification. The level of loosely or unbound 2HT2M increased to approximately 10 % due to the surface of the LB becoming more saturated with 2HT2M molecules and there being fewer available ion exchange sites for the 2HT2M molecules to strongly adsorb to.

The TGA analysis of LRD showed a similar general pattern to LB with increasing the level of organic modification resulting in a linear increase in the level of 2HT2M present on the LRD (Figure 4.8)

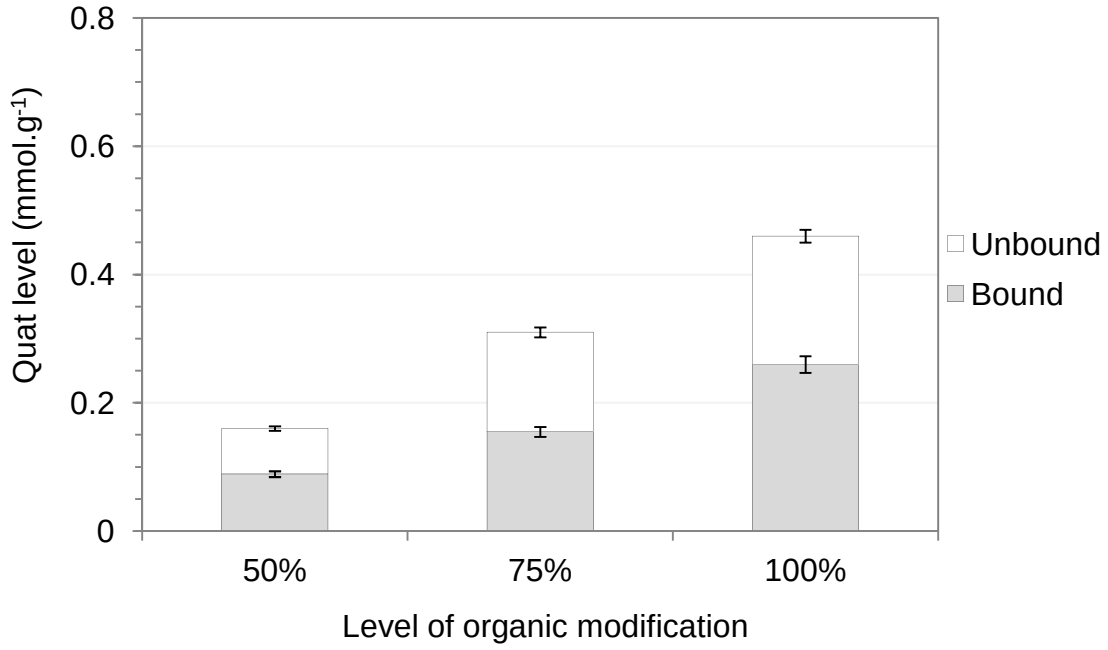

Figure 4.8: Amount of organic modifier present on LRD after modification with 2HT2M. The total length of the bar represents the overall surfactant level whilst the grey portion represents the level of bound surfactant and the white bar represents the level of unbound surfactant. Demonstrating the increase in organic material with increasing OM.

The cation exchange capacity of LRD was 53.9 meq/100 g which is almost half that of LB at 98.62 meq/100 g. As a result less organic modifier was required to reach the CEC, and this was reflected in the lower overall level of 2HT2M on LRD at each CEC in comparison to LB. The main difference between the LRD and LB samples was the proportion of loosely/unbound to bound 2HT2M with

there being approximately 50 % unbound at each CEC for LRD. As the level of bound 2HT2M increased with increasing OM it was not the case that the LRD platelets had become saturated at low levels of OM resulting in high levels of unbound 2H2TM. The main difference between the two Laponite® substrates was the lower CEC of LRD as a result of fewer negative charges spread across the platelet surface. The lower CEC may have resulted in less of a driving force for the 2HT2M to enter the galleries between the LRD platelets in comparison to LB, consequently more molecules would be adsorbed around the edges of the platelets. This may have led to a greater blocking of gallery entrances (pores) in LRD. As a result there would be fewer accessible cation exchange sites and a greater proportion of the 2HT2M molecules would be weakly adsorbed to the surface rather than held via ionic attractions.

The TGA results for F800 organically modified with 2HT2M via a dry mix method are given (Figure 4.9).

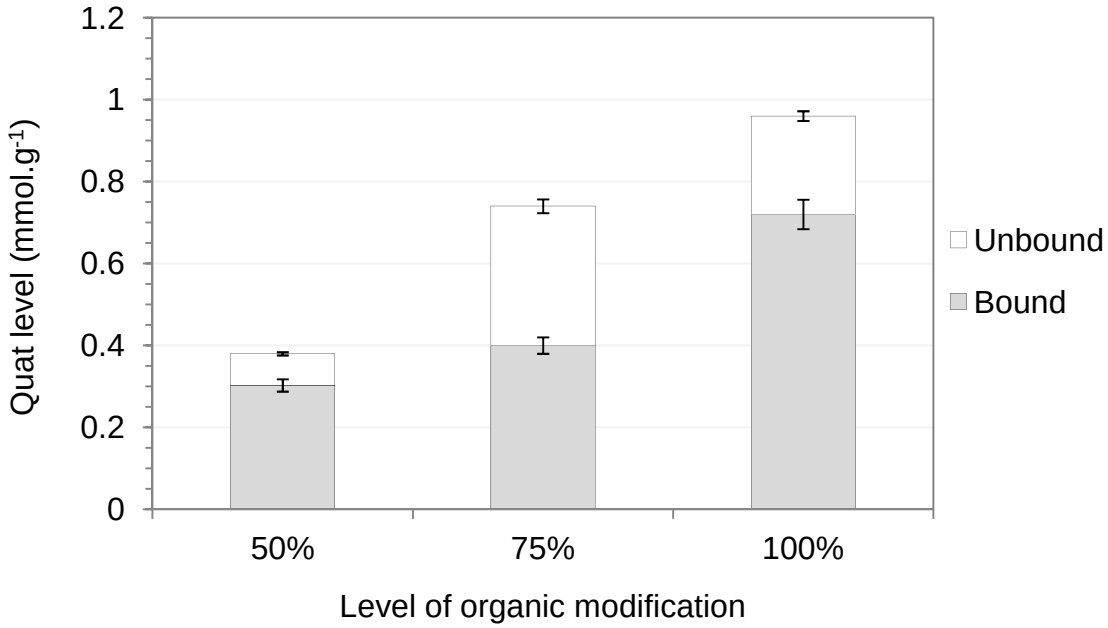

Figure 4.9: Amount of organic modifier present on F800 after modification with 2HT2M via a dry mix method. The total length of the bar represents the overall surfactant level whilst the grey portion represents the level of bound surfactant and the white bar represents the level of unbound surfactant. Demonstrating the increase in organic material present of F800 with increasing OM.

As with the Laponite® substrates the general trend observed for F800 OM with 2HT2M via the dry mix method was increasing levels of 2HT2M present on the substrate with increasing levels of OM. The proportion of unbound to bound 2HT2M also exhibited a similar pattern to that observed with the Laponite®s. F800 has a higher CEC (128.08 meq/100 g) than the Laponite® substrates thus to achieve the same percentage of cation exchange a greater mass of 2HT2M was required (i.e. for 50 % OM F800 required 0.59 mmol.g^{-1} in comparison LB required 0.26 mmol.g^{-1}). Despite the greater amount of 2HT2M added for F800 the level present as determined by TGA was of a similar level as that for LB. This may indicate that fewer 2HT2M molecules were able to enter the galleries between the platelets and therefore a lower proportion of the available cation exchange sites being utilised. F800 has a larger aspect ratio than the Laponite®s therefore more of the surface area is between the platelets, as a result blocking of the galleries by 2HT2M molecules would result in more of the surface area being restricted in comparison to the Laponite®s thus reducing the level of cation exchange able to take place.

The F800 organically modified with 2HT2M via a wet mix method displayed a similar pattern of results as the dry mix samples (Figure 4.10). As with the dry mix samples the level of 2HT2M present on the F800 was low in comparison to the level of 2HT2M initially added, indicating that a larger proportion of the cation exchange sites of the F800 remained unoccupied, relative to those of the Laponite® substrates. This was expected as the XRD data indicated that interlayer space between the F800 platelets was not sufficient to accommodate the 2HT2M molecules. The F800 samples modified via a wet mix method also exhibited a slightly lower level of 2H2TM molecules present in comparison to the F800 modified via a dry mix method. This indicates that the filtration and washing process removed a small amount of 2HT2M molecules that had not yet undergone cation exchange In Section 4.5.1.1 it was shown that the 2HT2M levels used were above the critical micelle concentration (CMC). It is likely that any micelles attached to the F800 would be easily removed during the filtration and washing process.

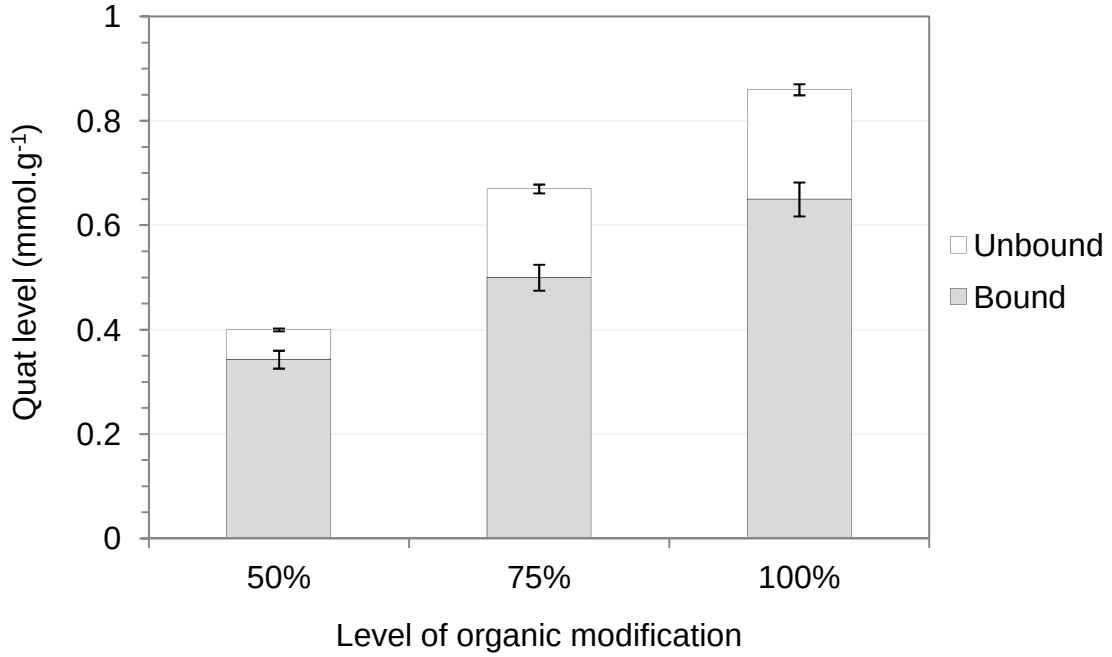

Figure 4.10: Amount of organic modifier present on F800 after modification with 2HT2M via a wet mix method. Bound fraction represents 2HT2M molecules which were successfully underwent ion exchange. Unbound fraction represents 2HT2M molecules which did not undergo ion exchange but were adsorbed onto the surface of the platelets. Demonstrating the increase in organic material present of F800 with increasing OM.

The F800 samples OM with CTAB via a wet mix method produced a different pattern of TGA results to the 2HT2M samples (Figure 4.11)

In contrast to the 2HT2M samples at 50 % OM the majority of the CTAB present on F800 was unbound (approximately 80 %). This was attributed to the lack of increase in interlayer spacing observed in Section 4.5.1.1. The interlayer space at 50 % OM was smaller than required to accommodate the CTAB molecules, thus no molecules could enter the galleries of the F800 resulting in all of the cation exchange taking place on edges of the platelets. As the edges of the platelets are only responsible for a fraction of the surface area the cation exchange sites would be limited resulting in the majority of the CTAB molecules remaining unbound.

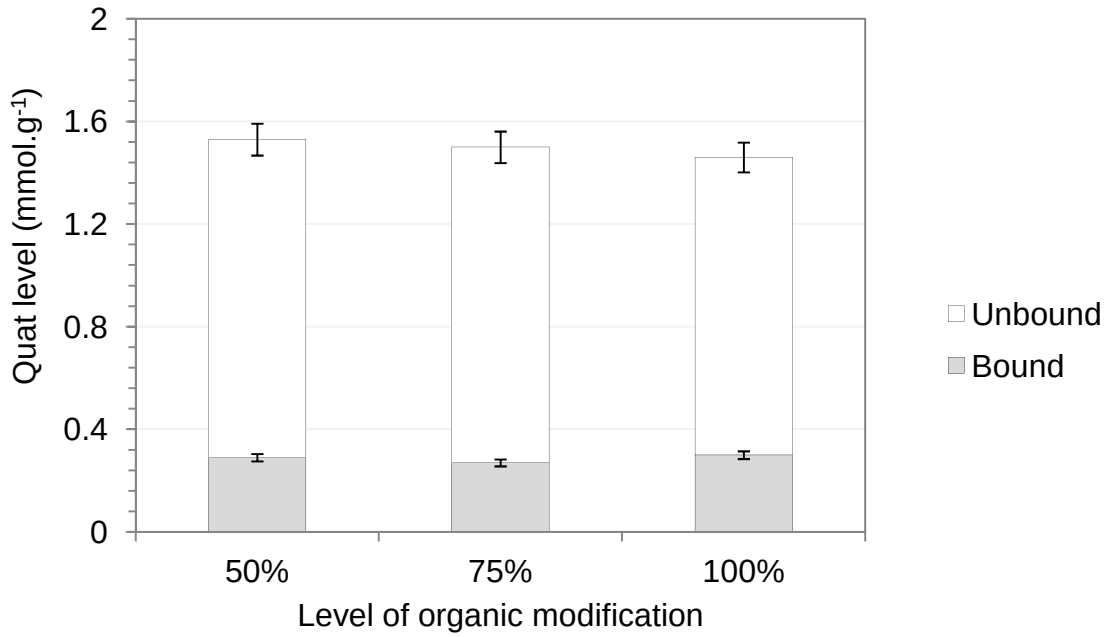

Figure 4.11: Amount of organic modifier present on F800 after modification with CTAB via a wet mix method. Bound fraction represents CTAB molecules which were successfully underwent ion exchange. Unbound fraction represents CTAB molecules which did not undergo ion exchange but were adsorbed onto the surface of the platelets. Demonstrating the lack of change in organic level with increasing OM, which indicated that the amount of bound surfactant had reached a limiting level at 50 % OM.

Increasing the level of OM to 75 % and 100 % had no effect on the level of bound CTAB molecules, indicating that the platelet edges had become saturated at 50 % OM and with the CTAB molecules unable to enter the galleries there were no available cation exchange sites for the additional CTAB molecules to attach to.

4.5.1.4 FTIR of OM substrates

To confirm the presence of the organic modifiers on the layered silicates DRIFTS-FTIR analysis was carried out. The OM would have intense aliphatic C–H stretch and bend vibrations from the alkyl tails as well as C–N stretches from the amine head. The amine vibrations would be present in the 1340 – 1020 cm^{-1} range with a medium intensity relative to the strongest peak. These

peaks are unlikely to feature on the OM MMT spectra as the Si–O–Si peak at 1100 cm^{-1} would be likely to mask them. The aliphatic CH_2 produces strong intensity stretching vibrations in the range 2960 – 2850 cm^{-1}; and the presence of these peaks would confirm the presence of the surfactant. The exact wavenumber of the methylene asymmetric stretching band ($\nu_{as}(CH_2)$) (approximately 2900 cm^{-1}) will also give information of the amount of ordering of the alky tails [134]. A shift to lower frequencies is indicative of an increase in the number all *trans* arrangements of the alkyl chains indicating self-assembly in to a quasi-crystalline array. Increasing the amount of OM would be expected to increase the ordering of the alky tails. The DRIFTS spectra for LB-2HT2M, F800-CTAB and F800-2HT2M (wet) are shown (Figures 4.12, 4.16 and 4.18 respectively).

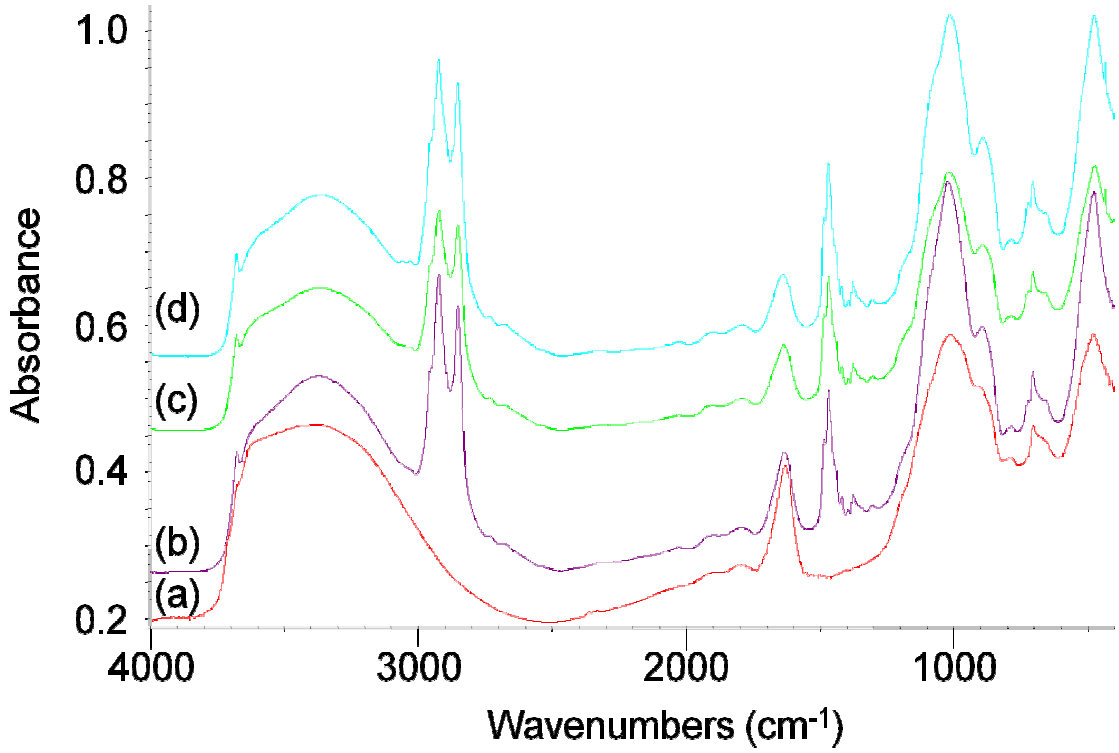

Figure 4.12: DRIFTS spectra of LB organically modified (OM) with 2HT2M at (a) Unmodified, (b) 50 % CEC, (c) 75 % CEC, (d) 100 % CEC. Demonstrating the presence of C-H stretch vibrations in the range 2800-3000 cm^{-1} as a result of OM.

The DRIFTS spectra of LRD (not shown) displayed the same peaks as LB. The only difference between the two Laponites® was the frequency of the $\nu_{as}(CH_2)$ stretch peak at approximately 2900 cm^{-1} for LB it was at 2922 cm^{-1} and for LRD

2924 cm^{-1}. This difference is not large enough to suggest any significant difference in the ordering of the alkyl tails, though the slightly lower frequency obtained for LB was consistent with an increased adsorption density in the gallery. The frequency of the $\nu_{as}(CH_2)$ stretch did not change with increasing surfactant level indicating that there was no greater ordering of the 2HT2M alkyl chains with increased modification.

The ratio of the absorbance peak of the C–H stretches to the Si–O stretch can be used as an indicator of the level of hydrocarbon present in the OM layered silicates. As the amount of Si–O remained constant the ratio can be used to determine whether increasing the level of OM resulted in an increase in hydrocarbons on the material. The effect of increasing OM on the ratio of C–H to Si–O and the platelet d-spacing for LB was compared (Figure 4.13).

Between 50 % and 75 % OM a rapid increase in the amount of hydrocarbon on the platelets of Laponite® B (Figure 4.13a) was observed, between 75 % and 100 % OM the amount of hydrocarbon stayed the same suggesting that the surface of the platelets had become saturated at 75 %. The increase in hydrocarbon with increasing surfactant level displayed a different pattern to the TGA data given in Section 4.5.1.3. At 50 % OM the hydrocarbon level obtained via DRIFTS appeared to be low in comparison to the same data for TGA. This may be as a result of the majority of the surfactant molecules being within the galleries of the LB. As a result the vibration of the bonds would be restricted leading to an underestimation of the hydrocarbon level [130].

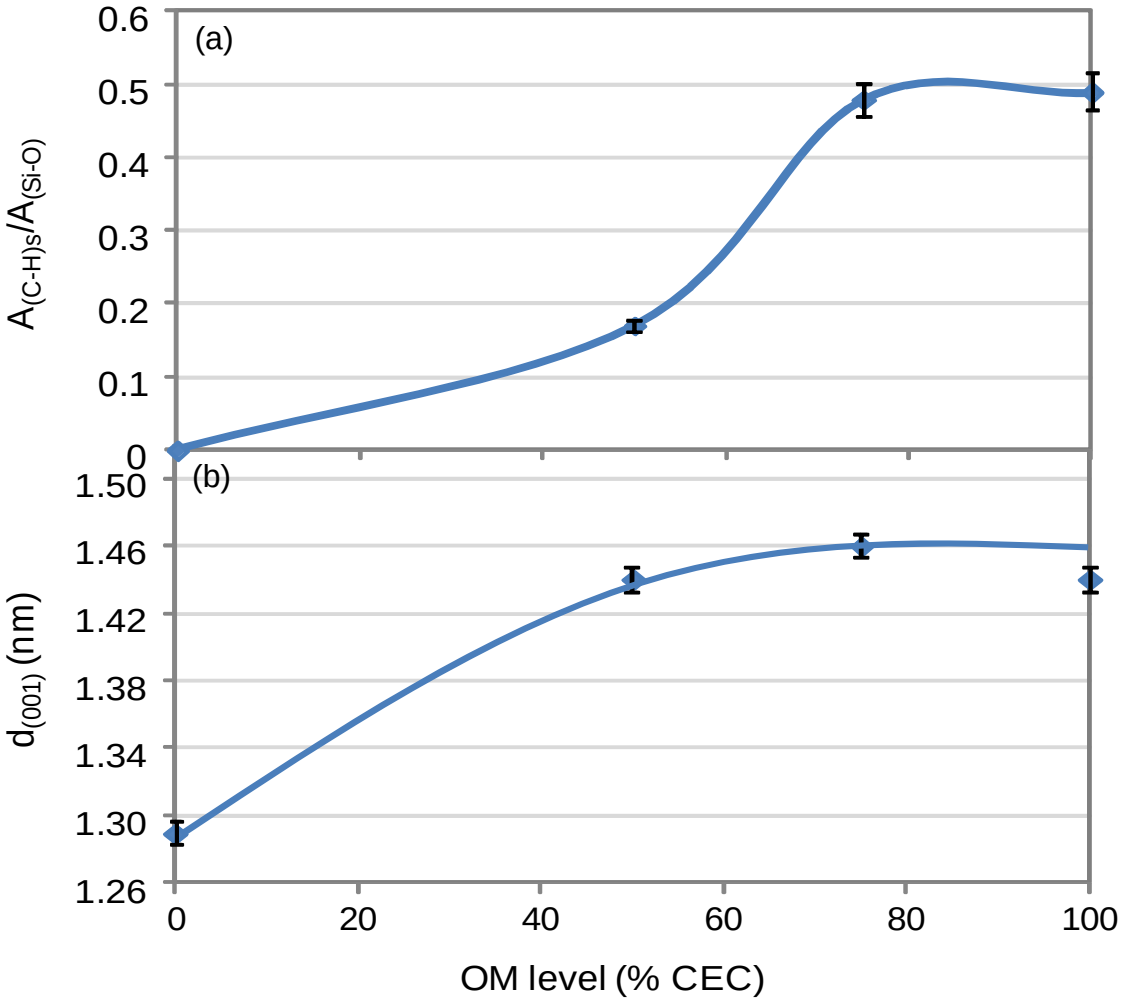

Figure 4.13: Data obtained from DRIFTS and XRD respectively plotted as a function of OM of LB (a) $A_{(C-H)S}/A_{(Si-O)}$, (b) d-spacing of platelets. Demonstrating the effect of increasing 2HT2M OM on the d-spacing of LB platelets, and the level of carbohydrate present on LB.

The DRIFTS data (Figure 4.13a) suggested that the LB became saturated at 75 % with no further increase in hydrocarbon level when the surfactant level was increased to 100 %, whereas the TGA data showed an increase in both bound and unbound surfactant from 75 % to 100 %. The difference between the two sets of data may be as a result of some of the unbound surfactant being present in a separate phase. The reflective nature of DRIFTS means that the bulk of the particles present in a separate phase may not be resolved fully [96] and therefore the intensity of the peak may be underestimated. In addition with the increased loading of surfactant molecules, restriction of the hydrocarbon chains may be increased further thus decreasing the intensity of the DRIFTS peak. The XRD data (Figure 4.13b) gave insight into why there was no ordering of the alky

tails observed on the FTIR spectrum. At 50 % OM the d-spacing had increased and as a result the interlayer space between the platelets was great enough to accommodate the alkyl tails of the surfactant as a horizontally adsorbed monolayer (Figure 4.14a). Ordering of the alkyl tails into a vertical arrangement (Figure 4.14b) would require an interlayer space of 2.54 nm and therefore a d-spacing of 3.46 nm.

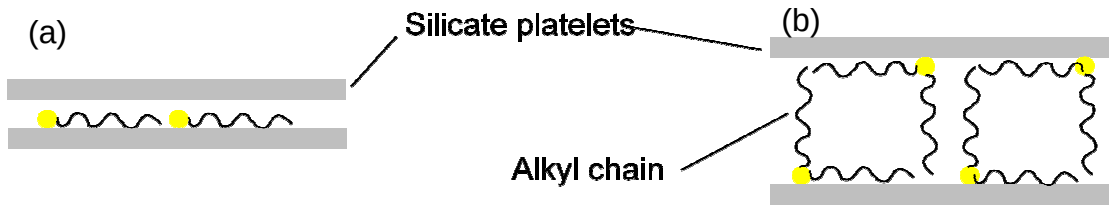

Figure 4.14: (a) surfactant alkyl tails arranged as a monolayer between platelets, (b) surfactant alkyl tails with vertical arrangement between platelets [100].

The adsorption density of surfactant within the LB galleries was not sufficient to change the mode of adsorption of the 2HT2M. At low adsorption levels, as observed with LB, both alkyl groups of the 2HT2M lay against the basal surface. However, at a critical adsorption level the drive to form self-assembled structures begins to dominate, resulting in one of the alkyl groups pointing upwards, away from the basal surface (Figure 4.14b).

Figure 4.15 shows the same data as Figure 4.13 but for Laponite® RD.

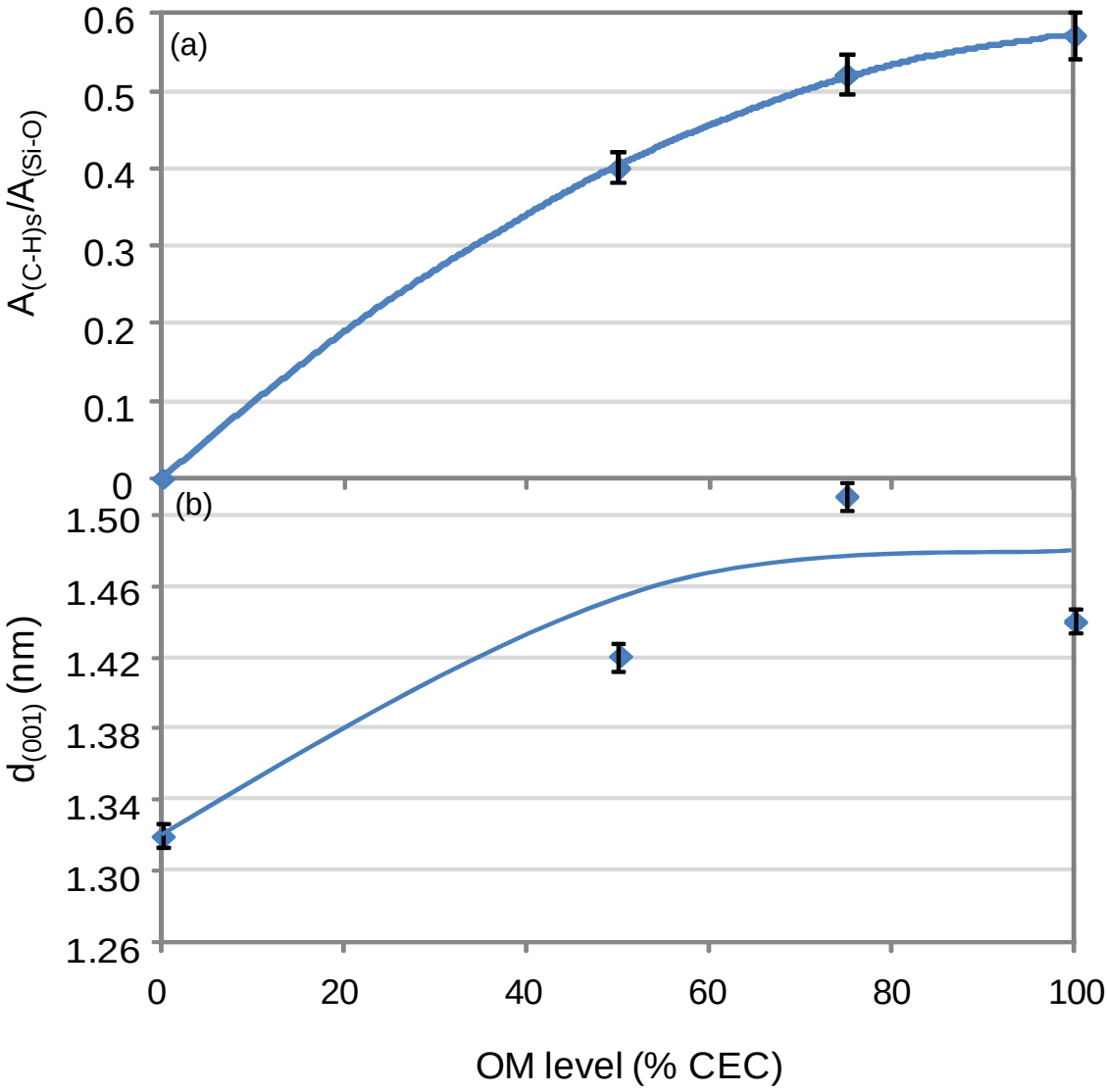

Figure 4.15: Data obtained from DRIFTS and XRD respectively plotted as a function of OM of LRD (a) $A_{(C-H)s}/A_{(Si-O)}$, (b) d-spacing of platelets. Demonstrating the increased d-spacing and carbohydrate level on LRD as a result of increasing 2HT2M OM.

The $A_{(C-H)s}/A_{(Si-O)}$ ratio for LRD at 50 % OM (Figure 4.15a) was approximately double that observed for LB, despite the TGA data indicating the surfactant level for LRD was approximately half that of LB. This indicated that the surfactant molecules were able to vibrate more freely when adsorbed onto LRD. This may be an indication that a greater proportion of the adsorbed molecules were situated on the edges of the platelets (and not within the galleries) for LRD in comparison with LB. From 50 % to 75 % OM there was an increase in the $A_{(C-H)s}/A_{(Si-O)}$ and a further increase from 75 % to 100 %. This mirrors the data obtained from TGA which indicted a linear increase in surfactant level with

increasing organic modification. The $A_{(C-H)s}/A_{(Si-O)}$ ratios at 75 % and 100 % for LRD were higher than those obtained for LB at the same levels of OM. In contrast the TGA data indicated that the surfactant levels on LRD were little over half those for LB. The apparently low $A_{(C-H)s}/A_{(Si-O)}$ ratios for LB in comparison to LRD may therefore be as a result of restriction of the surfactant molecules adsorbed onto LB due to the higher density of packing and a higher proportion located within the galleries of the substrate. This would result in reduced vibration of the C–H bonds of the alkyl chains and a less intense peak on the DRIFTS spectrum. As a result the hydrocarbon level may have been underestimated via DRIFTS.

The FTIR spectra for Fulcat® 800 after OM with different levels of CTAB was demonstrated (Figure 4.16).

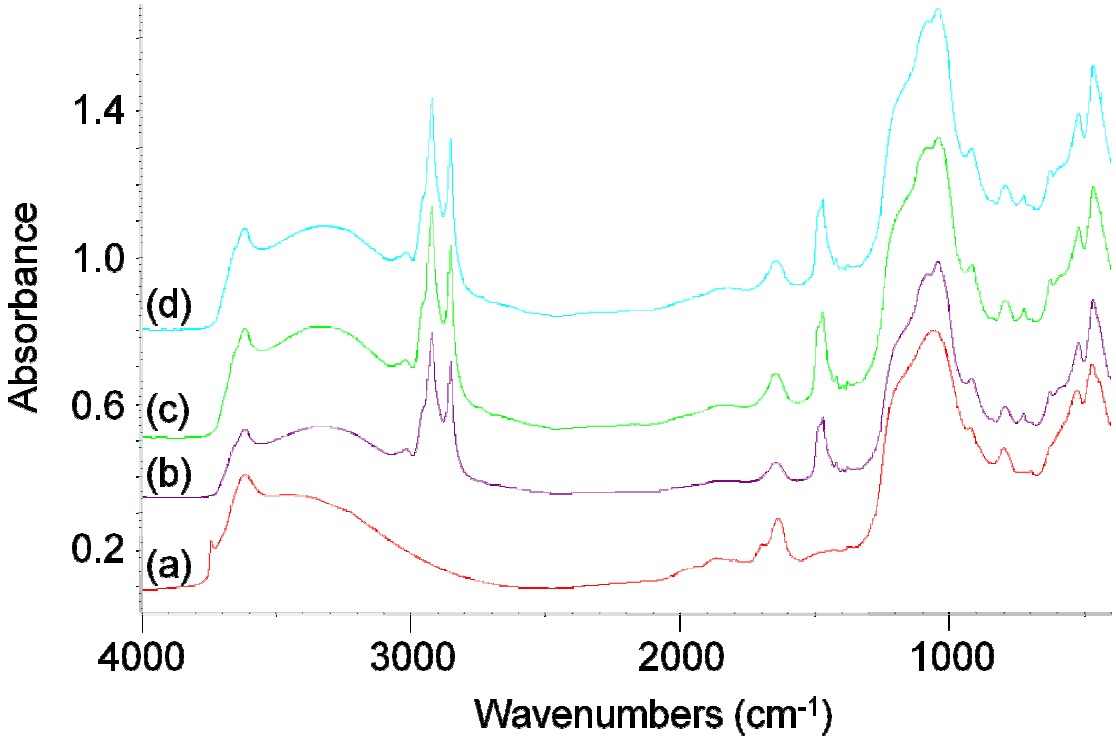

Figure 4.16: FTIR spectra of F800 OM with CTAB at (a) Unmodified, (b) 50 % CEC, (c) 75 % CEC, (d) 100 % CEC. Demonstrating the presence of C-H stretch vibrations in the range 2800-3000 cm^{-1} as a result of OM.

The frequency of the $\nu_{as}(CH_2)$ stretch for F800 OM with CTAB was similar to the Laponites® with the C–H stretch occurring slightly lower at 2921 cm^{-1}. As with the Laponites®, increasing the level of OM did not result in a shift in the

wavenumber of the C–H stretch vibrations indicating that there was not a higher amount of ordering of the CTAB alkyl chains with increasing surfactant level. The lower value for the $\nu_{as}(CH_2)$ stretch may be related to CTAB only having one alky chain whereas 2HT2M has two. This will result in more space for the alkyl chains reducing the likelihood of them being forced into *gauche* conformations.

The $A_{(C\text{-}H)s}/A_{(Si\text{-}O)}$ ratios for the CTAB modified F800 were plotted (Figure 4.17) for comparison of the effect of increasing surfactant level and the amount of hydrocarbon present on the substrate.

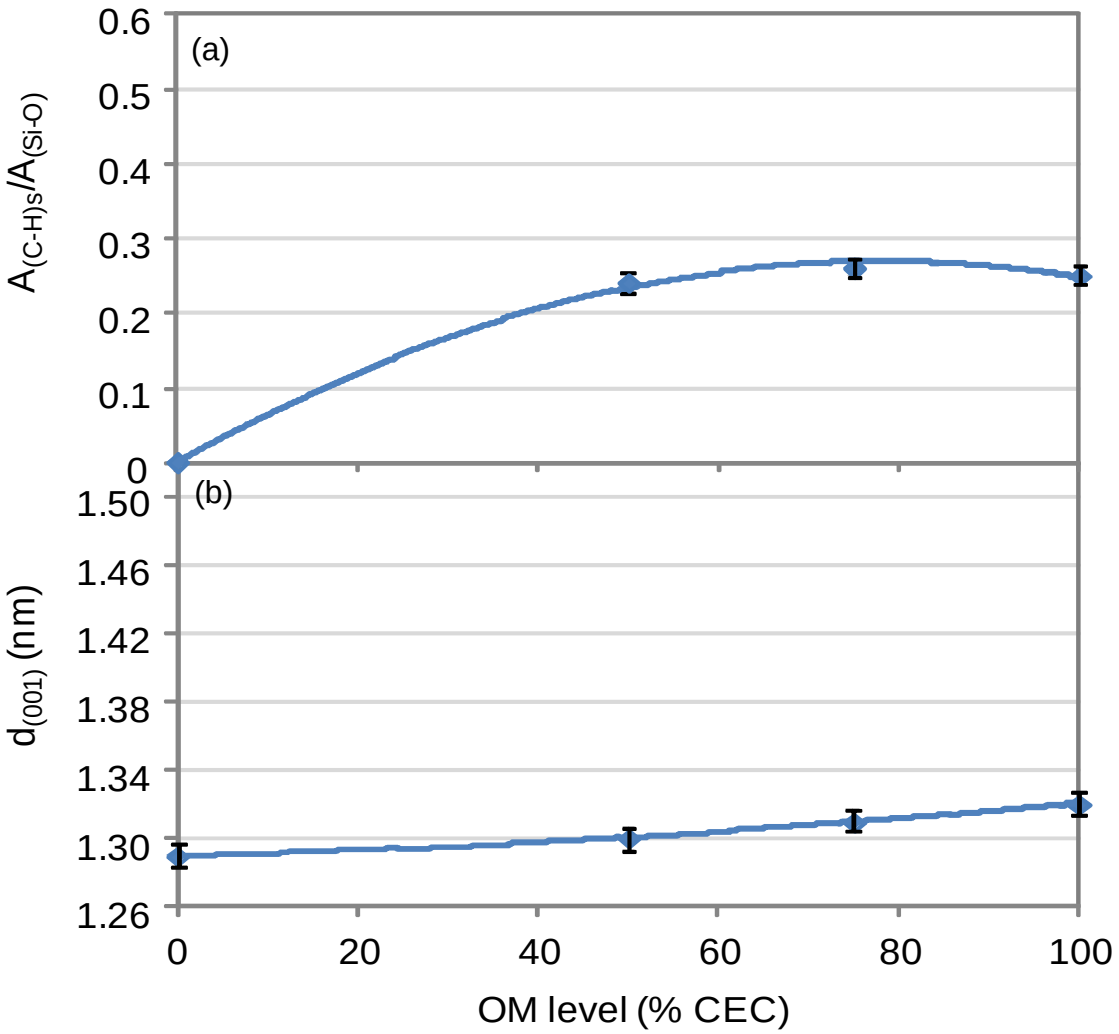

Figure 4.17: Data obtained from DRIFTS and XRD respectively plotted as a function of OM of F800 with CTAB; (a) $A_{(C\text{-}H)s}/A_{(Si\text{-}O)}$, (b) d-spacing of platelets. Demonstrating the increase in carbohydrate level as a result of CTAB OM and the lack of effect OM had on the d-spacing of F800.

At 50 % OM the ratio of $A_{(C-H)s}$ to $A_{(Si-O)}$ was 0.25 (Figure 4.17a), which was similar to that observed for LB. Increasing the level of surfactant had no effect on the level of hydrocarbon present on the F800. The lack of increase in hydrocarbon level with increasing OM was also observed via TGA in Section 4.5.1.3. The lower level of hydrocarbon on the substrate as measured by DRIFTS indicated that the high level of unbound surfactant observed in Section 4.5.1.3 may be in a separate phase and therefore the bulk of the unbound material was not detectible by DRIFTS. Two factors may have resulted in the low uptake of surfactant; as discussed in Section 4.5.1.1 the CTAB modification took place in an aqueous environment which may have facilitated the formation of micelles, resulting in fewer surfactant molecules available and the potential blocking of the F800 pores by the micelles. As a result the number of surfactant molecules that would have been able to enter the galleries and adsorb to the surface would have been reduced. In addition, the d-spacing of the platelets (Figure 4.17b) did not significantly increase with OM (0.3 nm from unmodified to 100 % OM) and as a result the interlayer spacing did not achieve the 0.4 nm required for the CTAB alkyl chains to fit between the galleries. This means that OM would only have been able to take place at the edge planes of the galleries and at the pores, explaining the lack of increase in the amount of hydrocarbon present at 75 and 100 % OM.

F800 modified with 2HT2M (both wet and dry) gave the same basic spectra as the other samples (Figure 4.18), with the only significant difference being the $\nu_{as}(CH_2)$.

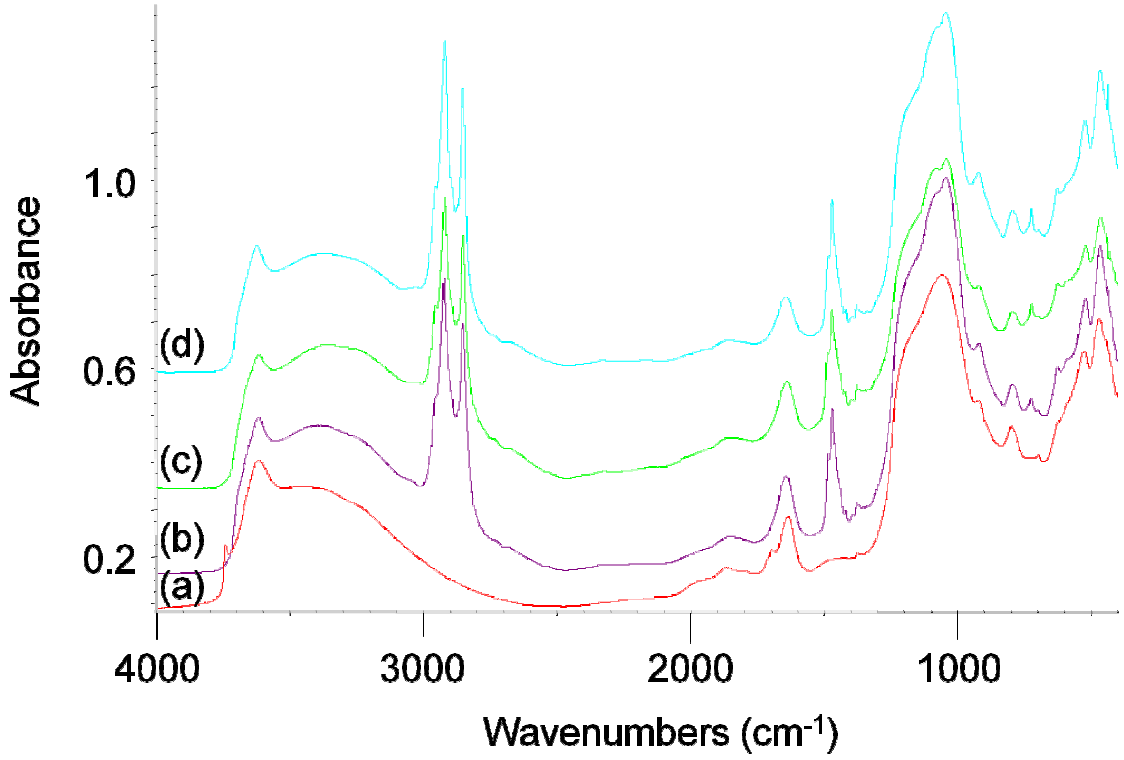

Figure 4.18: DRIFTS spectra of F800 OM with 2HT2M (wet) at (a) Unmodified, (b) 50 % CEC, (c) 75 % CEC, (d) 100 % CEC. Demonstrating the presence of C-H stretch vibrations in the range 2800-3000 cm^{-1} as a result of OM.

For the wet modified F800 at 50 % OM the frequency of the C–H stretch was 2922 cm^{-1}. Increasing the OM to 75 % resulted in the C–H stretch shifting to 2919 cm^{-1}. The d-spacing values (Figure 4.19b) did not show any evidence of expansion of the distance between the platelets to allow vertical alignment of the alkyl chains and therefore the decrease in $\nu_{as}(CH_2)$ between 50 % and 75 % OM was not due to this effect. At 50 % the d-spacing taken from the XRD data (Figure 4.19b) indicated intercalation of the surfactant molecules in a horizontal arrangement, giving an interlayer space of 0.4 nm. Interestingly at 75 % and 100 % OM there was a contraction in the d-spacing and therefore the surfactant molecules had not entered the galleries of the substrate (Section 4.5.1.1). As a result, the surfactant would be predominantly adsorbed (possibly in multi-layers) at the exposed basal and edge planes. The alkyl tails of the surfactant in the said multi-layers may be able to self-assemble resulting in the further reduction in $\nu_{as}(CH_2)$.

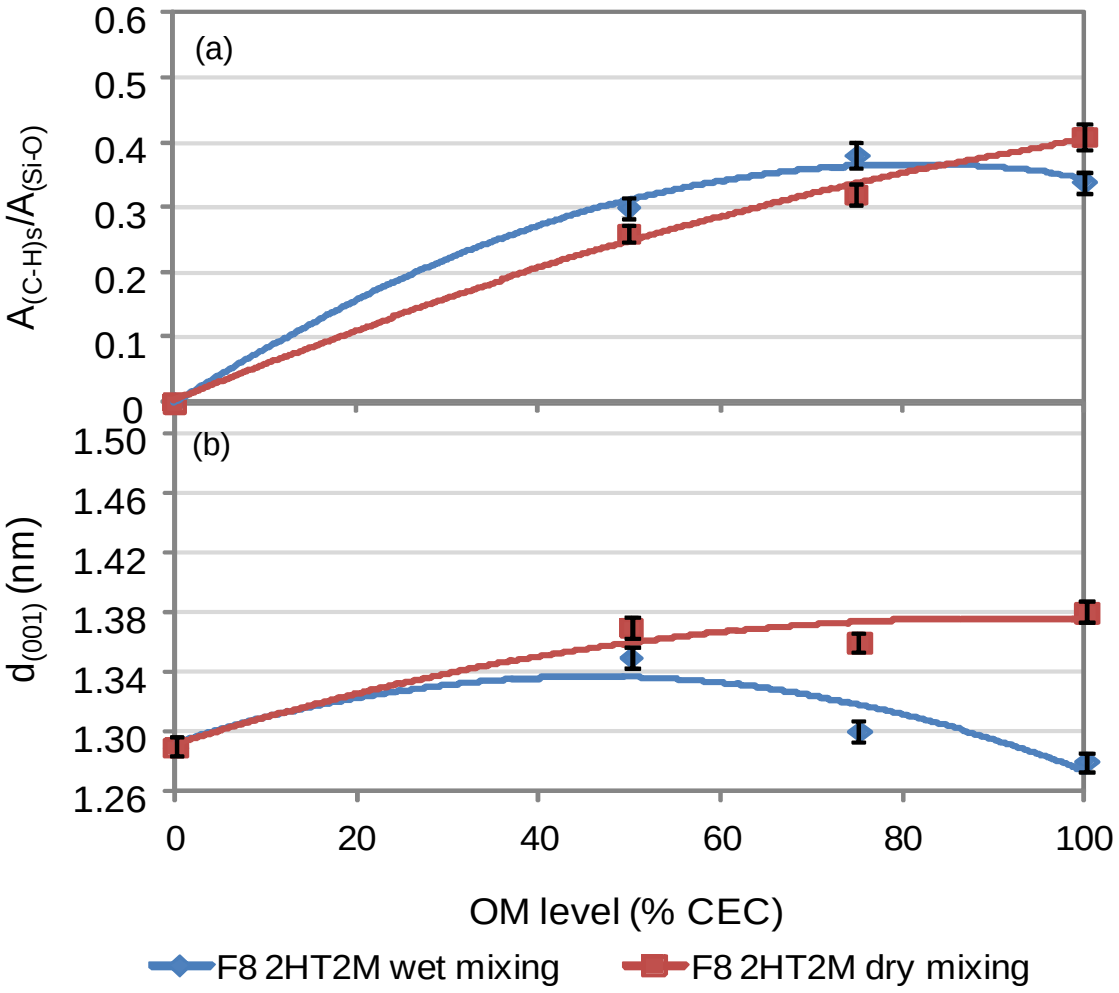

Figure 4.19: Data obtained from DRIFTS and XRD respectively plotted as a function of OM of F800 with 2HT2M using a wet mixing method and F800 with 2HT2M using a dry mixing method; (a) $A_{(C-H)s}/A_{(Si-O)}$, (b) d-spacing of platelets. Demonstrating the effect of increasing 2HT2M OM on the d-spacing of F800 platelets, and the level of carbohydrate present on F800.

In the case of F800 with 2HT2M OM applied using a dry mix method a significant decrease in $\nu_{as}(CH_2)$ was observed with increasing surfactant level; $\nu_{as}(CH_2)$ values were 2921 cm^{-1}, 2919 cm^{-1} and 2916 cm^{-1} for 50 %, 75 % and 100 % OM respectively. At the same time there was a increase in the amount of the surfactant present on the substrate as evidenced by an increasing $A_{(C-H)s}/A_{(Si-O)}$ ratio (Figure 4.19a). This appears to indicate that there may have been some self-assembly of the alkyl tails with increasing levels of OM. However, the XRD data (Figure 4.19b) indicated that it was most unlikely that these self-assembled structures were residing in the galleries as $d_{(001)}$ was too small. At higher surfactant levels, with the galleries already filled, the additional surfactant

would then adsorb around the edges of the material (resulting in the ratio of basal/edge bound to gallery bound molecules to increase in comparison with 50 % OM). The surfactant molecules adsorbed (possibly in multi-layers) on the edge and exposed basal planes a would have a lower $\nu_{as}(CH_2)$ as they may be in a more crystalline state. As a result at higher surfactant levels the average $\nu_{as}(CH_2)$ would decrease resulting in the shifts observed.

For Na-MMT, increasing the level of OM has been shown to be effective at increasing the ordering of alkyl chains. Liauw *et al.* (2007), showed that di(hydrogenated tallow) benzyl methyl ammonium chloride (2HTBM) and stearyl benzyl dimethyl ammonium chloride (SB2M) exhibited increases in the number of vertically aligned tails with increasing OM [130]. They also demonstrated that OM with two alkyl chains 2HTBM gave a higher level of ordering than one alky chain (SB2M). This explains the lack of ordering observed for CTAB modification of F800 compared to 2HT2M, due to the greater interaction between the alky chains of 2HT2M. The lack of ordering of alkyl tails within the Laponites® could be due to a number of factors; firstly the amount of organic modifier on the substrates was lower, with 100 % OM of LRD equating to 0.3 $mmol.g^{-1}$ and 100 % OM of LB equating to 0.61 $mmol.g^{-1}$ compared to 50 % and 100 % 2HT2M on F800 equating to 0.59 and 1.19 $mmol.g^{-1}$ respectively. The lower amount of OM coupled to the higher surface area of the Laponites® would result in the alkyl chains being further apart than with F800.

4.5.1.5 Summary

Overall analysis of the OM substrates suggests that 2HT2M OM had a much greater beneficial effect on the Laponite® materials than on F800. Not only did the Laponites® exhibit adsorption levels of mineral oil equal to or greater than the unmodified at certain levels of OM, but they also showed the capacity for the interlayer space to increase with OM providing more space for the adsorption of molecules into the area between the platelets. F800 did not exhibit this ability for increase in interlayer space and it is possible that this contributed to its poor adsorption after 2HT2M modification.

Modification of F800 with CTAB appeared to be more beneficial than 2HT2M, with oil absorption increasing steadily with increasing OM after an initial drop in adsorption at 50 % OM. As with the 2HT2M OM however, the levels of oil absorption achieved for CTAB modified F800 did not reach those seen for the unmodified substrate.

4.5.2 Gas chromatography adsorption studies of EO onto OM substrates

The GC adsorption results were obtained in the same way as for the unmodified (UM) layered silicates (Section 3.5.2) The reduction of each EO molecule for the adsorption liquor was obtained using calibration curves, and the data obtained was used to calculate an estimated overall level of adsorption of the EO.

4.5.2.1 Adsorption of EO onto OM Fulcat® 800 determined by GC

The adsorption results for F800 OM with cetyl trimethyl ammonium bromide (CTAB) are given (Figure 4.20).

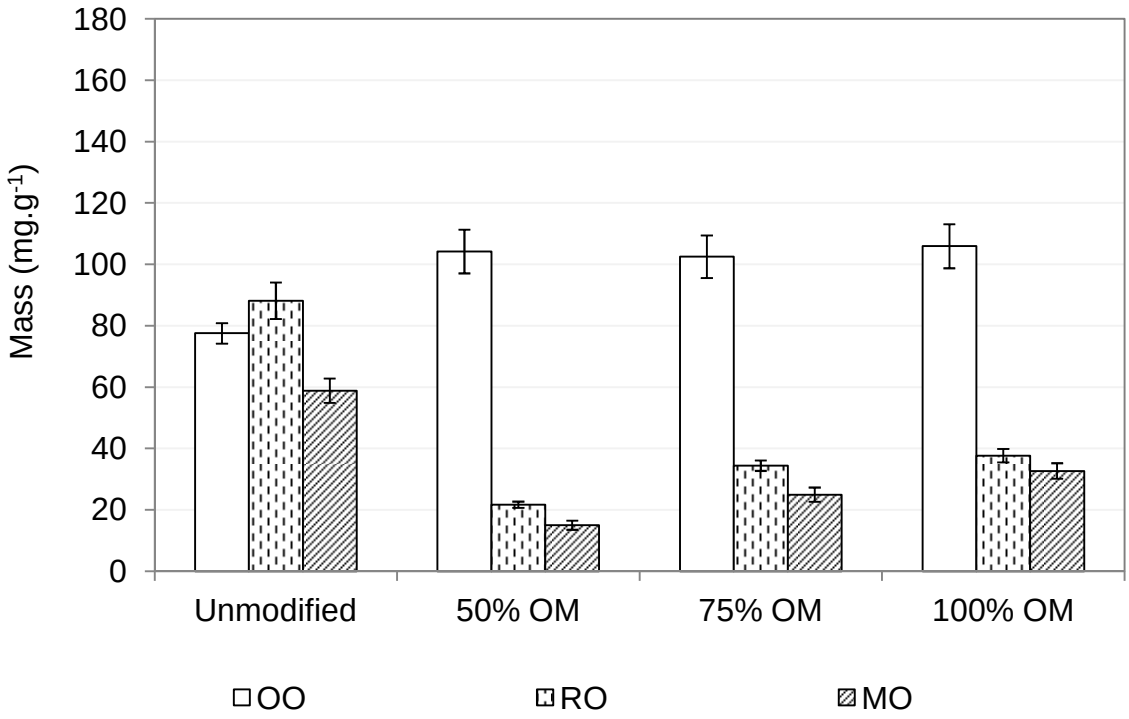

Figure 4.20: Comparison between mass of adsorption achieved for unmodified (UM) and CTAB modified F800. Demonstrating the decrease in adsorption at 50 % OM for RO and MO, followed by increased adsorption with increasing OM, OO adsorption was increased at all three levels of OM over UM.

The results for rosewood oil (RO) and manuka oil (MO) followed the same pattern. At 50 % OM there was a significant drop in the mass of oil adsorbed per gram of substrate. Increasing the level of organic modification resulted in a

gradual increase in the level of adsorption achieved. The effect of OM on the adsorption of oregano oil (OO) was considerably different to that seen for the other oils. At 50 % OM there was an increase of approximately30 $mg.g^{-1}$, however increasing the level of modification above 50 % appeared to have little further effect. The difference in the way OM affected adsorption of the oils was likely to be due to the difference in chemical makeup. Manuka oil was comprised mainly of molecules with no hydrophilic functional groups; therefore OM should increase the amount of adsorption as the more organophilic nature of the F800 after OM should be more attractive to the manuka oil molecules. It is possible that the reduced adsorption observed results from the alkyl tails of the organic modifier restricting the space available for adsorption into the galleries of the bulky bicyclic manuka oil molecules. With increasing OM, the environment becomes more organophilic and it was possible that the molecules are attracted enough to the organic nature of the galleries to partially overcome the reduction in adsorption caused by the reduced space. For rosewood oil, if linalool was adsorbing onto the hydrophilic sites on the surface of the substrates, via its OH group, then blocking the sites with alkyl chains from the OM would result in the reduced level of adsorption seen at 50 % OM. With increasing OM, the organophilic nature could attract the alkyl chain portion of linalool thus increasing its adsorption into the interlayer spaces of the galleries of the substrates. Oregano oil had a much more organic character than rosewood oil, and was comprised of predominantly acyclic or monocyclic molecules, making the average molecular size smaller than that of manuka oil. As it has fewer molecules with hydrophilic functional groups than rosewood oil, adsorption of the oregano oil molecules would be less affected by the blocking of the hydrophilic adsorption sites on the surface of the MMT substrate. The smaller molecular size compared to manuka oil means that the reduced space between the platelets of the F800 would have less of a restricting effect on the adsorption of the oregano oil molecules. It is possible that these two factors were responsible for the increase level of adsorption of oregano oil observed when manuka oil and rosewood oil displayed a reduction in adsorption.

Organic modification of F800 with di(hydrogenated tallow) dimethyl ammonium chloride (2HT2M) using the wet mix method had a similar effect on the levels of adsorption as CTAB (Figure4.21).

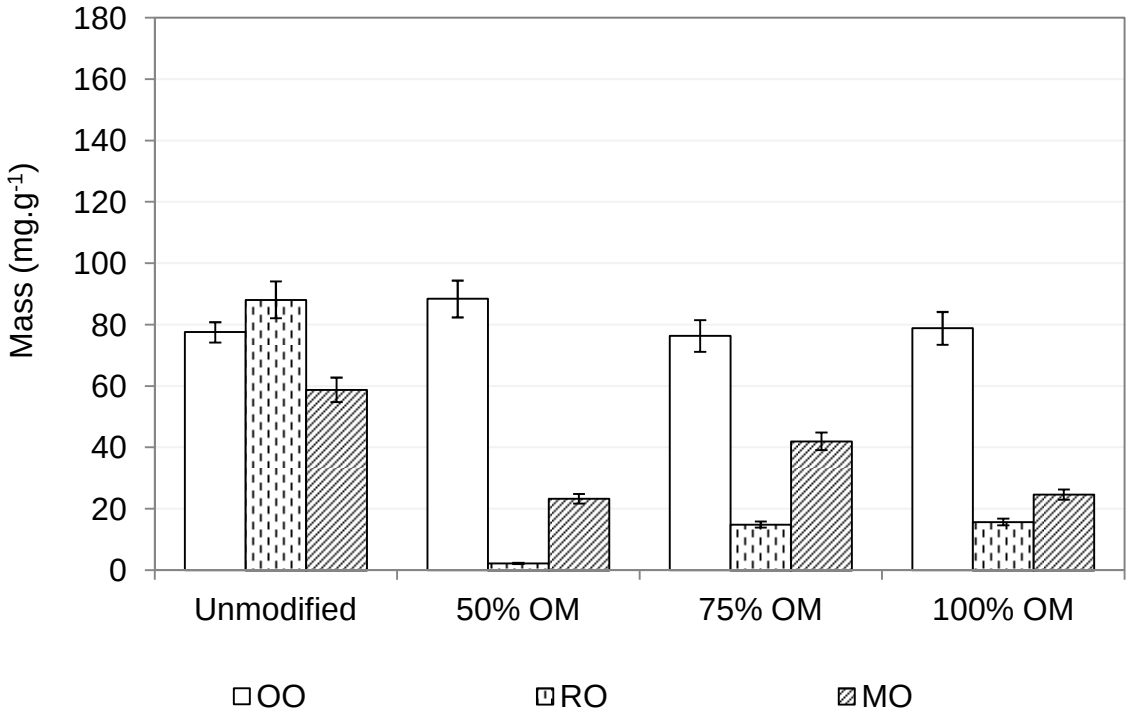

Figure 4.21: Comparison between mass of adsorption achieved for UM and 2HT2M modified (wet method) F800. Demonstrating the reduction in adsorption of RO and MO at 50% OM, OO adsorption was unaffected by OM.

The reduction in adsorption of rosewood oil from UM to 50 % was more pronounced than for the CTAB OM F800, suggesting that the CTAB alkyl chain was blocking more of the surface adsorption sites. At 75 % OM, adsorption of rosewood oil caused the OM F800 to form a gel. At 100 % OM adsorption all three of the EO resulted in gel formation.

Organic modification of F800 with 2HT2M using the dry mixing method resulted in a few differences when compared to the wet mix results. The affect of going from unmodified to 50 % OM was the same as for the wet mix method samples (Figure 4.22). However, at 75 % OM a drop in the level of adsorption of oregano oil was observed, which was maintained for 100 % OM. This large drop indicates a restriction on adsorption due to the drop in available surface area, or a filling of the interlayer space with the alkyl chains of the 2HT2M modifier.

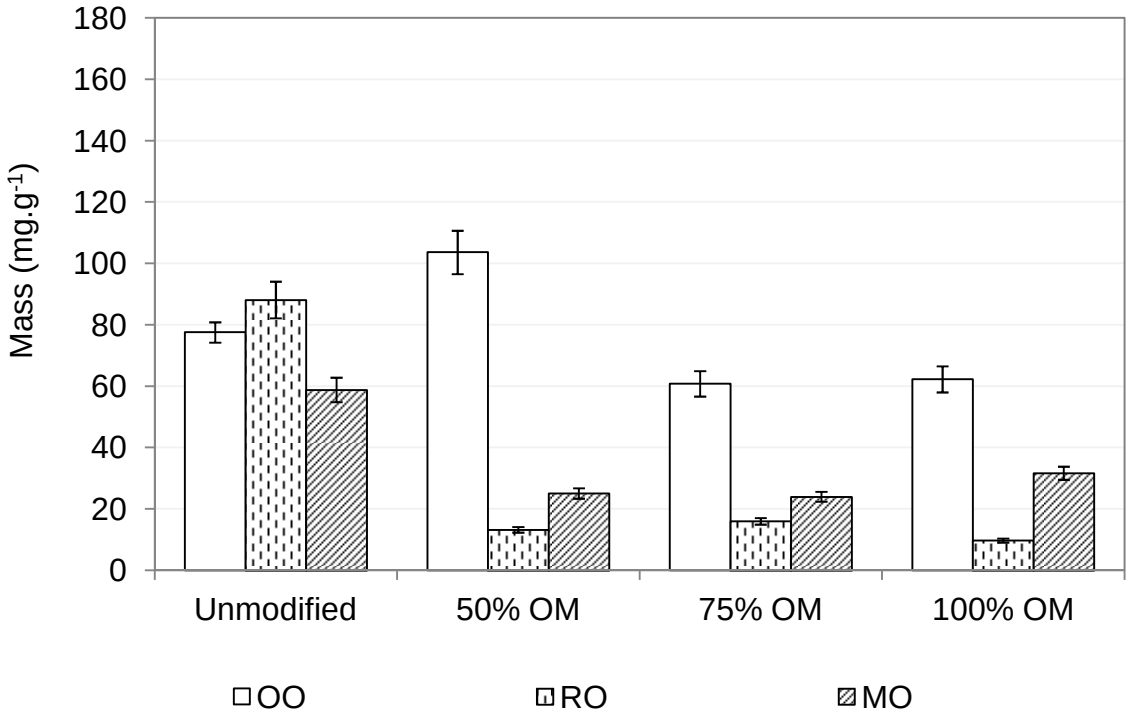

Figure 4.22: Comparison between mass of adsorption achieved for UM and 2HT2M modified (dry method) F800. Demonstrating that overall OM resulted in a decrease in the adsorption of the three EO.

During the adsorption studies it was noted that at 75 % OM adsorption of manuka oil and rosewood oil resulted in the substrate forming a gel, gel formation also occurred for the adsorption of manuka oil at 100 % OM.

4.5.2.2 Adsorption of EO onto OM Laponite® RD and OM Laponite® B determined by GC

The adsorption results for the three EO onto Laponite® RD (LRD) modified with 2HT2M were demonstrated (Figure 4.23). As with the other substrates, 50 % OM resulted in an increase in adsorption for oregano oil and a decrease for both manuka oil and rosewood oil. Manuka oil adsorption behaved in the same manner with increasing organophilic character resulting in a gradual increase in adsorption as the environment of the substrate became more attractive to the organic oil molecules. Increasing the level of OM did not have any effect on the level of adsorption of rosewood oil. The reduction in surface area between 50 and 75 % OM was greater for LRD (approximately 70 $m^2.g^{-1}$) than for the F800 samples (2HT2M (dry) – approximately 30 $m^2.g^{-1}$, 2HT2M (wet) – approximately

16 $m^2.g^{-1}$, and CTAB – approximately 4 $m^2.g^{-1}$). This indicated that the increase in organophilic character was not sufficient to overcome the more significant loss of surface adsorption sites due to the OM. The greater reduction in surface area appeared to have an effect on oregano oil oil adsorption as well, resulting in a reduction in adsorption at 75 % OM to less than half that achieved at 50 % OM. As there was no further decrease in surface area from 75 to 100 % OM, the greater organophilicity (and therefore a higher attraction for the EO molecules) resulted in an increase in adsorption to approximately the levels achieved by the unmodified substrate.

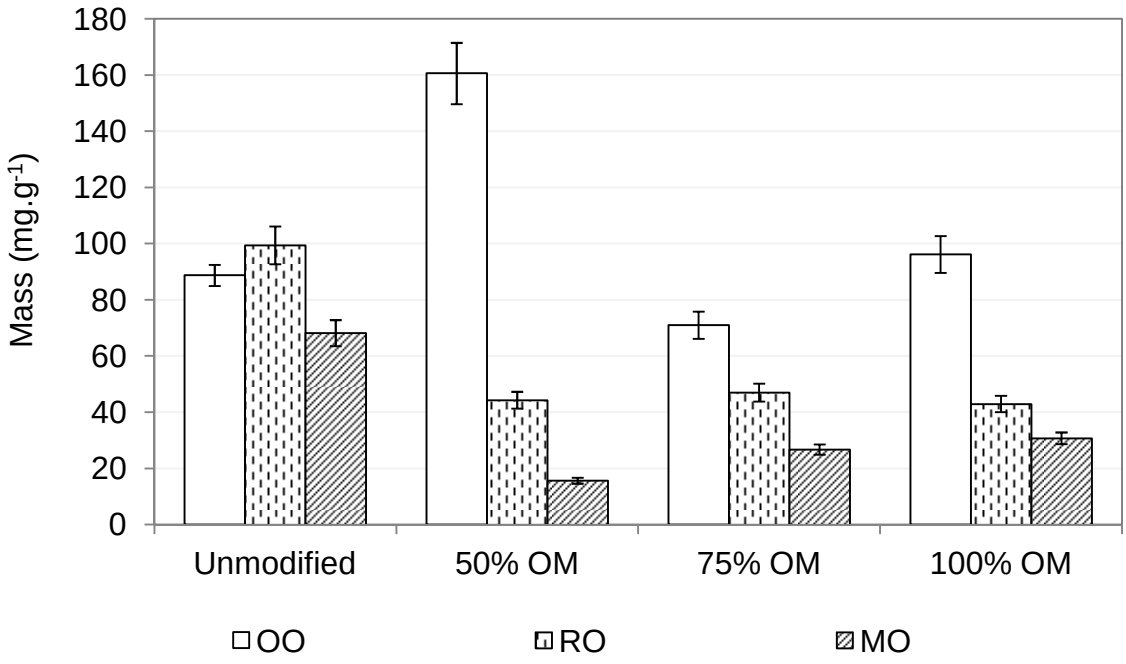

Figure 4.23: Comparison between mass of adsorption onto UM and 2HT2M modified LRD. Demonstrating the general pattern for a reduction in adsorption of EO with 50 % OM in comparison to the unmodified LRD. Followed by an increase in adsorption with increasing OM.

The reduction in the level of adsorption for rosewood oil was less severe for LRD at 50 % OM than that observed for F800 samples. X-ray diffraction data for LRD, F800-2HT2M (dry) and F800-CTAB revealed that the LRD had the largest increase in interlayer spacing, 0.12 nm compared to a 0.04 nm reduction for F800-2HT2M (dry) and 0.02 nm increase for F800-CTAB. As a result the interlayer space for the F800 samples was 0.37 and 0.36 nm respectively, whereas the interlayer space for LRD was 0.5 nm. The interlayer spaces for the

F800 samples were not large enough to accommodate the EO hydrocarbons which were approximately 0.4 nm, where as the interlayer space for LRD would accommodate the EO molecules. This may explain lower reduction in adsorption of rosewood oil for LRD compared to the F800 substrates.

Organic modification of LB showed the same general pattern for rosewood oil and manuka oil that had been observed for the majority of the other MMT substrates (Figure 4.24).

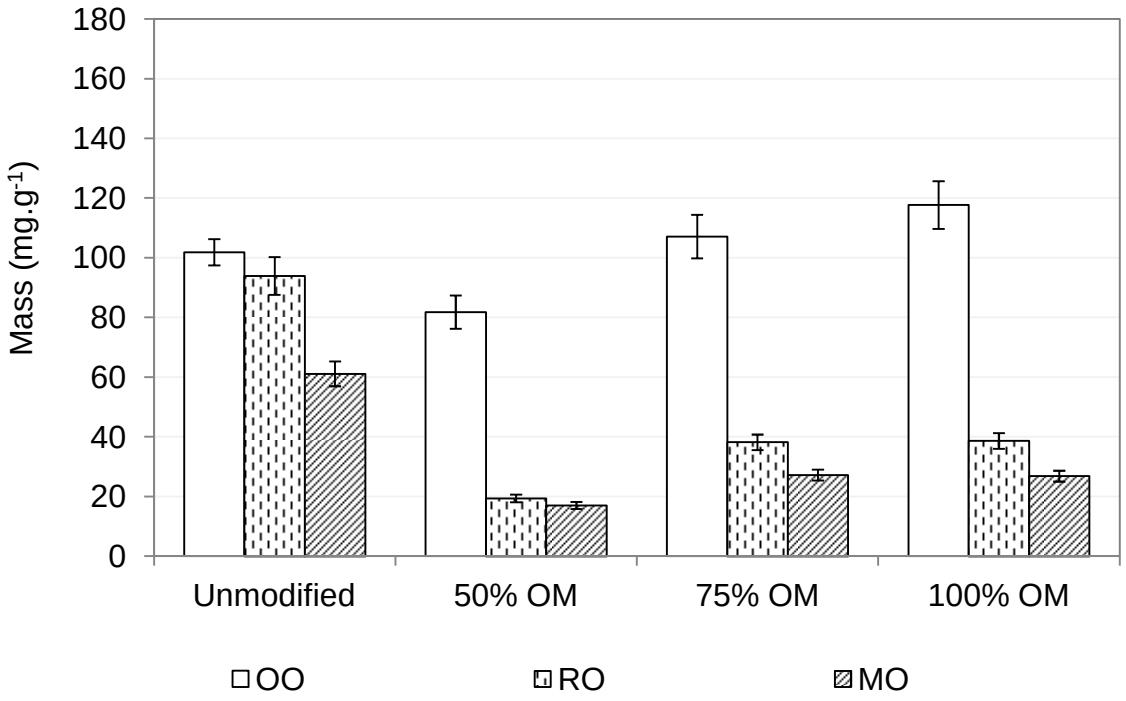

Figure 4.24: Comparison between mass of adsorption onto unmodified and 2HT2M modified LB. Demonstrating the initial reduction in adsorption as a result of 50 % OM followed by a gradual increase with increasing OM.

Instead of an increase in adsorption of oregano oil at 50 % OM, as observed with the other samples, in the case of LB there was a decrease of approximately 20 $mg.g^{-1}$. Subsequent increases in OM resulted in increases in adsorption of oregano oil. LB exhibited the largest loss of surface area from UM to 50 % OM with approximately a 400 $m^2.g^{-1}$ reduction. The low level of oregano oil adsorption achieved at 50 % OM indicates that the loss of adsorption sites on the surface was a more important factor on adsorption than the increase in organophilic character, compared to the other substrate samples.

4.5.2.3 Summary

None of the OM substrates tested achieved higher levels of adsorption for rosewood oil and manuka oil than the UM substrates. Organically modified Laponite® RD (75 %) achieved the best levels of adsorption for rosewood oil of any of the OM substrates, Fulcat® 800 OM with 100 % CTAB achieved the highest amount of adsorption for manuka oil and Laponite® RD OM with 50 % 2HT2M achieved the highest level of adsorption for oregano oil. Of the OM substrates the results suggest that Laponite® RD OM with 50 % 2HT2M would give the best adsorption for the antimicrobial EO blend (rosewood oil and oregano oil) identified as having the highest antimicrobial activity in Section 3.2. The adsorption characteristics of the EO onto the OM substrates was further investigated using FMC.

4.5.3 Flow micro-calorimetry analysis of adsorption of EOs onto organically modified substrates

As in Chapter 3 the OM substrates were analysed for adsorption of the EOs using FMC. This was done to investigate the overall levels of adsorption and to provide information on the mode of adsorption. The 100 % OM substrates could not be analysed in this way as they formed a gel when combined with the EOs which resulted in a blocking of the FMC cell.

4.5.3.1 FMC adsorption of EO onto OM Fulcat® 800

The adsorption and desorption data for F800 OM with 2HT2M using a dry mixing method was demonstrated (Figure 4.25). From the unmodified substrate to 50 % OM there is a large drop in the enthalpy of adsorption for all three EO. For oregano oil and manuka oil the majority of this reduction in heat was attributed to the reduced mass of adsorption resulting from 50 % OM of the substrate. With fewer molecules adsorbed, there will be fewer surface interactions such as hydrogen bonding, resulting in the lowered observed enthalpy. In addition, a greater proportion of the EO molecules adsorbed in the cases of manuka oil and oregano oil were able to desorb from the substrate. This was shown by the more even ratio of mass of desorption to mass of adsorption for 50 % OM samples compared with the unmodified F800. This indicates that the molecules that were able to adsorb were undergoing weaker interactions with the substrate. The aminyl head group and to a lesser extent the alkyl chains of the OM, lying horizontal to the surface of the substrate (see Section 4.5.1.1), will block at least a proportion of the surface silanol groups. This would result in a reduction in the amount of molecules able to undergo hydrogen bonding or electrostatic interactions with the surface.

Adsorption of rosewood oil onto the 50 % OM F800 also resulted in a much reduced enthalpy of adsorption in comparison to the unmodified substrate. However, unlike manuka oil and oregano oil there was only a slight reduction in the mass of rosewood oil adsorbed. The reduced availability of surface sites for interactions such as hydrogen bonding was therefore the main cause for the reduction in the enthalpy of adsorption. The high enthalpy of desorption for rosewood oil at 50 % OM and the low mass of desorption in comparison to the

enthalpy and mass of adsorption indicated that although there were fewer molecules undergoing surface interactions, the molecules that were able to undergo surface interaction were more strongly bonded in comparison with the unmodified F800. This may have been due to an underestimation in the mass of rosewood oil molecules desorbing as described in Section 3.5.4.1. Increasing the level of OM to 75 % of the CEC resulted in a slight reduction in the enthalpies of adsorption/desorption. This indicated that the rise in hydrocarbon present on the substrate (Section 4.5.1.3) resulted in a slightly weaker attraction between the substrate and the rosewood oil molecules. The mass of adsorption was largely unaffected by the increase in surfactant level. When considering the lower enthalpy of adsorption at 75 % this indicated that there were fewer surface interactions. This was likely as a result of increased blocking of adsorption sites such as silanol groups. The mass of rosewood oil desorbed was higher than the mass adsorbed. This anomaly is likely to be due to release of unbound surfactant during adsorption, which resulted in an underestimate of the amount adsorbed. Similarly, loss of unbound surfactant during the desorption phase may also have led to an over estimate of the amount desorbed. Displacement of unbound surfactant during adsorption would result in a faster increase in refractive index of the cell effluent and hence an underestimate of the amount adsorbed. The very low mass of rosewood oil desorbed at 50 % compared to 75 % OM may indicate an underestimation of the mass desorbed at 50 % considering the heats of desorption were very similar.

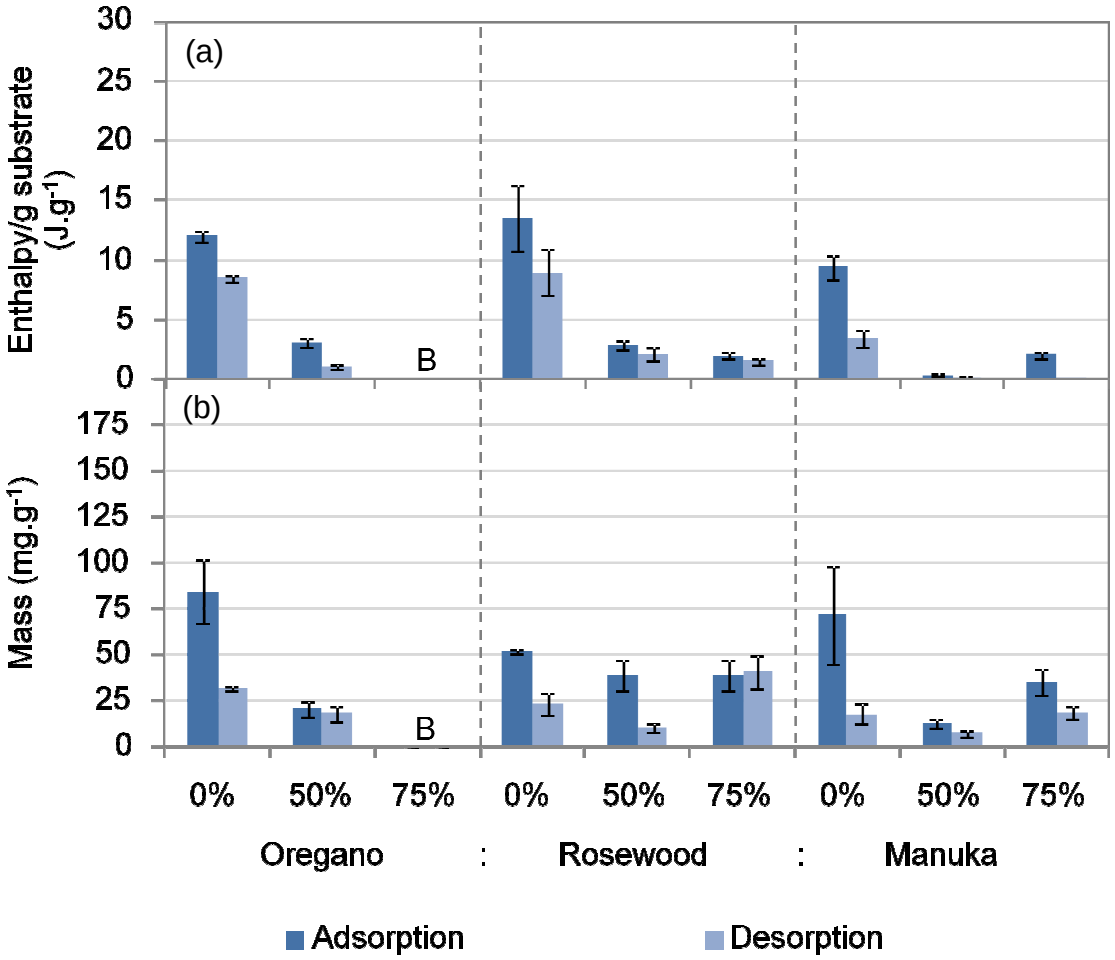

Figure 4.25: Effect of OM of F800 with 2HT2M using a dry mixing method on adsorption, comparison between unmodified (0 %) and modified at 50 % and 75 % CEC (a) Enthalpy of adsorption and desorption in joules per gram of substrate. (b) Mass of adsorption and desorption in milligrams per gram of substrate. B – Blockage of cell due to gel formation therefore data not obtained. Demonstrating the reduction in the mass of EO adsorbed as a result of OM in comparison to unmodified F800.

At 75 % OM there was an increase in the enthalpy of adsorption for manuka oil in comparison to 50 % OM. It is unlikely that the rise in heat observed was a result of stronger bonding of the manuka oil molecules to the substrate as the observed enthalpy of desorption showed a reduction from 50 to 75 % OM. The increase in mass of adsorption was the most likely cause of the higher enthalpy of adsorption. The increase in mass adsorbed could be attributed to the higher amount of hydrocarbon present on the F800 (Section 4.5.1.3) resulting in a more receptive environment for the organophilic manuka oil molecules. The low enthalpy of desorption and high mass of desorption (in proportion to mass of

adsorption) indicates that the strength of adsorption was reduced in comparison to 50 % OM. This will be as a result of more blocking of surface adsorption sites by the surfactant alkyl chains. The effect of OM on the mass adsorbed for rosewood oil and manuka oil mirrored the pattern observed with the GC adsorption (Section 4.5.2). However, the actual masses determined were slightly higher in general with FMC indicating that the constantly replenishing concentration of EO used in FMC had a beneficial effect on adsorption.

The results obtained from the adsorption/desorption of EO on F800 OM with CTAB are displayed (Figure 4.26).

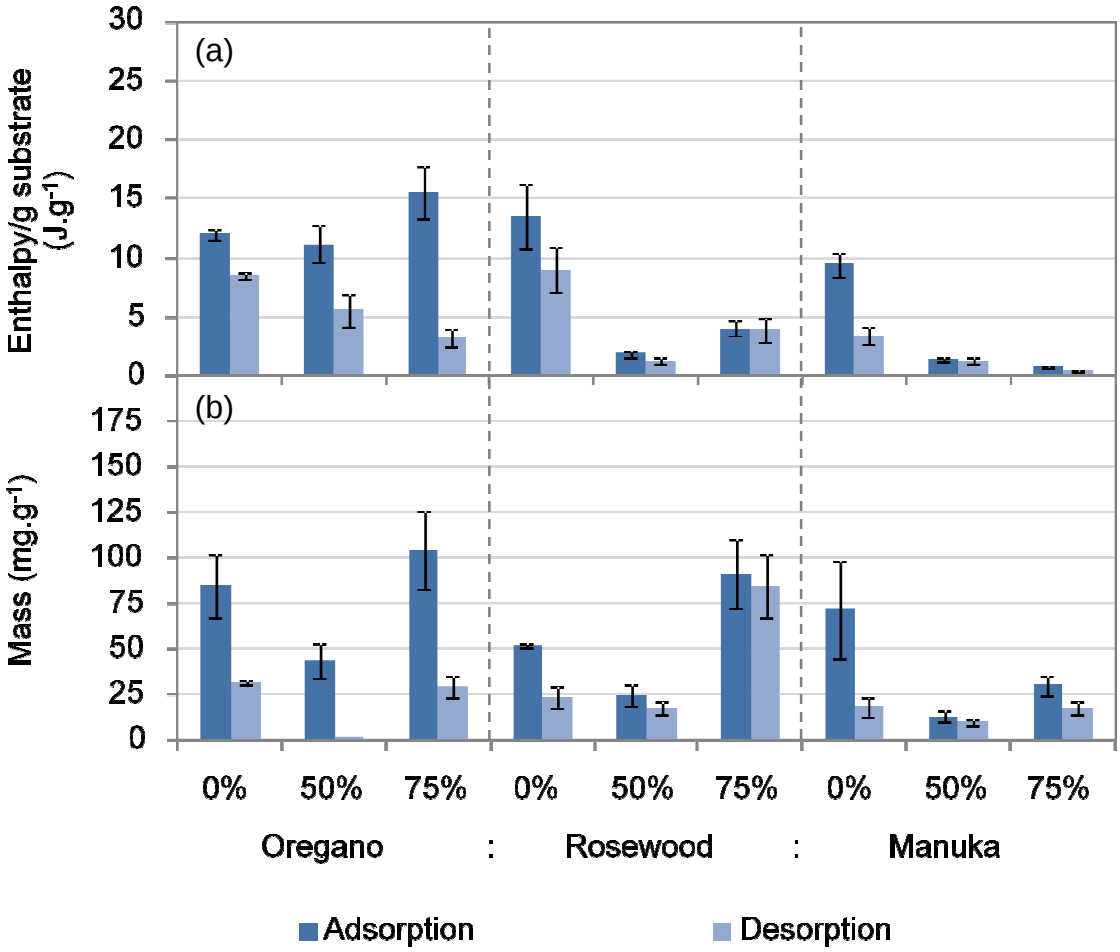

Figure 4.26: Effect of OM of F800 with CTAB using wet mixing method on adsorption, comparison between unmodified (0 %) and modified at 50 % and 75 % CEC (a) Enthalpy of adsorption and desorption in joules per gram of substrate. (b) Mass of adsorption and desorption in milligrams per gram of substrate. Demonstrating a reduction in mass of OO and RO adsorbed at 50 % OM, followed by an increase in mass adsorbed at 75 %.

The adsorption of oregano oil onto F800 with 50 % CTAB modification resulted in a slight reduction in the enthalpy of adsorption in comparison with the unmodified substrate. However, when taking into account the masses of adsorption due to the reduction in mass adsorbed at 50 % compared with the unmodified the effect was a 2 fold increase in the enthalpy per gram of oil adsorbed. This indicated that the strength of adsorption of each molecule had increased with 50 % OM. This may be related to additional intermolecular forces (such as dispersive interactions) between the organic EO molecules and the alky chain of CTAB being added to the already present hydrogen bonding between polar functional groups and any available/accessible surface silanol groups. The very low mass of oregano oil desorbed would appear to confirm the increase in strength of adsorption onto F800 with 50 % CTAB OM.

At 75 % OM despite an increase in enthalpy of adsorption the strength of adsorption of oregano oil molecules appeared reduced due to a high mass of oil adsorbed. With adsorption of both manuka oil and rosewood oil at 50 % OM, a large reduction in the heat produced in comparison to the unmodified substrate was observed. In both cases this was attributed to a large drop in the mass of oil adsorbed (potentially due to the less of adsorption sites due to the presence of the alkyl chain of CTAB). The loss of adsorption sites had a greater effect on the enthalpy of adsorption of rosewood oil suggesting hydrogen bonding between the linalool OH and surface silanol groups had been significantly reduced. The weak strength of adsorption for rosewood oil was further evidenced by the high proportion of the oil molecules that had adsorbed which were able to desorb on flushing the cell with solvent. An increase in mass adsorbed was observed for all three oils at 75 % OM (oregano oil and rosewood oil also exhibited an increase in enthalpy of adsorption), despite the fact that there was no apparent increase in the hydrocarbon present on the OM F800 (Section 4.5.1.3) and there was no increase in the d-spacing of the platelets (Section 4.5.1.1).

4.5.3.2 FMC adsorption of EOs onto OM Laponite® RD

The results obtained from the FMC analysis of EO adsorption onto LRD OM with 2HT2M are plotted in Figure 4.27.

At 50 % OM a decrease in the entalpy of adsoption was observed for all three EO in comparison with adsorption onto the unmodified LRD. Initially this indicated a reduction in the strength of adsorption of the EO molecules to the surface of the substrate, attributed to the blocking of surface adsorption sites by the alkyl chains of the 2HT2M. A reduction in the mass of adsorption for all three oils was also observed, for manuka oil the reduction in mass was inline with the reduction in enthalpy. This indicated that the strength of adsorption at 0 % OM and 50 % OM was similar for manuka oil and the reduction in enthalpy was purely a result of fewer molecules being able to adsorb due to the restriction of available space caused by the presence of the OM alkyl chains.

The reduction in the mass of adsorption for oregano oil and rosewood oil for 0 % to 50 % OM was proportionately larger than the reduction in the enthalpy of adsorption. As a result of this the enthalpy of adsorption per gram of oil adsorbed increased at 50 % OM, indicating that although fewer molecules were able to adsorb, those that did adsorb underwent stronger interactions with the substrate. The combination of hydrogen bonding with the surface silanols, and inter molecular attraction between the organophilic regions of the oregano oil and rosewood oil molecules and the alky chains of the surfactant is the most likely reason for the increased strength of adosrption. Further evidence for a stronger interaction between the oregano oil and rosewood oil molecules and LRD at 50 % OM comes from the evidence that the enthalpy of desorption for each oil, in comparison to enthalpy of adsorption, is proportionately higher for the organically modified LRD compared to the unmodified LRD. In addition, the enthalpy of adsorption per gram of oil desorbed had increased from 0 % to 50 % OM. This indicates that a greater amount of energy was required for desorption of the oil molecules at 50 % OM than for the unmodified substrate.

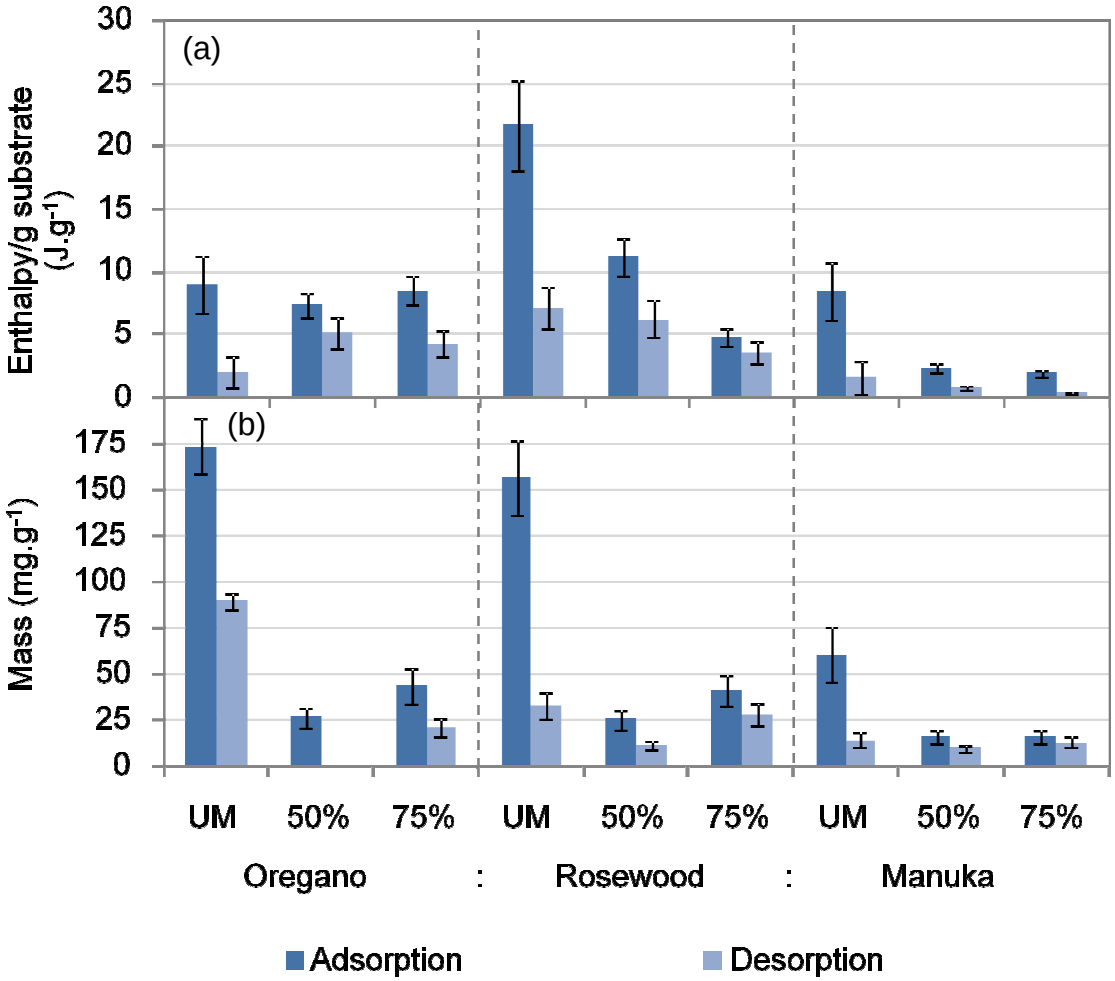

Figure 4.27: Effect of OM of LRD with 2HT2M on adsorption, comparison between unmodified (0 %) and modified at 50 % and 75 % CEC (a) Enthalpy of adsorption and desorption in joules per gram of substrate. (b) Mass of adsorption and desorption in milligrams per gram of substrate. Demonstrating the reduction in mass of adsorption, and increase in strength of adsorption, as a result of organic modification.

Increasing the level of OM to 75 % of the CEC had little effect on the adsorption of manuka oil, despite the increase in hydrocarbon present (Section 4.5.1.3). It was anticipated that the increase level of OM would result in a more organophilic environment which should have been more receptive to the manuka oil molecules. It was therefore evident that the increase in the number of surfactant molecules resulted in a reduction of the space available for the bulky manuka oil molecules. The enthalpy of desorption in relation to mass desorbed also decreased for 50 % to 75 % OM. This could be attributed to the reduction in the interaction between π-electrons present in manuka oil

component molecules and the substrate silanols due to the increased blocking of the silanols by surfactant molecules.

At 75 % OM there was a slight increase in enthalpy of adsorption for oregano oil. This was attributed to the increase in mass of oil adsorbed rather than an increase in the energy of adsorption per gram of oil. The desorption data indicated that the strength of adsorption had decreased from 50 % to 75 % OM with the enthalpy of desorption decreasing despite a large increase in the mass of desorption. In contrast to manuka oil the increase in organophilic character had a beneficial effect on the mass of adsorption. As oregano oil molecules were in general smaller than the manuka oil molecules, the increase in d-spacing (Section 4.5.1.1) may have provided enough extra space between the platelets to overcome the restriction in space imposed by the greater number of surfactant molecules.

Adsorption of rosewood oil at 75 % OM resulted in a reduction of the enthalpy of adsorption to approximately half that at 50 % OM indicating weaker adsorption. The increase in mass adsorbed indicated that although the increase in the organophilic character of the substrate resulted in a better environment for adsorption of rosewood oil, the presence of the surfactant molecules resulted in significant blocking of the surface adsorption sites thus preventing interactions between the rosewood oil molecules and the substrate. Further evidence for a weakening of the interaction between rosewood oil molecules and the OM LRD was provided by the high mass of desorption observed in proportion to the mass adsorbed.

4.5.3.3 FMC adsorption of EO onto OM Laponite® B

From unmodified to 50 % OM of LB there was a large reduction in the enthalpy of adsorption of manuka oil (Figure 4.28), indicating that the presence of the surfactant molecules reduced the number and intensity of surface interactions. In contrast to adsorption onto LRD, the reduction in enthalpy of adsorption was accompanied by a large increase in the mass of adsorption. There were two differences between the 50 % organically modified LRD and LB which can explain the difference in adsorption behaviour; LB had a larger d-spacing (Section 4.5.1.2) than LRD at 50 %, LB had no unbound 2HT2M molecules present at 50 % OM compared with 50 % of the 2HT2M molecules being

unbound for LRD (Section 2.5.1.3). The unbound 2HT2M molecules were more likely to be at the edges of the platelets than within the galleries, and therefore it was possible that at 50 % OM LRD had a higher proportion of 2HT2M molecules around the pores of the galleries. This may have resulted in blocking of the pores and restriction of the adsorption of the manuka oil molecules. The combination of these factors may have resulted in more space between the galleries and also greater ease of access to the galleries for LB in comparison to LRD. Therefore the increased organophilic character of LB 50 % OM, relative to unmodified LB resulted in the increase in mass of adsorption. The relatively high mass of manuka oil able to desorb indicated that whilst more manuka oil molecules were adsorbed, the strength of adsorption was decreased with respect to the unmodified substrate. At 75 % OM, a large decrease in the mass of manuka oil adsorbed was observed. This indicated that the higher surfactant loading had resulted in a blocking effect preventing the EO molecules from getting close enough to the surface of the LB to be adsorbed. It was observed in Section 4.5.1.3 that at 75 % OM there were unbound 2HT2M molecules present (in contrast to 50 % OM). It is possible that the presence of these unbound molecules resulted in greater blocking of the LB galleries, further restricting adsorption of the manuka oil molecules.

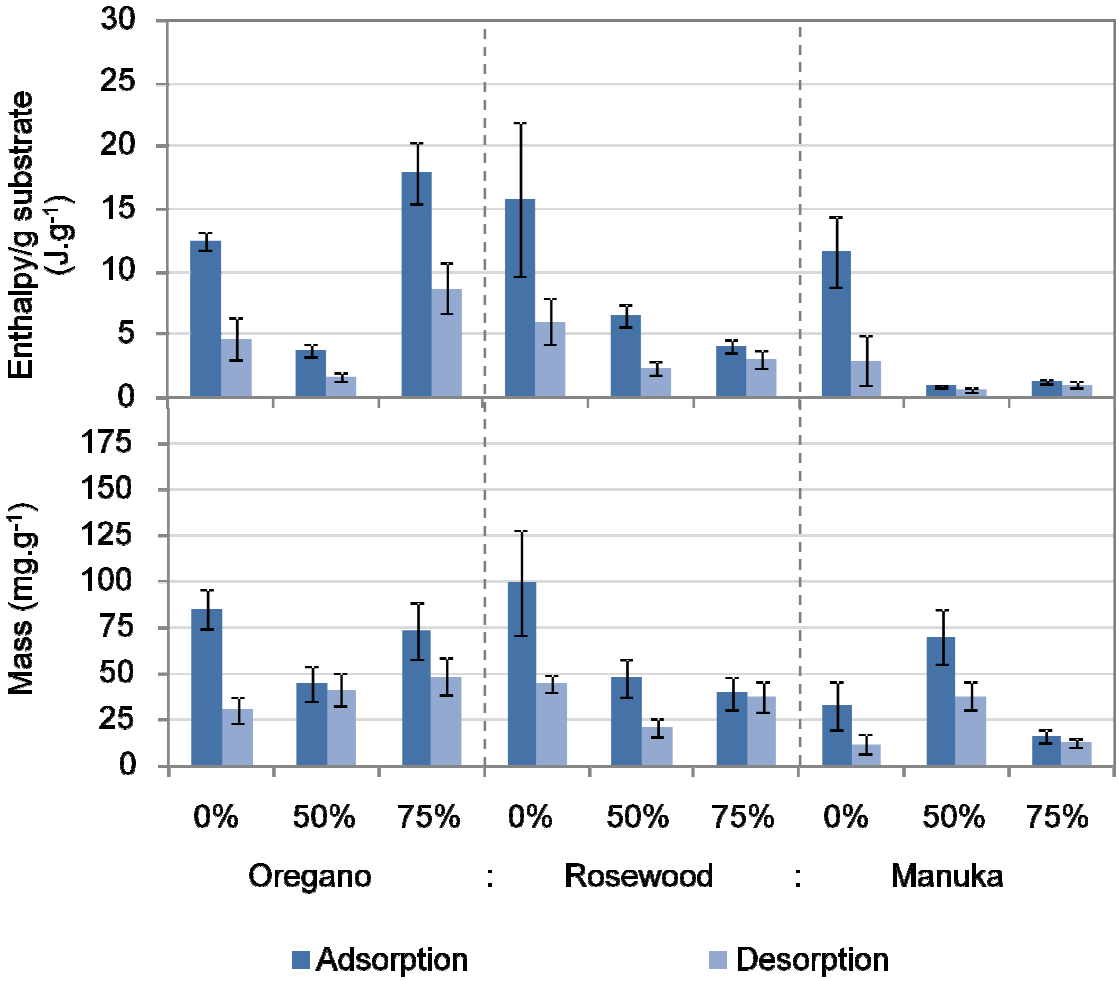

Figure 4.28: Effect of OM of LB with 2HT2M on adsorption. Comparison between unmodified (0 %) and modified at 50 % and 75 % CEC (a) Enthalpy of adsorption and desorption in joules per gram of substrate. (b) Mass of adsorption and desorption in milligrams per gram of substrate. Demonstrating a decrease in mass of adsorption as a result of OM in most cases, coupled to weaker strength of adsorption.

50 % OM of LB resulted in a decrease in the enthalpy of adsorption of oregano oil and rosewood oil relative to the unmodified substrate. This reduction was attributed in part to the reduced mass of the oils adsorbed and in part to a weaker strength of interaction between the EO molecules and the substrate. The reduced strength of adsorption was more evident for oregano oil; in this case almost all the molecules adsorbed were able to desorb back off of the substrate on flushing the cell with solvent. At 75 % OM the increased organic character had a beneficial effect on the mass of oregano oil adsorbed and an

increase in the enthalpy of adsorption such that that the enthalpy of adsorption per gram of oil adsorbed was higher than at 50 % OM.

Increasing the level of OM to 75 % resulted in a reduction in the enthalpy of adsorption of rosewood oil; however the mass of rosewood oil adsorbed did not appear to be significantly affected. This indicates that the higher number of surfactant molecules present at 75 % resulted in blocking of the silanols at the surface of the Laponite®, thus preventing hydrogen bonding with the linalool component of rosewood oil.

4.5.3.4 Summary

Adsorption of manuka oil was in general negatively affected by OM due to the larger molecular size of the components compared to the other EOs, resulting in the surfactant molecules blocking EO adsorption onto the substrates. For LB at 50 % OM TGA data suggested that there was no unbound quat present on the substrate. Therefore, the organic modification would not result in a blocking of the entry to the galleries and adsorption sites. The increased level of adsorption observed for LB with 50 % OM was therefore possibly due to the combination of increased organophillic character and good availability of adsorption sites and gallery pores.

Organic modification of F800 with 2HT2M resulted in low strength of adsorption for rosewood oil and oregano oil, Weak adsorption was likely to result in fast desorption of the EO molecules which would be undesirable for controlled release of the antimicrobial EO blend.

F800 OM with CTAB resulted in high mass and strength of adsorption of oregano oil, however it also exhibited very weak adsorption of rosewood oil.

LRD exhibited a good strength of adsorption of both oregano oil and rosewood oil especially at 50 % OM. However, the mass adsorbed via FMC of the two oils which were used in the antimicrobial EO blend was low in comparison with the other substrates.

LB OM with 2HT2M led to relatively high masses of adsorption for both rosewood oil and oregano oil. However, in contrast to LRD the strength of adsorption was low especially for oregano oil at 50 % OM and rosewood oil at 75 % OM where in both cases almost all of the EO adsorbed was removed during the desorption process.

4.6 Conclusions

- The lack of increase in the interlayer space of F800 indicated that the surfactant molecules could not enter the galleries of the material.
- OM of the layered silicate substrates resulted in a reduction in the adsorption of manuka oil both in GC and FMC studies. There was some FMC evidence that a lower surfactant loading may have enhanced the level of adsorption of manuka oil onto the organically modified layered silicates.
- For the EO which was to be used in the antimicrobial blend (oregano oil and rosewood oil), LRD at 50 % OM gave the best adsorption performance.
- The weak adsorption of both oregano oil and rosewood oil onto the OM F800 indicated that it would not be suitable as a substrate for controlled release applications.
- The high strength of adsorption of the EOs onto LRD 50 % OM in addition to the relatively high surface area led to its selection as the substrate which may provide the best properties for adsorption of EO and controlled release. As the rate of desorption of the EO from the substrate is the main mechanism of controlled release, a slow rate of desorption would be required for a successful material. A high strength of adsorption would mean that a high energy was required to remove the EO molecules from the surface of the substrate. This high desorption energy should result in a slow rate of desorption.

CHAPTER 5

Antimicrobial polymers

Abstract

This study examined the addition of EOs to polymer materials for the confirmation of their antimicrobial properties. The antimicrobial EO blend identified in Chapter 2 was added to linear low density poly ethylene (LLDPE), silicone elastomer (SE) and a solvent based paint. The EO blend was pre-adsorbed onto an organically modified layered silicate (OMLS) before addition to the polymer formulation. Control samples were also prepared where the EO blend was added directly. The polymer materials were tested for their ability to reduce the number of viable bacterial cells of both *Acinetobacter baumannii* and methicillin resistant *Staphylococcus aureus*. All of the polymer samples containing the directly added EO blend displayed good antimicrobial activity, achieving at least a 1 log reduction in the number of bacterial cells within 2 hours of exposure. Pre-adsorption of the EO blend onto the OMLS improved the antimicrobial activity of the SE and paint samples (in some cases by up to a 2 log reduction). However, pre-adsorption resulted in a reduction in the antimicrobial activity of LLDPE samples in comparison with controls containing the directly added EO blend. The release of the EO molecules from the polymers was assessed using head-space gas chromatography. Pre-adsorption of the EO blend led to more sustained release of molecules in SE and LLDPE. Overall it was shown that antimicrobial properties could be conferred to polymer materials via the addition of EOs. Adsorption of the EOs onto LRD with 50 % organic modification before addition to the polymers was shown to improve antimicrobial properties and reduce the rate of EO molecule release from the polymers.

5.1 Introduction

The final stage of this study was to add the antimicrobial EO blend (both directly, and pre-adsorbed on to the layered silicate substrates) to a range of polymer materials. It was hypothesised that comparison of the antimicrobial

performance afforded by these modes of addition would provide insight into the effect of pre-adsorption of EO on the controlled release of the antimicrobial blend.

5.1.1 Thermoplastics

Plastics are synthetic polymers made from organic monomers (such as ethene) isolated from crude oil. Plastics are split into two categories; thermoplastics and thermosets. Thermosets undergo crosslinking of the polymer chains during curing reactions and therefore will not melt once set. Thermoplastic polymer chains are not crosslinked. The shape of items made from thermoplastics is set either by the polymer melt going below its glass transition temperature (T_g) and/or crystallisation of the polymer. The latter depends on whether or not the thermoplastic is amorphous or semi-crystalline, respectively. On re-heating a thermoplastic will return to its melt state and can be reshaped to a different item. Approximately 80 % of all plastics used are thermoplastics such as polyethylene and polypropylene, therefore addition of the antimicrobial EO blend to a thermoplastic would result in a material with a much wider range of uses than addition to a thermosetting plastic [135, 136].

Polyethylene (Figure 5.1) was discovered in 1933 by Reginald Gibson and Eric Fawcett while working at Imperial Chemical Industries (ICI), by heating a mixture of ethylene and benzaldehyde to 170 ℃ at a pressure of 1700 atm. It is the highest consumed polymer worldwide due to its versatility and high performance [137, 138].

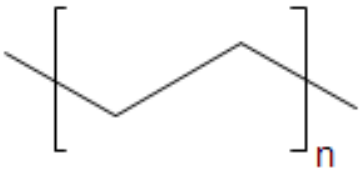

Figure 5.1: Skeletal representation of polyethylene (PE) showing one repeating unit.

Low density polyethylene (LDPE) is a form of polyethylene where there are long branches off of the main polymer chain. This means that the polymer chains cannot pack as closely together as they can in high density polyethylene (HDPE) (which has minimal chain branching) [138] and therefore they have a higher crystalline content and higher density. Linear low density polyethylene (LLDPE) is in some senses a version of LDPE which utilises low pressure Zeigler – Natta polymerisation techniques normally used to produce HDPE. The branches in LLDPE are introduced via copolymerisation of ethene with higher 1-alkenes such as hex-1-ene and oct-1-ene. The number, type and distribution of branches in LLDPE can therefore be tightly controlled, though LLDPE lacks long chain branches. This results in “high chemical stability, high performance characteristics both at relatively high and low temperatures, high resistance to cracking, and improved resistance to puncture” [139]. LLDPE typically has a density of 0.92 $g.cm^{-2}$. In 2010 approximately 30 % of polyethylene used worldwide was LLDPE and annual consumption of LLDPE worldwide is expected to grow at an average of 7 % [140]. LLDPE is versatile and has a wide range of uses including film applications, carrier bags, wire and cable coatings, injection moulded parts and pipes [141].

5.1.2 Silicone elastomer

Elastomers are polymers of generally of high molar mass (long chains) combined with light crosslinking of the chains, which must be far above T_g at room temperature. This allows the polymer to display rubber-like elasticity. The chains readily uncoil on stretching, but due to the cross-links, they are unable to slide relative to one another, therefore on release of the load the chains return to their original coiled state [142].

Silicone based polymers are defined as “polymers comprising of alternate silicon and oxygen atoms in which the silicon atoms are joined to organic groups” [143]. Organosilicone compounds were first predicted by Dumas in 1840 and in 1857 Buff and Wohler produced trichlorosilane (the first example of an organosilicone). The first silicone polymer, a viscous oil, was developed in 1872 by Ladenburg and was comprised of a siloxane backbone with organic branches off of the silicon atoms. The first commercial grades of silicone elastomers were produced in1943 by the Dow corning corporation, following

work started in 1931 at the corning glass works to develop heat resistant resins as a flexible electrical insulating medium for glass fabrics [144].

Silicone elastomers (SE) are divided into two groups, high temperature vulcanised (HTV), where crosslinking occurs at high temperatures (over 100 ℃), and room temperature vulcanisation (RTV) where crosslinking occurs at room temperature. RTV SEs can be cured by either exposure to water (RTV-1) or the use of a catalyst (RTV-2). This study will explore the performance of the antimicrobial EO blend in both an RTV-2 type SE and the semi-crystalline thermoplastic LLDPE (crystalline melting point (T_m) approximately 120 ℃). This will enable the effect of the relatively high processing temperature of LLDPE on the antimicrobial EO blend to be assessed. RTV-2 SEs can be further divided into two groups, condensation cure systems where a silanol-terminated polydimethylsiloxanes are reacted with an organosilicon cross-linking agent [145], and addition cure systems (used in this study) where two separate polymers are cross-linked using a catalyst (usually platinum or tin based). In addition cure SE systems, the first polymer (part-A) usually contains Si-H groups, while the second polymer the second polymer (part-B) contains Si-$CH{=}CH_2$ groups the catalyst is also present in the part-B polymer (Figure 5.2) [146].

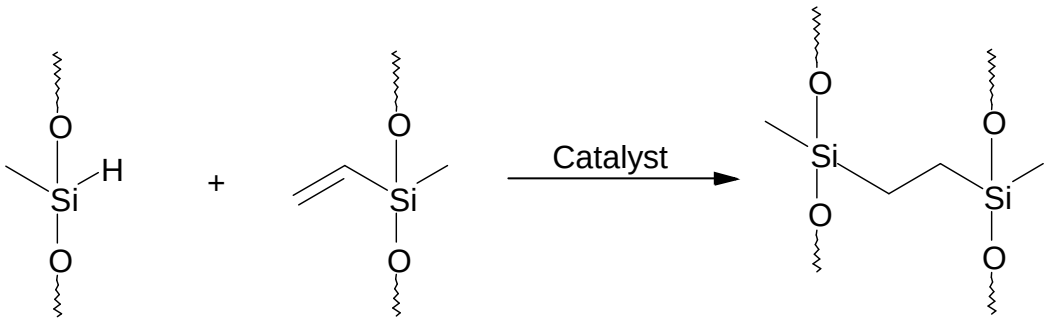

Figure 5.2: Reaction scheme for an RTV-2 SE addition cure system, demonstrating cross linking of polymer chains via a catalyst to create the solid polymer matrix [146].

Silicone elastomers find a wide variety of uses, in particular in medical devices, but also materials such as sealants for use around baths and sinks [145]. Addition of an antimicrobial (such as developed in Section 2.5.2) to the SE in sealants may provide a material which resists the build up of molds.

5.1.3 Solvent based paint

Coating surfaces in healthcare facilities with an antimicrobial paint may help to reduce the number of HCAI by reducing the overall number of bacterial cells present in the healthcare environment; therefore the risk of cross contamination will be reduced. Paints consist of three main parts; pigments, binders and solvents. The binder portion of the paints is the polymer film and is the most important part of the paint: It is responsible for the adhesion of the paint to a surface, as well as having a significant influence on the properties of the paint. Binders are often organic polymers such as acrylics or polyesters but can also be unsaturated oils. Paint solvents are liquids used to dilute the paint binder and are used to adjust the physical properties of the paint such as the rheology and drying characteristics. There are two types of solvent used in paints; water, or organic solvents such as petroleum distillates. In water based paints the organic binder has to be emulsified to enable stable dispersion in the water. This is done using surfactants such as polyoxyethyene alcohol. In solvent based paints the organic binders are miscible with the solvents and therefore there is no need for surfactants to be used.

The antimicrobial EO blend used in this study is an organic material, therefore a solvent based paint was selected for the evaluation of the antimicrobial EO blend in paint films.

5.2 Objectives

- Successfully create a range of antimicrobial polymers via the addition of the previously identified antimicrobial EO blend, either as free oil, or pre-adsorbed onto porous layered silicate reservoir/carriers.
- Provide insight into the effect of pre-adsorption of EO onto layered silicates on the antimicrobial properties of polymers.
- Investigate the release of the EO from polymer materials to determine whether adsorption onto porous layered silicates resulted in controlled release, increased antimicrobial activity.

5.3 Materials

5.3.1 Polymer samples

M511 addition curing maxillofacial Silicone elastomer (SE) (Technovent Limited, Bridgend, UK) was used for production of all SE based samples (Section 5.4.1.1). SE was used as an example of a room temperature processing and room temperature cure polymer in which the potential effects of thermal processing could be eliminated.

Dulux trade High Gloss pure brilliant white (ICI, UK) was used as the base for all paint samples (Section 5.4.1.2)

Linear low density polyethylene (LLDPE) was used as an example of a thermoplastic. The LLDPE used for all samples (Section 5.4.1.3) was Borealis Borstar® FB2230 the physical properties of the LLDPE were; specific gravity 0.923, melting point 124 ℃, melt flow rate 1 g 10 min^{-1} (190 ℃/5.0 Kg).

5.3.2 Culture media

Vide supra 2.3.1.

5.3.3 Microorganisms

Vide supra 2.3.2

5.4 Experimental

5.4.1 Production of antimicrobial polymers via addition of essential oils adsorbed onto layered silicates

Reference samples were prepared via direct incorporation of the most effective antimicrobial EO blend (rosewood and oregano oils) in to a number of different polymer samples. This trial would establish whether or not the antimicrobial activity of the EO could be transferred to the selected polymers. Substrates treated with the antimicrobial EO blend were prepared prior to addition to the polymers by adding the desired substrate (5 g) to heptane (100 ml). The antimicrobial EO blend (2.5 g) was then added to the slurry and stirred. The mixture was left in the draft of a fume cupboard to allow the heptane to evaporate, thereby forcing adsorption of the antimicrobial EO blend on to the substrate, resulting in approximately 33.3 % loading of EO on the substrate.

5.4.1.1 Production of silicone elastomer samples containing EO

Samples of M511 maxillofacial SE, containing no antimicrobial EO blend were prepared as a positive control. Part A (silicone polymer with H groups) (40 g) and Part B (silicone polymer with organic side chains, plus catalyst) (4 g) were added to a vacuum mixing pot. Part B was then folded carefully into part A and then mixed using a pallet knife. The SE mix was then mixed under vacuum using a Multivac® 4 (Degussa AG, Germany) at full vacuum for 30 seconds. After mixing, the SE was allowed to sit for 15 minutes before being poured into a 130 mm x 130 mm x 1mm mould, and spread within the cavity using a pallet knife. The mould was then placed on a vibrating table to bring any air bubbles to the surface, the bubbles were burst with a thin piece of wire. The excess SE was scrapped off so that the surface of the SE was flush to the top of the mould, and the mould was placed on a flat surface for 24 h to allow the SE to cure. After curing the SE sheet was removed from the mould and sealed in a plastic bag.

Using the same basic method SE samples containing: Laponite® RD 50 % OM with 2HT2M (SE+LRD50 2HT2M), Laponite® RD 50 % OM with 2HT2M with

33.3 % EO blend adsorbed (SE+(LRD50 2HT2M+EO)), Laponite® RD 100 % OM with 2HT2M with 33.3 % EO blend adsorbed (SE+(LRD100 2HT2M+EO)), and 3.33 % EO blend were made (SE+EO). The masses of the individual components of the SE are given (Table 5.1).

Table 5.1. Masses required of silicone, substrate and EO to produce the SE samples for antimicrobial and controlled release analysis.

	Silicone part A (g)	Silicone part B (g)	Substrate (g)	Free EO (g)
SE+(LRD50 2HT2M)	27.00	2.70	3.30	N/A
SE+(LRD50 2HT2M+EO)	27.00	2.70	3.30	N/A
SE+(LRD100 2HT2M+EO)	27.00	2.70	3.30	N/A
SE+EO	28.36	3.54	N/A	1.10

For all of the SE samples containing the antimicrobial EO blend the approximate final EO content was 3.33 % (m/m). The SE+EO sample was made using an 8:1 part A to part B ratio as the addition of the EO to a 10:1 mix did not cure completely

5.4.1.2 Production of solvent based paint containing EO

As with the SE samples the test paint samples contained 10 % of the required substrate and approximately 3.33 % EO blend. Paint samples containing Laponite® RD 50 % OM with 2HT2M (Paint+LRD50 2HT2M), Laponite® RD 50 % OM with 2HT2M with 33.3 % EO blend adsorbed (Paint+(LRD50 2HT2M+EO)), Laponite® RD 100 % OM with 2HT2M with 33.3 % EO blend adsorbed (Paint+(LRD100 2HT2M+EO)), and 3.33 % EO blend were made (Paint+EO). The masses for the individual components of the paint samples are given (Table 5.2). After addition of the required components to the paint each sample was mixed thoroughly using a Dispermat® CV using a 40 mm shear

blade at 2000 rpm for 30 min. After mixing the paint samples were transferred to 250 ml airtight bottles for storage.

Table 5.2. Masses of paint, substrate and EO required for each paint formulation for antimicrobial and controlled release testing.

	Paint (g)	Substrate (g)	Free EO (g)
Paint+(LRD50 2HT2M)	210.00	23.33	N/A
Paint+(LRD50 2HT2M+EO)	210.00	23.33	N/A
Paint+(LRD100 2HT2M+EO)	210.00	23.33	N/A
Paint+EO	210.00	N/A	7.31

5.4.1.3 Production of linear low density polyethylene samples containing EO

LLDPE formulations were mixed using a Haake Rheomix 600 mixing chamber (Thermo Scientific, UK) fitted with roller rotors and driven by a Haake Polydrive (Thermo Scientific, UK). Settings were as follows: mixing chamber temperature was 160 ℃, mixing speed 70 rpm and mixing time 6 minutes.

For the pure LLDPE sample the mass of LLDPE required to fill the mixing chamber to 70 % capacity was calculated from the density to be 44.90 g. After mixing, the sample was removed from the mixing chamber and placed between two metal plates, and then hand pressed into a pre-form patty. The sample was compression-moulded using a 130 mm x 130 mm x 1 mm frame mould, at 160 ℃ using an electrically heated hydraulic press. Compression moulding was carried out as follows: the mould plates were pre-heated in the press for 5 minutes. The polymer sample was then placed in the mould and the platens brought up to contact for 2 minutes in order to melt, but not completely squash, the sample. The pressure was increased to 40 tons and held for 2 minutes to

mould the sample. The mould was then transferred to an electric cooling press, set to 15 ℃, and held at maximum pressure until co ol to touch.

For formulations containing added substrates or the antimicrobial EO blend the following modification to the mixing method was made: LLDPE was added to the mixing chamber and mixed for 1.5 minutes to allow the LLDPE to melt. At 1.5 minutes after mixing started the material to be added was introduced to the mixing chamber, the polymer formulation was then allowed to mix for a further 4.5 minutes.

The following LLDPE formulations were made for testing using the method described above, LLDPE containing: Laponite® RD 50 % OM with 2HT2M (LLDPE+LRD50 2HT2M), Laponite® RD 50 % OM with 2HT2M with 33.3 % EO blend adsorbed (LLDPE+(LRD50 2HT2M+EO)), Laponite® RD 100 % OM with 2HT2M with 33.3 % EO blend adsorbed (LLDPE+(LRD100 2HT2M+EO)), and 3.33 % EO free within polymer (LLDPE+EO) Formulations containing the substrates all had a 10 % (m/m) substrate loading, resulting in a final oil loading of 3.33 % (m/m).

The masses of polymer, substrate and free EO for each formulation are given (Table 5.3).

Table 5.3: Required masses of LLDPE, substrate and EO for each polymer formulation used in the antimicrobial assays, and controlled release studies.

	LLDPE (g)	Substrate (g)	Free EO (g)
LLDPE+(LRD50 2HT2M)	40.41	4.49	N/A
LLDPE+(LRD50 2HT2M+EO)	40.41	4.49	N/A
LLDPE+(LRD100 2HT2M+EO)	40.41	4.49	N/A
LLDPE+EO	43.40	N/A	1.50

5.4.2 Antimicrobial testing of polymer samples

In order to test the antimicrobial efficacy of the polymer samples described in Section 5.4.1, a novel method was developed.

For the SE and LLDPE based samples, 1 cm x 1 cm plaques of the polymer material were cut out. For the paint samples, 0.2 mm thick, 1 cm x 1cm 304 stainless steel (2b finish) supports were cut out. The sample to be tested was then painted directly onto the support such that the average dried and conditioned coating thickness was 70 µm. The conditioning process proceeded as follows: after allowing the paint to dry, the samples were left for 72 hours to allow residual solvent to evaporate and then placed in a 1 % (m/v) solution of washing up liquid (C4 concentrated hand wash detergent, Jeyes Professional) for 48 hours (in order to leach out cobalt carboxylate present in the paint) in preparation for testing. The extended drying time was used as it was found that if the paint was tested with the minimum drying time required no bacteria would survive on the positive controls. The latter process was carried out as even after allowing the residual solvent to evaporate out, the test bacteria still did not survive on the positive controls. It was theorised that the cobalt was responsible for the inherent antimicrobial activity.

The polymer plaques were disinfected by dipping into 70 % ethanol and then passing through a blue Bunsen flame. After being placed in a sterile Petri dish, each plaque was inoculated with 100 µl of an overnight broth culture adjusted to 10^7 CFU, so that there were 10^6 CFU on the surface of the plaque. The plaques were then placed in a drying cabinet at 40 ℃ to dry the bacterial suspension onto the surface. Immediately after drying (Time 0) plaques of each of the polymer samples being tested were transferred into sterile universals containing 10 ml peptone water with 0.5 % tween 20 added. Each universal was vortexed for 1 min to transfer the bacterial cells from the polymer surface to the peptone water. Using a Whitley Automated Spiral Plater (Don Whitley Scientific, UK) (set to deposit 50 µl per plate), the cell suspension extracted from the plaque into each universal was plated onto 2 agar plates (nutrient agar for MRSA, Columbia blood agar for *A. baumannii*) and the plates were incubated at 37 ℃ for 24 h to allow any viable bacterial cells to grow. After incubation the spiral agar plates were read using a Synbiosis aCOLyte plate reader. The number of colonies on the agar plate was used to back calculate the number of viable cells that were

on the surface of the polymer plaque. Comparing this to the known initial number of viable cells (10^6) inoculated onto the surface allowed a quantitative measure of the level of cell death caused by the polymer sample. Further samples were taken at 2, 6, and 24 h after the drying phase.
Each experiment was carried out in triplicate and positive (bacterial suspension placed onto pure polymer) and negative (100 µl sterile nutrient broth placed onto polymer samples) controls were used.

Testing was undertaken for MRSA and *A. baumannii* on pure Silicone elastomer, SE+LRD50 2HT2M, SE+(LRD50 2HT2M+EO), SE+(LRD100 2HT2M+EO), SE+EO, pure LLDPE, LLDPE+LRD50 2HT2M, LLDPE+(LRD50 2HT2M+EO), LLDPE+(LRD100 2HT2M+EO), and LLDPE +EO samples.
MRSA was also tested on pure paint, paint+LRD50 2HT2M, paint+(LRD50 2HT2M+EO), paint+(LRD100 2HT2M+EO), and paint+EO samples.

Antimicrobial testing was carried out in triplicate, with each of the three replicates sampled twice for the number of viable bacterial cells. Reported values were the mean of the 6 values obtained for each replicate. Where statistical analysis was required a Student's T test was carried out using Minitab (Minitab, Inc. Pennsylvania).

5.4.3 Controlled release of essential oils from polymer samples

In order to monitor the release of the antimicrobial EO blend from the polymer samples 1 cm^2 polymer samples were made in the same way as described in Section 5.4.2 for the pure polymer, polymer plus antimicrobial EO blend, polymer plus Laponite® RD 50 % 2HT2M, and polymer plus Laponite® RD 50 % 2HT2M with antimicrobial EO blend. Individual plaques for each polymer sample were placed in headspace vials (20 ml) (Crawford Scientific, UK) and the vials were sealed. Hexane (10 µl) (HPLC grade >99.9 % Sigma Aldrich, UK) was then added to each vial using a chromatography syringe for use as an internal standard. The vials were then sampled using a PerkinElmer HS 40 headspace auto sampler (Perkin Elmer, UK) connected to a Hewlett Packard 6890 GC (Agilent, UK) with a 5973 MSD (Agilent, UK). The head space conditions were as follows; Vial temperature 100 ℃, loop temperature 140 ℃,

transfer line temperature 150 ℃, vial equilibration time 15 min, vial pressurisation time 0.20 min, loop fill time 0.20 min, loop equilibration time 0.05 min, inject time 1 min, vial pressure 19 psi and carrier flow pressure 8 psi. The GC temperature programme was 60 to 210 ℃ at 5 ℃ min^{-1}, with a split of 1 ml min^{-1}, injector port temperature 275 ℃, and detector temperature 250 ℃. Samples were run in triplicate, and an average value taken.

Plaques of the polymer were placed in an oven at 50 ℃ in order to accelerate loss of the antimicrobial EO blend held within the polymer. At time periods of 1, 2, 4 and 8 days, samples were removed from the oven, sealed in headspace vials and analysed using the above method.

In order to determine the level of controlled release of the antimicrobial EO blend from the polymers, the EO peaks which showed up after the headspace analysis of the initial samples that had not been aged at 50 ℃ were ratioed against the hexane internal standard peak. By comparing these peak ratios to the ratios of the same peaks from the heat aged samples it allowed determination of how long the polymer samples were retaining the antimicrobial EO blend and therefore get a measure of the degree of control of EO release from the polymer was calculated.

In cases where the EO molecules were present in both samples containing free EO and samples containing EO adsorbed to a substrate student's t-tests were carried out to determine if the difference in the level of molecules retained was significant.

Controlled release studies were carried out in triplicate, the reported values for each molecule were taken as the mean of the three replicates. Student's t testing was used to determine the statistical significances of the difference in level of the individual molecules at each time period.

5.5 Results and discussions

5.5.1 Assessment of polymer samples after addition of EO

As described in Section 5.4.1 three different types of polymer were treated with the antimicrobial EO blend (oregano oil and rosewood oil) as an oil, and the antimicrobial EO blend adsorbed onto layered silicate substrates. Following the adsorption studies Laponite® RD 50 % CEC 2HT2M was selected as the substrate for adsorption of the antimicrobial EO blend. As a comparison samples were also made where the EO had been adsorbed onto Laponite® RD 100 % CEC 2HT2M. The oil blend was preprepared at a ratio of 3:1 oregano to rosewood as this was the blend that showed best activity in the antimicrobial testing (Section 2.5.2).

5.5.1.1 Physical properties of silicone elastomer samples containing EO

The addition of the Laponite® RD to the SE presented a number of challenges. First it was found that when the Laponite® RD was added it resulted in the evolution of bubbles in the SE material. The SE samples were originally placed in a mould between two plates and pressed using a screw press during the curing process in order to ensure smooth surfaces and accurate width of sample (1 mm). The bubbles evolved from the addition of Laponite® RD to the SE were trapped within the SE due to the pressure and this resulted in a material with a high number of defects.

It was proposed that the bubbles were either nucleated by the layered silicate, or as a result of the polymer displacing gas adsorbed to the LRD surface. Therefore, heating the mixture of silicone part A and layered silicate, before adding the catalyst, may have reduced the number of bubbles formed. Whilst heating did reduce the number of defects, there were still too many to allow the SE pieces to be used. Furthermore, the heat could also drive off some of the EO from the SE samples containing the layered silicate with oil adsorbed. Because of this and the fact that there were still a high number of bubbles it was decided that heating the mixture before adding the catalyst would not be useful.

As the bubbles were being trapped within the SE by the pressure exerted by the mould plates, it was proposed that by not using the top mould plate and not applying pressure the bubbles may be allowed to leave the SE as it cured resulting in fewer defects. In order to achieve a uniform thickness and flat surface this required the removal of excess SE from the mould. This was done by carefully dragging a thin metal plate across the surface of the mould containing the SE, so that the depth of SE in the mould was approximately 1 mm. Once the excess SE had been removed the mould was covered and the SE was allowed to cure. This process enabled useable SE test pieces to be made.

Addition of the OM modified Laponite® RD without adsorbed EO resulted in SE pieces with a relatively good distribution of layered silicate particles. Addition of OM Laponite® RD with adsorbed EO however, resulted in macroscopically visible agglomerates of layered silicate particles, which introduced defects into the sample. This may not unduly compromise antimicrobial performance, but the agglomeration would have to be reduced if the SE were to be used in industry. The SE elastomer samples were cut into 10 mm x 10 mm squares for use in the antimicrobial assays

5.5.1.2 Solvent based paint containing EO either free within the matrix or adsorbed to a substrate

A solvent based paint was selected as a matrix for the antimicrobial EO blend and antimicrobial EO blend loaded layered silicates. For this proof of concept study, water based paint was avoided due to miscibility related concerns, which would be particularly applicable to the control sample in which the antimicrobial EO blend was directly added. The paint used was Dulux Trade high gloss, purchased of the self from B&Q, UK. After thorough mixing (see Section 5.4.1.2) all, of the OM layered silicate samples dispersed well within the paint used. There were no visible agglomerates in the paint even when painted in thin layers onto a substrate.

5.5.1.3 Physical properties of linear low density polyethylene samples containing EO

LLDPE samples were prepared containing either Laponite® RD + 50 % 2HT2M (LLDPE+LRD50), Laponite® RD + 100 % 2HT2M (LLDPE+LRD100), Laponite® RD + 50 % 2HT2M with EO adsorbed (LLDPE+(LRD50+EO)) or Laponite® RD + 100 % 2HT2M with EO adsorbed (LLDPE+(LRD100+EO)).

The LLDPE+LRD50 had a good dispersion of the Laponite® through the polymer matrix with no visible aggregates within the sample. In comparison the LRD100 was not so well distributed through the matrix with visible aggregation in the polymer sample. Both of the LLDPE samples containing the EO loaded Laponite® exhibited a brown discolouration due to the presence of the EO. There were a greater number of aggregates visible in both the samples containing EO loaded Laponite® compared to the LLDPE containing just Laponite®.

The LLDPE – layered silicate interactions were investigated in order to determine the effect of increasing the level of OM, and the how addition of the antimicrobial EO blend affected the stiffness of the materials. The stiffness of the polymer samples was compared using flexural modulus, determined via a three point bending test using a Hounsfield H10KS tensometer manufactured by Hounsfield Test Equipment Co. The stiffness of the LLDPE based samples provided some insight into both the state of dispersion of the Laponite® platelets and the interaction between the Laponite® platelets and the polymer matrix. Differences in stiffness were taken to be significant if the standard deviation error bars did not overlap. In general, addition of layered silicate type materials resulted in an increase in stiffness. This was due to constraint of the matrix provided by the interface between the layered silicate and the polymer [147]. The flexural modulus data for the LLDPE samples is given below (Figure 5.3).

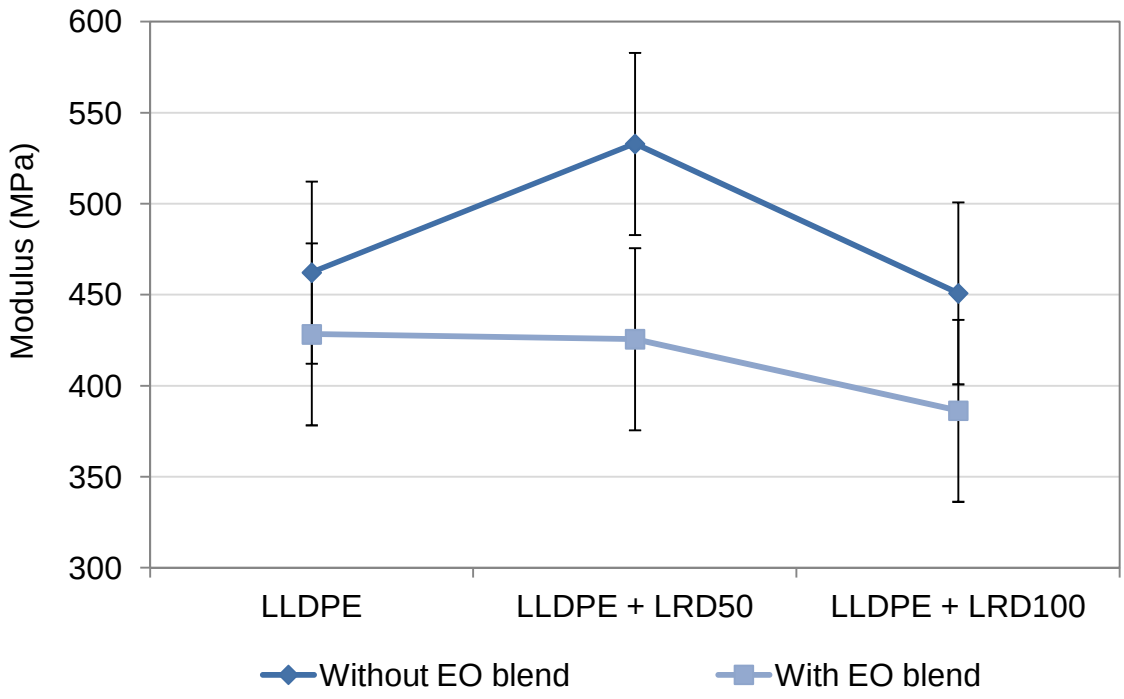

Figure 5.3: Flexural test data for LLDPE samples ahowing the affect of addition of organically modified LRD with and without EO on flexural modulus. Demonstrating the increased stiffness of the LLDPE as a result of organic modification; explained by the increased interaction between the LRD platelets and the polymer matrix.

Addition of the antimicrobial EO blend to the LLDPE resulted in a reduction in the stiffness. This may be explained by plasticization of the amorphous regions by the antimicrobial EO blend. Pre-adsorption of the antimicrobial EO blend onto Laponite® RD 50 % (to give EO-LRD50) led to a reduction in stiffness relative to when the antimicrobial EO blend was absent. This is most probably due to poor dispersion of the EO-LRD50 (aggregates were visible to the naked eye), though the adsorption of the EO may have led to reduced aggregate / matrix interaction. Additionally, the plasticising effect of the EO molecules on the amorphous regions of the LLDPE would further reduce stiffness. In studies of SE/organically modified montmorillonite (o-MMT)/triclosan ternary composite systems studied by Liauw [98], a reduction in composite stiffness was related by WAXS data to re-aggregation of the o-MMT platelets in to uniformly spaced tactoids. The latter effect arose due to enhanced self-assembly of quat alkyl tails caused by co-intercalation of the galleries by triclosan molecules. A similar effect maybe in operation here, though due to the lower CEC of the LRD, and

lower aspect ratio of the LRD platelets, together with non-homogeneous dispersion of platelets / aggregates, the WAXS data (see next paragraph) was not particularly revealing. Addition of EO-LRD100 led to a further reduction in stiffness relative to EO-LRD50 for the same reasons though the effect was enhanced due to the increased levels of quat and EO. While the addition of the EO antimicrobial did cause a reduction in stiffness it was only significant in the case of the EO antimicrobial first being adsorbed onto LRD50. This indicates that there was no negative effect on the LLDPE stiffness as a result of the addition of the various different formulations.

Wide angle X-ray scattering (WAXS) was carried out on LRD50 and LRD100, both alone and loaded with the antimicrobial EO blend (Figures 5.4 and 5.5 respectively). WAXS data LLDPE based composites containing the latter were also obtained in order to determine the effect of the polymer and melt processing on the dispersion of the LRD platelets.

For unmodified LRD the (001) reflection occurred at 6.8°. After 50 % OM the (001) reflection shifted to a lower angle (5.7°) which reflected a small increase in the average interlayer spacing to 0.61 nm. Adsorption of EO onto LRD50 resulted in a shift in the (001) reflection to 5.2° indicating that the oil molecules entering the galleries had the effect of forcing the platelets further apart and increasing the interlayer spacing to 0.76 nm. OM also resulted in a broadening of the (110) reflection at 20°. This was indicative of increasing randomisation of orientation of LRD platelets within aggregates. The broadening of the (110) reflection increased with EO adsorption adding further evidence for the adsorption of the EO resulting in an increased interlayer space and a change in the dispersion of LRD platelets within aggregates.

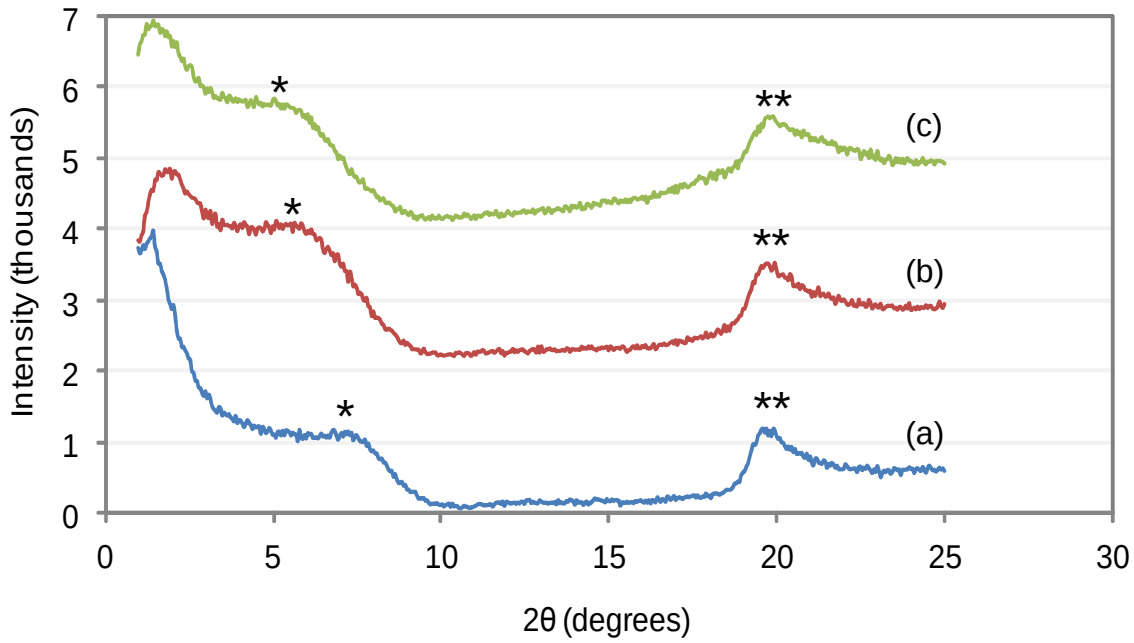

Figure 5.4: WAXS data for (a) LRD, (b) LRD50, and (c) EO-LRD50. Showing the effect of OM and EO adsorption on the position and shape of the (001) reflection (*) and (110) reflection (**). Demonstrating the increased d-spacing as a result of organic modification, resulting in the (001) reflection shifting to lower angles.

WAXS data for the LRD100 based powders displayed the same general pattern as seen with the LRD50 powder series; the (001) reflections were shifted to lower angle and broadening of the (110) reflection was observed. Due to the higher level of quat in LRD100, the (001) reflection occurred at 5.1°, relative to 5.7° for LRD50. Considering the low CEC of LRD, the increase in layer spacing was not expected to be significant as the alkyl tails of the quat were likely to be lying flat against the platelets at both quat levels. Addition of the antimicrobial EO blend to LRD100 made little difference the interlayer spacing with the (001) reflection occurring at 5.0° for EO-LRD100. A similar figure (5.2°) was obtained for EO-LRD50. However, in EO-LRD100 an intense and well defined peak was evident at 2.4° which corresponded to an (001) spacing of 3.68 nm, and an interlayer spacing of 2.74 nm. This may indicate that a fraction of the platelets had been co-intercalated with the EO to the extent that the quat alkyl chains were no longer laying on the basal surface and were angled away from it.

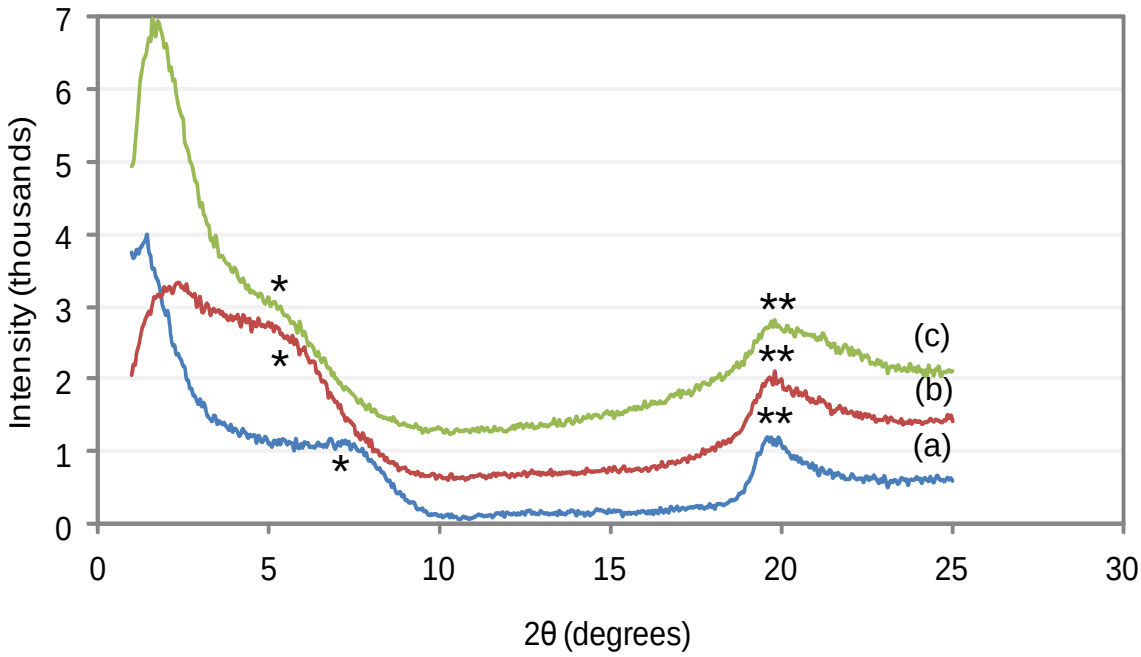

Figure 5.5: WAXS data for (a) LRD, (b) LRD100, and (c) EO-LRD100. Showing the effect of OM and EO adsorption on the position and shape of the (001) reflection (*) and (110) reflection (**). Demonstrating the increase in d-spacing of LRD with organic modification, and the further increase as a result of EO adsorption, as the (001) reflection shifts to lower angles.

The WAXS data for the LLDPE samples containing Laponite® RD are shown (Figure 5.6). Comparison of the (001) reflections of the Laponite® samples before and after addition to LLDPE gave information as to how the polymer and substrate were interacting. It should be noted from the outset that the reflection peak at 2θ = 4.3° observed in all the samples (including the LLDPE (unfilled) with antimicrobial EO blend) was an artefact that is also present in LLDPE. The origin of the latter is not yet known.

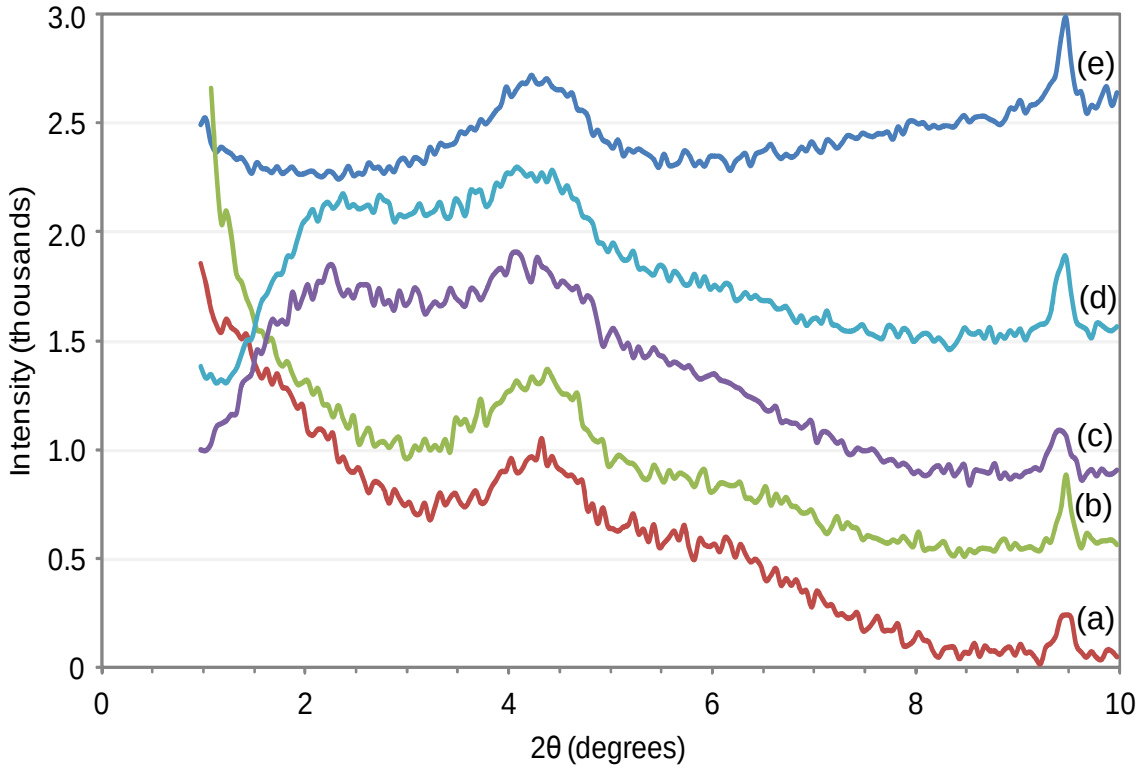

Figure 5.6: WAXS data for LLDPE based composites containing 10 % (m/m) of (a) LRD50, (b) LRD50+EO, (c) LRD100, (d) LRD100+EO, (e) 3.3 % (m/m) EO. Demonstrating the increased d-spacing of the Laponite® as a result of interaction with the polymer matrix.

Addition of the LRD samples to LLDPE resulted in the (001) reflection shifting to lower angles than for the Laponite® RD samples before addition. For LLDPE/LRD50 there was no distinctive (001) relection due to there being a very random/broad distribution of layer spacings, some of which were likely to be too large for the instrument to measure. This indicates a high level of intercalation of LRD50 by the LLDPE, and may have led to the relatively high stiffness of this composite (Figure 5.3). Addition of the antimicrobial EO blend to LRD50 (to give EO-LRD50) resulted in similar WAXS data to LLDPE/LRD50, though the intensity of the data at 2° and 6° was somewhat low er, and the count intensity as 1° was approached, was higher in LLDPE/EO-LRD50. These subtle changes may be indicative of increased exfoliation when the antimicrobial EO blend is present, however the composite stiffness data does not support this proposition. Perhaps poor macro-dispersion, plasticization of the amorphous regions by the EO and reduction in filler-matrix interaction, are dominant factors leading to reduced composite stiffness.

At low angles the two LRD100 based composites gave very different WAXS data to the equivalent LRD50 based composites. In the latter case the counts increased at 1° was approached whilst in the former case (for composites based on LRD100) the data was on a downward trend, forming the base of a reflection peak at approximately 2° (giving an aver age interlayer spacing of 2.74 nm for LRD100 and 4.1 nm for EO-LRD100). This observation may be interpreted as there being more widely spaced (possibly exfoliated) platelets in the LRD50 based composites than in those based on LRD100. It should be noted that both LRD100 and particularly EO-LRD100 were not as well dispersed in the LLDPE as the two 50 % OM LRD powders. The EO-LRD100 based composite showed a slightly narrower band of reflection peaks over the range 1° to 8°, indicating that addition of the EO led to slight narrowing of the distribution of layer spacings. The latter could be due to co-intercalation of the LRD100 by the antimicrobial EO blend that may have resulted in more effective interaction between quat alkyl chains on opposing platelets. Similar observations made by Liauw *et al*. (2011) in SE/o-MMT/triclosan ternary systems [98], have been reviewed previously. In these cases co-intercalation of the o-MMT with triclosan in SE led to high levels of ordering of layer spacing to the extent that multiple higher order reflections became evident. Such dramatic effects were not obtained in the LLDPE/OM-LRD/antimicrobial EO blend systems examined here due the different morphology of LRD and that EOs consist of mixtures of molecules.

5.5.2 Antimicrobial testing of polymer samples

The three different polymer samples were tested over a 24 hour period for their antimicrobial efficacy, with samples taken at time periods of 0, 2 6 and 24 hours. The intended use of the materials was to maintain a low bacterial load between regular cleaning. Therefore, rapid kill of cells (high cell death at 0 and 2 hours) coming into contact with the polymers would be a desirable characteristic. The assay time was extended to 24 h to provide more detailed information on how the materials functioned, but prolonged activity over this period was not a necessity.

The testing of the antimicrobial efficacy of the polymer samples containing EO provided significant methodology challenges. Initially disc diffusion tests were attempted by placing 5 mm diameter discs cut from the polymer samples onto agar plates that had 1 ml of 10^6 CFU per ml bacterial suspension spread over it in a lawn. After incubation it was expected that zones of inhibition would be visible on the agar around the polymer discs where the EO had inhibited the growth of the bacteria. However, no zones of inhibition were observed. This could be due to two factors: either the EO in the polymer was not at high enough concentration to inhibit growth, or the EO was unable to diffuse from the polymer sufficiently. To assess the reason for the lack of zone of inhibition 5 mm diameter filter discs had a drop of the undiluted antimicrobial EO blend added onto them. The discs were then placed on a bacterial lawn as with the polymer discs. After incubation there were no zones of inhibition visible around the filter paper discs. As the EO was at a concentration above that required for inhibition, and the EO would be able to diffuse out of the filter paper, it was concluded that the lack of inhibition was due to the EO molecules not being able to diffuse through the agar. Therefore a zone of inhibition approach was not suitable for assessment of the antimicrobial efficacy of the polymer samples.

The next method attempted was to take five 1 cm x 1 cm plaques of the polymer samples and add them to 10 ml of nutrient broth containing 0.5 % tween 20 in a sterile 25 ml universal bottle. The tween 20 acts as an emulsifying agent helping the EO molecules to diffuse through the broth. To this 100 µl of bacterial suspension at 10^8 CFU per ml was added, and the universal was incubated. If the polymer samples had been effective at inhibiting growth then the universals with EO treated polymers should have fewer bacterial cells after incubation than the positive controls. After incubation, it was found that all the universals containing EO polymers had the same level of growth as the positive controls. Therefore it was concluded that this method was also unsuitable for assessment of antimicrobial efficacy of the polymers.

It was proposed that the bacterial cells would have to be in direct contact with the polymer samples for a true reflection of antimicrobial efficacy to be obtained. The method described in Section 5.4.2 was developed in order to satisfy this criterion. Initially the test method was going to be run by adding a 100 µl drop of

bacterial suspension to the surface of the polymer plaques and then leaving the sample for set time periods before washing the bacterial suspension into peptone water and testing for viable bacterial cells. However, the SE samples stuck to the bottom of Petri dishes, so that when it came to place them into peptone water they had to be peeled off of the surface. During the process of removing the SE samples from the Petri dish the bacterial suspension ran off the surface preventing analysis. Drying the bacterial suspension on to the surface of the polymer solved this problem. However it would be important to ensure that the drying process did not kill the bacterial cells rather than the EO in the polymer. The latter was verified by taking SE plaques, which contained no EO, and adding bacterial suspension (100 µl, 10^7 CFU per ml) to the surface which was then dried on for 90 minutes at 40 ℃. After drying the plaques were vortex mixed in 10 ml peptone water containing 0.5 % tween 20 to remove the attached cells. The peptone water was then plated on agar to determine whether the bacteria had survived the drying process. It was found that 95 % of the bacteria that had been added to the polymer could be successfully retrieved after drying and grown on agar for *Acinetobacter baumannii* and methicillin resistant *Staphylococcus aureus* (MRSA). However with *Pseudomonas aeruginosa* no viable cells could be recovered from the surface of the polymers. It was proposed that the temperature used to dry the *P. aeruginosa* cells onto the surface of the polymers may have caused cell death. In an attempt to avoid this, the conditions were modified. Ten microlitres of 10^8 CFU per ml bacterial suspension was inoculated onto the polymer plaque which was incubated at 30 ℃ for 1 hr. At the reduced temperature it was found that no viable *P. aeruginosa* cells could be recovered from the plaque. Therefore it is likely that the process of drying was responsible for the cell death thus the method would not be suitable for testing the antimicrobial efficacy of the polymer materials against *P. aeruginosa*. Thus the method developed was used only with *A. baumannii* and MRSA.

5.5.2.1 Assessment of antimicrobial activity of silicone elastomer samples containg EO

All of the SE samples that contained EO displayed antimicrobial activity against MRSA (Figure 5.7) and *A. baumannii* (Figure 5.8).

Immediately after the drying process was completed (time = 0) the plaques containing EO all showed at least a 3 log reduction in the number of viable bacterial cells on the surface compared to the pure SE sample. The SE sample containing only LRD50 and no EO also exhibited strong antimicrobial activity initially. Quaternary ammonium compounds (quats) such as 2HT2M have been shown to have antimicrobial activity [148-150], thus it is likely that the antimicrobial activity is a result of the 2HT2M within the SE. No other tests displayed such a strong antimicrobial activity for the polymer samples containing 2HT2M only, and at 6 and 24 h. The SE samples containing 2HT2M did not exhibit antimicrobial activity against MRSA. This indicates that there may have been some unbound quat available in the samples at 0 and 2 h which had an effect on the growth of the MRSA. It is therefore unlikely that in general the polymer samples with no EO and just Laponite® RD with 2HT2M would provide significant antimicrobial activity.

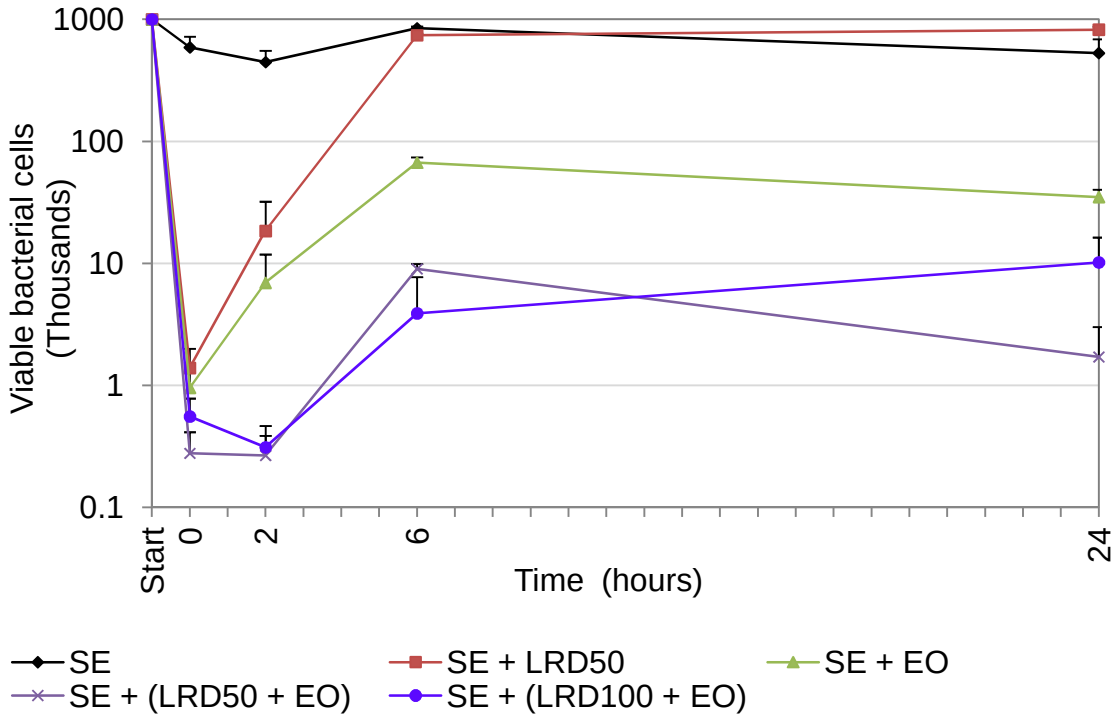

Figure 5.7: Antimicrobial testing of SE against MRSA, demonstrating the successful conferment of antimicrobial activity to the SE after addition of the EO antimicrobial. The graph also highlights the increased efficacy obtained by adsorbing the EO onto LRD. LRD50 = Laponite® RD 50 % CEC 2HT2M, LRD50 + EO = Laponite® RD 50 % CEC 2HT2M with EO blend adsorbed, LRD100 + EO = Laponite® RD 100 % CEC 2HT2M with EO blend adsorbed.

The three SE samples containing EO gave similar levels of performance initially (after the drying phase), with the antimicrobial EO blend achieving a 3 log reduction and the EO adsorbed onto Laponite® RD 50 % 2HT2M achieving a 3.5 log reduction (highest level of antimicrobial activity). With increasing time the difference in antimicrobial of the EO polymer samples became clear. Over the course of the 24 h the number of viable bacterial cells increased from the initial level observed after drying. This is possibly because as the cells were dried onto the surface they would have stacked on each other resulting in a number of the cells not being in contact with the surface. The cells at the bottom of the stack will have been killed by the EO in the polymer resulting in the reduction at time = 0. Cells which were towards the top of stacks may have been far enough away from the polymer surface to not be affected by the EO. Over the 24 h they could then have slowly replicated resulting in the observed

increase in viable bacterial cells. Alternatively, if the surface was having a bacteriostatic effect at the early time periods the cells may be in shock and unable to grow when plated. As time increased the cells would overcome the shock and be able to grow, giving the appearance of increased numbers of viable cells on the polymer samples. Scanning electron microscopy (SEM) images of polymer samples, which have not had the bacterial cells washed off, may provide information as to what is happening to the cells and why they are increasing over the 24 h after an initial reduction. If the action of the surfaces is bacteriostatic then the cells would be intact when viewed using SEM. If the action of the surfaces was bactericidal then the cells would show visible signs of damage and structural disintegration.

The increase in viable bacterial cells over 24 h was greater for the SE containing EO only (approximately 1.5 log increase compared to > 1 log increase at 24 h for SE + (LRD 50 + EO)). This was due to fewer cells being killed initially and therefore there being more cells able to multiply. Between 6 and 24 h, there was a drop in viable bacterial cells for SE + EO (approximately 90 %) and SE + (LRD 50 + EO) (approximately 98 %). This indicated that the EO molecules were desorbing from the polymer and coming into contact with the cells held away from the polymer surface resulting in death of the MRSA cells. The lower antimicrobial effect observed for the SE + EO sample is likely to be as a result of EO molecules being lost more rapidly from the material. The curing process of the SE took 24 hours and during this time the SE samples were open to the air. Adsorption of the EO molecules onto the LRD would have resulted in less molecules being able to evaporate from the SE during the curing time thus explaining the greater antimicrobial activity.

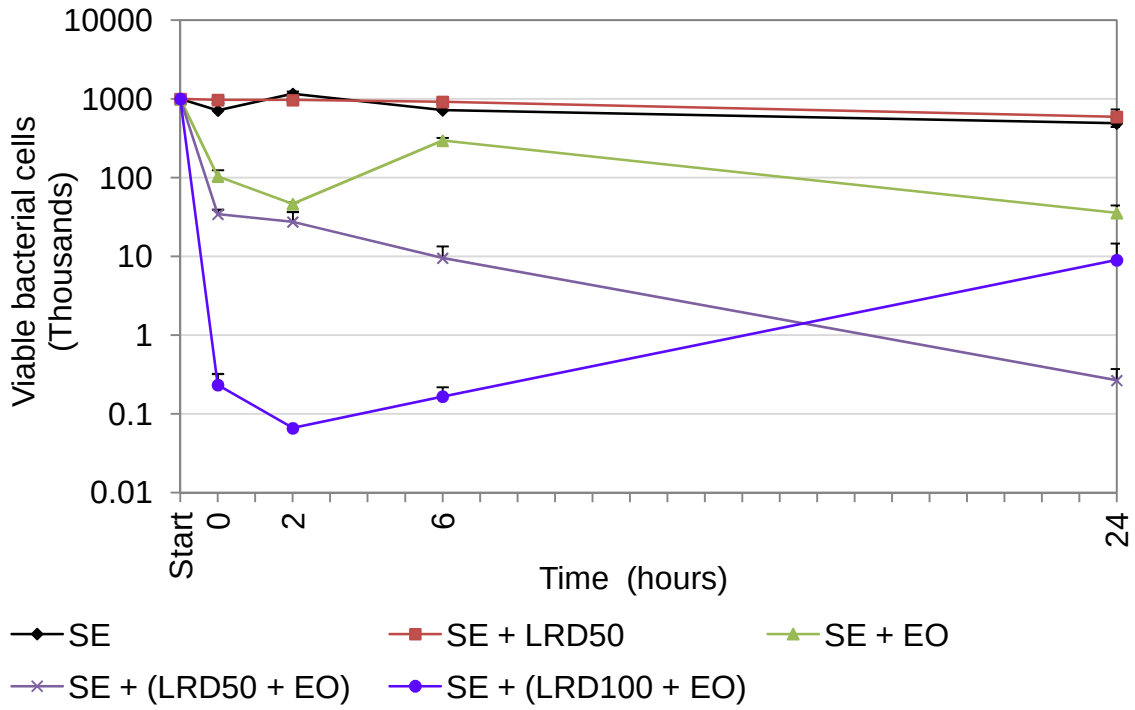

Figure 5.8: Antimicrobial testing of SE against *A. baumannii*. LRD50 = Laponite® RD 50 % CEC 2HT2M, LRD50 + EO = Laponite® RD 50 % CEC 2HT2M with EO blend adsorbed, LRD100 + EO = Laponite® RD 100 % CEC 2HT2M with EO blend adsorbed. Demonstrating the antimicrobial effect of adding EO's to SE, and the improvement in efficacy obtained by adsorbing the EO's onto an organically modified substrate prior to addition.

As with the MRSA test, all three SE samples containing EO caused a reduction in the number of *A. baumannii* viable bacterial cells immediately after the drying phase (time = 0) (Figure 5.8). The SE + (EO-LRD100) significantly outperformed the SE + (EO-LRD50) and the SE + EO samples. Over the 24 h test period the SE + (EO-LRD50) exhibited a steady decline in the number of viable bacterial cells. This indicates that enough of the EO was able to desorb out of the sample at a high enough rate to prevent the cells stacked away from the surface from multiplying. The SE + (EO-LRD100) resulted in stable numbers of viable bacterial cells for the first 6 h then there was approximately a 2 log increase between 6 and 24 h indicating that the EO was too strongly adsorbed into the LRD to allow sufficient EO molecules to desorb out of the SE and kill the cells which had stacked away from the surface.

From the SE results, it is clear that there is a benefit to adsorbing the EO onto LRD before addition to polymers. Against MRSA the greatest benefit was seen for the SE + (EO-LRD50) composite. Against *A. baumannii* SE + (EO-LRD100) gave the greatest benefit initially, but despite the SE + (EO-LRD50) giving low initial antimicrobial it resulted in a more sustained level of antimicrobial activity. Freely added EO is likely to exist within the polymer as a dispersed phase; possibly spherical inclusions with ligaments of material in between that will be effectively untreated. These ligaments may have reduced antimicrobial activity in comparison to the areas with high EO concentration, and the bacteria would have a greater chance of survival in these regions. The adsorption of the EO onto the OM LRD helped to improve the distribution of the EO through the polymer; with a more uniform distribution, the bacterial cells are more likely to come into contact with EO molecules and be inhibited or killed. This may explain the increased antimicrobial activity of the samples containing pre adsorbed EO as it was likely that the EO would be more evenly distributed throughout the polymer increasing the likely hood of the bacterial cells coming into contact with the EO. It was likely that the adsorption of the EO onto LRD prevents the EO molecules evaporating during the processing of the SE, resulting in a higher concentration of EO in the SE samples with the adsorbed EO than the SE +EO samples.

5.5.2.2 Assessment of antimicrobial activity of paint samples containing EO

The antimicrobial assays on the EO treated paints provided a significant challenge. Initially the painted samples were tested for antimicrobial efficacy immediately after the paint had been allowed to dry. These initial tests resulted in no viable bacterial cells being recovered from any samples including the positive controls. It was apparent that the paint itself had a level of antimicrobial activity. This was initially thought to be due to residual solvent remaining within the paint that was driven out by the heat of the drying process and had an inhibitory effect on the bacterial cells. To ensure that all residual solvent was removed from the paint before antimicrobial testing the painted plaques were left for 72 h after drying. However again no bacteria could be recovered from the positive controls, indicating that the solvent in the paint was not necessarily the cause of the lack of viable cells. The Dulux trade high gloss paint used contains cobalt carboxylate, which is used as a drying agent in paints [151]. Cobalt has been shown to posses antimicrobial properties [152, 153] and therefore it was possible that the cobalt present in the paint was responsible for the lack of viable bacterial cells on the surface of the paint. To test this, plaques which had been painted, allowed to dry and left for 72 h to allow the solvent to evaporate were then placed in a 1 % solution of washing up liquid in water for 48 hours to allow the cobalt carboxylate to leach out of the paint. After this period the plaques were allowed to dry and were then inoculated with MRSA bacterial culture as described above. For positive control samples around 95 % of the bacteria initially dried onto the surface of the paint could be recovered, enabling the antimicrobial assays to be run.

The results for MRSA antimicrobial assay on the paint samples showed successful conferment of the EO blend antimicrobial properties to the polymer (Figure 5.9).

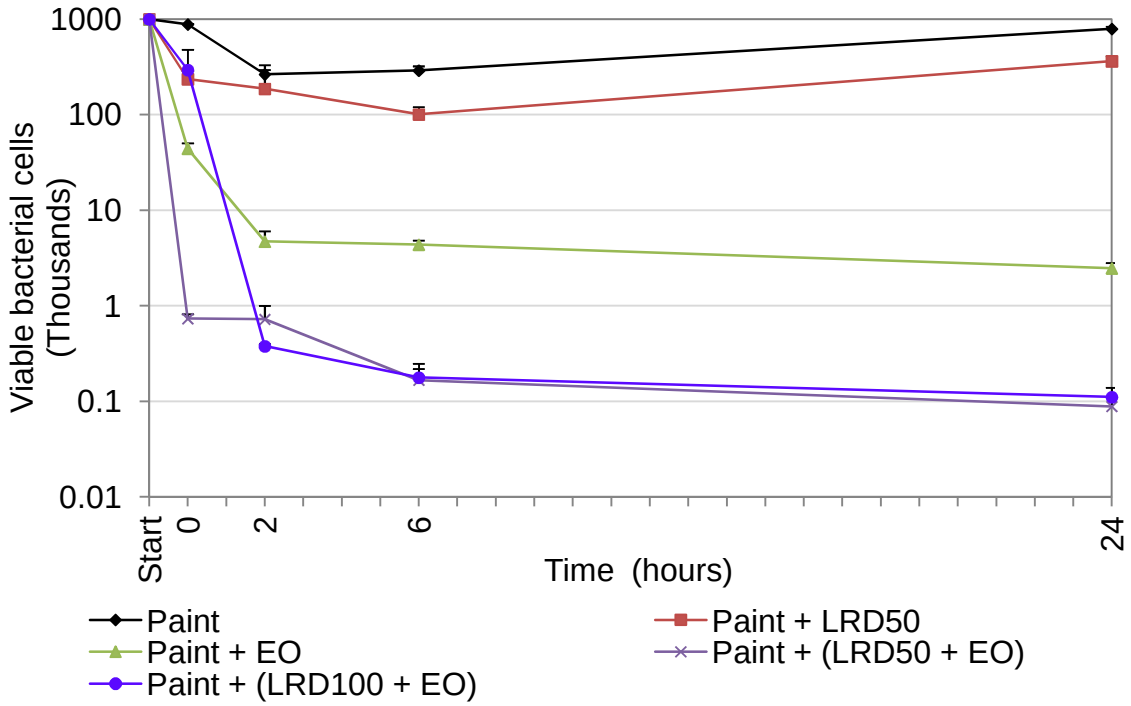

Figure 5.9: Antimicrobial testing of paint samples against MRSA. LRD50 = Laponite® RD 50 % CEC 2HT2M, LRD50 + EO = Laponite® RD 50 % CEC 2HT2M with EO blend adsorbed, LRD100 + EO = Laponite® RD 100 % CEC 2HT2M with EO blend adsorbed.

As with the SE samples all of the paint samples that contained EO showed high levels of antimicrobial activity. At t = 0, paint + (LRD50 + EO) caused approximately 2.5 log reduction compared to the positive controls, with paint + EO causing a 1 log reduction. At t = 0 paint + (LRD100 + EO) did not exhibit any reduction in viable bacterial cells compared to the positive controls, indicating that the high organophilic nature of the OM Laponite® may be resulting in the EO molecules being more strongly bound to the MMT than in the paint + (LRD50 + EO) sample, restricting the amount of EO available at the surface of the paint. At t = 2h the paint + EO samples had cause a further 1 log reduction in the number of viable bacterial cells indicating that more of the EO had been released from the paint and affected the MRSA cells. The paint + (LRD100 + EO) sample caused a 2 log reduction in the number of viable bacterial cells between t = 0 and t = 2, giving evidence to the concept that the EO molecules were more tightly bound in the layered silicate substrate and therefore took longer to be released to the surface and have an antimicrobial effect. By the end of the 24 h the two layered silicate adsorbed samples

resulted in approximately the same reduction in viable bacterial cells (3.5 log compared to positive controls) and approximately a 1.5 log greater reduction than the paint + EO samples.

Due to the need for method development to enable meaningful antimicrobial assessment of the paint surfaces, there was insufficient time available to investigate the antimicrobial activity of the paint surfaces against *A. baumannii.*

5.5.2.3 Assessment of antimicrobial activity of linear low density polyethylene samples containing EO

The LLDPE samples which contained EO exhibited different patterns in antimicrobial activity relative to the SE and paint samples. Against MRSA (Figure 5.15) the LLDPE + (LRD50 + EO) resulted in a 1 log reduction in the level of viable bacterial cells at t = 0, at 6 h the reduction of viable bacterial cells had increased to 1.5 log (or 95 % of cells initially added).

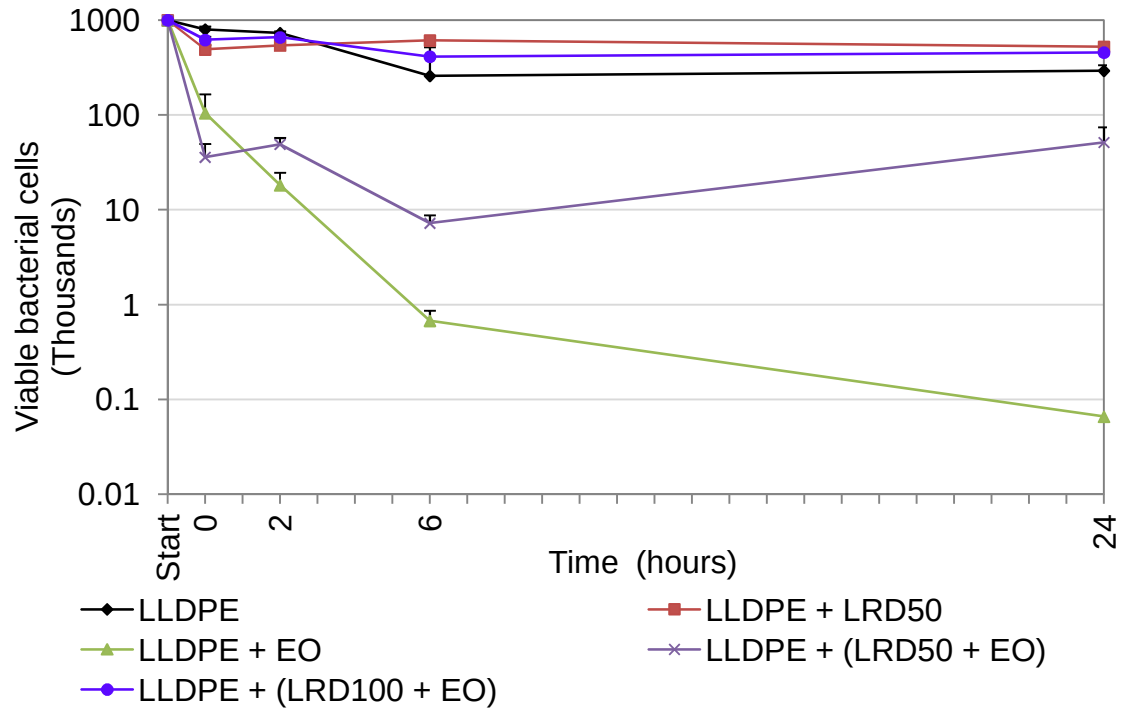

Figure 5.10: Antimicrobial testing of LLDPE samples against MRSA. LRD50 = Laponite® RD 50 % CEC 2HT2M, LRD50 + EO = Laponite® RD 50 % CEC 2HT2M with EO blend adsorbed, LRD100 + EO = Laponite® RD 100 % CEC 2HT2M with EO blend adsorbed. Demonstrating the antimicrobial activity of LLDPE when treated with the EO blend, and the reduction in efficacy caused by adsorption of the EO onto LRD50 before addition to LLDPE.

At t = 0, the LLDPE + EO sample exhibited slightly weaker antimicrobial effects than LLDPE + (LRD50 + EO). By t = 2h LLDPE + EO was exhibiting a stronger antimicrobial effect than layered silicate adsorbed samples, and at t = 6 the LLDPE + EO was resulting in a 1 log greater reduction in viable bacterial cells compared to LLDPE + (LRD50 + EO). Between 6 h and 24 h the number of viable bacterial cells on the LLDPE + (LRD50 + EO) samples had increased resulting in approximately a 1 log reduction compared to the positive controls. In contrast LLDPE + EO exhibited a further reduction in viable bacterial cells resulting in a > 3 log reduction at 24 h. This difference in activity between the layered silicate adsorbed EO and the free EO samples indicates that initially there is more EO available at the surface of the (LRD50 + EO) sample enabling a greater initial reduction of bacterial cells. The increase in activity of the LLDPE + EO with time indicated that the EO molecules are able to bloom/sweat out from the polymer matrix and affect the bacterial cells that are not in direct

contact with the surface. The opposite trend was seen for the (LRD50 + EO) samples, which indicated that the EO molecules were more tightly bound to the LRD50 within the polymer and are not able to bloom to the surface, thereby allowing the multiplication of MRSA cells that were not in contact with the surface. The controlled release analysis in Section 5.5.3.3, provided data which agreed with the analysis of the antimicrobial activities of the LLDPE samples containing EO.

It was observed that the LLDPE + (LRD100 + EO) sample exhibited no antimicrobial activity, suggesting that the high level of OM of the Laponite® RD resulted in the EO being too strongly adsorbed preventing it from desorbing out. The WAXS data for this composite supports this explanation (Section 5.5.1.3)

The antimicrobial assay results for LLDPE against *A. baumannii* followed a similar pattern to that observed with MRSA (Figure 5.11). Due to high levels of contamination the results for samples at t = 6 were deemed to be unreliable and therefore not included, as with the MRSA assay the LLDPE + EO gave the highest reduction in the number of viable bacterial cells overall. At t = 0 the LLDPE + (LRD50 + EO) resulted in an 80 % reduction in the number of viable bacterial cells compared to the positive controls, whereas the LLDPE + EO achieved a 95 % reduction. Due to the low numbers of viable bacterial cells recovered from the positive control it was not apparent whether these reductions were significant. Statistical analysis of both sets of data using Student's T test gave T values of 3.45 and 4.35 respectively. Both values were greater than the required value for synergism of 2.57, therefore the reduction in viable bacterial cells caused by both samples was significant. At 24 h the LRD50 + EO and the free EO + LLDPE sample exhibited a high level of antimicrobial activity resulting in approximately 2.5 log and 3 log reductions respectively. This indicates that for both samples enough EO was able to desorb out of the polymer to be able to kill the *A. baumannii* which were not in contact with the polymer surface. The LLDPE + (LRD100 +EO) sample again exhibited little or no antimicrobial activity initially (at t = 0 and 2), but by t = 24 there was approximately a 95 % reduction in the number of viable bacterial cells compared to the positive controls. This supports the idea that the EO molecules were more strongly bound within the galleries of LRD100 compared to the LRD50 samples, resulting in a longer time required for enough of the EO to desorb to the surface (and out of) the polymer to have an antimicrobial effect.

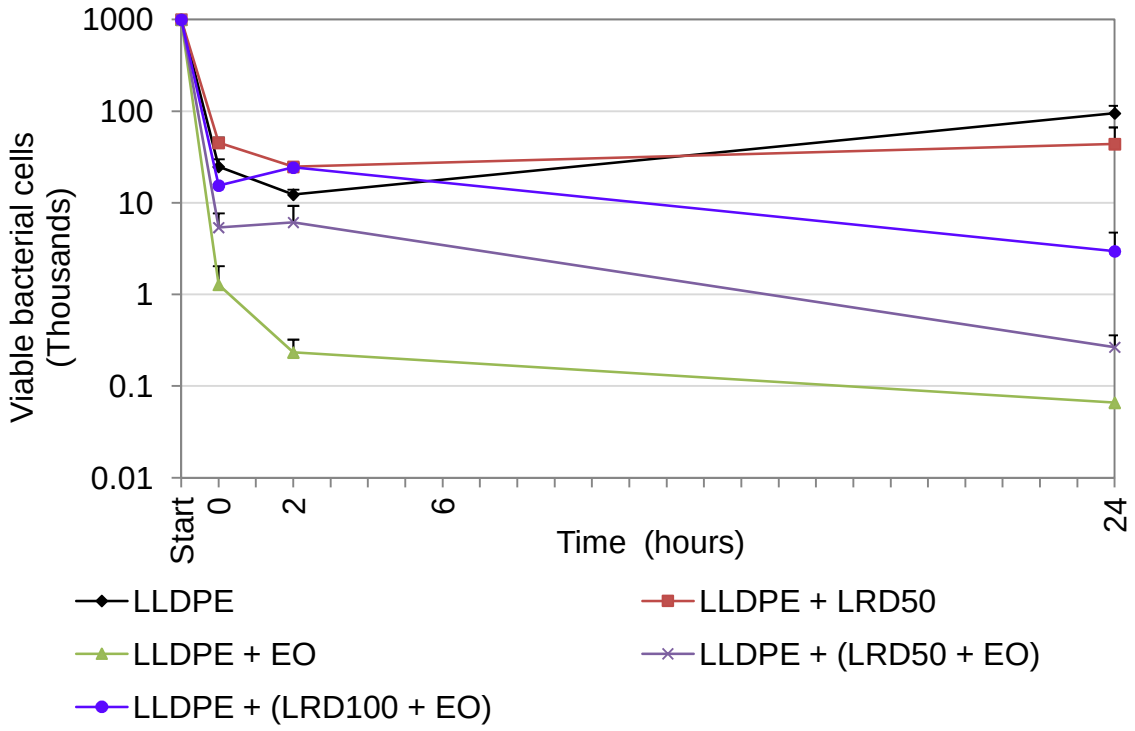

Figure 5.11: Antimicrobial testing of LLDPE samples against *A. baumannii*. LRD50 = Laponite® RD 50 % CEC 2HT2M, LRD50 + EO = Laponite® RD 50 % CEC 2HT2M with EO blend adsorbed, LRD100 + EO = Laponite® RD 100 % CEC 2HT2M with EO blend adsorbed. Demonstrating the antimicrobial effect obtained when EO's are added to LLDPE and the reduction in efficacy caused by adsorption onto LRD50 prior to addition.

All of the polymer samples containing EO (with the exception of LLDPE + (LRD100 + EO) against MRSA) showed a level of activity. For the SE and paint samples, adsorption of the antimicrobial EO blend onto OM LRD before addition to the polymers resulted in an increase in antimicrobial activity, in comparison to the samples which contained the free EO. This is potentially due to a better distribution of the EO throughout the polymer matrix and a greater concentration of EO retained within the polymer during production. For the LLDPE samples it was observed that the LLDPE containing free EO was more antimicrobial than the LLDPE containing EO adsorbed onto OM LRD. There were a number of potential reasons for the difference in behaviour for LLDPE in relation to the other polymers. The relatively high polarity/polarisability of the paint solvent and binder would make it more compatible with the EO molecules than the SE and LLDPE matrices. Therefore the EO molecules are more likely to desorb out of

the galleries of the OM RD and into the paint making them more available at the surface of the paint increasing antimicrobial activity. For the SE and the LLDPE, the EO molecules were more likely to stay within the galleries of the OM LRD due to being incompatible with the polymer. The difference in antimicrobial activity of the SE and LLDPE based samples containing EO-LRD was due the vast difference in structure/morphology of LLDPE relative to SE. The LLDPE crystalline matrix had a lower level of free volume (particularly in the crystalline regions) than the SE and therefore EO molecules that desorb out of the galleries of OM LRD will move slowly through the matrix of the LLDPE. The SE has more free volume, due to its lower T_g, and amorphous nature; these features will result in higher permeability relative to LLDPE. This will result in freer movement of the EO molecules through the matrix making them more available at the surface and increasing the antimicrobial activity. The difference between the LLDPE + EO and the LLDPE + (LRD + EO) samples was likely to be due to the incompatibility of the EO and the LLDPE. This incompatibility will result in the majority of the EO molecules in the LLDPE + EO being at or near the surface and therefore the limited movement of the EO molecules through the matrix will have little effect on the antimicrobial activity. For the LLDPE + (LRD + EO) samples the EO molecules will not desorb readily into the LLDPE from the galleries of the LRD, and the molecules that do desorb will move slowly through the matrix of the LLDPE due to the low permeability. This will result in fewer EO molecules being available at the surface of the LLDPE compared to the LLDPE + EO sample reducing the antimicrobial activity.
The differences in permeability of the SE and LLDPE should result in the EO molecules being retained within the LLDPE for a longer period of time than the SE.

The antimicrobial activity displayed by the EO treated polymers compares favourably with other antimicrobial polymers reported in literature.
Polymers treated containing methylene blue have been shown to cause a 3.5 log reduction in the number of viable MRSA cells with 8 mins contact time or a 3.5 log reduction in 5 mins if the polymer also contains nano Ag^+ present [154]. The paint and SE samples tested gave similar levels of reduction at the first time period analysed, while the LLDPE gave lower levels of antimicrobial activity. In order to achieve this antimicrobial the methylene blue polymers

needed to be irradiated with laser light for activation. The EO loaded antimicrobial polymers developed in this project do not require activation of antimicrobial properties after production.

Polyurethane containing 5 % mass zeolite containing 2.5 % Ag^+ (ZEOMIC AJ10D) resulted in approximately 87.5 % reduction in MRSA viable bacterial cells after 24 h contact, and SE containing the 5 % ZEOMIC resulted in a 40 % reduction in MRSA viable bacterial cells after 24 h [155]. All of the EO treated polymers tested in this research project achieved a greater reduction in viable bacterial cells of MRSA after 24 h than was achieved by the polymers containing Zeomic.

Sun *et al*. (2012), have described antimicrobial polymers created by covalently bonding 5,5-Dimethylhydantoin to polyurethane and then chlorinating to create an n-halamine polyurethane [156]. The chlorine acts as the antimicrobial and they were able to achieve a 4 log reduction of MRSA cells in 30 mins contact. This 4 log reduction is slightly higher than the best reduction achieved using the EO polymers, however chlorine based antimicrobials require water to be present to function which is not the case for the antimicrobial EO blends.

5.5.3 Assessment of controlled release behaviour of the composites

The main function of adsorbing the EO onto a MMT substrate was to prolong the antimicrobial lifetime of the polymers by slowing the release of the EO molecules. Assessing the level of the release of EO molecules was a complex issue; it was not possible to perform leaching studies into aqueous solutions, as commonly done [157], due to the immiscibility of the EO molecules making measuring of the level of release into aqueous media impossible. Performing leaching into an organic solvent was not desirable as it would not mimic real world conditions of the polymers. We proposed exposing plaques of the EO treated polymers to air at a set temperature, to allow the EO molecules to evaporate out of the polymers. In order to accelerate the evaporation process 50 ℃ was chosen as the set temperature, and the level of EO molecules remaining in the polymers was to be analysed at 0, 1, 2, 4, and 8 days of heating. EO molecules are volatile it was proposed that this would allow headspace (HS) GC analysis to detect the level of the molecules remaining in the polymer after heating. To do this the polymer plaques were sealed in a gas

tight HS vial, and the heated to 100 ℃ for 15 mins to drive the molecules remaining in the polymers into the atmosphere of the vial. The HS of the vial was then sampled and run through a GC-MS, any peaks visible in the resulting spectra could be taken to be EO molecules present in the polymer. To enable quantitative analysis of the EO molecules 10 µl of hexane was added to each vial before heating as an internal standard, the EO molecules could then be ratioed against the hexane for standardisation allowing comparison between samples.

The six most abundant molecules in the RO:OO blend were selected for analysis; these were p-cymene, linalool, thymol, carvacrol, and *trans*-caryophyllene and *cis*-calamenene. From the antimicrobial activity data (Section 5.5.2) it was decided that as the 50 % OM Laponite® RD samples provided the best antimicrobial activity they would be use for the release studies. The 100 % OM Laponite® RD samples were not analysed due to their in general poor antimicrobial performance. In addition, as they were more organophilic, the amount of EO that could be driven from the galleries of the layered siliactes would be low and therefore difficult to measure. It was also necessary to limit the number of samples tested to prevent the analysis becoming too time consuming.

5.5.3.1 EO release from silicone elastomers comparison of samples containing free EO and adsorbed EO

The results of the release studies for the SE samples containing free EO (Figure 5.12) showed that the SE did not retain the EO molecules. Of the six EO components selected for analysis only three could be detected in the positive controls (0 days heating), these were thymol, carvacrol and *cis*-calemenene.

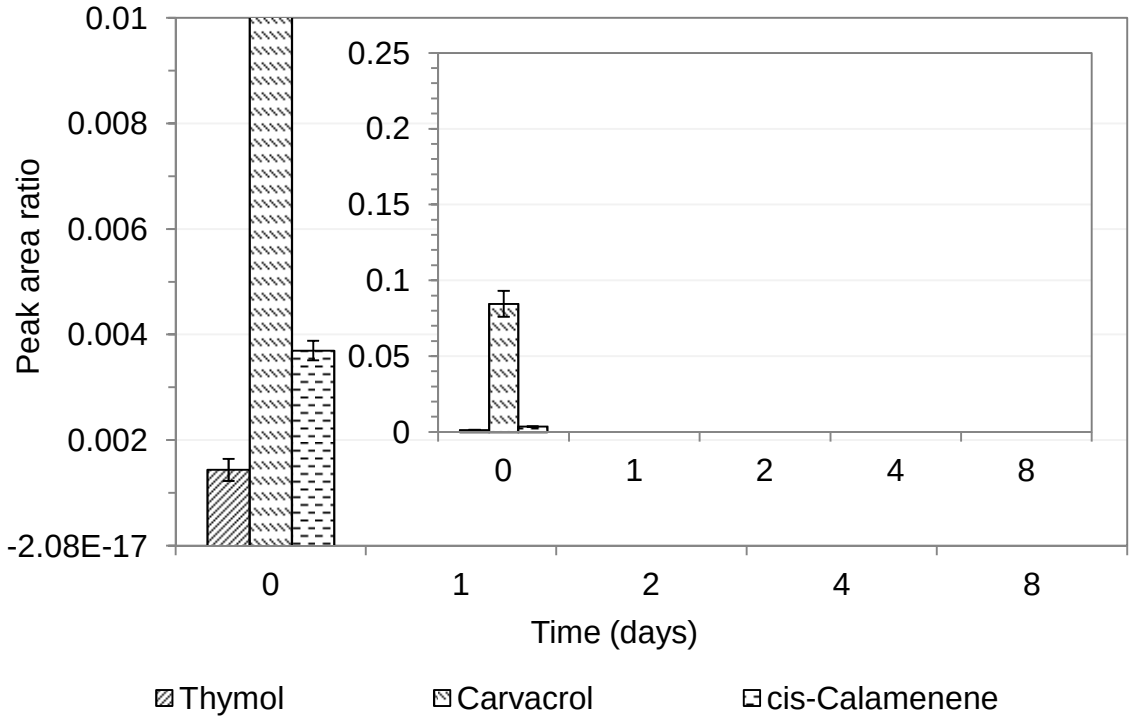

Figure 5.12: EO molecules detected from SE + EO samples after heating to 50 ℃. Displaying the lack of retention of EO antimicr obial when added directly to the SE matrix. Inset full scale displaying data for cavacrol at 0 days.

After 24 h heating no EO molecules could be detected from the SE samples using HS, indicating that there was no controlled release of the EO molecules and that antimicrobial activity of the SE+EO would be lost rapidly.

For the results of the SE + (LRD50 +EO) samples (Figure 5.13), with the adsorption of the EO onto the layered silicates, it was speculated that the EO molecules should be more tightly held within the polymer and therefore should persist within the polymer for longer.

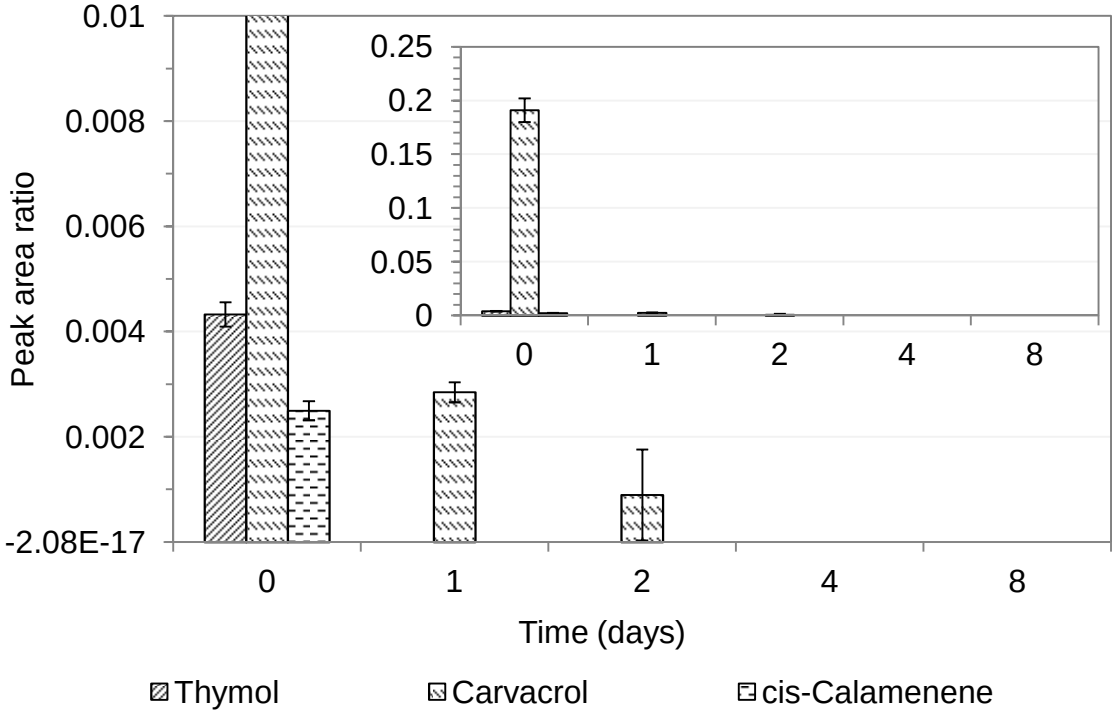

Figure 5.13: EO molecules detected from SE + (LRD50 + EO) samples after heating to 50 ℃. Displaying the improved retention of carvacrol n provided by adsorption of the EO antimicrobial to LRD50. Inset full scale showing data for carvacrol at 0 days.

In the control SE + (LRD50 + EO) the amount of thymol and carvacrol present was twice that found in the (SE + EO) samples. This helps to explain why the samples containing EO adsorbed onto OM Laponite® RD gave a higher level of antimicrobial activity (Section 5.5.2.1) because the level of EO molecules present was higher than that in the SE + EO samples. After 1 days heating thymol and *cis*-calamenene were not detected. This indicates that there is no level of controlled release of these two molecules. Carvacrol was detected in the polymer after 2 days of heating, indicating that there was some control of release of the molecule. As carvacrol is the most abundant molecule in the antimicrobial EO blend, adsorption of the antimicrobial EO blend onto OM RD before addition to SE should help to prolong the antimicrobial properties of the SE.

Statistical analysis could only be carried out at t=0 due to the lack of EO molecules in the SE at all other time points when the EO blend was free in the SE. For thymol, carvacrol and *cis*-calamenene at t=0 the t values were 16.1, 13.2 and 8.1, the degree of freedom for all samples was 4 and therefore the

required t value for p = 0.05 was 2.78. Therefore, it can be said that the increased retention of EO molecules due to adsorption onto LRD50 at t=0 was significant.

5.5.3.2 EO release from paint comparison of samples containing free EO and adsorbed EO

The paint positive control samples (Figure 5.14) yielded 4 of the 6 molecules selected for analysis; linalool, thymol, carvacrol and *trans*-caryophyllene.

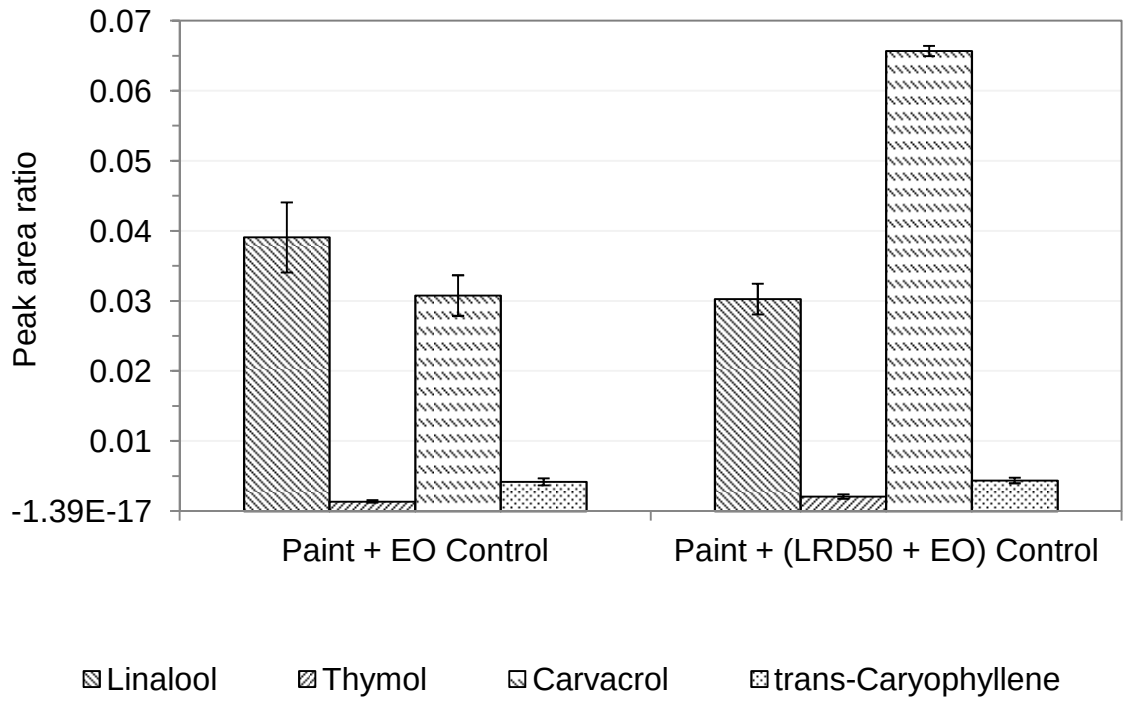

Figure 5.14: Positive control sample results for paint samples containing EO, showing level of EO molecules determined via headspace. Demonstrating the difference in EO molecule levels between samples containing the EO antimicrobial free within the paint, and samples where the EO antimicrobial was adsorbed onto LRD50.

Three of the molecules (thymol, carvacrol and *trans*-caryophyllene) detected from the paint samples were present in larger quantities for the paint + (LRD50 + EO) sample. There was approximated to be twice as much carvacrol detected from the paint + LRD50 + EO sample than the paint + EO, highlighting why the

antimicrobial effect was greater for the samples where the EO was adsorbed onto the layered silicates compared to the paint + EO samples. After 24 h of heating at 50 ℃ no EO molecules could be detected from either the paint + EO or paint + (LRD50 + EO) samples. This was because of the small volume of paint present on the steel supports 10 x 10 x 0.007 mm compared to the 10 x 10 x 1 mm sample size used for the SE and LLDPE samples.

In order to understand the difference in EO molecule levels in the two paint samples t-testing was carried out to determine whether the increased levels due to adsorption onto the substrate were significant. The degree of freedom for the analysis was four and therefore the threshold for significance was $t > 2.78$. For linalool a higher level was observed in the paint containing the free EO, however the calculated t value was $t=2.77$, $p>0.05$, $n=4$, therefore the difference between the samples was not significant. The paint sample containing the EO blend adsorbed onto the substrate had higher levels for thymol, carvacrol and *trans*-caryophyllene. The t values for these three molecules were as follows, 3.30, 20.23 and 0.54 respectively. The statistical data showed that for thymol and carvacrol the increased levels in paint + (LRD50 + EO) was significant, explaining the higher antimicrobial efficacy against MRSA for paint + (LRD50 + EO) compared to paint + EO.

5.5.3.3 EO release from linear low density polyethylene comparison of samples containing free EO and adsorbed EO

Five EO molecules were detected from the positive control linear low density polyethylene (LLDPE) samples p-cymene, linalool, thymol, carvacrol, and *trans*-caryophyllene.

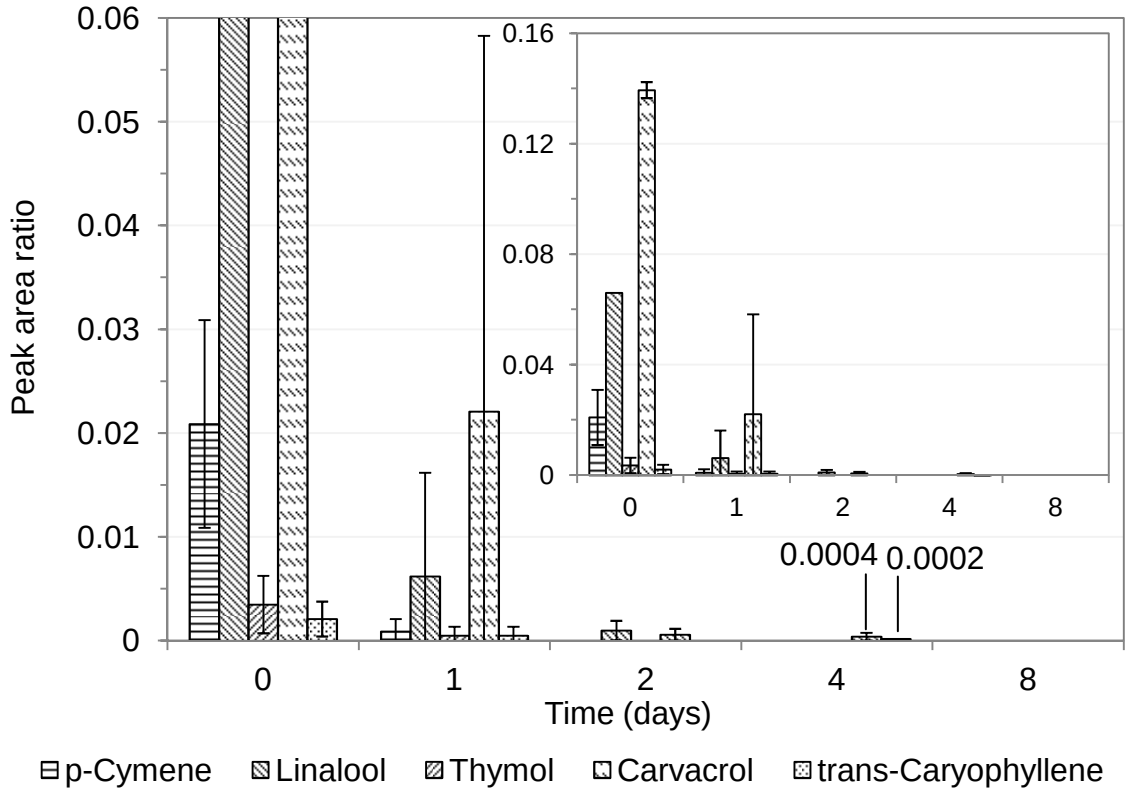

Figure 5.15: EO molecules detected from LLDPE + EO samples after heating to 50 ℃. Demonstrating the level of EO molecule retention achieved when the EO blend is added free into the polymer matrix. Inset at full scale showing complete linalool and carvacrol bars at day 0.

The results for the LLDPE + EO samples (Figure 5.15) support the idea presented in Section 5.5.2.3 that the EO molecules do not move as freely through the LLDPE, due to lower free volume and higher crystallinity, as the SE. This can be seen by the fact that the EO molecules are present in higher quantities initially and they can be detected from the polymer after heating whereas the SE + EO had no EO molecules present after 24 h heating. The two major molecules (linalool and carvacrol) in the antimicrobial EO blend were still detected after 2 days of heating at 50 ℃, with carvacrol still present in low quantities after 4 days. This indicates that the LLDPE + EO samples would

retain their antimicrobial properties for a longer period of time compared to the SE + EO samples.

The LLDPE + (LRD50 + EO) samples (Figure 5.16) exhibited the same increase in the retention of EO molecules as was observed for the SE samples. Unlike the SE and paint samples, before aging the LLDPE + (LRD50 + EO) control had similar levels of EO molecules present compared to the LLDPE + EO control. The statistical data confirmed that there was no significant difference between of *para*-cymene, linalool, carvacrol and *trans*-caryophyllene as a result of adsorption (t values = 0.69, 1.59, 0.88 and 0.48 at p = 0.05 and n = 4 respectively). For thymol, the difference was significant resulting in a t value of 7.68. The lack of a difference in the retention of the majority of EO molecules (especially carvacrol as it was the most abundant molecule in the belnd) may partially explain why the LLDPE + (LRD50 + EO) did not perform better than the LLDPE + EO in the antimicrobial testing (Section 5.5.2.3). The LLDPE samples had a higher initial level of EO molecules in comparison to the SE samples. This was because of the reduced capacity for EO molecules to move through the LLDPE polymer matrix. In addition the SE samples were left exposed to the air for 24 hours prior to synthesis in order to allow the vulcanisation process to take place; differing from the LLDPE samples which were sealed in airtight bags immediately after processing. During the vulcanisation time a proportion of the EO molecules are likely to have evaporated out from the SE.

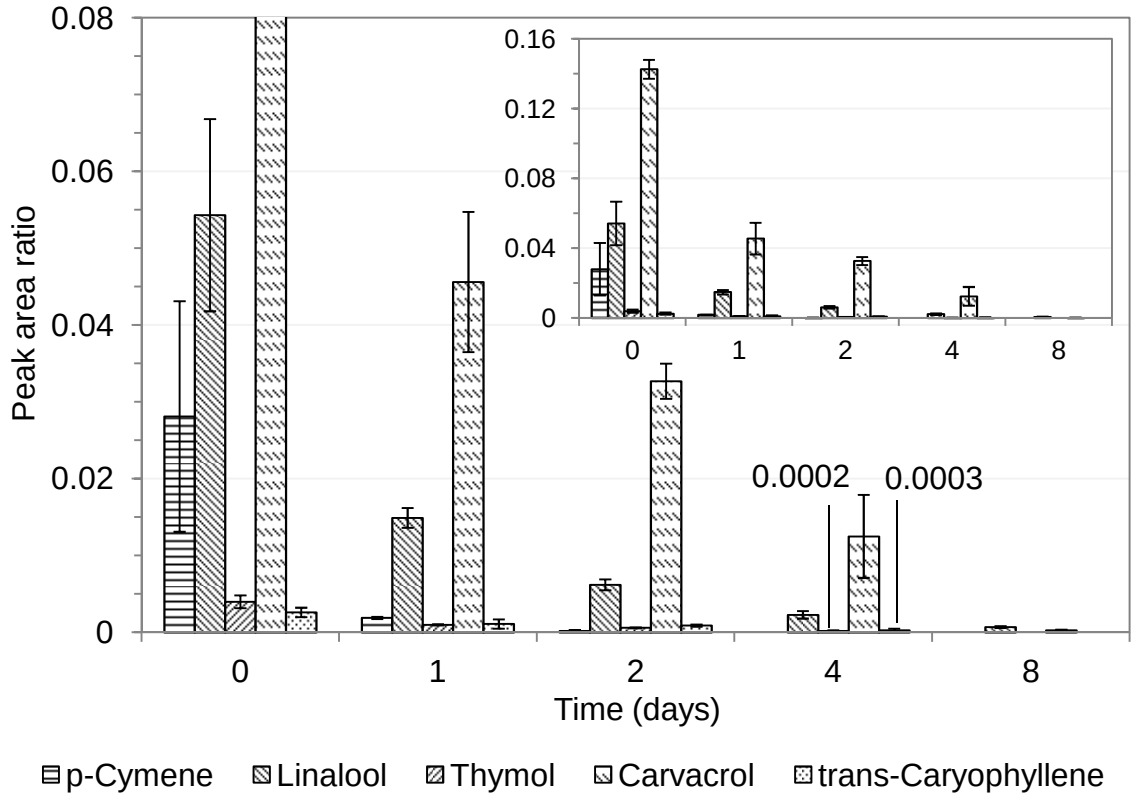

Figure 5.16: EO molecules detected from LLDPE + (LRD50-EO) samples after heating to 50 ℃, demonstrating the improved level of retention of EO molecules after heating, in comparison to LLDPE + EO (Figure 5.15). Inset displays full scale for day 0 carvacrol data.

The level of EO molecules retained within the LLDPE + (LRD50 + EO) after heating were considerably higher than those for LLDPE + EO. After 1 day heating the differences in retention were not statistically different, resulting in t values of 1.43, 1.49, 1.00, 1.10, and 1.00 for *para*-cymene, linalool, thymol, carvacrol and *trans*-caryophyllene respectively. This indicated that the retention of the EO molecules was initially controlled by the polymer matrix rather than adsorption onto the substrate. After 2 days heating all five of the EO molecules present in the control were still detected compared to only two present (linalool and thymol) at the same time for LLDPE + EO. Statistical analysis confirmed that the increased retention of linalool and thymol as a result of adsorption was significant (t values of 7.68 and 23.5 respectively). After 4 days heating only p-cymene (the lowest molecular weight) was not detected in the LLDPE + (LRD50 + EO). This showed considerable improvement compared to LLDPE +EO where only carvacrol was still present. The significantly higher amount of carvacrol detected at 4 days for LLDPE + (LRD50 + EO) compared to LLDPE + EO adds

further evidence to the improved performance of LLDPE + (LRD50 + EO) with peak area ratios of 0.0125 and 0.0004 respectively ($t = 3.87$, $p = 0.05$, $n = 4$). At 8 days linalool and carvacrol were still present, representing 4 time greater retention for linalool and two times greater retention for carvacrol. The controlled release data from two days onwards indicated that although initially the release of EO molecules was controlled by the movement of the molecules through the matrix, with extended aging the mechanism of controlled release shifted to the adsorption of the EO onto LRD50.

These results indicated that although the LLDPE + EO gave higher levels of antimicrobial activity (Section 5.5.2.3), the life time of antimicrobial should be significantly extended by adsorption of the antimicrobial EO blend into the galleries of OM LRD.

5.6 Conclusions

- Antimicrobial properties were successfully conferred onto thermoplastic, silicone elastomer and solvent paint materials via the addition of an antimicrobial EO blend. The resultant antimicrobial polymers were effective against selected gram-negative and gram-positive organisms.
- Adsorption of the antimicrobial EO blend onto organically modified porous/layered silicates before addition to the polymers resulted in improved antimicrobial activity for silicone elastomer and solvent based paint systems.
- Adsorption of the antimicrobial EO blend onto organically modified porous/layered silicates resulted in the major molecular components of the EO being retained within the thermoplastic and silicone elastomer for longer time periods than when the EO was added free to the polymers. This confirms the controlled release action of the porous silicate substrates.

CHAPTER 6

Overall conclusions and further work

6.1 Conclusions

Concluding statements are given at the end of each preceding chapter; this section will address overall conclusions and the success of the original aims.

This project set out to determine whether the addition of selected essential oils (EO) to polymer materials would result in the conferment of antimicrobial properties. In addition, the benefits of adsorbing the EO onto layered silicate substrates within the polymers were also investigated.

As part of the work, a suitable antimicrobial agent needed to be identified. Of the oils tested, oregano oil and manuka oil gave the highest activity against the test bacteria, but neither exhibited good activity against all three bacteria tested. By blending the EO together increased antibacterial activity was obtained, comprising oregano oil and rosewood oil in a 3:1 ratio. The addition of synthetic biocides to the antimicrobial EO blends was investigated in an attempt to further increase the antimicrobial potency of the blend. In general, the synthetic biocides did not provide a significant increase in antimicrobial activity, with the exception of PHMB which exhibited a synergistic effect with all seven of the antimicrobial EO blend combinations tested.

Six layered silicates were assessed for adsorption of the EOs. Natural montmorillonites (both acid activated and standard) had catalytic effects on the components of the EO and were therefore unsuitable. Synthetic layered silicates and a chemically modified natural montmorillonite were found to adsorb the EO without the negative effects of the natural montmorillonites.
In an attempt to improve adsorption of the organic EO molecules onto the layered silicates, organic modification of the layered silicates was undertaken. Of the modified substrates, LRD with 50 % CEC of di(hydrogenated tallow)

dimethyl ammonium chloride was adjudged to have the most significant desirable improvement of properties and characteristics.

The work has shown that addition of these EO to a range of different polymers resulted in a level of antimicrobial activity. Adsorption of the EO onto layered silicates before the addition to polymer materials exhibited significant benefits. Improvements in the antimicrobial activity resulted in a higher level of cell death (up to 90 % reduction in some cases from free EO to adsorbed EO). Controlled release studies showed that adsorbed EO were retained within the polymer materials for longer time periods than EO which were free within the polymer. The best antimicrobial activity was obtained with addition of the antimicrobial EO blend (oregano and rosewood in a 3:1 ratio) adsorbed onto an organically modified Laponite® into a silicone elastomer. The best controlled release was obtained with addition of the antimicrobial EO blend adsorbed onto an organically modified Laponite® into linear low density polyethylene.

6.2 Further work

The initial antimicrobial screening investigated the use of synthetic biocides in combination with the antimicrobial EO blends. PHMB was found to have a synergistic effect with the antimicrobial EO blend of oregano oil and rosewood oil in broth dilution methods. There was not time during the project to asses the effect of addition of PHMB to the EO-layered silicate material. The adsorption of PHMB onto the layered silicate substrates and subsequently the production of polymers containing layered silicates with EO and PHMB adsorbed for antimicrobial testing should be investigated.

The adsorption of the EO onto the layered silicates was only assessed as individual oils. Competitive adsorption studies between oregano oil and rosewood oil would help with the understanding of how the antimicrobial EO blend adsorbed onto the substrates. Adsorption studies of the antimicrobial EO blend onto the layered silicates would also be worthwhile.

LB at 50 % OM had a low level of hydrocarbon present ($A_{(C\text{-}H)s}/A_{(Si\text{-}O)}$ ratio of 0.2), and achieved the highest level of manuka oil adsorption. In an attempt to

achieve better levels of manuka oil adsorption on the other OM layered silicates it may be beneficial to organically modify them at lower cation exchange capacity (CEC) (such as 25 %) resulting in a lower hydrocarbon level on the substrate.

The organically modified Laponites® in this study did not exhibit any signs of self assembly of the surfactant alkyl chains, unlike other layered silicates reported in literature. The lack of self assembly could be due to the low surfactant level used, or the low aspect ratio of the Laponite® platelets. Organic modification at higher percentages of the CEC or with a Laponite® with a higher CEC could allow for further investigation into the reasons for lack of self assembly. In addition, organo montmorillonites that are known to form these self assembled arrays could be studied for adsorption of the EO to determine whether self assembly of the alkyl chains has a beneficial effect on adsorption.

In order to provide further understanding of the effects of organic modification on the substrates SEM and transition electron microscopy (TEM) imaging should be undertaken. This would provide information as to how organic modification affected the platelets of the substrates on the micro and nanoscale. The images should also provide information as to how the organic modifier is interacting with the surface of the substrates.

The antimicrobial polymers produced were shown to be effective against two bacteria; testing against other microbes such as fungi would provide more information as to how effective they are as a general biocidal material, or as a targeted product. If the materials are effective at killing moulds commonly found in bathrooms there may be the potential for addition to grouting and sealants to prevent the build up of mould on these materials.

The antimicrobial testing of the treated polymers was fundamental and focused on proof of concept of the treatment of polymers with EO to achieve antimicrobial activity. Further analysis needs to be carried out to enable better understanding of the polymers antimicrobial properties. Scanning electron microscopy (SEM) should be used on plaques which have not had the cells washed off; this would enable the determination as to whether cell lysis had occurred. Lysis of the bacterial cells would confirm that the cells were being killed by the EO in the polymers, rather than being shocked into a viable but nonculturable state.

Staining of the positive controls after the bacterial cells had been washed off should be carried out to determine the retention of cells that had been left on the surface. Using a live dead stain would allow for the determination of the number of viable bacterial cells remaining on the polymer plaques. This information would improve the understanding of the antimicrobial action of the materials.

The addition of soiling to the surface with soils such as blood plasma would allow for the investigation into how common soils found in healthcare environments affected the antimicrobial activity of the polymers.

Polymer plaques that have been through one cycle of antimicrobial testing should be retested. This will clarify whether the EO molecules at the surface are depleted during the process of acting on the bacterial cells. The results of such testing will confirm whether the polymer materials will be able prevent multiple colonisations of surfaces.

It was proposed that the distribution of the EO throughout the polymer materials may have an effect on their antimicrobial activity of the materials. Since there were areas of high EO concentration with good activity surrounded by areas of low EO concentration that may have reduced activity. Atomic force microscopy (AFM) could be used to assess the coefficient of friction of the sample surfaces, to investigate whether there were large areas with no EO present. An area with no EO present should have a lower coefficient of friction that an area with a high concentration of EO.

As with the antimicrobial testing of the polymers, the controlled release studies also focused on the proof of concept, that adsorption of the EO onto a substrate would increase the retention of the EO molecules within the polymer. Further work needs to be carried out determine whether the increased retention would result in a useful lifetime of the materials. For example, antimicrobial testing of the polymers after aging to confirm whether the level of EO molecules retained was sufficient for antimicrobial activity. In addition release rate kinetics studies could be used to determine how the controlled release of the EO antimicrobial would occur at room temperature.

Literature indicates that cyclisation of linalool results in the formation of α-terpineol. However, this study found evidence for the cyclisation of linalool to limonene catalysed by the natural montmorillonites. It was proposed that the formation of limonene may be as a result of the lack of available OH within the pores of dried montmorillonite. The proposed formation of limonene could be investigated via the addition of pure linalool to dried montmorillonite and then extraction of the resulting products. In addition, addition of linalool to hydrated montmorillonite followed by analysis of the products may provide evidence for available OH to be present for the formation of α-terpineol.

Artificially aging the level of EO in the polymer materials by heating gave evidence for the adsorption of the EO onto layered silicates providing better retention of the EO components in comparison to EO free within the polymer, and therefore adsorption of the EO resulted in controlled release. It is important to test the antimicrobial efficacy of the polymer materials after artificial aging of the EO level to show that the improved controlled release provided by adsorption onto layered silicates results in an increase in the antimicrobial lifetime of the polymers.

In addition, as the layered silicates have been shown to adsorb the EO it may be possible to reimpregnate the layered silicate within the polymer materials once the initial EO has desorbed out. This would provide a simple way to further increase the antimicrobial life time of the polymer materials. To determine if this is possible, polymer samples which contain the EO adsorbed to the layered silicate would have the EO driven out using heat, a simple wiping of a solution containing fresh antimicrobial EO blend over the polymer material would be undertaken and the EO solution allowed to dry. Using the headspace GC method the polymer would then be analysed for presence of volatile components of EOs.

For each of the three polymers used in this study, only one formulation containing the EO adsorbed onto the organically modified layered silicate was investigated (10 % (m/m) of substrate containing approximately 33.3 % (m/m) EO). Formulations containing different volumes of EO adsorbed onto the layered silicate, and also different percentage loadings of the layered silicate

within the polymer should be investigated to allow for the optimisation of the antimicrobial properties. In addition, during this work mechanical (i.e. flexibility and hardness), stability (i.e. photo, thermal and colour) and aging testing should be undertaken to determine whether the properties required for commercial use of the polymers can be achieved.

References

1. Garner, J.S., Jarvis, W.R., Emori, T.G., Horan, T.C., and Hughes, J.M., *CDC definitions for nosocomial infections, 1988.* American Journal of Infection Control, 1988. **16**(3): p. 128-140.
2. *Summary Points on Clostridium difficile Infection (CDI)* 2011, Health Protection Agency: London.
3. *Summary Points on Meticillin Resistant Staphylococcus aureus (MRSA) Bacteraemia* 2011, Health Protection Agency: London.
4. *Pseudomonas spp. and Stenotrophomonas maltophilia bacteraemia in England, Wales, and Northern Ireland, 2004 to 2008*. 2009, Health Protection agency: London. p. 10.
5. *Surveillance of Surgical Site Infections in NHS hospitals in England 2010/2011*. 2011, Health Protection Agency: London.
6. Petersen, M.H., Holm, M.O., Pedersen, S.S., Lassen, A.T., and Pedersen, C., *Incidence and prevalence of hospital-acquired infections in a cohort of patients admitted to medical departments.* Danish Medical Journal, 2010. **57**(11).
7. Klevens, R.M., *Estimating health care-associated infections and deaths in U.S. Hospitals, 2002.* Public health reports, 2007. **122**(2): p. 160-166.
8. *Trends in Antimicrobial Resistance in England and Wales, 2004-2005*. 2006, Health Protection Agency: London.
9. Coello, R., Charlett, A., Wilson, J., Ward, V., Pearson, A., and Borriello, P., *Adverse impact of surgical site infections in English hospitals.* Journal of Hospital Infection, 2005. **60**(2): p. 93-103.
10. Kilgore, M.L., *The costs of nosocomial infections.* Medical Care, 2008. **46**(1): p. 101-104.
11. Sánchez-Velázquez, L.D., Ponce de León Rosales, S., and Rangel Frausto, M.S., *The Burden of Nosocomial Infection in the Intensive Care Unit: Effects on Organ Failure, Mortality and Costs. A Nested Case-Control Study.* Archives of Medical Research, 2006. **37**(3): p. 370-375.
12. Tortora, G.J., Funke, B.R., and Case, C.L., *Microbiology an Introduction*. 9 ed. 2007, San Francisco: Pearson Benjamin Cummings.
13. Singleton, P., *Bacteria in Biology, Biotechnology and Medicine*. 6 ed. 2004, Chichester: John Wiley and Sons.
14. Kaiser, G.E. *Structure of a Gram-Positive Cell Wall*. 21/01/2007 [cited 2012 20/07/2012]; Available from: http://faculty.ccbcmd.edu/courses/bio141/labmanua/lab12/diseases/blood/u1fig9b.html.
15. Kaiser, G.E. *Structure of a Gram-Negative Cell Wall*. 21/01/2007 [cited 2012 13/01/2012]; Available from: http://faculty.ccbcmd.edu/courses/bio141/labmanua/lab16/diseases/gonococcus/u1fig10b.html.
16. El-Mougy, N.S., *Effect of some essential oils for limiting early blight (Alternaria solani) development in potato field.* Journal of Plant Protection Research, 2009. **49**(1): p. 57-62.
17. Williams, D., *Lecture Notes on Essential Oils*. 1989, Long Melford: Bush Boake Allen Ltd.
18. Lambert, R.J.W., Skandamis, P.N., Coote, P.J., and Nychas, G.J.E., *A study of the minimum inhibitory concentration and mode of action of*

oregano essential oil, thymol and carvacrol. Journal of Applied Microbiology, 2001. **91**(3): p. 453-462.
19. Adams, M., Berset, C., Kessler, M., and Hamburger, M., *Medicinal herbs for the treatment of rheumatic disorders--A survey of European herbals from the 16th and 17th century.* Journal of Ethnopharmacology, 2009. **121**(3): p. 343-359.
20. Yoon, C., Kang, S.-H., Yang, J.-O., Noh, D.-J., Indiragandhi, P., and Kim, G.-H., *Repellent activity of citrus oils against cockroaches Blattella germanica, Pariplaneta americana, and P. fuliginosa.* Journal of Pesticide Science, 2009. **34**(2): p. 77-88.
21. Melo, F.H.C., Moura, B.A., de Sousa, D.P., de Vasconcelos, S.M.M., Macedo, D.S., Fonteles, M.M.d.F., Viana, G.S.d.B., and de Sousa, F.C.F., *Antidepressant-like effect of carvacrol (5-Isopropyl-2-methylphenol) in mice: involvement of dopaminergic system.* Fundamental & Clinical Pharmacology, 2011. **25**(3): p. 362-367.
22. Tumen, I., Süntar, I., Keleş, H., and Akkol, E.K., *A Therapeutic Approach for Wound Healing by Using Essential Oils of Cupressus and Juniperus Species Growing in Turkey.* Evidence-Based Complementary and Alternative Medicine, 2012. **2012**.
23. Chao, C., Wu, P., Chang, H., and Su, H., *The effects of evaporating essential oils on indoor air Quality*, in *Indoor Air 2005: 10th International Conference on Indoor Air Quality and Climate*. 2005, Tsinghua University Press: Beijing, Peoples Republic of China.
24. Maji, T.K., Baruah, I., Dube, S., and Hussain, M.R., *Microencapsulation of Zanthoxylum limonella oil (ZLO) in glutaraldehyde crosslinked gelatin for mosquito repellent application.* Bioresource Technology, 2007. **98**(4): p. 840-844.
25. Parris, N., Cooke, P.H., and Hicks, K.B., *Encapsulation of Essential Oils in Zein Nanospherical Particles.* J. Agric. Food Chem., 2005. **53**(12): p. 4788-4792.
26. Keawchaoon, L. and Yoksan, R., *Preparation, characterization and in vitro release study of carvacrol-loaded chitosan nanoparticles.* Colloids and Surfaces B: Biointerfaces, 2011. **84**(1): p. 163-171.
27. Paula, H.C.B., Sombra, F.M., Cavalcante, R.d.F., Abreu, F.v.O.M.S., and de Paula, R.C.M., *Preparation and characterization of chitosan/cashew gum beads loaded with Lippia sidoides essential oil.* Materials Science and Engineering: C, 2011. **31**(2): p. 173-178.
28. B. Giménez, M.C. Gómez-Guillén, M.E. López-Caballero, J. Gómez-Estaca, and Montero, P., *Role of sepiolite in the release of active compounds from gelatin-egg white films.* Food Hydrocolloids, 2012. **27**(2): p. 475-486.
29. Mitchell, J.K. and Soga, K., *Fundamentals of Soil Behaviour*. 2005: John Wiley & Sons.
30. Shiragami, T., Matsumoto, J., Inoue, H., and Yasuda, M., *Antimony porphyrin complexes as visible-light driven photocatalyst.* Journal of Photochemistry and Photobiology C: Photochemistry Reviews, 2005. **6**(4): p. 227-248.
31. Phillips, C. and Fisher, K., *The mechanism of action of a citrus oil blend against Enterococcus faecium and Enterococcus faecalis.* Journal of Applied Microbiology, 2009. **106**(4): p. 1343-1349.

32. Greene-Kelly, R., *Sorption of aromatic organic compounds by montmorillonite: Part 1. - Orientation studies.* Transactions of the Faraday Society, 1955. **51**: p. 412-424.
33. Moronta, A., Oberto, T., Carruyo, G., Solano, R., Sánchez, J., González, E., and Huerta, L., *Isomerization of 1-butene catalyzed by ion-exchanged, pillared and ion-exchanged/pillared clays.* Applied Catalysis A: General, 2008. **334**(1-2): p. 173-178.
34. Nistor, D., Dron, P., Surpățeanu, G., Siminiceanu, I., Miron, N., and Azzouz, A., *Optimized procedure for clay pillaring with aluminum species used in depollution.* Journal of Thermal Analysis and Calorimetry, 2006. **84**(2): p. 527-530.
35. Stathi, P., *Heavy-metal uptake by a high cation-exchange-capacity montmorillonite:The role of permanent charge sites.* Global nest, 2010. **12**(3): p. 248-255.
36. Alexandre, M. and Dubois, P., *Polymer-layered silicate nanocomposites: preparation, properties and uses of a new class of materials.* Materials Science and Engineering: R: Reports, 2000. **28**(1-2): p. 1-63.
37. Hammer, K.A., Carson, C.F., and Riley, T.V., *Antimicrobial activity of essential oils and other plant extracts.* Journal of Applied Microbiology, 1999. **86**(6): p. 985-990.
38. Edwards-Jones, V., Buck, R., Shawcross, S.G., Dawson, M.M., and Dunn, K., *The effect of essential oils on methicillin-resistant Staphylococcus aureus using a dressing model.* Burns, 2004. **30**(8): p. 772-777.
39. Sikkema, J., De Bont, J.A.M., and Poolman, B., *Mechanisms of Membrane Toxicity of Hydrocarbons.* Microbiological Reviews, 1995. **59**(2): p. 201-222.
40. Lv, F., Liang, H., Yuan, Q., and Li, C., *In vitro antimicrobial effects and mechanism of action of selected plant essential oil combinations against four food-related microorganisms.* Food Research International, 2011. **44**(9): p. 3057-3064.
41. Cox, S.D. and Markham, J.L., *Susceptibility and intrinsic tolerance of Pseudomonas aeruginosa to selected plant volatile compounds.* Journal of Applied Microbiology, 2007. **103**(4): p. 930-936.
42. *Bioactivity of Essential oils and Their Components*, in *Flavours and Fragrances Chemistry, Bioprocessing and Sustainability*, R.G. Berger, Editor. 2007, Springer Verlag: Berlin. p. 87-115.
43. Uribe, S., Ramirez, J., and Pena, A., *Effects of β-pinene on yeast membrane functions.* Journal of Bacteriology, 1985. **161**(3): p. 1195-1200.
44. Bassolé, I.H.N. and Juliani, H.R., *Essential oils in combination and their antimicrobial properties.* Molecules, 2012. **17**(4): p. 3989-4006.
45. Hagvall, L., Sköld, M., Bråred-Christensson, J., Börje, A., and Karlberg, A.-T., *Lavender oil lacks natural protection against autoxidation, forming strong contact allergens on air exposure.* Contact dermatitis, 2008. **59**(3): p. 143-150.
46. Davis, P., *Aromatherapy an A-Z*. 1999, Saffron Waldon: C.W. Daniel. 320.
47. Khalaj, L. and Farzin, D., *P.2.d.004 Evaluation of antidepressant activities of rose oil and geranium oil in the forced swim test in mouse.* European Neuropsychopharmacology, 2006. **16, Supplement 4**(0): p. S334-S335.

48. Schelz, Z., Molnar, J., and Hohmann, J., *Antimicrobial and antiplasmid activities of essential oils.* Fitoterapia, 2006. **77**(4): p. 279-285.
49. Rosato, A., Vitali, C., De Laurentis, N., Armenise, D., and Antonietta Milillo, M., *Antibacterial effect of some essential oils administered alone or in combination with Norfloxacin.* Phytomedicine, 2007. **14**(11): p. 727-732.
50. Kunicka-Styczyńska, A., Sikora, M., and Kalemba, D., *Antimicrobial activity of lavender, tea tree and lemon oils in cosmetic preservative systems.* Journal of Applied Microbiology, 2009. **107**(6): p. 1903-1911.
51. Porter, N.G. and Wilkins, A.L., *Chemical, physical and antimicrobial properties of essential oils of Leptospermum scoparium and Kunzea ericoides.* Phytochemistry, 1999. **50**(3): p. 407-415.
52. George, D.R., Smith, T.J., Shiel, R.S., Sparagano, O.A.E., and Guy, J.H., *Mode of action and variability in efficacy of plant essential oils showing toxicity against the poultry red mite, Dermanyssus gallinae.* Veterinary Parasitology, 2009. **161**(3-4): p. 276-282.
53. Russo, M., Galletti, G.C., Bocchini, P., and Carnacini, A., *Essential Oil Chemical Composition of Wild Populations of Italian Oregano Spice (Origanum vulgare ssp. hirtum (Link) Ietswaart): A Preliminary Evaluation of Their Use in Chemotaxonomy by Cluster Analysis. 1. Inflorescences.* Journal of Agricultural and Food Chemistry, 1998. **46**(9): p. 3741-3746.
54. De Azeredo, G.A., Stamford, T.L.M., Nunes, P.C., Gomes Neto, N.J., De Oliveira, M.E.G., and De Souza, E.L., *Combined application of essential oils from Origanum vulgare L. and Rosmarinus officinalis L. to inhibit bacteria and autochthonous microflora associated with minimally processed vegetables.* Food Research International, 2011. **44**(5): p. 1541-1548.
55. Sivropoulou, A., Papanikolaou, E., Nikolaou, C., Kokkini, S., Lanaras, T., and Arsenakis, M., *Antimicrobial and Cytotoxic Activities of Origanum Essential Oils.* Journal of Agricultural and Food Chemistry, 1996. **44**(5): p. 1202-1205.
56. Bukovská, A., Čikoš, Š., Juhás, Š., Il'ková, G., Rehák, P., and Koppel, J., *Effects of a Combination of Thyme and Oregano Essential Oils on TNBS-Induced Colitis in Mice.* Mediators of Inflammation, 2007. **2007**.
57. Inouye, S., Uchida, K., Maruyama, N., Yamaguchi, H., and Abe, S., *A Novel Method to Estimate the Contribution of the Vapor Activity of Essential Oils in Agar Diffusion Assay.* Japanese Journal of Medical Mycology, 2006. **47**: p. 91-98.
58. Sampaio, L.d.F.S., Maia, J.G.S., de Parijós, A.M., de Souza, R.Z., and Barata, L.E.S., *Linalool from Rosewood (Aniba rosaeodora Ducke) Oil Inhibits Adenylate Cyclase in the Retina, Contributing to Understanding its Biological Activity.* Phytotherapy Research, 2012. **26**(1): p. 73-77.
59. *MRSA - Information for patients*. 2010, Health Protection Agency: London.
60. Madigan, M.T., Martinko, J.M., and Parker, J., *Biology of Microorganisms*. 9 ed. 2000, London: Prentice-Hall International.
61. Cohen, J.O., *Medical Microbiology*. 2 ed, ed. S. Baron. 1986, Menlo Park: Addison-Wesley.
62. Hanberger, H., Walther, S., Leone, M., Barie, P.S., Rello, J., Lipman, J., Marshall, J.C., Anzueto, A., Sakr, Y., Pickkers, P., Felleiter, P., Engoren, M., and Vincent, J.-L., *Increased mortality associated with meticillin-resistant Staphylococcus aureus (MRSA) infection in the Intensive Care*

Unit: results from the EPIC II study. International Journal of Antimicrobial Agents, 2011. **38**(4): p. 331-335.
63. *Pseudomonas aeruginosa*. 2012 [cited 2012 24/02/2012]; Available from: http://www.hpa.org.uk/Topics/InfectiousDiseases/InfectionsAZ/PseudomonasAeruginosa/.
64. Peleg, A.Y., Seifert, H., and Paterson, D.L., *Acinetobacter baumannii: Emergence of a Successful Pathogen.* Clinical Microbiology Reviews, 2008. **21**(3): p. 358-582.
65. Hidron, A.I., Edwards, J.R., Patel, J., Horan, T.C., Sievert, D.M., Pollock, D.A., and Fridkin, S.K., *NHSN annual update: antimicrobial-resistant pathogens associated with healthcare-associated infections. Annual summary of data reported to the National Healthcare Safety Network at the Centers for Disease Control and Prevention, 2006-2007.* Infection control and hospital epidemiology 2008. **29**(11).
66. Doi, Y., Onuoha, E.O., Adams-Haduch, J.M., Pakstis, D.L., McGaha, T.L., Werner, C.A., Parker, B.N., Brooks, M.M., Shutt, K.A., Pasculle, A.W., Muto, C.A., and Harrison, L.H., *Screening for Acinetobacter baumannii Colonization by Use of Sponges.* Journal of Clinical Microbiology, 2010. **49**(2): p. 154-158.
67. *Gas chromatography-mass spectoscopy background*. 1998 20/01/1998 [cited 2012 24/02/2012]; Available from: http://www.gmu.edu/depts/SRIF/tutorial/gcd/gc-ms2.htm.
68. Renneberg, J., *Definitions of Antibacterial Interactions in Animal Infection Models.* Journal of Antimicrobial Chemotherapy, 1993. **31**(Supplement D): p. 167-175.
69. Sivropoulou, A., Kokkini, S., Lanaras, T., and Arsenakis, M., *Antimicrobial activity of mint essential oils.* Journal of Agricultural and Food Chemistry, 1995. **43**(9): p. 2384-2388.
70. Vokou, D., Kokkini, S., and Bessiere, J.-M., *Geographic variation of Greek oregano (Origanum vulgare ssp. hirtum) essential oils.* Biochemical Systematics and Ecology, 1993. **21**(2): p. 287-295.
71. Kpadonou Kpoviessi, B.G.H., Ladekan, E.Y., Kpoviessi, D.S.S., Gbaguidi, F., Yehouenou, B., Quetin-Leclercq, J., Figueredo, G., Moudachirou, M., and Accrombessi, G.C., *Chemical Variation of Essential Oil Constituents of Ocimum gratissimum L. from Benin, and Impact on Antimicrobial Properties and Toxicity against Artemia salina Leach.* Chemistry & Biodiversity, 2012. **9**(1): p. 139-150.
72. Gauvin, A., Lecomte, H., and Smadja, J., *Comparative investigations of the essential oils of two scented geranium (Pelargonium spp.) cultivars grown on Reunion Island.* Flavour and Fragrance Journal, 2004. **19**(5): p. 455-460.
73. Mesa-Arango, A.C., Montiel-Ramos, J., Zapata, B., Durán, C., Betancur-Galvis, L., and Stashenko, E., *Citral and carvone chemotypes from the essential oils of Colombian Lippia alba (Mill.) N.E. Brown: composition, cytotoxicity and antifungal activity.* Memórias do Instituto Oswaldo Cruz, 2009. **104**(6): p. 878-884.
74. Limoncu, M.H., Ermertcan, S., Çetin, Ç.B., Cosar, G., and Dinç, G., *Emergence of phenotypic resistance to ciprofloxacin and levofloxacin in methicillin-resistant and methicillin-sensitive Staphylococcus aureus strains.* International Journal of Antimicrobial Agents, 2003. **21**(5): p. 420-424.

75. Lambert, R.J.W., *Comparative analysis of antibiotic and antimicrobial biocide susceptibility data in clinical isolates of methicillin-sensitive Staphylococcus aureus, methicillin-resistant Staphylococcus aureus and Pseudomonas aeruginosa between 1989 and 2000*.* Journal of Applied Microbiology, 2004. **97**(4): p. 699-711.
76. Pendland, S.L., Neuhauser, M.M., Garey, K.W., Prause, J.L., and Jung, R., *Comparative killing rates of gatifloxacin and ciprofloxacin against 14 clinical isolates: impact of bacterial strain and antibiotic concentration.* Diagnostic Microbiology and Infectious Disease, 2002. **44**(1): p. 59-61.
77. Kõljalg, S., Naaber, P., and Mikelsaar, M., *Antibiotic resistance as an indicator of bacterial chlorhexidine susceptibility.* Journal of Hospital Infection, 2002. **51**(2): p. 106-113.
78. Fisher, K. and Phillips, C., *The mechanism of action of a citrus oil blend against Enterococcus faecium and Enterococcus faecalis.* Journal of Applied Microbiology, 2009. **106**(4): p. 1343-1349.
79. Allen, M.J., White, G.F., and Morby, A.P., *The response of Escherichia coli to exposure to the biocide polyhexamethylene biguanide.* Microbiology, 2006. **152**(4): p. 989-1000.
80. Bagamboula C.F., Uyttendaele M., and J, D., *Inhibitory effect of thyme and basil essential oils, carvacrol, thymol, estragol, linalool and p-cymene towards Shigella sonnei and S. flexneri.* Food Microbiology, 2004. **21**: p. 33-42.
81. Gupta, N., Saxena, G., and Kalra, S.S., *Antimicrobial activity pattern of certain terpenoids.* International Journal of Pharma and Bio Sciences, 2011. **2**(1): p. 87-91.
82. Gianotti, V., Benzi, M., Croce, G., Frascarolo, P., Gosetti, F., Mazzucco, E., Bottaro, M., and Gennaro, M.C., *The use of clays to sequestrate organic pollutants. Leaching experiments.* Chemosphere, 2008. **73**(11): p. 1731-1736.
83. Parolo, M.E., Avena, M.J., Pettinari, G.R., and Baschini, M.T., *Influence of Ca^{2+} on tetracycline adsorption on montmorillonite.* Journal of Colloid and Interface Science, 2012. **368**(1): p. 420-426.
84. Sannino, F., Filazzola, M.T., Violante, A., and Gianfreda, L., *Adsorption and Desorption of Simazine on Montmorillonite Coated by Hydroxy Aluminum Species.* Environmental Science & Technology, 1999. **33**(23): p. 4221-4225.
85. Wang, X.-p., Shan, X.-q., Luo, L., Zhang, S.-z., and Wen, B., *Sorption of 2,4,6-Trichlorophenol in Model Humic Acidâˆ'Clay Systems.* Journal of Agricultural and Food Chemistry, 2005. **53**(9): p. 3548-3555.
86. Shin, W., Song, D., Choi, S., and Kim, J., *Multi-step competitive sorption and desorption of chlorophenols in surfactant modified montmorillonite.* Water, air, and soil pollution, 2005. **166**(1-4): p. 367-380.
87. *Fulcat 400 clay catalyst and adsorbent*. Rockwood Additives Limited Product Bulletin [cited 2012 20/02/2012]; Available from: http://www.rockwoodadditives.com/product_bulletins_eu/PB%20Fulcat%20400.pdf.
88. Bartholomew, C.H. and Farrauto, R.J., *Fundamentals of Industrial Catalytic Processes*. 2 ed. 2005: Wiley.
89. *Fulcat 435 clay catalyst and adsorbent*. Rockwood Additives Limited Product Bulletin [cited 2012 20/02/2012]; Available from: http://www.rockwoodadditives.com/product_bulletins_eu/PB%20Fulcat%20435.pdf.

90. Bovey, J. and Jones, W., *Characterisation of al-pillared acid activated clay catalysts.* Journal of Materials Chemistry, 1995. **5**(11).
91. Tyagi, B., Chudasama, C.D., and Jasra, R.V., *Determination of structural modification in acid activated montmorillonite clay by FT-IR spectroscopy.* Spectrochimica Acta Part A: Molecular and Biomolecular Spectroscopy, 2006. **64**(2): p. 273-278.
92. Falaras, P. and Lezou, F., *Electrochemical behavior of acid activated montmorillonite modified electrodes.* Journal of Electroanalytical Chemistry, 1998. **455**(1-2): p. 169-179.
93. *Product bulletin Fulacolor XW*. Rockwood Additives Limited Product Bulletin [cited 2012 15/02/2012]; Available from: http://www.rockwoodadditives.com/product_bulletins_eu/PB%20Fulacolor%20XW.pdf.
94. *Laponite Technology*. 2010 [cited 2012 19/02/2012]; Available from: http://www.scprod.com/pdfs/Laponite%20Technology%20Feb%202010.pdf.
95. Ploehn, H.J. and Liu, C., *Quantitative Analysis of Montmorillonite Platelet Size by Atomic Force Microscopy.* Industrial & Engineering Chemistry Research, 2006. **45**(21): p. 7025-7034.
96. Rothon, R.N., *Particulate-Filled Polymer Composites (2nd Edition)*. 2003, Smithers Rapra Technology: Shrewsbury.
97. Peña, J.M., Allen, N.S., Liauw, C.M., Edge, M., Valange, B., and Santamaría, F., *Factors affecting the adsorption of stabilisers on to carbon black (flow micro-calorimetry studies) Part III Surface activity study using acid/base model probes.* Journal of Materials Science, 2001. **36**(18): p. 4443-4457.
98. Liauw, C.M., Taylor, R.L., Maryan, C., Kato, R., Wilkinson, A.N., and Cheerarot, O., *Organo-Montmorillonite as a Controlled Release Reservoir for Triclosan in Silicone Elastomer: A Flow Micro-Calorimetry and Leaching Study.* Macromolecular Symposia, 2011. **301**(1): p. 96-103.
99. Jones, A., *Novel approaches to high temperature stabilisation of polypropylene*, in *Biology Chemistry and Health Science*. 2011, Manchester Metropolitan University: Manchester. p. 150.
100. Kádár, F., Százdi, L., Fekete, E., and Pukánszky, B., *Surface Characteristics of Layered Silicates: Influence on the Properties of Clay/Polymer Nanocomposites.* Langmuir, 2006. **22**(18): p. 7848-7854.
101. MacEwan, D.M.C., *Complexes of clays with organic compounds. I. Complex formation between montmorillonite and halloysite and certain organic liquids.* Transactions of the Faraday Society, 1948. **44**.
102. Wilson, M.J., *Clay Minerology: Spectroscopic and Chemical Determinative Methods*. 1 ed. 1994, London: Chapman and Hall.
103. Dalaran, M., Emik, S., Güçlü, G., İyim, T., and Özgümüş, S., *Removal of acidic dye from aqueous solutions using poly(DMAEMA–AMPS–HEMA) terpolymer/MMT nanocomposite hydrogels.* Polymer Bulletin, 2009. **63**(2): p. 159-171.
104. López-Linares, F., Carbognani, L., Sosa-Stull, C., Pereira-Almao, P., and Spencer, R.J., *Adsorption of Virgin and Visbroken Residue Asphaltenes over Solid Surfaces. 1. Kaolin, Smectite Clay Minerals, and Athabasca Siltstone.* Energy & Fuels, 2009. **23**(4): p. 1901-1908.

105. Yu, W., Wen , M., Yang, L., and Li Liu, Z., *Ferric Chloride Catalyzed Isomerization and Cyclization of Geraniol, Linalool and Nerol.* Chinese Chemical Letters, 2002. **13**(6): p. 495-496.
106. Bedoukian, P.Z., *Perfumery Synthetics and Isolates*. 1951, New York: D. Van Nostrand Company.
107. Scheuing, D.R., *Fourier Transform Infrared Spectroscopy in Colloid and Interface Science An Overview*, ed. D.R. Scheuing. 1990: American Chemical Society.
108. Li, Z., Jiang, W.-T., and Hong, H., *An FTIR investigation of hexadecyltrimethylammonium intercalation into rectorite.* Spectrochimica Acta Part A: Molecular and Biomolecular Spectroscopy, 2008. **71**(4): p. 1525-1534.
109. Bedoukian, P.Z., *Perfumery and Flavoring Synthetics*. 3 Revised ed. 1986, Carol Stream: Allured Publishing Corporation.
110. *CRC Handbook of Chemistry and Physics*. 92 ed, ed. W.M. Haynes. 2011, Boulder: CRC Press.
111. Tiwari, R.R., Khilar, K.C., and Natarajan, U., *Synthesis and characterization of novel organo-montmorillonites.* Applied Clay Science, 2008. **38**(3-4): p. 203-208.
112. Ciullo, P.A., *Industrial Minerals and Their Uses - A Handbook and Formulary*. 1996, William Andrew Publishing/Noyes.
113. Ozdes, D., Duran, C., and Senturk, H.B., *Adsorptive removal of Cd(II) and Pb(II) ions from aqueous solutions by using Turkish illitic clay.* Journal of Environmental Management, 2011. **92**(12): p. 3082-3090.
114. De Pablo, L., Chávez, M.L., and Abatal, M.a., *Adsorption of heavy metals in acid to alkaline environments by montmorillonite and Ca-montmorillonite.* Chemical Engineering Journal, 2011. **171**(3): p. 1276-1286.
115. Smith, C.R., *Base Exchange Reactions of Bentonite and Salts of Organic Bases.* Journal of the American Chemical Society, 1934. **56**(7): p. 1561-1563.
116. Jordan, J.W., *Organophilic Bentonites. I. Swelling in Organic Liquids.* The Journal of Physical and Colloid Chemistry, 1949. **53**(2): p. 294-306.
117. Jordan, J.W., Hook, B.J., and Finlayson, C.M., *The Organophilic Bentonites. II. Organic Liquid Gels.* The Journal of Physical and Colloid Chemistry, 1950. **54**(8): p. 1196-1208.
118. Salehi-Mobarakeh, H., Yadegari, A., Khakzad-Esfahlan, F., and Mahdavian, A., *Modifying montmorillonite clay via silane grafting and interfacial polycondensation for melt compounding of nylon-66 nanocomposite.* Journal of Applied Polymer Science, 2012. **124**(2): p. 1501-1510.
119. Jarrar, R., Mohsin, M.A., and Haik, Y., *Alteration of the mechanical and thermal properties of nylon 6/nylon 6,6 blends by nanoclay.* Journal of Applied Polymer Science, 2012. **124**(3): p. 1880-1890.
120. Chen, Y., Guo, Z., and Fang, Z., *Relationship between the distribution of organo-montmorillonite and the flammability of flame retardant polypropylene.* Polymer Engineering & Science, 2012. **52**(2): p. 390-398.
121. Chan, M.-l., Lau, K.-t., Wong, T.-t., Ho, M.-p., and Hui, D., *Mechanism of reinforcement in a nanoclay/polymer composite.* Composites Part B: Engineering, 2011. **42**(6): p. 1708-1712.

122. Liu, G., van de Ven, M., Wu, S., Yu, J., and Molenaar, A., *Influence of organo-montmorillonites on fatigue properties of bitumen and mortar.* International Journal of Fatigue, 2011. **33**(12): p. 1574-1582.
123. Ake, C.L., Wiles, M.C., Huebner, H.J., McDonald, T.J., Cosgriff, D., Richardson, M.B., Donnelly, K.C., and Phillips, T.D., *Porous organoclay composite for the sorption of polycyclic aromatic hydrocarbons and pentachlorophenol from groundwater.* Chemosphere, 2003. **51**(9): p. 835-844.
124. Carmody, O., Frost, R., Xi, Y., and Kokot, S., *Adsorption of hydrocarbons on organo-clays--Implications for oil spill remediation.* Journal of Colloid and Interface Science, 2007. **305**(1): p. 17-24.
125. Akçay, G., KilInç, E., and Akçay, M., *The equilibrium and kinetics studies of flurbiprofen adsorption onto tetrabutylammonium montmorillonite (TBAM).* Colloids and Surfaces A: Physicochemical and Engineering Aspects, 2009. **335**(1-3): p. 189-193.
126. Kostyniak, P.J., Giese, R.F., Costanzo, P.M., and Syracuse, J.A., *ANTIMICROBIAL COMPOSITIONS*, W.I.P. Oganization, Editor. 1997: US.
127. Zaghouane-Boudiaf, H. and Boutahala, M., *Preparation and characterization of organo-montmorillonites. Application in adsorption of the 2,4,5-trichlorophenol from aqueous solution.* Advanced Powder Technology, 2011. **22**(6): p. 735-740.
128. Ishida, H. and Agag, T., *Handbook of Benzoxazine Resins*. 1 ed. 2011: Elsevier.
129. Kim, S. and Park, S.-J., *Interlayer spacing effect of alkylammonium-modified montmorillonite on conducting and mechanical behaviors of polymer composite electrolytes.* Journal of Colloid and Interface Science, 2009. **332**(1): p. 145-150.
130. Liauw, C.M., Lees, G.C., Rothon, R.N., Wilkinson, A.N., and Limpanapittayatorn, P., *Evaluation of an alternative modification route for layered silicates and synthesis of poly(styrene) layered silicate nanocomposites by in-situ suspension polymerisation.* Composite Interfaces, 2007. **14**(4): p. 361-386.
131. Guang-Guo, Y., *Fate, behavior and effects of surfactants and their degradation products in the environment.* Environment International, 2006. **32**(3): p. 417-431.
132. Anderson, M.T., Martin, J.E., Odinek, J.G., and Newcomer, P.P., *Effect of Methanol Concentration on CTAB Micellization and on the Formation of Surfactant-Templated Silica (STS).* Chemistry of materials, 1998. **10**(6): p. 1490-1500.
133. Xi, Y., Martens, W., He, H., and Frost, R.L., *Thermogravimetric analysis of organoclays intercalated with the surfactant octadecyltrimethylammonium bromide.* Journal of Thermal Analysis and Calorimetry, 2005. **81**(1): p. 91-97.
134. Vaia, R.A., Teukolsky, R.K., and Giannelis, E.P., *Interlayer Structure and Molecular Environment of Alkylammonium Layered Silicates.* Chemistry of Materials, 1994. **6**(7): p. 1017-1022.
135. *Plastics*. Nobelprize.org 27/02/2012]; Available from: http://www.nobelprize.org/educational/chemistry/plastics/readmore.html.
136. *Thermosoftening plastics and Thermosetting plastics*. 27/02/2012]; Available from:

http://www.lgschemistry.org.uk/PDF/Thermosoftening_and_thermosetting_plastics.pdf.
137. *Historical Review: Discovery of Polyethylene*. Royal Society of Chemistry 20/02/2012]; Available from: http://www.rsc.org/Chemsoc/Activities/ChemicalLandmarks/UK/Polyethylene.asp.
138. Vasile, C. and Pascu, M., *Practical Guide to Polyethylene*. 2005, Shawbury: Rapra Technology Limited.
139. *Linear Low-Density Polyethylene (LLDPE)*. DAco-Trade 1/10/2010 19/02/2012]; Available from: http://daco-trade.com/info/lldpe/.
140. Borruso, A., *Linear Low-Density Polyethylene (LLDPE) Resins*. 2011, Chemical Economics Handbook.
141. *Linear low density polyethylene (LLDPE)*. Environmental Product Declarations of the European Plastics Manufacturers 2008 01/11/2008 27/02/2012]; Available from: http://www.plasticseurope.org/Documents/Document/20100312112214-FINAL_LLDPE_270409-20081215-019-EN-v1.pdf.
142. Clayden, J., Greeves, N., Warren, S., and Wothers, P., *Organic Chemistry*. 2007, Oxford: Oxford University Press.
143. Saunders, K.J., *Organic Polymer Chemistry*. 2 ed. 1988, London: Chapman and Hall.
144. Brydson, J., *Plastics Materials (7th Edition)*. 7 ed. 1999, Oxford: Butterworth-Heinemann.
145. AZoM.com. *Silicone Rubber*. 2001 25/09/2001 24/02/2012]; Available from: http://www.azom.com/article.aspx?ArticleID=920#_Room_Temperature_Vulcanising.
146. Brook, M.A., *Silicon in Organic, Organometallic, and Polymer Chemistry*. 2000, Chichester: Wiley-Interscience.
147. Yun-Yun, S. and Chin-Hsing, C., *PMMA/montmorillonite nanocomposites by bulk polymerization: Mechanical and thermal properties*, in *16th International Conference on Composite Materials*. 2007: Kyoto, Japan.
148. Garcia, M.T., Campos, E., Sanchez-Leal, J., and Ribosa, I., *Anaerobic degradation and toxicity of commercial cationic surfactants in anaerobic screening tests.* Chemosphere, 2000. **41**: p. 705-710.
149. Dean-Raymond, D. and Alexander, M., *Bacterial metabolism of quaternary ammonium compounds.* Applied and Environmental Microbiology, 1977. **33**(5): p. 1037-1041.
150. Tischer, M., Pradel, G., Ohlsen, K., and Holzgrabe, U., *Quaternary Ammonium Salts and Their Antimicrobial Potential: Targets or Nonspecific Interactions?* ChemMedChem, 2012. **7**(1): p. 22-31.
151. Hawkins, M., *Why we need cobalt.* Applied Earth Science: Transactions of the Institution of Mining & Metallurgy, Section B, 2001. **110**(2): p. 66–71.
152. Ranquet, C., Ollagnier-de-Choudens, S., Loiseau, L., Barras, F.d.r., and Fontecave, M., *Cobalt Stress in Escherichia coli.* Journal of Biological Chemistry, 2007. **282**(42): p. 30442-30451.
153. Hatamie, S., Nouri, M., Karandikar, S.K., Kulkarni, A., Dhole, S.D., Phase, D.M., and Kale, S.N., *Complexes of cobalt nanoparticles and polyfunctional curcumin as antimicrobial agents.* Materials Science and Engineering: C, 2012. **32**(2): p. 92-97.

154. Perni, S., Piccirillo, C., Pratten, J., Prokopovich, P., Chrzanowski, W., Parkin, I.P., and Wilson, M., *The antimicrobial properties of light-activated polymers containing methylene blue and gold nanoparticles.* Biomaterials, 2009. **30**(1): p. 89-93.
155. Kaali, P., Stromberg, E., Aune, R.E., Czel, G., Momcilovic, D., and Karlsson, S., *Antimicrobial properties of Ag+ loaded zeolite polyester polyurethane and silicone rubber and long-term properties after exposure to in-vitro ageing.* Polymer Degradation and Stability, 2010. **95**(9): p. 1456-1465.
156. Sun, X., Cao, Z., Porteous, N., and Sun, Y., *A N-halamine-based rechargeable antimicrobial and biofilm controlling polyurethane.* Acta Biomaterialia, 2012(0).
157. Ruiz, J.-C., Alvarez-Lorenzo, C., Taboada, P., Burillo, G., Bucio, E., De Prijck, K., Nelis, H.J., Coenye, T., and Concheiro, A., *Polypropylene grafted with smart polymers (PNIPAAm/PAAc) for loading and controlled release of vancomycin.* European Journal of Pharmaceutics and Biopharmaceutics, 2008. **70**(2): p. 467-477.

Appendices

Appendix 1: Essential oil calibration graphs for calculating percentage concentration from gas chromatography data.

Appendix 1 (a) Rosewood oil.

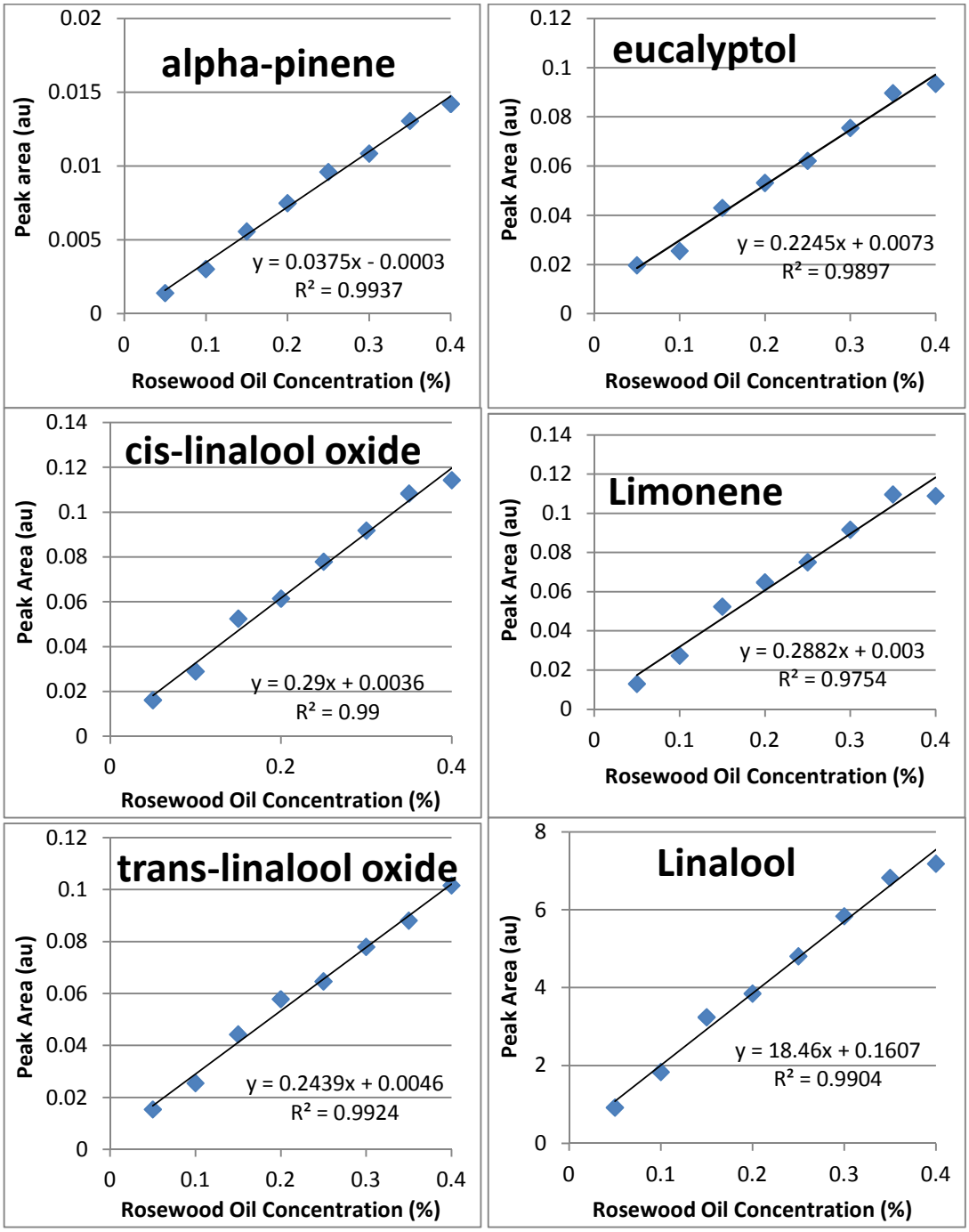

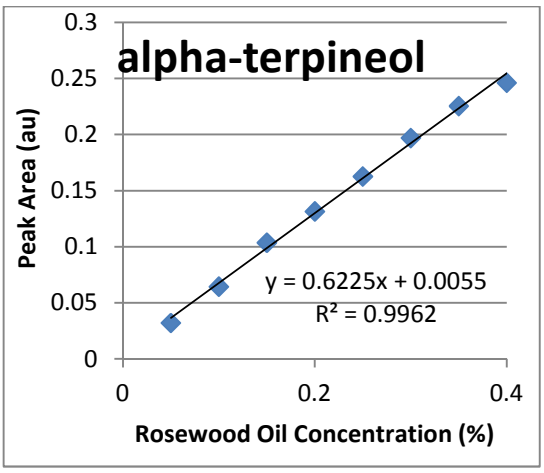

Appendix 1 (b) Oregano oil

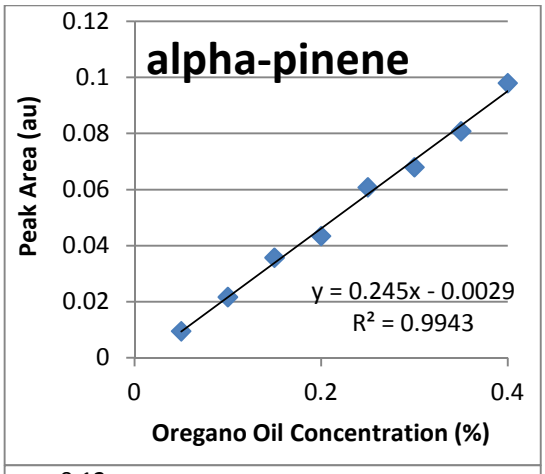

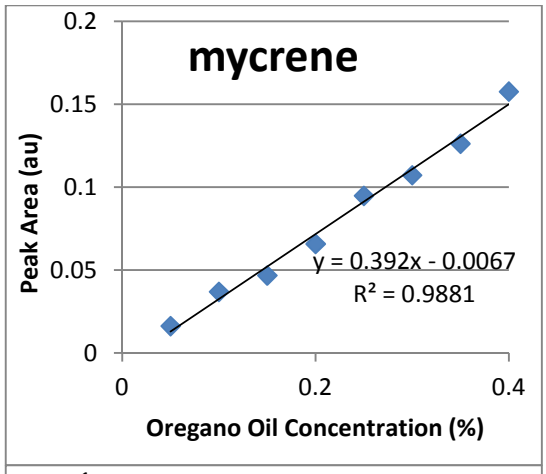

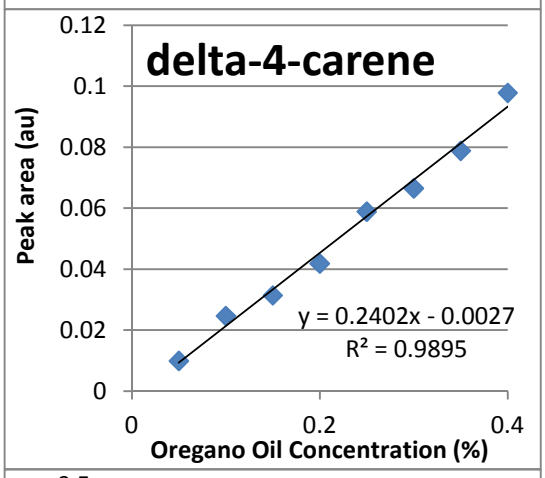

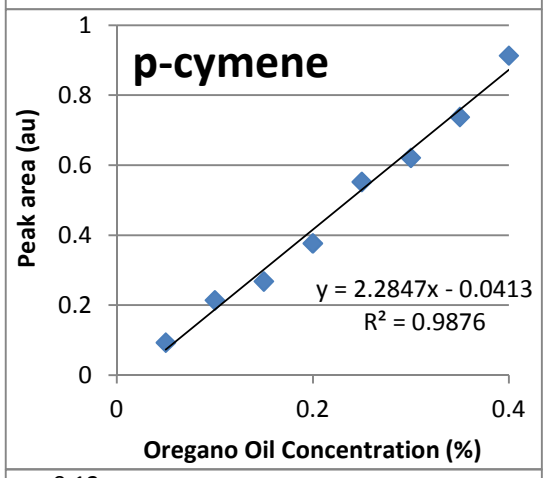

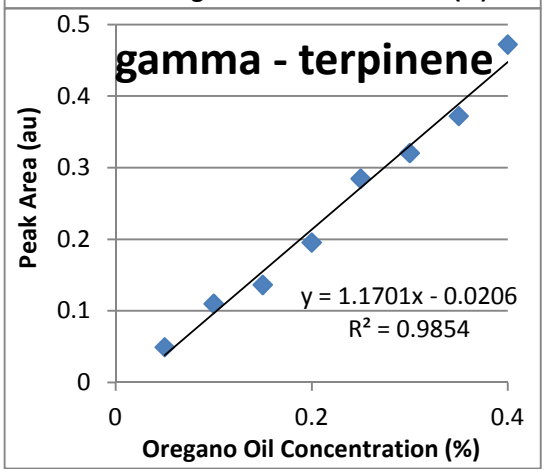

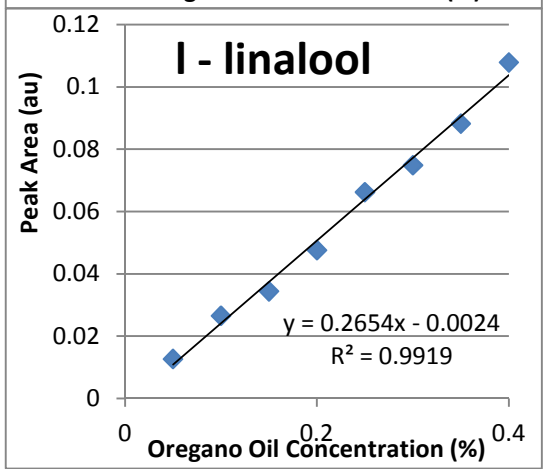

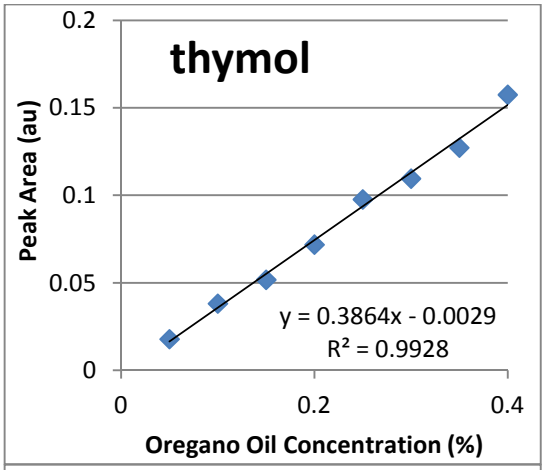

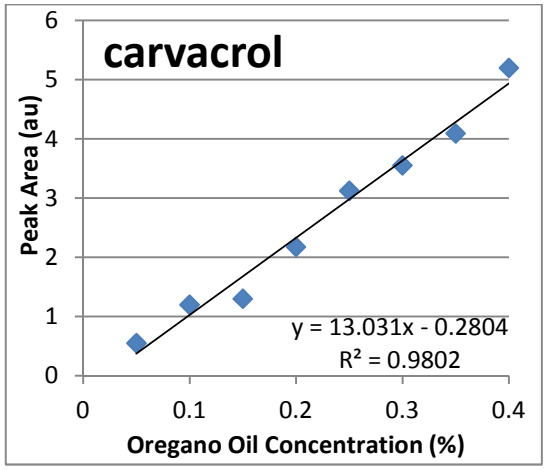

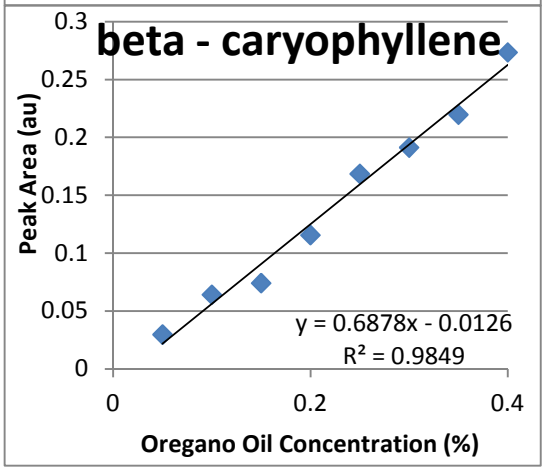

Appendix 1 (c) Manuka oil

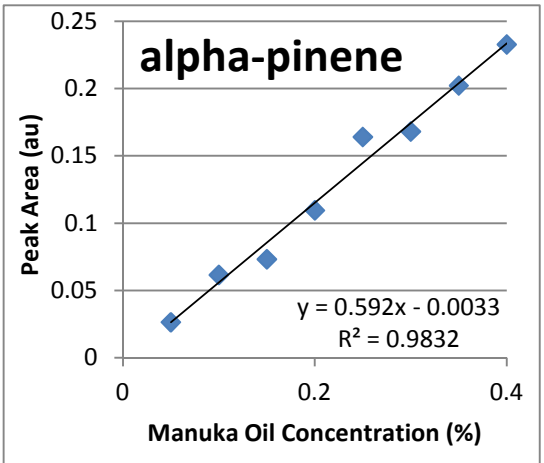

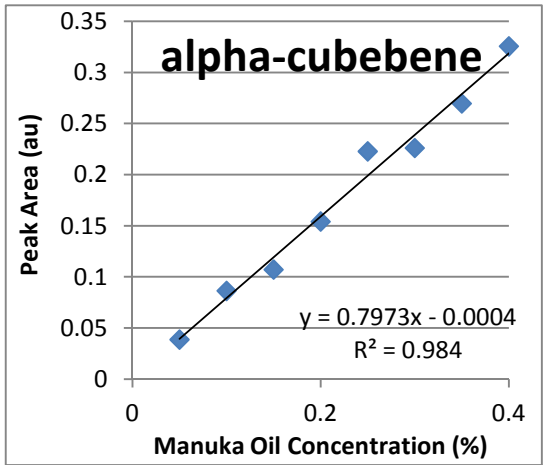

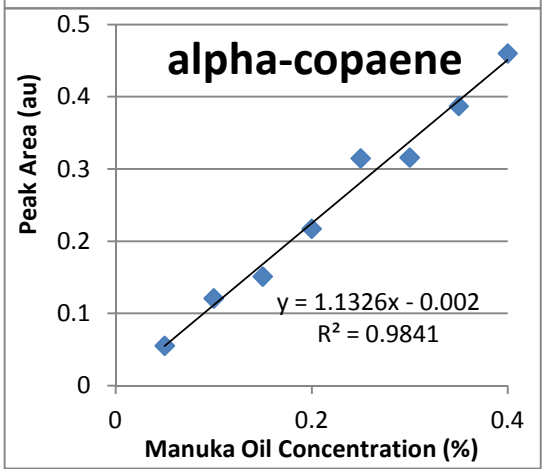

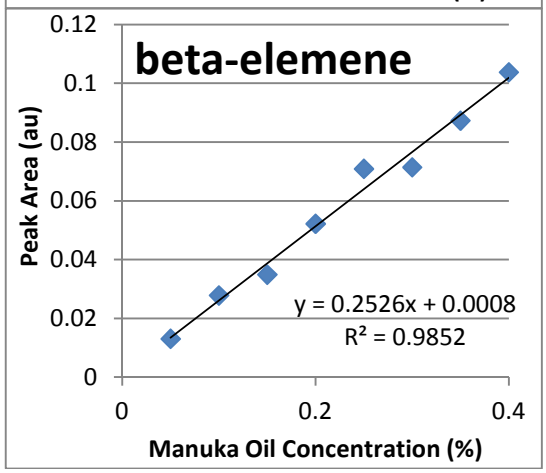

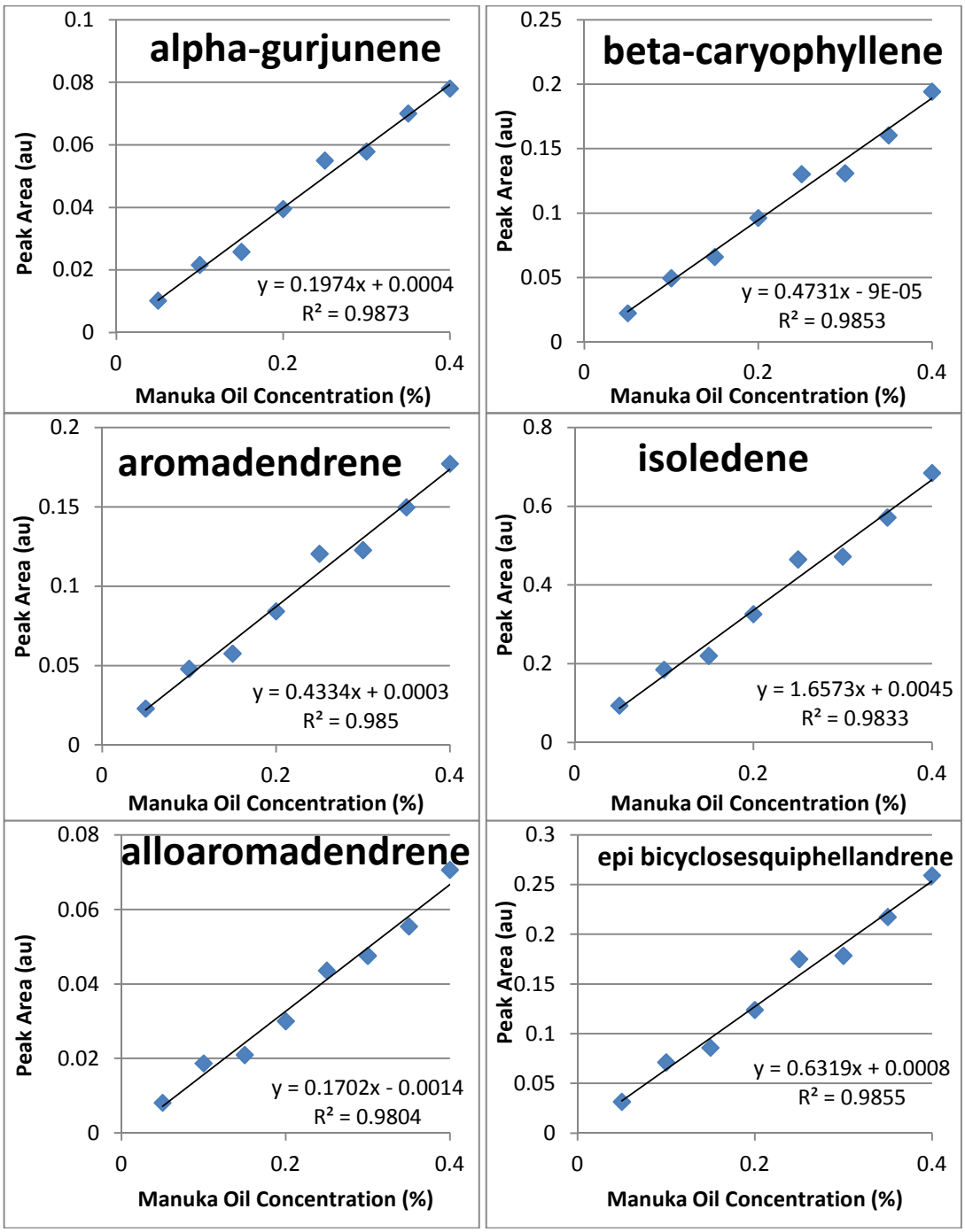
alpha-gurjunene
Peak Area (au)
Manuka Oil Concentration (%)
y = 0.1974x + 0.0004
R² = 0.9873
beta-caryophyllene
y = 0.4731x - 9E-05
R² = 0.9853
aromadendrene
y = 0.4334x + 0.0003
R² = 0.985
isoledene
y = 1.6573x + 0.0045
R² = 0.9833
alloaromadendrene
y = 0.1702x - 0.0014
R² = 0.9804
epi bicyclosesquiphellandrene
y = 0.6319x + 0.0008
R² = 0.9855

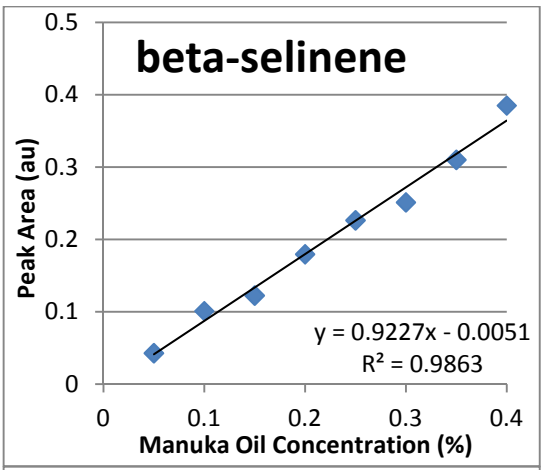

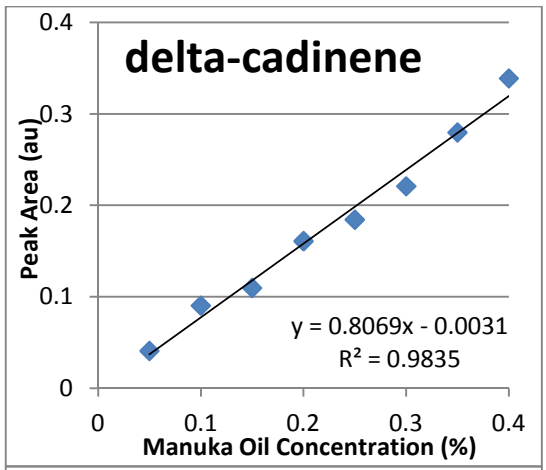

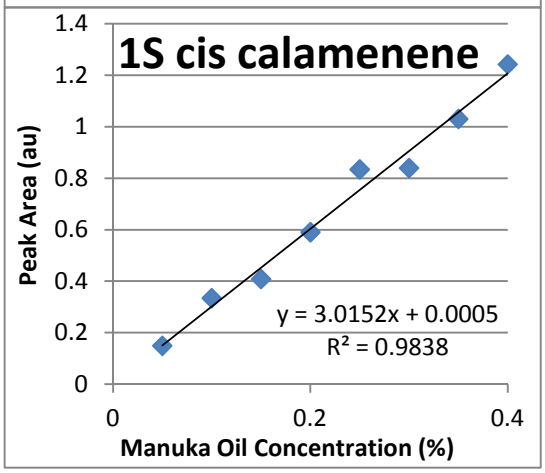

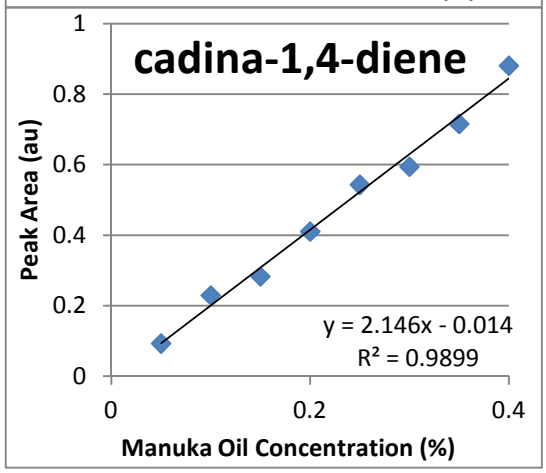

Appendix 1 (d) Lavender oil

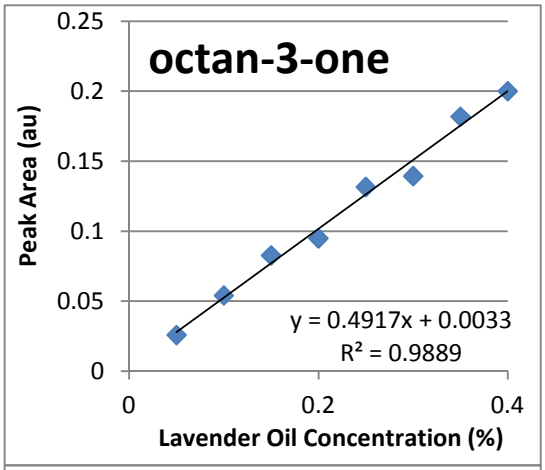

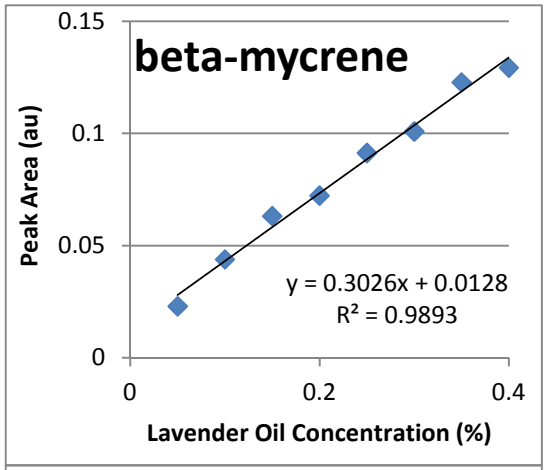

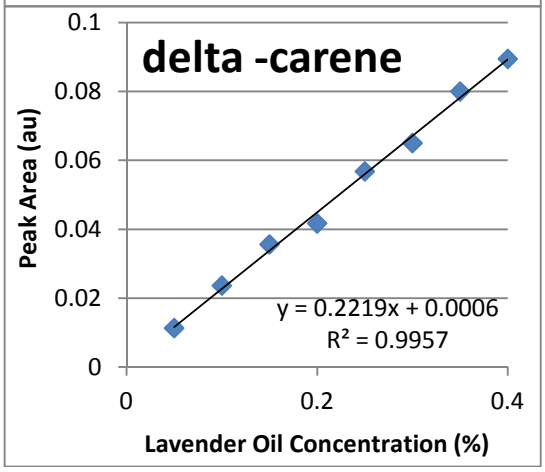

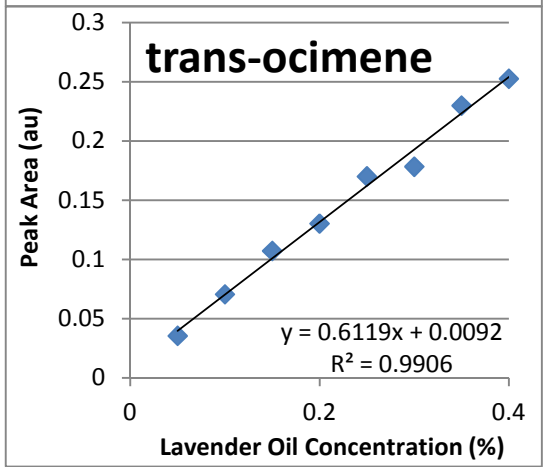

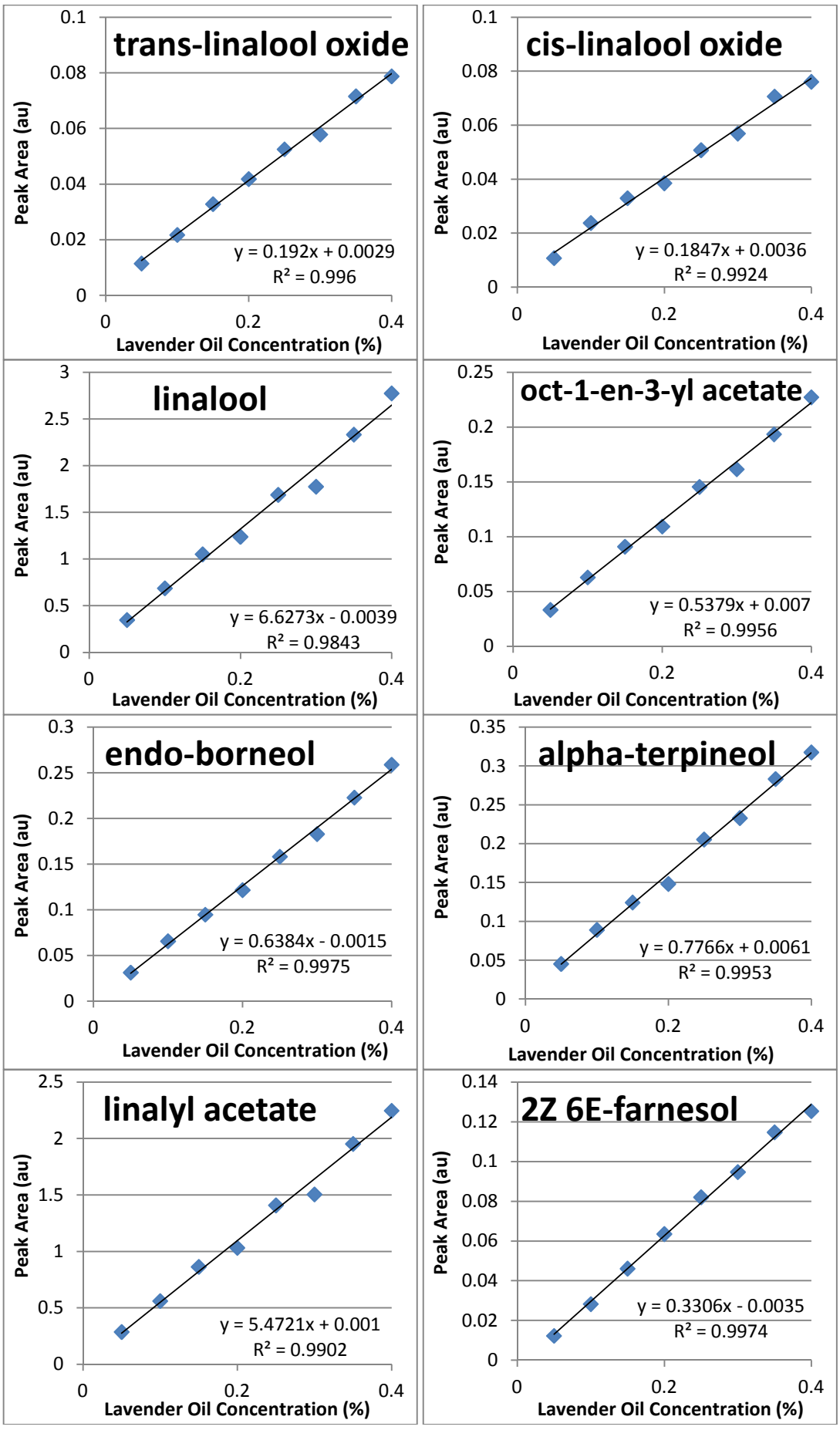
trans-linalool oxide
y = 0.192x + 0.0029
R² = 0.996
cis-linalool oxide
y = 0.1847x + 0.0036
R² = 0.9924
linalool
y = 6.6273x - 0.0039
R² = 0.9843
oct-1-en-3-yl acetate
y = 0.5379x + 0.007
R² = 0.9956
endo-borneol
y = 0.6384x - 0.0015
R² = 0.9975
alpha-terpineol
y = 0.7766x + 0.0061
R² = 0.9953
linalyl acetate
y = 5.4721x + 0.001
R² = 0.9902
2Z 6E-farnesol
y = 0.3306x - 0.0035
R² = 0.9974
Peak Area (au)
Lavender Oil Concentration (%)

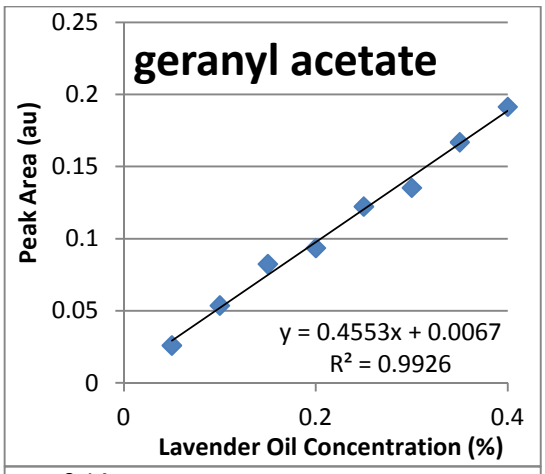

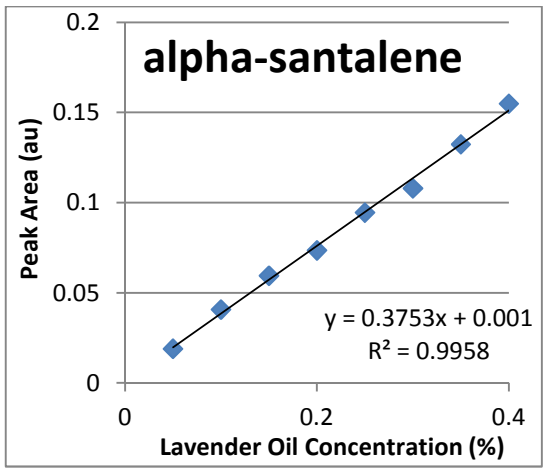

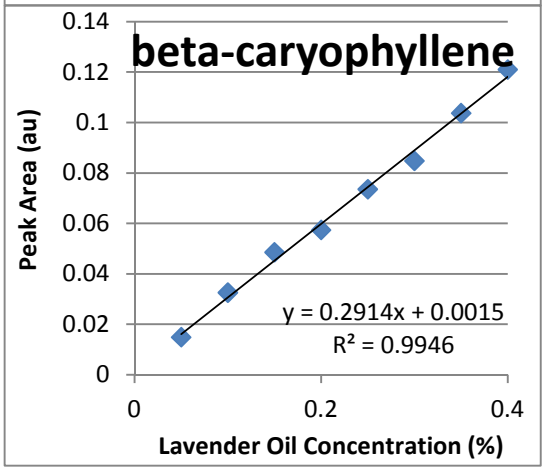

Appendix 1 (e) Geranium oil

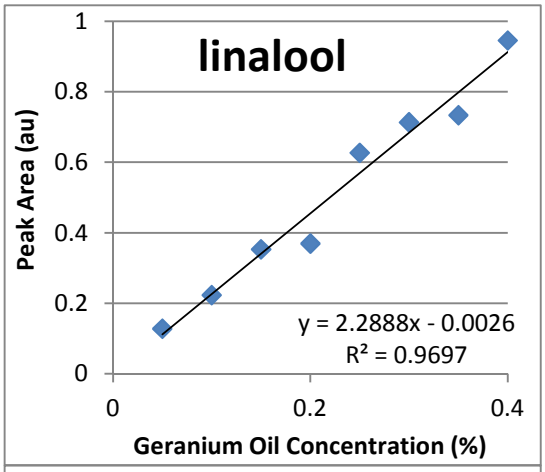

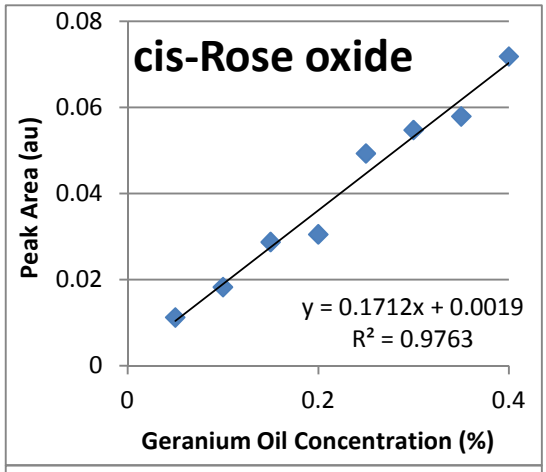

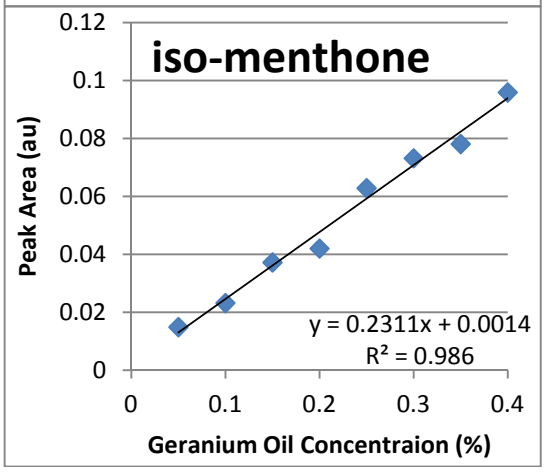

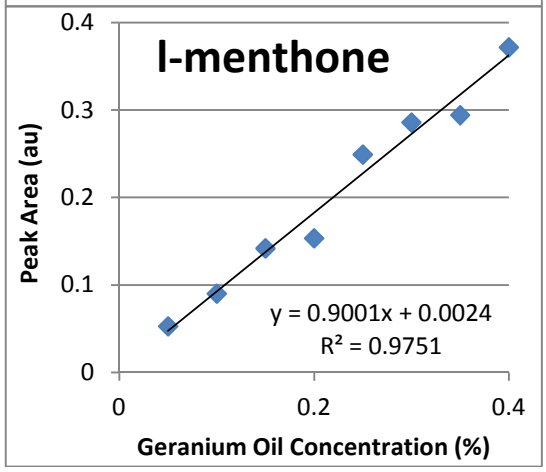

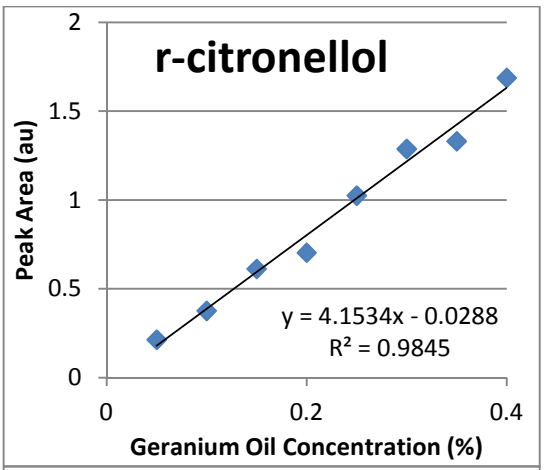
r-citronellol
Peak Area (au)
Geranium Oil Concentration (%)
y = 4.1534x - 0.0288
R² = 0.9845

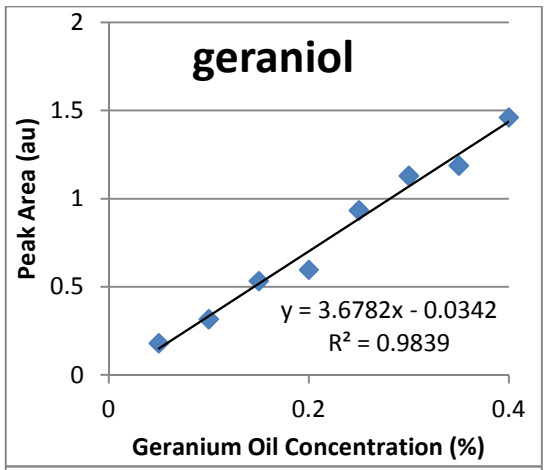
geraniol
Peak Area (au)
Geranium Oil Concentration (%)
y = 3.6782x - 0.0342
R² = 0.9839

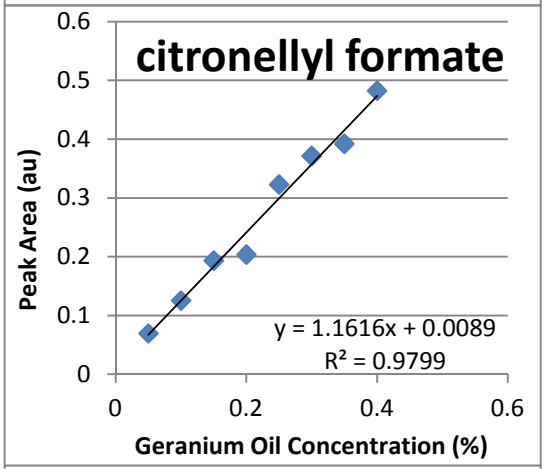
citronellyl formate
Peak Area (au)
Geranium Oil Concentration (%)
y = 1.1616x + 0.0089
R² = 0.9799

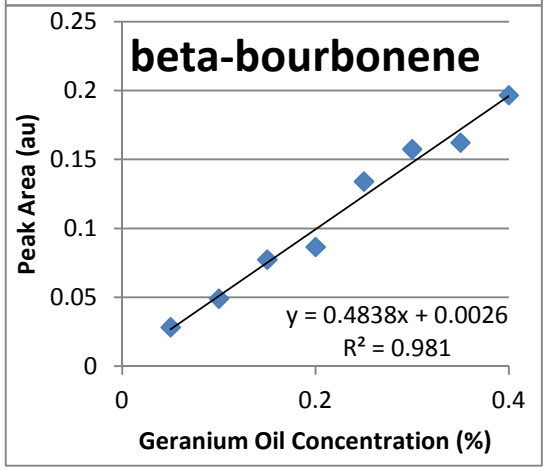
beta-bourbonene
Peak Area (au)
Geranium Oil Concentration (%)
y = 0.4838x + 0.0026
R² = 0.981

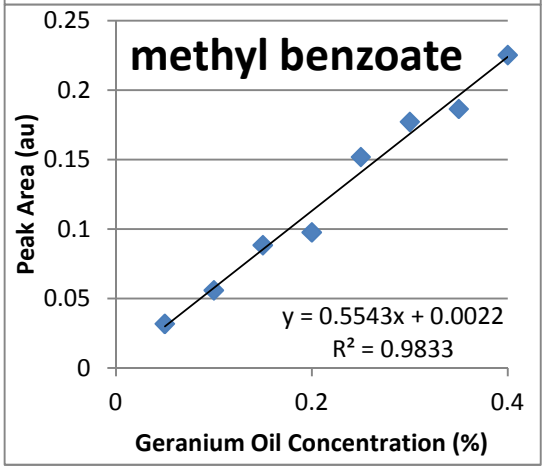
methyl benzoate
Peak Area (au)
Geranium Oil Concentration (%)
y = 0.5543x + 0.0022
R² = 0.9833

Appendix 2: Abstract for VITAE Postgraduate Researchers in Science Medicine conference October 2009.

Nano-layered inorganic-organic hybrid materials for the controlled delivery of antimicrobials to protect against healthcare associated infections.

M Kinninmonth, C Liauw, V Edwards-Jones, J Verran, R Taylor and D Shaw

Keywords: antimicrobial, essential oil, montmorillonite

Healthcare-associated infections (HAI) are a major problem in modern medicine, with reports suggesting that approximately 10% of patients acquire a HAI. Such infections have a considerable impact both economically and socially, and therefore it is important to investigate ways in which they can be prevented.
The aim of this project is to blend essential oils (EO), which have been shown to inhibit many HAI causing bacteria, in a way that will create a broad spectrum antimicrobial. The EO blend will then be adsorbed into the structure of a porous inorganic substrate.
The substrate-EO complex will then be incorporated onto materials such as plastics and fibers, the treated materials could then be used to create antimicrobial surfaces and textiles for use in healtchare facilities. This would create a reduced microbe environment and help to reduce the chances of a patient getting a HAI.
The majority of the work in the first year has concentrated on finding the optimum blends from five oils (manuka, oregano, geranium, lavender and rosewood), and combining the oil blends with man made biocides to improve the antimicrobial activity further.
The next stages of the project will be looking at the adsorption of the oils onto a range of inorganic substrates to determine the optimum substrate for adsorption and controlled release.

Appendix 3: Abstract for Manchester Metropolitan University Annual Research Student Conference September 2009 (poster presentation given)

Nano-layered inorganic-organic hybrid materials for the controlled delivery of antimicrobials

Malcolm Kinninmonth[1], Christopher Liauw[1], Joanna Verran[1], Rebecca Taylor[1], Valerie Edwards-Jones[2], David Shaw[3]

[1] School of Biology Chemistry and Health Science, Manchester Metropolitan University, Manchester, M1 5GD, UK.
2 R.E.D. Office, Manchester Metropolitan University, Chester Street, Manchester, M1 5GD, UK.
[3] Technical Manager, Rockwood additives Ltd, Moorfield Road, Widnes, Cheshire, WA8 3AA UK

Healthcare-associated infections (HAI) are a major problem in modern medicine, with reports in Scotland suggesting that approximately 10% of patients acquire a HAI[1]. Such infections have an additional impact both economically and socially. With antibiotic resistance making it difficult to treat many HAI, it is important to find methods to prevent infection [2].

Essential oils (EO), which are natural oils isolated from plant material, have been shown to be effective in limiting the growth of many pathogenic microbes responsible for HAI [3, 4]. If EO were present on surfaces in healthcare facilities it could reduce the numbers of pathogenic microbes in the environment and therefore reduce the incidence of HAI. By encapsulating EO in a substrate it could potentially be implanted into surfaces during production creating a long lasting reliable delivery mechanism. Research into the encapsulation of EO has concentrated on using organic polymers. Polyvinyl alcohols have been used to create microcapsules of EO using coacervation followed by cross-linking, the coacervated cross-linked membrane had a permeability coefficient of between 10-4 and 10-6 cm/s for santosol oil [5]. Organic materials can be susceptible to extreme conditions often used in manufacturing processes. If the EO could be incorporated into an inorganic substrate, such as the montmorillonite, this would create a complex resistant enough to the conditions used in manufacturing to allow the impregnation of surfaces directly. The pores running through the material form a large internal area in which the antimicrobial can be encapsulated. A major requirement of any successful material would be to confer long term antimicrobial properties, and the greater the volume of EO that could be encapsulated the longer the materials lifetime would be. Work at MMU has shown that organically modified montmorillonites can offer controlled release of the organic biocide 5-chloro-2-(2,4-dichlorophenoxy)phenol (triclosan) [7].

References:

1. Reilly, J., et al., Results from the Scottish National HAI Prevalence Survey. Journal of Hospital Infection, 2008. 69(1): p. 62-68.

2. Trends in Antimicrobial Resistance in England and Wales, 2004-2005. London, Health Protection Agency 2006.
3. Hammer, K.A., et al., Antimicrobial activity of essential oils and other plant extracts. Journal of Applied Microbiology, 1999. 86(6): p. 985-990.
4. Edwards-Jones, V., et al., The effect of essential oils on methicillin-resistant Staphylococcus aureus using a dressing model. Burns, 2004/ 30(8): p. 772-777.
5. Bachtsi, A.R., et al., Synthesis and release studies of oil-containing poly(vinyl alcohol) microcapsules prepared by coacervation. Journal of Controlled Release, 1996. 38(1): p. 49-58.
6. Liauw, C. M., et al., Controlled Release of Triclosan from Organically Modified Montmorillonite in a Maxillofacial Silicone Elastomer. In: 4th International Symposium on Nanostructured and Functional Polymer-Based Materials and Nanocomposites, Nanofun Poly and European Centre for Nanostructured Polymers, Rome, Italy, 16th-18th April 2008

Appendix 4: Abstract for Manchester Metropolitan University Annual Research Student Conference February 2011 (oral presentation given)

Nano-layered inorganic-organic hybrid materials for the controlled delivery of antimicrobials.

KINNINMONTH, M.A., & LIAUW, C.M., & VERRAN, J., & EDWARDS-JONES, V.
School of Engineering and Technology, Division of Mechanical Engineering, Manchester Metropolitan University, Manchester, M1 5GD, UK.

Introduction

Healthcare-associated infections (HAI) are a major problem in modern medicine, with reports in Scotland suggesting that approximately 10% of patients acquire a HAI (Health Protection Agency, 2006), and it is important to find methods to prevent infection.

Essential oils (EO), have been shown to be effective in limiting the growth of many pathogenic microbes responsible for HAI (Hammer, 1999), (Edwards-Jones, 2004). If EO were present on surfaces in healthcare facilities it could reduce the numbers of pathogenic microbes in the environment and therefore reduce the incidence of HAI. This study aims to encapsulate a broad spectrum EO antimicrobial into montmorillonites (MMT) which are porous Aluminosilicates. The EO loaded inorganic will then be incorporated into polymers for the manufacture of antimicrobial surfaces.

Results and conclusions

Five EO (oregano, manuka, lavender, rosewood and geranium) were tested against *Pseudomonas aeruginosa*, *Acinetobacter baumannii*, Methicillin Resistant *Staphylococcus Aureus*, both as individual oils and in blend formulations. Oregano was found to be the most effective at inhibiting growth. Of the blends tested oregano+rosewood was the most effective, inhibiting the growth of all three test bacteria at concentrations of less than 0.2 %. Flow Micro Calorimetry was to analyse the adsorption characteristics of EO onto montmorillonite (MMT) materials. The initial MMT materials tested only gave low levels of adsorption (between 5 and 20 %). In an attempt to achieve higher levels of adsorption the MMT will be organically modified, to make them more hydrophobic. EO loaded MMT were incorpotated to a number of polymer matrices, the polymers were then tested for antimicrobial activity. Using organically modified MMT as carriers the antimicrobial properties of rosewood oil were successfully transferred to a silicone elastomer, with the treated silicone showing a log 3 reduction in microbial growth compared to untreated silicone.

References

Trends in Antimicrobial Resistance in England and Wales, 2004-2005. London, Health Protection Agency 2006.

Edwards-Jones, V., et al., *The effect of essential oils on methicillin-resistant Staphylococcus aureus using a dressing model.* Burns, 2004/ 30(8): p. 772-777.

Hammer, K.A., et al., *Antimicrobial activity of essential oils and other plant extracts.* Journal of Applied Microbiology, 1999. 86(6): p. 985-990.

Appendix 5: Abstract for Eurofillers 2011 Dresden September 2011 (oral presentation given)

Nano-layered inorganic-organic hybrid materials for the controlled delivery of antimicrobials.

KINNINMONTH, M.A.[1], & LIAUW, C.M.[1], & VERRAN, J.[2], TAYLOR, R.L.[2], EDWARDS-JONES, V.[3], & SHAW, D.[4]

[1] School of Engineering, Manchester Metropolitan University, Manchester, M1 5GD, UK.
[2] School of Healthcare Science, Manchester Metropolitan University, Chester Street, Manchester, M1 5GD, UK.
[3] R.E.D. Office, Manchester Metropolitan University, Chester Street, Manchester, M1 5GD, UK.
[4] Technical Manager, Rockwood additives Ltd, Moorfield Road, Widnes, Cheshire, WA8 3AA UK

Healthcare-associated infections (HAI) are a major problem in modern medicine, with reports in Scotland suggesting that approximately 10% of patients acquire a HAI [1] and it is important to find methods to prevent infection.
Essential oils (EO), have been shown to be effective in limiting the growth of many pathogenic microbes responsible for HAI [2,3]. If EO were present on surfaces in healthcare facilities it could reduce the numbers of pathogenic microbes in the environment and therefore reduce the incidence of HAI. This study aims to encapsulate an EO antimicrobial into montmorillonites (MMT). The EO loaded inorganic will then be added to polymers for the manufacture of antimicrobial surfaces. Previous work at MMU has shown MMT can be used as a controlled release reservoir for Triclosan ® [4] the EO antimicrobial used in this work should be able to inhibit the growth of a broader range of microbes.

Montmorillonites provided by Rockwood Additives Ltd. have been analysed for their ability to adsorb three EO (oregano, manuka, and rosewood). These oils were selected on the basis of earlier work which had shown them to have good antimicrobial activity against a number of bacteria, both as individual oils and in blend formulations. Oregano having the highest individual antimicrobial activity and the blend of oregano and rosewood showing the highest activity overall.

Flow Micro Calorimetry (FMC) was to analyse the adsorption characteristics of EO onto montmorillonite (MMT) materials. The initial MMT materials tested only gave low levels of adsorption, not high enough to produce the reservoir effect that was required. To achieve higher levels of adsorption the MMT samples were organically modified, using Quats, to make them more organophillic. Gas chromatography was also used to analyse adsorption, this allowed us to analyse what was happening to the individual components of the EO, where FMC gave a broad overview of adsorption.
The EO loaded MMT have been incorporated to a number of polymer matrices, the polymers were then tested for antimicrobial activity. Using organically modified MMT as carriers the antimicrobial properties of rosewood oil were

successfully transferred to a silicone elastomer, with the treated silicone showing a log 3 reduction in microbial growth compared to untreated silicone.

[1] *Trends in Antimicrobial Resistance in England and Wales, 2004-2005*. London, Health Protection Agency 2006.

[2] Hammer, K.A., et al., *Antimicrobial activity of essential oils and other plant extracts.* Journal of Applied Microbiology, 1999. 86(6): p. 985-990.

[3] Edwards-Jones, V., et al., *The effect of essential oils on methicillin-resistant Staphylococcus aureus using a dressing model.* Burns, 2004. 30(8): p. 772-777.

[4] Liauw, C.M., et al., *Organo-Montmorillonite as a controlled release reservoir for Triclosan in silicone elastomer: A Flow Micro-Calorimetry and leaching study,* Macromolecular Symposia Special Issue: Eurofillers**,** 2011. 301(1): p 96-103

Appendix 6: Abstract for paper submitted to Macromolecular Symposia to be published in the proceedings volume for Eurofillers (Dresden; Germany) – Paper currently under review.

Nano-layered inorganic-organic hybrid materials for the controlled delivery of antimicrobials.

Malcolm Kinninmonth,[1] *Christopher Liauw*,*[1] *Joanna Verran,*[2] *Rebecca Taylor,*[2] *Valerie Edwards-Jones,*[3] *David Shaw*[4]

[1] School of Engineering, Manchester Metropolitan University, Manchester, M1 5GD, UK.
[2] School of Healthcare Science, Manchester Metropolitan University, Chester Street, Manchester, M1 5GD, UK.
[3] R.E.D. Office, Manchester Metropolitan University, Chester Street, Manchester, M1 5GD, UK.
[4] Technical Manager, Rockwood additives Ltd, Moorfield Road, Widnes, Cheshire, WA8 3AA UK

Summary: An essential oil (EO) blend has been identified that provides a broad spectrum potent antimicrobial effect. Adsorption of the EO onto porous silicate materials (Rockwood Additives: Laponite® B, Laponite® RD and Fulcat® 800) and has been analysed and it was found that Laponite® RD organically modified with dihydrogenated tallow dimethyl ammonium chloride (2HT2M) at 50% cation exchange capacity gave the highest levels of adsorption. The Laponite® RD 2HT2M with EO blend adsorbed has been added to polymer materials to produce an antimicrobial polymer. The adsorption of the EO onto the Laponite® RD was done to achieve controlled release of the EO to prolong the antimicrobial effect within the polymer.
Addition of the EO loaded substrates into silicone elastomer has resulted in successfully conferring a high level of antimicrobial activity to the polymer.

Keywords: Organoclay; Silicones; Essential oil; Antimicrobial; Controlled release